BUCKLING BEHAVIOUR OF GUSSET PLATES IN BUCKLING RESTRAINED BRACED FRAMES

BENJAMIN ALEXANDER WESTENENG

A thesis submitted in partial fulfilment of the requirements for the degree of Master of Engineering endorsed in Earthquake Engineering

Supervised by:
Senior Lecturer Chin-Long Lee
Associate Professor Gregory A. MacRae

Department of Civil and Natural Resources Engineering
University of Canterbury
Christchurch
New Zealand

October 2016

ABSTRACT

This thesis describes a finite element study of BRB gusset plates under in-plane loading to determine how their strengths compare with those of experiments, and with those of methods in current design standards. Limitations of current standards, such as the calibration of the equivalent column method, with its effective length, Whitmore width and Thornton length, and the lack of explicit considerations for frame action effects are described. In addition, a stiffness based BRB system stability method is developed.

It is shown that the finite element modelling replicated behaviour and strengths of gusset plates in BRB system tests. Also, a number of other gusset plate connections were analysed where it was found that current design methods predicted greater strengths than that obtained from the analysis, or from experimental tests, due to limitations in the development of these design methods.

The major limitation of the design method is the calibration for the equivalent column strut using the Whitmore length and Thornton length together with a particular buckling curve, and an effective length factor. This effective length factor, K, has recommended values ranging from the fully fixed brace case (i.e. $K = 0.5$) to the fixed-free sway boundary condition case (i.e. $K = 2.0$), in the literature. In the NZ standard, it is recommended that $K = 0.70$. Current design methods for the fixed-free sway boundary condition case (i.e. $K = 2.0$) rather than 0.70 estimated greater capacities than those from previous experiments and analysis. Also, variations of Whitmore width and Thornton length did not always produce the expected changes in performance indicating that they may not be reliable for determining gusset plate buckling capacity.

Finite element models of a BRB frame considering frame action forces acting, and not acting, showed that frame action can decrease gusset plate buckling capacity.

A simple stiffness based BRB element stability method was developed to determine how different BRB system elements affected buckling capacity. Flexibilities of the frame beam-column joint and all other elements of the BRB system are considered. Effects of residual stresses and yielding from the column curve are considered. The buckling capacity of the system was determined based on the minimum eigenvalue of the system's stiffness matrix. A sensitivity study found that buckling capacity significantly decreases if one element of the system has relatively lower stiffness.

ACKNOWLEDGEMENTS

I would like to thank my parents, Kevin Westeneng and Hilary Westeneng, and my brother, Oliver Westeneng, for their support throughout the development of this thesis.

I also would like to thank my supervisors, Chin-Long Lee and Greg MacRae, as well as Audsley Jones. I am grateful for their guidance, time and support.

I would also like to acknowledge support from the Earthquake Commission (EQC) New Zealand for their financial assistance from their University Post-Graduate Research Programme.

TABLE OF CONTENTS

LIST OF TABLES

LIST OF FIGURES

LIST OF NOTATIONS

α_b	member section constant, $\alpha_b = 0.5$ for gusset plates
Δ_X	displacement at a particular end of the beam element
θ_X	rotation at a particular end of the beam element
λ_c	slenderness coefficient
λ_r	equivalent slenderness ratio used with the AIJ elasto-plastic column curves to determine N_{cr}^r
ν	Poisson's ratio
ξ	ratio of connection length to BRB casing length
ξL_0	connection region length
$\xi\kappa_{Rg}$	normalised rotational stiffness of the gusset plate and beam-column joint
π	pi
A_0	vertical gusset plate length along column interface
a_r	initial imperfection at the BRB end
B_0	horizontal gusset plate length along beam interface
b_0	short bounded edge length of gusset plate
b_1	bending line length
b_b	width between outermost splice plate bolts or width between splice plate welds
b_e	Whitmore effective width
c	column curve factor
E	elastic modulus
EI	gusset plate flexural rigidity
$\left(\frac{EI}{L}\right)_C$	flexural stiffness of the yielding core plate
$\left(\frac{EI}{L}\right)_R$	flexural stiffness of the restrainer including the outer casing and concrete filling
$\left(\frac{EI}{L}\right)_g$	flexural stiffness of the gusset plate
$(EI)_{eff,i}$	effective rigidity of beam element
E_t	tangent stiffness modulus
I	second moment of area of beam element
I_c	second moment of area of connection, or non-yielding segment at end of BRB casing

i_c	radius of gyration of connection region
K	effective length factor
K_{equiv}	equivalent effective length factor
k_{BC}	beam-column joint rotational stiffness
k_{RE}	rotational spring stiffness of BRB end
k_g	finite element model constant
l_b	length between outermost splice plate bolts or length of splice plate welds
L	gusset plate length, beam element length, Thornton length
L_b	length, from end of BRB casing to centre of beam-column joint
L_c	connection length, from end of BRB casing to beam or column flange
M_0^r	initial bending moment at the BRB ends produced by out-of-plane drift
M_X	moment at a particular end of the beam element
M_p^g	plastic bending strength of the gusset plate including axial force effects
M_p^r	moment transfer capacity at the BRB ends
N^*	applied axial load on beam element
N_{cr}^B	elastic buckling strength of the BRB considering the effects of connection bending stiffness and gusset plate rotational stiffness
N_{cr}^r	elastic buckling strength of the connection region without bending moment transfer capacity
N_s	axial section yield capacity
P	applied load to beam element
P_{cr}	gusset plate buckling capacity
P_{cr1}	buckling capacity assuming elastic springs for gusset plates
P_{cr2}	buckling capacity assuming plastic hinges at the gusset plate ends
r	radius of gyration
S_L	splice plate length
S_W	splice plate width
SRF_i	stiffness reduction factor
V_X	shear force at a particular end of the beam element

1 INTRODUCTION

1.1 Background

Steel braced frames are a common structural system used in areas of high seismic risk. For concentrically braced frames (CBFs), their ability to resist earthquake forces is generally limited by the diagonal brace member's compressive buckling capacity. An alternative solution is to use buckling restrained braces (BRBs). These members consist of a slender steel core, and an outer casing to limit buckling of the core. Because the steel core is restrained, the BRB will instead yield in compression.

BRBs are well suited to resist seismic loads due to their unique properties. As the ground shakes in an earthquake, a structure must sustain cyclic displacements. The BRB dissipates seismic energy by yielding in both compression and tension.

To maintain structural integrity between members in a braced frame, it is vital that the connections are robust. BRBs are connected to the braced frame with gusset plates. These plates need to be designed to transfer the forces in the braced frame though the BRB without any damage to the plate itself or the surrounding members.

1.1.1 Gusset Plates

Gusset plates are typically used to connect a diagonal brace member to a beam and column in a frame. They are often rectangular with the corner clipped where the brace meets the plate, but can also be designed to other shapes.

Gusset plates are generally designed to behave elastically as it is desired that the majority of the yielding will occur in the BRB. This is achieved by designing the gusset plate for the brace overstrength force, the maximum force that can occur in the BRB. The capacity of the gusset plate is dependent on the gusset plate geometry, thickness, the presence of any stiffeners and the material yield strength.

The gusset plate is sized such that the connection between the gusset plate and the beam and column is sufficient to transfer force through the gusset plate to the beam and column. For welded gusset plates, the size may be governed by the length of the weld required to transfer the force.

The connection between the diagonal brace member and the gusset plate can be welded, bolted or pinned. Additional splice plates can also be welded or bolted between the brace and the gusset plate. The length of the connection of the brace to the gusset plate is dependent on its ability to transfer force to the gusset plate. This length can also govern the gusset plate size.

When the gusset plate is subjected to compressive forces from the connected brace member, the design of the gusset plate must consider buckling in addition to yielding. Buckling may cause the member to become unstable and deform laterally.

1.1.2 Gusset Plate Buckling

Gusset plate buckling, such as that shown in Figure 1.1-1, is undesirable. The common way to design gusset plates used in braced frames not to buckle is to consider the gusset plate as an equivalent column with assumed boundary conditions.

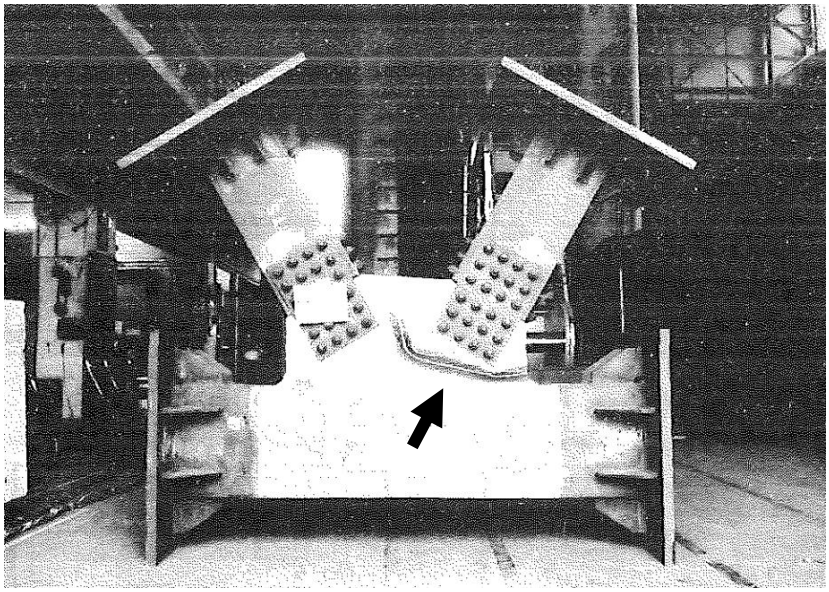

Figure 1.1-1: Local buckling of a gusset plate in a truss joint (Yamamoto et al. 1985)

Boundary conditions at the interface of the gusset plate to the beam and column, and the interface of the gusset plate to the brace, are sometimes assumed to be restrained in all degrees of freedom so that they are unable to translate or rotate in any direction. Because of this fixed-fixed boundary condition assumption, the effective length of a gusset plate framing into these boundaries is less than that if some boundary flexibility existed. For example, for a gusset plate connected between rigid boundaries in a braced frame, the effective length of the equivalent buckling column is considered to be one half of the total length.

If the interface between the gusset plate and the brace is unable to provide any translational or rotational restraint, then the interface can be considered free in all degrees of freedom. Under this condition, the gusset plate will buckle by sway instead of braced (or local) buckling. If the beam and column to gusset plate connection is assumed to be rigid, then the effective length of the equivalent buckling column, representing the gusset plate, is now twice the total length. The buckling capacity of a gusset plate to resist sway buckling failure is significantly less than the capacity required to resist local buckling failure. Such sway buckling has been seen in actual experiments, as shown in Figure 1.1-2.

In realistic frames, there is no lateral restraint at the brace end of the gusset plate, and the mode of buckling involves sway. If the rotational stiffness at the interfaces at both ends of the gusset plate is less than rigid, then the effective length will be greater than unity and it tends to infinity for low rotational flexibilities. The strength of the gusset plate is therefore directly related to the rotational stiffness at both ends of the gusset plate.

Figure 1.1-2: Sway buckling of a gusset plate in a BRB frame (Chen et al. 2004)

Gusset plates used in a number of BRB frame experiments have failed by sway buckling (Chou et al. 2012; Koetaka et al. 2008; Tsai et al. 2002, 2004). These gusset plates were designed with current buckling design methods assuming gusset plate effective lengths less than unity, which implies a braced failure.

There is currently no single agreed upon buckling capacity design procedure for gusset plates in BRB frames. However, it is clear that a potential failure mode is buckling by sway failure due to the end of the BRB forming a hinge.

Different design methods that currently exist considering the sway buckling capacity of a gusset plate in a BRB frame have been proposed by Chou et al. (2012) and Tsai and Hsiao (2008). Both of these methods consider an effective length equal to twice the total length of the equivalent buckling column, indicating sway buckling. These methods are in good agreement with in-plane experimental testing on BRB frames considered by each paper. However, it is currently unclear if these methods will be conservative and accurate for all gusset plates in BRB frames. Takeuchi et al. (2014) have also proposed a method considering sway, which considers element yielding.

Current design methods only consider the force from the brace. Additional forces from the beam-column joint opening or closing during lateral loading can also act on the gusset plate. These forces, known as frame action forces, may change the brace force required to buckle the gusset plate.

The effect of other elements, including the beam-column joint and BRB, on gusset plate buckling capacity is not also considered by most current design methods. The beam-column joint is usually assumed to be rigid in buckling capacity design. However, for chevron configuration braced frames, where two BRBs meet at a central beam joint, the rotational stiffness of the beam joint is significantly lower than being rigid.

1.2 Issues

Based on the information above, there is a need for further research. This thesis will attempt to investigate gusset plate sway buckling by answering the following questions:

1) What gusset plate buckling capacity design methods are currently used and are their assumptions valid for gusset plate sway buckling?
2) Are current design methods able to conservatively estimate gusset plate buckling capacity considering sway buckling for a range of gusset plates?
3) Are the relationships assumed by current design methods between their parameters and gusset plate buckling capacity representative of the true relationships?
4) Do frame action forces have an effect on gusset plate buckling capacity in BRB frames?
5) What is the sensitivity of other elements in the BRB system on gusset plate sway buckling failure?

1.3 Outline

The issues and questions raised above will be addressed in the chapters of this thesis to better understand the buckling behaviour of gusset plates in BRB frames, and to evaluate if an appropriate design method can be recommended for gusset plates in BRB frames in New Zealand.

Chapter 2 presents a literature review of gusset plate behaviour and design. This chapter reports prior knowledge on gusset plates and determines the areas that require further investigation. It includes a review of BRBs, buckling behaviour in experimental tests of gusset plates, buckling behaviour of gusset plates in experimentally tested BRB frames, and available design methods for gusset plate buckling.

Chapter 3 presents the current buckling capacity design methods for gusset plates and discusses the assumptions and limitations of each available method. Each method was evaluated against two experimentally tested BRB frames that have failed by gusset plate sway buckling (Chou et al. 2012; Tsai et al. 2004) to determine if the method is conservative and accurate.

Chapter 4 discusses the effects of frame action forces in gusset plate buckling capacity. A finite element model of a BRB frame was developed to determine if frame action forces have a direct effect on gusset plate buckling capacity when the BRB is in compression. It was then evaluated whether this effect should be considered in buckling capacity design methods of gusset plates in BRB frames.

Chapter 5 assesses the validity of the assumption made by Chou et al. (2012) and Tsai and Hsiao (2008) that the gusset plate effective length factor is equal to 2.0 for a variety of gusset plates. An effective length factor of 2.0 is representative of a gusset plate that has boundary conditions that are fixed at one end and free at the other end. No gusset plate has been experimentally tested with these boundary conditions. To remedy this, validated finite element models of experimentally tested gusset plates were analysed under fixed-free boundary conditions.

Chapter 6 assesses the assumptions made for each parameter considered by the Thornton method (Thornton 1984). This was done to identify why the Thornton method, and methods that are based on the Thornton method such as the methods proposed by Chou et al. (2012) and Tsai and Hsiao (2008), are unable to conservatively and accurately predict the buckling capacity of gusset plates. A parametric study of a range of gusset plate finite element models was done to evaluate each parameter's relationship to gusset plate buckling capacity and then compared to the Thornton method.

Chapter 7 investigates the effect of other elements in a BRB frame on gusset plate buckling capacity and develops a design method that considers these elements. These elements included the beam-column joint, the gusset plate, the connection region, the BRB end rotational stiffness, and the BRB. A design method was developed by forming a stiffness matrix of the sub-structural system considering the flexural or rotational stiffness of each element. The buckling load was then determined using eigenvalue analysis. A sensitivity study was undertaken to evaluate the effect of each element's stiffness on the buckling capacity of the BRB system.

Finally, Chapter 8 provides conclusions summarised from the previous chapters.

2 LITERATURE REVIEW

This literature review was conducted to understand and review the previous research that has been performed on experimentally tested gusset plates, and gusset plates in BRB frames, to better understand gusset plate buckling behaviour. Current design methods developed to determine the buckling capacity of gusset plates have also been reviewed to determine what methods are available to a designer to prevent buckling failure. A brief review of BRBs has been included to increase understanding of BRB frames.

2.1 Review of Buckling Restrained Braces

A BRB is an energy dissipation device that can dissipate comparable amounts of energy under both tension and compression. This results in a large amount of energy being dissipated, making BRBs ideal for use in seismically designed structures to resist lateral earthquake loads.

Standard concentric braces buckle when loaded in compression before the compressive yield capacity is reached. The braces are more effective at dissipating energy in tension than compression. This behaviour can be seen in Figure 2.1-1. The BRB consists of a steel core section that is generally restrained by a steel outer casing and restraining medium so that it is unable to buckle in compression. The provided restraint significantly increases the amount of energy that is dissipated during lateral loading of the braced frame, as seen in Figure 2.1-2.

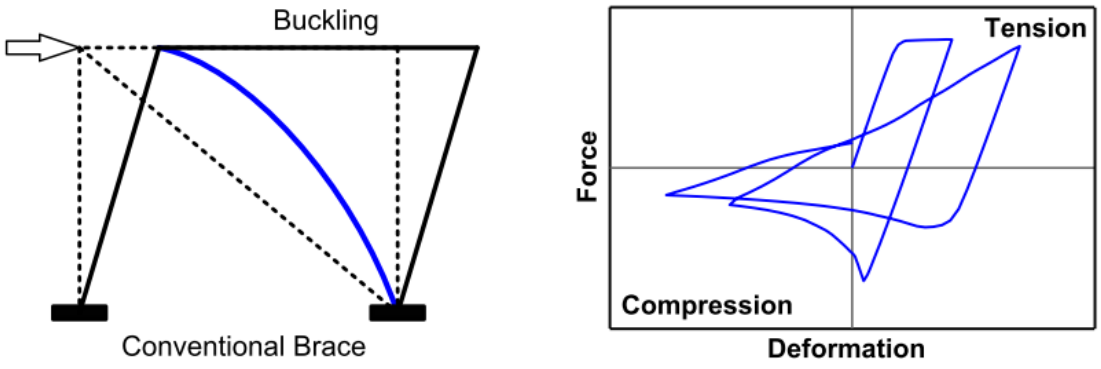

Figure 2.1-1: Concentric brace behaviour (Lin et al. 2012)

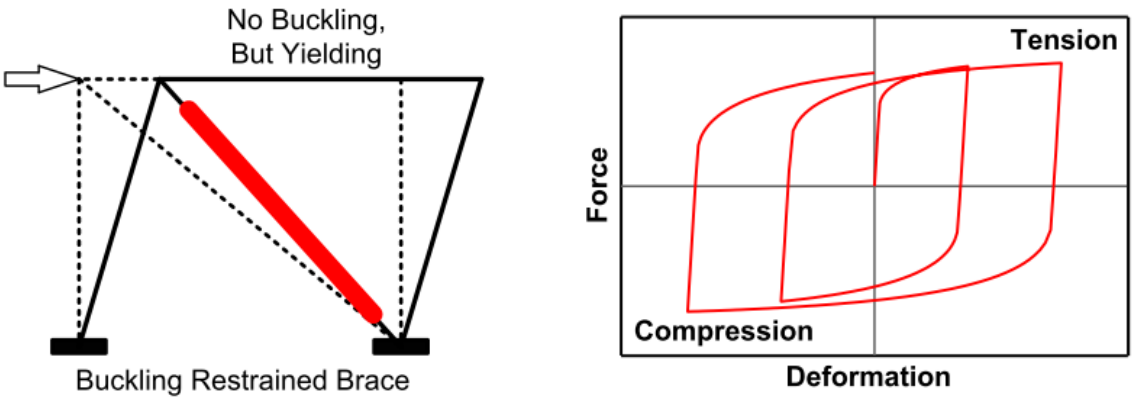

Figure 2.1-2: Buckling restrained brace behaviour (Lin et al. 2012)

There are many different types and configurations of BRBs. The most common BRB consists of a steel core section which is coated with an unbonding layer and surrounded by a restraining medium such as concrete or grout. A steel tube confines the restraining medium and also provides additional restraint. Together, the steel tube and restraining medium are often referred to as the restrainer. Some all-steel BRBs have also been developed that do not require concrete or grout in the restrainer (Ma et al. 2008; Tsai et al. 2008). The unbonding layer ensures that the steel core can yield in compression or tension without engaging the restraining medium and behaving as a composite section. The result is a brace that has axial properties dependent on the steel core and buckling properties dependent on the restrainer.

The steel core consists of different segments, as seen in Figure 2.1-3. The yielding segment is fully restrained and is responsible for the energy dissipation during loading. The non-yielding segment of the steel core is wider to ensure stability at the ends of the BRB casing.

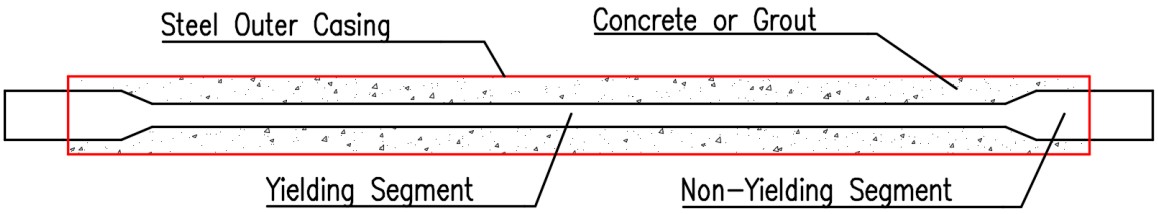

Figure 2.1-3: Segments of buckling restrained brace

The earliest form of BRB was developed and tested by Wakabayashi et al. (1973) which consisted of a flat steel plate clamped between two reinforced precast concrete panels. The modern form of BRBs with a steel plate, unbonding layer, concrete restraining medium and steel outer casing were developed in the 1980s by Nippon Steel in Japan (Watanabe et al. 1988). These designs were patented as unbonded braces. Further research and development on BRBs have been performed in Japan, the United States, India, and Taiwan (Uang et al. 2004).

BRBs are connected to the surrounding frame through gusset plate connections. The BRB can either be welded, pinned, or bolted to the gusset plate. Bolted connections are often preferred due to their ease of on-site installation during construction. This thesis explicitly considers bolted gusset plate connections, although the findings may apply to other connection types. Gusset plates in BRB frames will experience higher compressive loading than gusset plates in concentrically braced frames as the brace is restrained from buckling.

2.2 Gusset Plate Behaviour

2.2.1 Experimentally Tested Gusset Plates

The following papers investigated experimentally tested gusset plates that did not exhibit the sway buckling failure observed in BRB frames. Nonetheless, it is important to review the experiments as they form the basis of Chapter 5, where a number of experimentally tested gusset plates were modelled in finite element software and then had their boundary conditions modified to consider sway buckling. Some of the papers also form the foundation for which the gusset plate design methods have been formulated. Additionally, trends such as the effect of gusset plate thickness on buckling capacity can be observed.

The mode shape and the buckling capacity of the buckled gusset plates are dependent on the boundary conditions of the gusset plate. The gusset plate boundary conditions and their buckling mode shapes that have been considered in this chapter can be seen in Figure 2.2-1.The boundary conditions of interest to this thesis are (a) fixed-fixed, (b) fixed-roller, and (c) fixed-free boundary conditions.

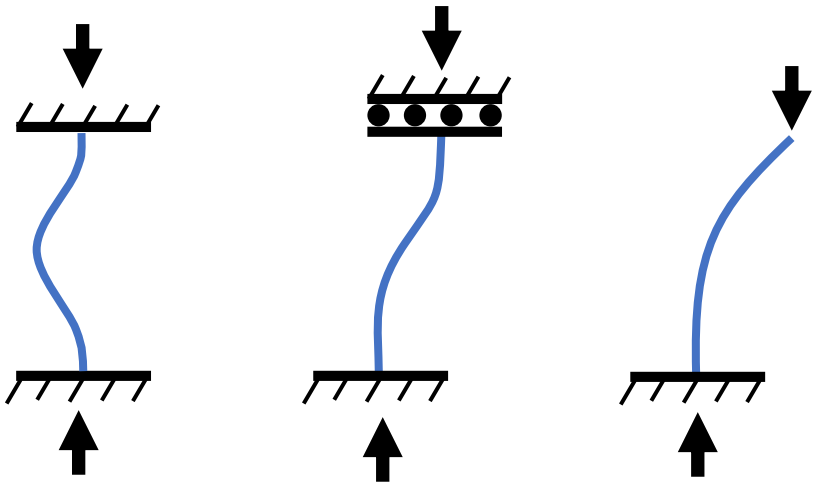

Boundary Condition	(a) Fixed - Fixed	(b) Fixed - Roller	(c) Fixed - Free
Theoretical K	0.5	1.0	2.0
NZS 3404 Design K	0.7	1.2	2.2

Figure 2.2-1: Considered boundary conditions with their column buckling mode shape and effective length factor values

2.2.1.1 Whitmore (1952)

Whitmore (1952) performed experiments on two connected gusset plates designed for a Warren truss joint to investigate stress distributions. The gusset plates tested were made from aluminium at ¼ scale and used a mixture of tight fitting bolts and pins to simulate rivets for connecting the brace to the gusset plate. Thirty strain gauges were attached to the gusset plate to monitor stress distribution as the gusset plates were loaded. One gusset plate was loaded in tension and the other in compression to simulate a typically loaded truss joint.

The Whitmore method was developed by Whitmore (1952) to determine if the maximum stress observed in the experiment by the strain gauges was similar to the maximum stress calculated by dividing the observed yield force by the Whitmore effective width and gusset plate thickness. A maximum stress of 4310 psi in the tension gusset plate and 4760 psi in compression gusset plate was calculated. The strain gauges determined a maximum normal stress of about 4000 psi in tension and 3500 psi in compression. The Whitmore method over predicted maximum stresses by approximately 8 % in tension and 36 % in compression, indicating the method was conservative.

However, stresses were not measured at the rivet holes, where stress concentration is likely to be higher. The paper concluded that the Whitmore method was likely to be less conservative in reality, but still a reasonable assumption of the maximum stress in a gusset plate.

It is unclear how the outcomes of the experiment would be different if a full-size gusset plate with steel instead of aluminium were used. It was considered that the high strength aluminium alloy possessed similar properties to structural steel. It was also believed that, despite the size reduction, the stresses would be representative of a full-size model.

A detailed explanation of the Whitmore method can be found in Section 2.4.1.

2.2.1.2 Hu and Cheng (1987)

A structural engineering report by Hu and Cheng (1987) detailed 14 experimental tests of six gusset plate connections in compression. The objectives of the report included providing experimental data for a range of design parameters, evaluating design methods available at the time and comparing test results with finite element models. The scope was limited to single gusset plate connections connecting a diagonal brace to a steel frame and the variables investigated were plate thickness, size, boundary conditions, and eccentricity. It was assumed all plates would fail by buckling elastically.

Two plate sizes of 850 mm by 550 mm and 850 mm by 700 mm were tested with two plate thicknesses at 6.70 mm and 3.11 mm thick. Single plate 13 mm splice plates were bolted to the gusset plate on each side to attach each gusset plate to the bracing member. Additionally, both plate sizes were tested at 6.70 mm thickness with only one 8.10 mm splice plate to evaluate an eccentrically loaded connection. The gusset plates were all tested for two separate boundary conditions, fixed-fixed, where both the bracing member and the test frame were fixed rotationally and laterally, and fixed-roller, where the test frame was free to translate out-of-plane by sitting on rollers. Figure 2.2-2 and Figure 2.2-3 show the experimental set-up.

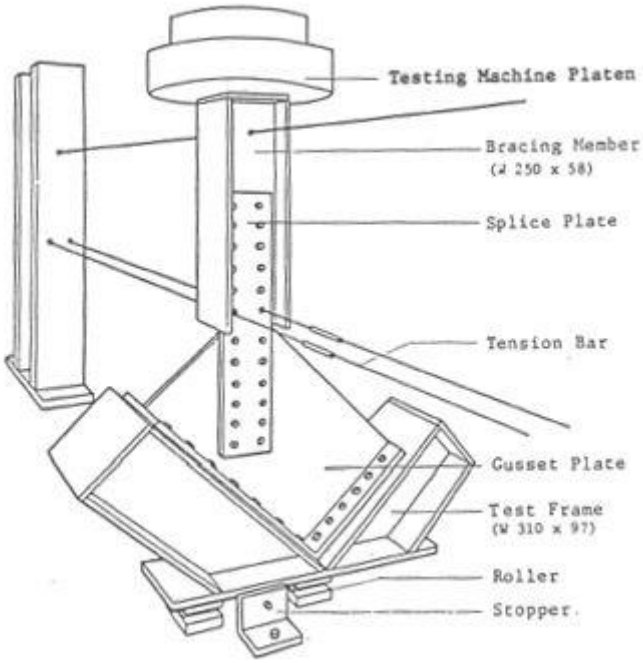

Figure 2.2-2: Experimental test schematic (Hu and Cheng 1987)

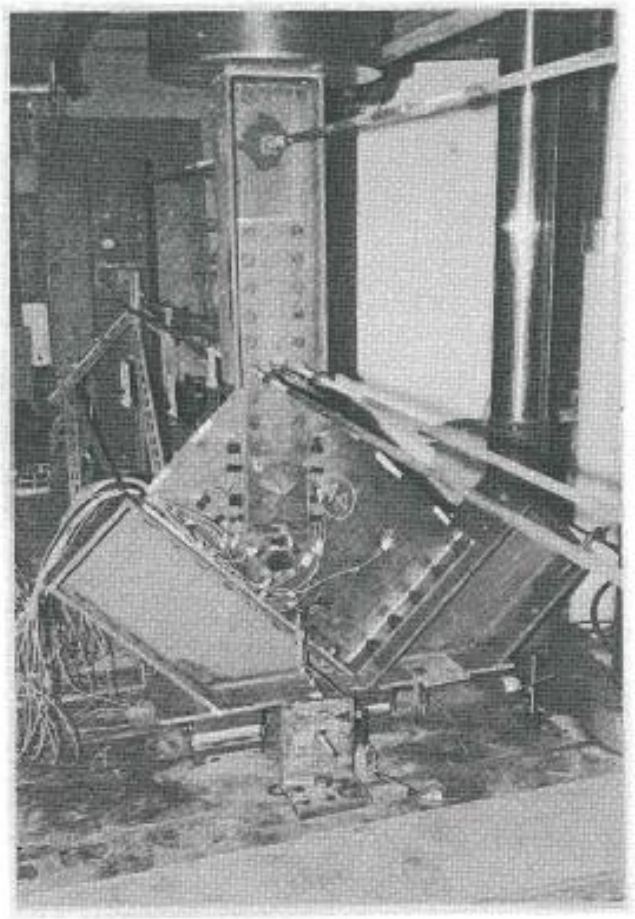

Figure 2.2-3: Experimental test photograph (Hu and Cheng 1987)

The results of the experiment were compared with the Whitmore method and an eigenvalue analysis of finite element models of each gusset plate. The paper shows that the Whitmore method significantly overestimated the gusset plate capacity. This overestimation was expected as the gusset plates buckled elastically at a lower compressive force than required for yielding to occur. The eigenvalue analysis was considered reasonably accurate for some gusset plates but was highly conservative in some cases and non-conservative in other cases.

Hu and Cheng (1987) show that increasing the stiffness of the splice plate would result in an increase in buckling capacity of the gusset plate. A recommendation of a flat splice plate two to four times the thickness of the gusset plate was made. This recommendation is unlikely to be a significant factor in gusset plate sway buckling in BRB frames as most splice plates have a rib plate in the centre that increases their flexural stiffness considerably.

It is important to note that the tension bars used to restrain rotational movement at the end of the gusset plate may be over constraining the specimen compared to gusset plates in braced frames. Additionally, no consideration was made to the frictional resistance of the rollers used in the experiment. With a large downward load applied, it may be possible that lateral translation was partially restrained by frictional forces and so true fixed-roller boundary conditions would not be achieved.

2.2.1.3 Gross and Cheok (1988)

Gross and Cheok (1988) tested three diagonally braced steel sub-assemblages to observe the compressive behaviour of gusset plates. The objectives of these tests were to determine the influence of framing members on (a) connection behaviour, (b) the effect of connection eccentricity, and (c) the validity of the AISC LRFD specification (1986) and equations by Richard (1986) used to size the gusset plate edge lengths. The experiment considered one sub-assemblage where the gusset plate line of action was concentric with the beam-column working point and one where the line of action was eccentric. A sub-assemblage was also tested where the column was orientated so that the gusset plate connected in the weak-axis direction.

The experimental test set-up is shown in Figure 2.2-4, where the upper gusset plate attached to the beam was the focus of the experiment. The gusset plate size was 584 mm by 279 mm with a thickness of 6.35 mm. The connected beam, braces and column were pinned at the ends, simulating the centre points of each frame member in a complete braced frame. It is possible that this test set-up may have resulted in lower buckling capacities than gusset plates that have been tested directly due to any frame forces acting on the gusset plate.

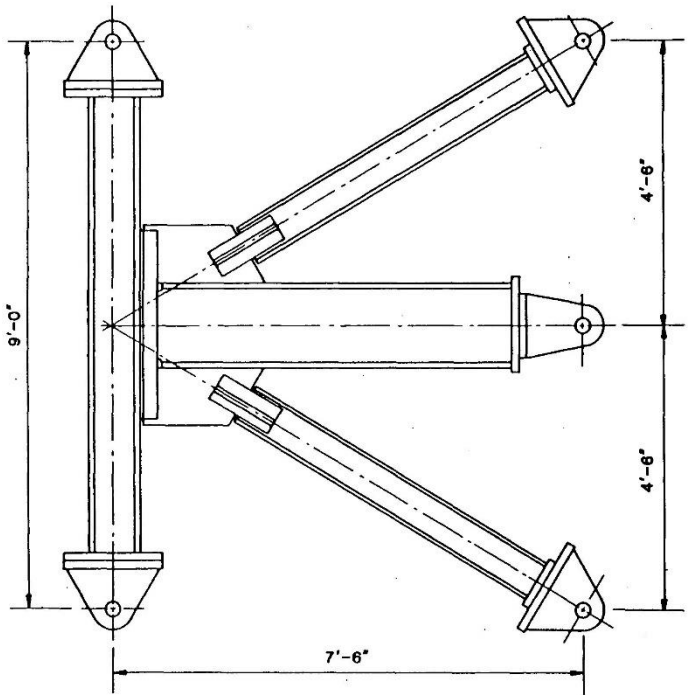

Figure 2.2-4: Experimental test schematic (Gross and Cheok 1988)

Test results for Specimen No. 1 found failure by bolt slip at the splice plate at 400 kN and then compressive buckling at 515 kN. It was calculated by the paper that the nominal buckling capacity was 320 kN using the Thornton method as prescribed in the AISC LFRD specification (1986), considering the average Thornton length. The paper also considered an effective length factor of $K = 0.5$ instead of 0.65 on the assumption that fixed-fixed boundary conditions are closely approximated in the experiment. Based on these results, the Thornton method was conservative by a factor of 1.6 for this experiment. Had an effective length factor of 0.65 been used, the Thornton method would be conservative by a factor of 1.9.

It is unclear if the bolt slip at the splice plate resulted in a reduced buckling capacity of the gusset plate.

2.2.1.4 Yamamoto et al. (1985)

Yamamoto et al. (1985) tested eight gusset plate specimens for Warren truss joints to determine the maximum load carrying capacity. The paper found that local buckling strength was the critical failure mechanism after yielding occurred for a range of material strengths and gusset plate thicknesses. The buckling load was determined as the point at which strain bifurcation occurs due to bending rather than the ultimate capacity of the specimen like most experiments. A buckled example of the gusset plate tested can be seen in Figure 2.2-5.

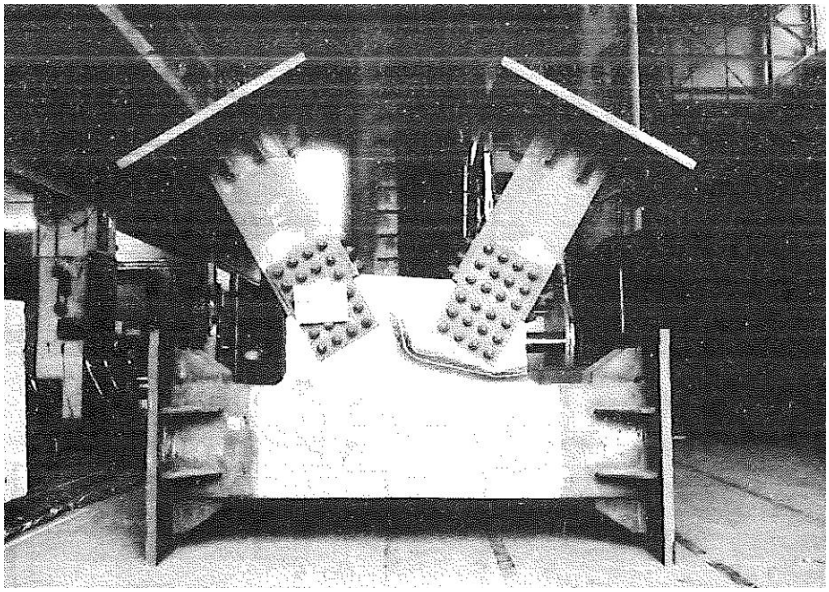

Figure 2.2-5: Buckled gusset plate truss joint (Yamamoto et al. 1985)

The paper presented a method for calculating buckling capacity using a right-angled triangular model of a gusset plate with the horizontal side considered simply supported, the vertical side free and the hypotenuse dependent on the appropriate boundary conditions of the gusset-brace connection. A stiffness matrix was then developed for the triangular model, and the eigenvalue was calculated. From the experimental data, buckling constants were developed for each boundary condition case. This method was limited to Warren truss joint gusset plates and required safety factors. It will not be considered as a potential buckling capacity method for gusset plates in BRB frames.

2.2.1.5 Yam and Cheng (1993)

Yam and Cheng (1993) experimentally tested 19 gusset plates to better understand their compressive behaviour and ultimate strength. Several parameters were investigated including thickness, size, and brace angle. The gusset plates mostly failed by sway failure with $K = 1.0$ mode shape as a result of the support frame sitting on rollers. The objectives of the study were to examine inelastic and elastic gusset behaviour, evaluate gusset plate parameters, compare results to current design methods, and find areas that require further investigation. The study also looked at eccentrically connected gusset plates and gusset plates with moments imposed on the attached beam and column.

Figure 2.2-6 shows the experimental set up for gusset plates with a brace attachment angle of 45 degrees. An additional experimental set-up, shown in Figure 2.2-7, was used for gusset plates with a 30-degree attachment angle as well as gusset plate tests with moments

imposed on the beam and column by the use of hydraulically tensioned rods. Rollers were used to consider any out-of-plane translation of the brace during buckling. Due to experimental testing limitations, the supporting frame was allowed to translate out-of-plane instead of the brace. The position of the rollers at the end of either the supporting frame or the brace should result in the same gusset plate buckling capacity.

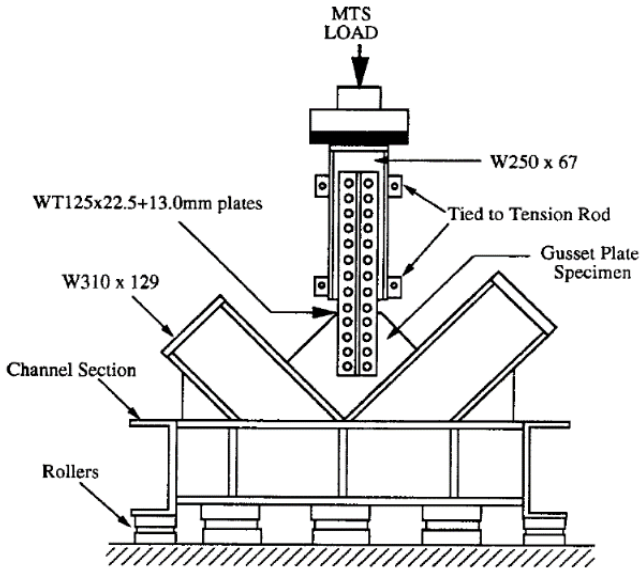

Figure 2.2-6: Experimental test schematic for 45° brace angle gusset plates (Yam and Cheng 1993)

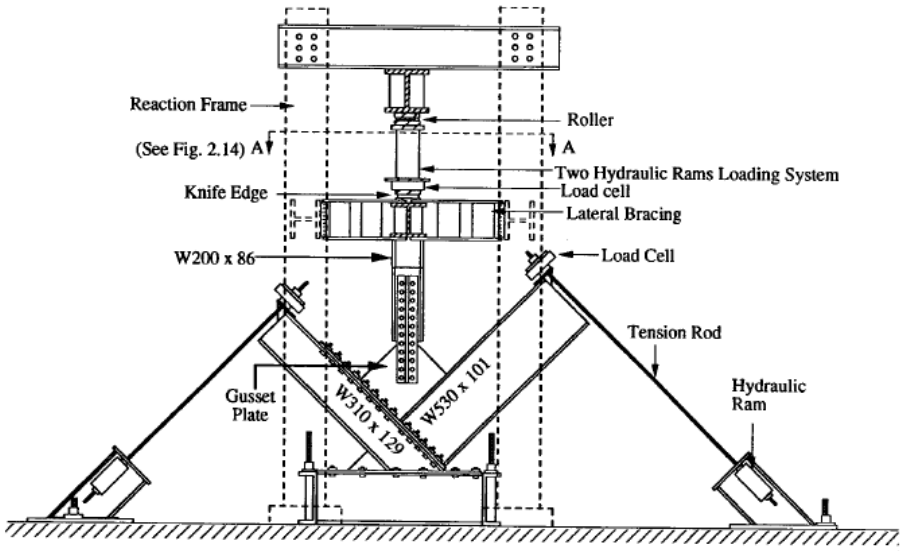

Figure 2.2-7: Experimental test schematic for 30° brace angle gusset plates and 45° gusset plates with moment imposed on attached beam and column (Yam and Cheng 1993)

Yam and Cheng (1993) compared the gusset plate ultimate compressive load to both the Whitmore method and the Thornton method. They considered the Thornton method with an average Thornton length and $K = 0.65$. This effective length factor was lower than the true

experimental boundary conditions corresponding to $K = 1.0$. However, the paper shows that the Thornton method conservatively predicted buckling capacity for all tested gusset plates except those eccentrically loaded. The paper also shows that the Whitmore method was conservative for most plates.

The paper shows that the additional beam and column moment did not affect the ultimate compressive capacity significantly. The ultimate load of eccentrically spliced gusset plates was significantly less than concentrically loaded gusset plates due to the low flexural stiffness provided by the single splice and the imposed moment from the eccentricity.

Yam and Cheng (2002) revisited the testing from Yam and Cheng (1993) and made the following conclusions:

- The failure mode of the gusset plates was sway buckling (as a result of the rollers allowing $K = 1.0$ buckling mode shape).
- Increasing gusset plate thickness resulted in an almost linearly proportional increase in buckling capacity.
- Buckling capacity of gusset plates with a 30° brace angle was slightly less than gusset plates with a 45° brace angle.

The finding that gusset plate thickness is almost linearly proportional to buckling capacity is significant because the Thornton method considers a cubic proportional relationship between gusset plate thickness and elastic buckling capacity. The relationship between gusset plate thickness and buckling capacity for inelastic buckling behaviour is also non-linear.

2.2.1.6 Rabinovitch and Cheng (1993)

Rabinovitch and Cheng (1993) investigated the cyclic behaviour of steel gusset plate connections. The experiment considered five gusset plate tests in a concentrically braced frame joint tested under cyclic loading. The design parameters considered were changing gusset plate thickness, adding free-edge stiffeners, and changing gusset plate geometry. The objectives of the experiment were to consider the effect of changing design parameters, to determine if ultimate capacity was affected by cyclic loading, and to determine the feasibility of using gusset plates as the primary energy absorption method in a concentrically braced frame.

Free-edge stiffeners are flat plates welded perpendicular to the free edge of the gusset plate. Their purpose is to increase the overall stiffness of the gusset plate, which increases gusset plate buckling capacity. There is currently no available design method to assess the increase in buckling capacity provided by free-edge stiffeners.

The experimental set-up can be seen in Figure 2.2-8, where the brace is held in place, and the distributing beam is laterally displaced by the load cells. Like Yam and Cheng (1993), the experimental test frame had rollers, allowing $K = 1.0$ sway failure mode shape. No calculations have been provided to determine if the deflections associated with the distributing beam during the testing influenced results. The testing cycles for the gusset plates began with two elastic cycles of tension and compression at 10 % and 50 % of the expected tensile yield capacity based on the Whitmore load. The gusset plates were then subjected to steadily increasing cycles from 100 % of the expected tensile yield capacity until failure. After the gusset plates had been observed to fail during compression, the gusset plates were loaded cyclically between zero compressive load and tensile loading until tensile rupture occurred.

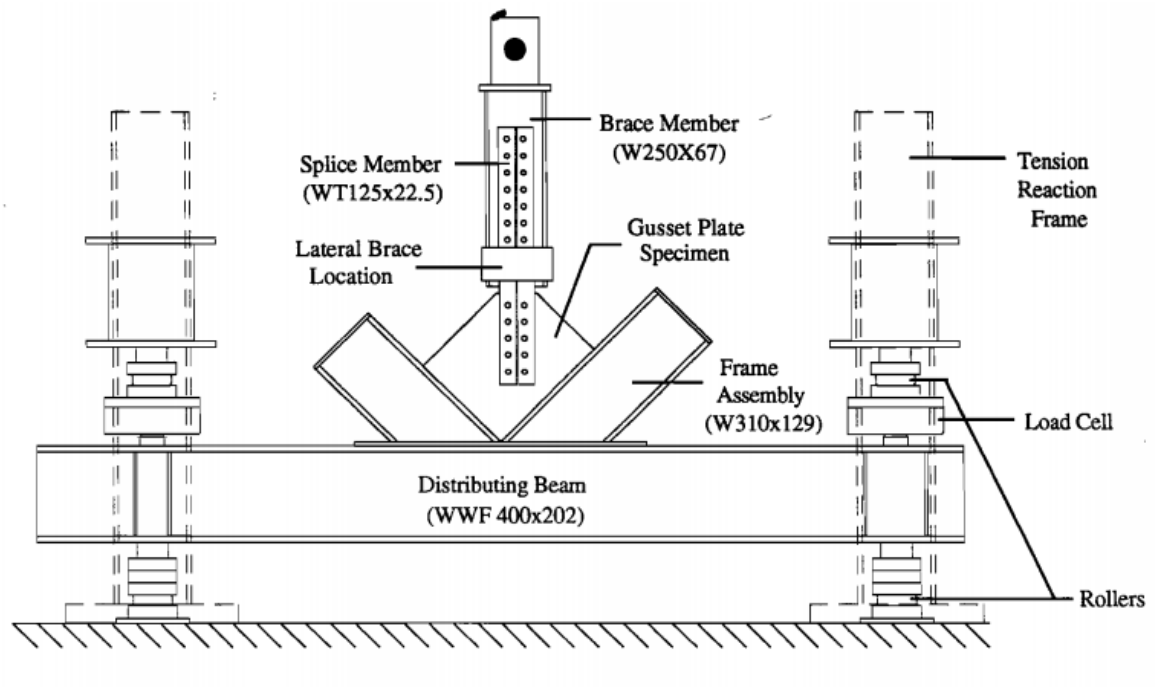

Figure 2.2-8: Experimental test schematic (Rabinovitch and Cheng 1993)

From the experimental testing, the following conclusions were made:

- Ultimate tensile and compressive capacity of the unstiffened gusset plates were roughly proportional to the thickness of each specimen.
- Free-edge stiffeners significantly improved the energy absorption behaviour and buckling capacity of the gusset plates tested. The effects of the free-edge stiffeners on buckling capacity of the gusset plates is dependent on the size and stiffness of the free-edge stiffener used.
- Unstiffened gusset plates have a sudden drop in compressive capacity but stiffened gusset plates have a stable post-buckling response with a gradual decrease in compressive capacity.
- The Thornton method conservatively estimates the buckling capacity of the gusset plates. The method cannot account for free-edge stiffeners.

These findings indicate that the addition of free-edge stiffeners to a gusset plate increases buckling capacity and results in a more stable failure mechanism if buckling were still to occur. For BRB frames, this behaviour would be beneficial.

2.2.1.7 Naghipour et al. (2013)

To investigate gusset plate behaviour in BRB frames, Naghipour et al. (2013) performed an analytical investigation of gusset plate compressive strength by finite element modelling. The finite element model was verified by a single full-scale experiment. The analytical investigation compares a number of parameters including gusset plate thickness, splice plate length, and gusset plate width to length ratio. From this analysis, a design method was recommended that follows the inelastic plate buckling method (Sheng et al. 2002). This method was modified slightly to consider the Whitmore width, instead of the bending line length used by Sheng et al. (2002). From the finite element models, the constant k_g was determined to allow a designer to determine buckling capacity through the use of charts and the inelastic buckling formula proposed. The use of free-edge stiffeners was also investigated.

The experimentally tested gusset plate had dimensions of 500 mm by 500 mm and a thickness of 8 mm. The plate was bolted to a supporting frame as well as a short, stocky I-beam brace, as shown in Figure 2.2-9. It was determined that the I-beam would behave sufficiently close to a BRB due to its slenderness ratio. The gusset plate buckled at 403 kN and the finite element model buckled at 416 kN, which was in good agreement.

Figure 2.2-9: Experimental test photograph (Naghipour et al. 2013)

Figure 2.2-10: Buckled gusset plate (Naghipour et al. 2013)

It can be seen in Figure 2.2-10 that the gusset plate has buckled locally and the I-beam has deformed out-of-plane, but a hinge has not formed.

The paper found the following conclusions:

- A simplified finite element model is sufficient to assess the ultimate load and buckling behaviour of an experimentally tested gusset plate.
- When gusset plate thickness is increased, buckling behaviour will change from elastic to inelastic.
- Higher buckling capacity can be achieved by increasing the depth of the splice plate section into the gusset plate.
- The addition of free-edge stiffeners increased gusset plate buckling capacity.

The paper only assessed gusset plates for local buckling failure, although acknowledgement of sway buckling failures in BRB frames was made in the literature review and was considered to be the primary reason for undertaking the research. By considering the BRB as an I-beam, the paper fails to account for a low rotational stiffness at the BRB end. Thus a plastic hinge is unable to form and allow the gusset plate to fail by sway. It is likely that the design method proposed by the paper would be inappropriate for gusset plate buckling in BRB frames.

The findings of this paper are in good agreement with findings of other papers in this literature review. It is clear from the assumptions made by the paper in designing the experiment that the findings can only be considered in the context of gusset plate local buckling and not sway buckling.

2.2.2 Finite Element Modelling

2.2.2.1 Cheng et al. (1994)

Cheng et al. (1994) developed finite element models based on gusset plates tested by Hu and Cheng (1987). The paper shows that the finite element models gave reasonable predictions of buckling capacity of the experimentally tested gusset plates, although these predictions ranged from 0.73 to 2.40 times the experimental capacity. A parametric study was then performed to investigate a number of parameters.

Cheng et al. (1994) show that increasing splice plate thickness increases buckling capacity of the gusset plate until a critical thickness where no further increase in buckling capacity is observed. Increasing splice plate length also resulted in an increase in buckling capacity.

Increasing gusset plate thickness was found to have an almost linear relationship to increasing buckling capacity. This finding matches findings by Yam and Cheng (2002) and indicates that the Thornton method does not accurately consider gusset plate thickness.

Fixed-pinned boundary conditions were investigated by removing the rotational restraint of the brace to the gusset plate. This change in boundary condition was found to have a negligible effect on buckling capacity. This would indicate that a hinge forming at a BRB end will not significantly reduce buckling capacity of the gusset plate if the BRB end is restrained from out-of-plane displacement.

Fixed -free boundary conditions were investigated by removing the rotational restraint of the brace to the gusset plate for the fixed-roller boundary condition case. This resulted in a significant reduction in buckling capacity. In one finite element model, the paper shows that the buckling capacity reduced from 144 kN to 14 kN, indicating a decrease in capacity by a factor of 10. However, most gusset plates had a decrease in buckling capacity by a factor of approximately 4.

This last conclusion is significant as the fixed-free boundary conditions result in an effective length factor equal to 2.0. This is the same effective length factor recommended by Tsai and Hsiao (2008) when designing gusset plates in BRB frames for sway buckling. The reduction in buckling capacity when changing from fixed-roller boundary conditions to fixed-free boundary conditions is a factor of 4 when considering elastic buckling. A decrease in buckling capacity by a factor of 10 was found in the finite element models analysed by Cheng et al. (1994). This indicates that the recommendation by Tsai and Hsiao (2008) may not

always be conservative when designing gusset plates considering fixed-free boundary conditions.

2.2.2.2 Sheng et al. (2002)

Sheng et al. (2002) performed a finite element model parametric study on gusset plate buckling capacity considering fixed-roller boundary conditions. Four gusset plate shapes were compared, as shown in Figure 2.2-11, to consider the effect of load dispersion angle. These gusset plates were then modified by increasing splice plate length, gusset plate thickness, and modifying rotational end restraint.

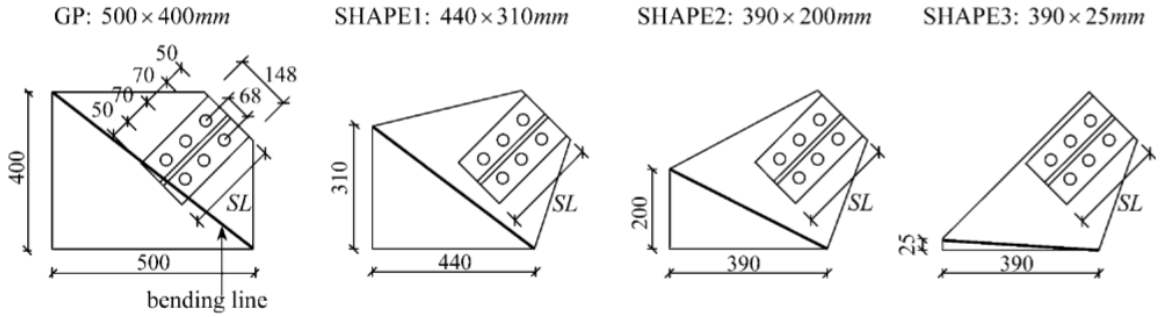

Figure 2.2-11: Gusset plate shapes used for finite element modelling (Sheng et al. 2002)

The following conclusions have been made from the parametric study:

- Buckling capacity can be reduced by modifying the gusset plate shape without altering the Whitmore width or the Thornton length.
- Increasing splice plate length into the gusset plate can have a significant increase in buckling capacity.
- SHAPE2 can achieve similar buckling capacity to GP if the splice plate length is increased. This is considered preferable as it reduces the size of the gusset plate connection.
- Gusset plates that are welded to the splice plate have 10 to 20 % higher buckling capacity than bolted splice plates. Welds also reduced stress concentrations.
- If the connecting brace member is unable to provide any rotational restraint at the end connecting to the gusset plate, buckling capacity is significantly reduced for all gusset plates.
- The addition of centreline stiffeners increases buckling capacity more than the addition of free-edge stiffeners.

The finding that buckling capacity is significantly reduced when the brace member is unable to provide rotational restraint at the end matches the behaviour of BRB frames that have buckled when a plastic hinge has formed at the BRB end.

2.2.2.3 Walbridge et al. (2005)

Walbridge et al. (2005) modelled gusset plates from Rabinovitch and Cheng (1993) and Yam and Cheng (1993) in finite element software. The models considered the effects of inelastic materials, large displacements and initial imperfections. The paper observed that the finite element models were in good agreement with the experimental gusset plates for both monotonic and cyclic loading.

A parametric study on the finite element models was then performed for cyclic loading. The paper showed that:

- The sequence of loading did not have a significant effect on the cyclic behaviour of the gusset plate.
- Local buckling of the gusset plate resulted in a small capacity reduction and stable cyclic behaviour.
- Gusset plate buckling may be preferable to concentric brace buckling in concentrically braced frames.
- Thicker gusset plates show fuller hysteresis loops for concentric braces.

These findings suggest that gusset plate buckling may be beneficial as an energy dissipation mechanism in concentrically braced frames. These findings will not apply to BRB frames as it is essential that no buckling occurs in any BRB frame element to maintain a stable hysteresis loop.

2.2.2.4 Palmer et al. (2016)

Palmer et al. (2016) used finite element modelling to simulate a BRB frame accurately from earlier experimental testing by Palmer (2012). A parametric study was performed with approximately 50 models to analyse the effects of gusset plate thickness, gusset plate taper, free-edge stiffeners, beam and column web reinforcement, and BRB strength and stiffness.

The paper observed that reducing gusset plate thickness reduced the beam and column demands at the gusset plate interface. This benefit is an interesting result as it runs counter to the idea that gusset plate thickness should be increased as a result of gusset plate buckling. A designer must, therefore, determine their primary motivation for sizing the gusset plate thickness and then mitigate the resulting adverse effect. Adding beam and column web reinforcement was found to be an alternative to reducing gusset plate thickness, as the web reinforcement reduced demands and local deformation.

It was also found that using thinner gusset plates with free-edge stiffeners reduced damage to the gusset plate, but increased the damage to the beam and column at a level that

was approximate to using a thicker gusset plate. This finding is in contrast to other research such as Chou and Liu (2012) which suggests that free-edge stiffeners are an effective means of reducing stresses that lead to damage in the beam and column.

Finally, the paper shows that designing gusset plate welds for the full strength of the gusset plate will significantly reduce local strain demand in the connection. This will result in reducing weld tearing and fracture, as seen in Mahin et al. (2004) and Christopulos (2005). It is current practice to only design gusset plate welds for the maximum BRB compressive load.

2.2.3 Other Papers Considering Gusset Plate Behaviour

2.2.3.1 Dowswell (2006)

Dowswell (2006) compared 59 experimental specimens and 56 finite element models to the expected buckling capacity using the Thornton method. Gusset plates were categorised into five different types, as shown in Figure 2.2-12. The paper observed that the Thornton method was significantly conservative in estimating local buckling capacity for many gusset plates.

Dowswell proposed updated effective length factors for each of the different gusset plate configurations. It was suggested that compact gusset plates need not consider the possibility of local buckling failure due to their stiffness. For non-compact gusset plates, however, the effective length factor was increased to 1.0, indicating that the Thornton method is sometimes not conservative using $K = 0.65$. It should be noted that one gusset plate from Hu and Cheng (1987) was still found not to be conservatively predicted when using $K = 1.0$.

Extended corner, single-brace and chevron type gusset plates had their effective length factors changed to 0.6, 0.7, and 0.75 respectively. The Thornton length was also recommended to be taken as the middle length, L_1, instead of the average Thornton length.

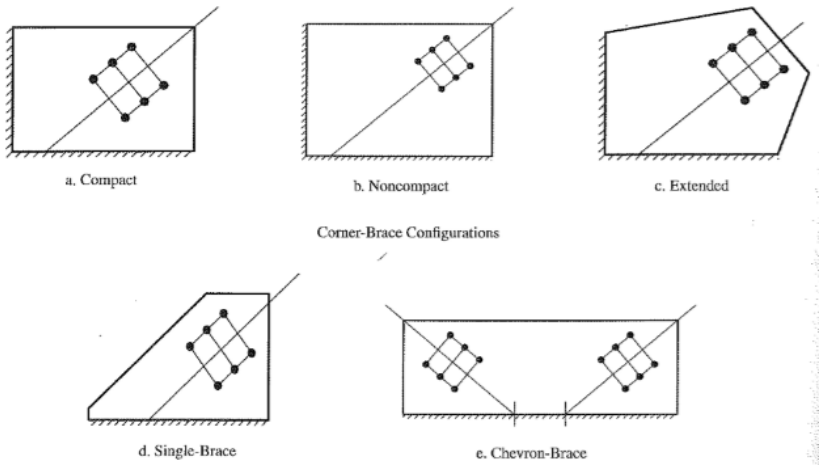

Figure 2.2-12: Different types of gusset plate configurations (Dowswell 2006)

This paper does not consider sway buckling failure observed in BRB frames, but it does highlight the inaccuracy of the Thornton method for many specimens. As such, any method to prevent sway buckling that is based on the Thornton method such as that proposed by Tsai and Hsiao (2008) must be considered carefully to ensure that it is conservative for all cases.

2.2.3.2 Wigle and Fahnestock (2010)

Wigle and Fahnestock (2010) investigated the concept that BRB frames are limited in performance due to connection failure modes. A calibrated finite element model based on testing by Fahnestock et al. (2007) was used to study BRB frame connection behaviour. Twelve different connection configurations were considered, and it was shown that connection configuration could have a significant impact on global system response and connection demands. The models considered bolted, welded, and pinned connections between the BRB and gusset plates. Having a splice in the connection beam at the end of the gusset plate was also considered. This feature acted like a hinge and reduced stress in the connection region.

The following conclusions were made by the paper:

- BRB force and deformation behaviour was not significantly affected by altering the connection configuration.
- Storey shear and drift behaviour was largely unaffected by connection type, but peak storey shear was reduced by 30 % when a spliced beam is considered.
- Thinner gusset plates have larger stresses. However, they are more evenly distributed. Thicker gusset plates result in a diagonal zone of concentrated stress which can lead to yielding.
- If a gusset plate is too thick compared to adjacent members, localised plastic strain demands increase at the beam and column.
- Calculating stress distribution at the gusset plate edges considering only the force from the BRB is insufficient. Frame action forces must be considered.
- Using a beam with a connection splice will significantly reduce the distributed stress at the gusset plate edges due to frame action forces.

This paper suggests that thicker gusset plates may not always be beneficial to BRB frame performance. A thicker gusset plate can lead to concentrated stress zones that can cause yielding. They can also cause additional local plastic strain if the beam and column are not proportionally sized. Increasing the buckling capacity of gusset plates can be achieved by increasing gusset plate thickness. It may, therefore, be difficult for a designer to design a gusset plate that is strong enough to prevent sway buckling failure in a BRB frame and prevent localised plate yielding.

2.2.3.3 Chou and Liu (2012)

Chou and Liu (2012) developed a design method to consider frame action forces on the gusset plate. When the BRB is in tension, the beam-column joint closes, resulting in frame forces that push against the gusset plate. The beam-column joint opens when the BRB is in compression and the frame action forces pull on the gusset plate. This has been illustrated in Figure 2.2-13. At large inter-storey drifts, the magnitude of these forces can be greater than the force on the gusset plate due to the BRB.

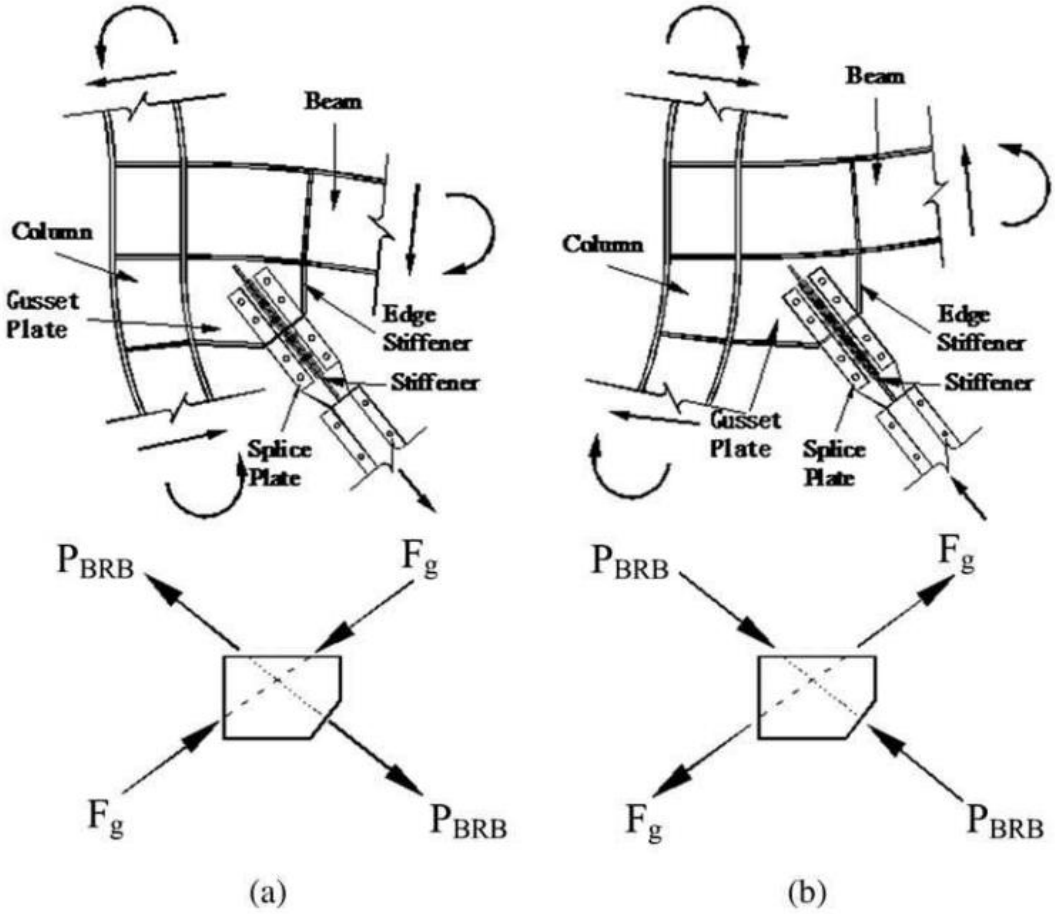

Figure 2.2-13: Effect of frame action forces on gusset plate for (a) joint closing, (b) joint opening (Chou and Liu 2012)

The stress profile along the gusset plate interface to the beam-column joint can be assumed to be triangular with the peak occurring at the end of the gusset plate connection to the beam or column. When the stress is large enough, the weld between the gusset plate and the beam-column joint can begin to tear out at this edge. This has been seen in a number of experimental tests where frame action forces have not been considered in the design of the gusset plate weld including tests by Christopulos (2005) and Mahin et al. (2004).

The design method presented by Chou and Liu (2012) assumes frame action forces behave as an equivalent strut across the gusset plate. The critical stress at the end of the gusset plate connection to the beam or column is also calculated.

The direct effect of frame action forces on the buckling capacity of a gusset plate has not been considered in research, and this will be explored in Chapter 4.

2.3 Gusset Plate Buckling in BRB Frames

Sway buckling failure of gusset plates in BRB frames has been observed in a number of experimental tests. In some cases, this failure was unexpected, and gusset plates were not the main focus of the experiment. It can be seen that gusset plates that have not been explicitly designed to prevent sway buckling failure can buckle at a much lower capacity than what the designer expected.

2.3.1 Tsai et al. (2002)

Tsai et al. (2002) tested an unsymmetrical "V" configuration BRB frame to verify connection design and details adopted in the Taipei County Administration Building. The test was a half scale, one bay, one storey frame, as shown in Figure 2.3-1. The frame was found to be suitable for the prescribed loads. However, when the frame was loaded to the prescribed cyclic inter-storey drift demand of up to 0.01 radians, buckling occurred. During the second cycle, the west brace buckled out-of-plane at the bottom beam joint near the brace with a hinge forming at the BRB end. When the load was reversed, the east brace also buckled at the lower beam joint, as shown in Figure 2.3-2.

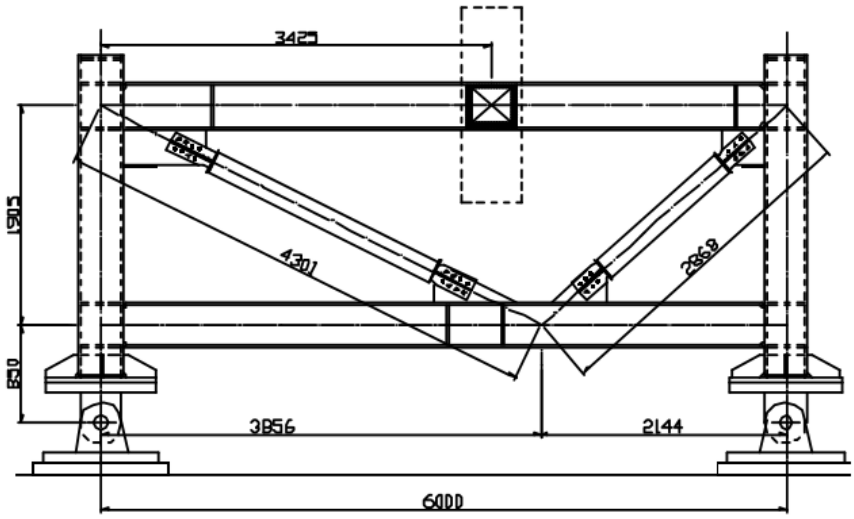

Figure 2.3-1: Experimental test schematic for single bay "V" configuration BRB frame test (Tsai et al. 2002)

Figure 2.3-2: Sway buckling of east brace, showing hinge at BRB end (Tsai et al. 2002)

The paper does not explicitly consider the role of the gusset plate on the buckling of the system but does introduce the working point method (see Section 2.4.7) as an explanation for the buckling. The method calculated a buckling capacity about 1.5 times the brace yield strength. This was considered to be a low critical strength and that the long connection joint length contributed to the buckling failure.

At the beam joint, there is usually one central gusset plate that connects both BRBs in a chevron configuration frame. For this experiment, two separate gusset plates were used, each with a central stiffener that extended to the beam joint to increase the flexural stiffness. It is likely that these gusset plates have a lower flexural stiffness than a central gusset plate as they were only restrained by one edge. Overall, the gusset plate flexural stiffness was not sufficient to prevent sway buckling. It is possible that the beam joint also contributed to the buckling failure with a low rotational stiffness. However, no information has been presented in the paper to indicate if the beam joint deflected after buckling.

2.3.2 Tsai et al. (2004)

Tsai et al. (2004), Chen et al. (2004), and Lin et al. (2004) tested a full-scale 3-storey 3-bay BRB frame with concrete-filled tube columns under scaled pseudo-dynamic earthquake loads. The BRBs were in chevron configuration, as shown in Figure 2.3-3. The purpose of the testing was to investigate the behaviour of a full-scale BRB frame under scaled earthquake ground motions. The tests were also used to confirm that peak storey drifts of the frame agreed with target design limits.

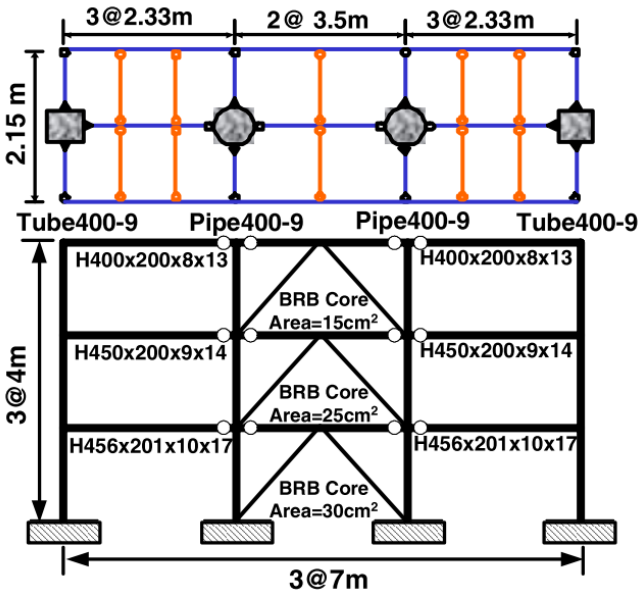

Figure 2.3-3: Experimental test schematic for 3-storey 3-bay BRB frame (Lin et al. 2004)

During Test No. 1, at the bottom storey, a hinge formed at the BRB end and the gusset plate buckled at a load of 805 kN, as shown in Figure 2.3-4. The test was then stopped and free-edge stiffeners were added to all of the top gusset plates and the web of the supporting beam. Rib plates were also added at the centre of the supporting beam to increase beam rotational stiffness, as shown in Figure 2.3-5. The buckled gusset plate and the hinged BRB were straightened before the next test. The failure occurred under loading of a scaled 50 % chance in a 50-year earthquake in Taiwan with a peak ground acceleration of 0.276 G.

Figure 2.3-4: Top gusset plate sway buckling failure at first storey chevron BRB frame (Chen et al. 2004)

Figure 2.3-5: Retrofitted connection region with free-edge stiffeners on gusset plates and rib stiffeners on beam (Chen et al. 2004)

Test No. 4 used the strongest earthquake loading with a scaled 2 % in 50-year Taiwan earthquake with a peak ground acceleration of 0.622 G. Cracking was observed at the concrete foundation near the gusset plate on the ground floor at the south BRB end. It was also noted that the north BRB on the ground floor was bending at the top gusset plate end, the same place which had buckled in Test No. 1. Free-edge stiffeners were then added to the bottom gusset plates on the first floor to prevent further out-of-plane deformation.

Test No. 7 involved cyclic increasing of storey drifts from 0.01 to 0.0375 radian. At the fourth 0.02 radian cycle, the third storey bottom gusset plate buckled by sway, as shown in Figure 2.3-6. This occurred at a load of 755 kN. It is interesting to note that in this case, the hinge formed outside the BRB casing end.

Figure 2.3-6: Bottom gusset plate sway buckling failure at third storey chevron BRB frame (Chen et al. 2004)

Additionally, in Test No. 7, at the first 0.025 radian cycle, both top ends of the BRBs on the second floor fractured. It has been described that the gusset plate then buckled by sway

with the supporting beam also deforming laterally, as shown in Figure 2.3-7. This is a remarkable failure as it indicates that a gusset plate stiffened by free-edge stiffeners and a beam joint stiffened by rib stiffeners is still able to deform out-of-plane. Because of the fracture at the end of the BRB, it could be said that the BRB end behaved like a perfect pin, with rotational stiffness equal to zero. This suggests that only one single element in the BRB system needs to have sufficiently less stiffness than the other elements to result in sway buckling of the system. This failure mode could potentially be ignored as the fracture of the BRB is more significant.

Figure 2.3-7: Out-of-plane displacement of beam and connection after BRB end fracture (Chen et al. 2004; Christopulos 2005)

The second phase of testing was performed with new BRBs and stiffened gusset plates. No buckling failure of gusset plates occurred in in the three subsequent tests. Chen et al. (2004) found that welding free-edge stiffeners to the gusset plates were effective in preventing buckling.

Overall, the gusset plate failures were unexpected, and it was assumed that by designing the gusset plates with $K = 0.65$, no buckling would occur. Tsai et al. (2008) came to the conclusion that designing with $K = 2.0$ closely matched the experimental results (see Section 2.4.7 for more detail). However, instead of redesigning the gusset plates assuming $K = 2.0$ to ensure that buckling did not occur, all gusset plates were retrofitted with free-edge stiffeners to increase their stiffness.

This testing is one of the few chevron configuration frames that have been tested that show the gusset plate buckling instead of the beam.

2.3.3 Mahin et al. (2004)

Mahin et al. (2004) tested a single storey, 1-bay BRB frame in diagonal brace configuration under cyclic loading to investigate whether the hysteretic behaviour in uniaxial tested BRBs matches the hysteretic behaviour of BRBs in frames. How gusset plates perform in BRB frames under expected building drifts was also considered. The test schematic can be seen in Figure 2.3-8.

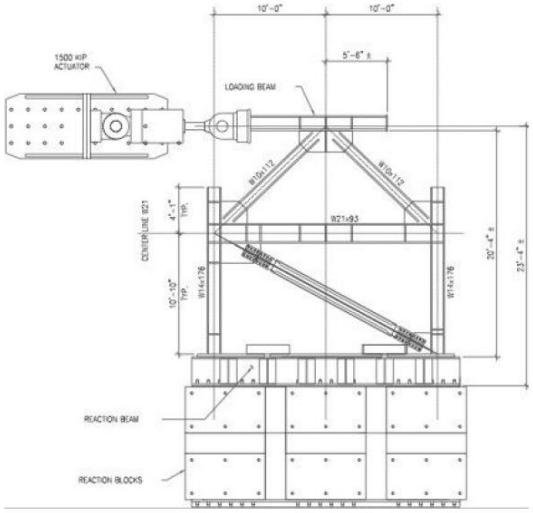

Figure 2.3-8: Experimental test schematic for diagonal configuration BRB frame (Mahin et al. 2004)

During the second test, the top gusset plate buckled while the BRB was in tension. This was an unexpected failure and occurred due to the result of frame pinching. When the BRB was in tension, the beam and column of the frame at the top gusset plate pinched inwards. The increased force on the gusset plate due to frame pinching was sufficient to buckle the gusset plate. Finite element modelling was performed to confirm the behaviour (Figure 2.3-9b). Weld cracking was also observed at the bottom of the top gusset plate welds to the column because of frame action forces.

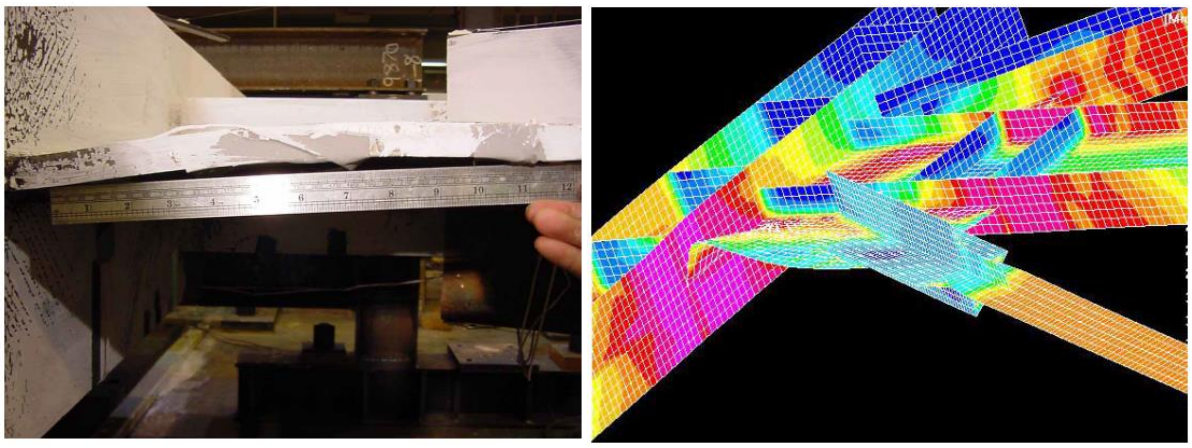

Figure 2.3-9: (a) Top gusset plate buckled under tension. (b) Finite element model showing tension buckling (Mahin et al. 2004)

Gusset plate buckling under tension is not currently a design consideration and requires further investigation. However, it will not be considered further in this thesis.

For the third test, a small free-edge stiffener was added to the bottom edge of the top gusset plate at the face of the column to reduce stresses and help prevent weld cracking. During the test, Mahin et al. found that at a cyclic loading of less than 1.7 % drift, the bottom flange of the beam, at the outside edge of the gusset plate, cracked across its entire width. A crack also formed 2 inches into the beam web. Because of this fracture in the beam, the gusset plate region lost torsional stability and buckled by sway with a hinge forming at the BRB end. This can be seen in Figure 2.3-10.

Figure 2.3-10: Buckling of gusset plate after beam fracture in BRB frame (Mahin et al. 2004)

The weld cracks and flange cracking that occurred in these tests were the result of increased stresses at the gusset plate tips due to frame pinching and pulling. This is commonly referred to as frame action effects (Chou and Liu 2012). The testing shows that the effects of frame action forces on the gusset plate connection can eventually lead to buckling failure of the system. It is currently unclear if frame action forces have a direct influence on buckling capacity, and this will be explored in Chapter 4.

2.3.4 Christopulos (2005)

Christopulos (2005) tested six BRB and gusset plate combinations inside a single storey, 1-bay horizontal frame in diagonal brace configuration, as seen in Figure 2.3-11. The gusset plate connections were modified in each test to observe the effect on the BRB frame. Sway buckling of the gusset plate and plastic hinging of the BRB end was found in all tests, as shown in Figure 2.3-12. Additionally, the sixth BRB test had an ultimate failure by weld fracture along the entire gusset plate weld connection to the beam and column, resulting in the gusset plate becoming detached from the frame, as seen in Figure 2.3-13.

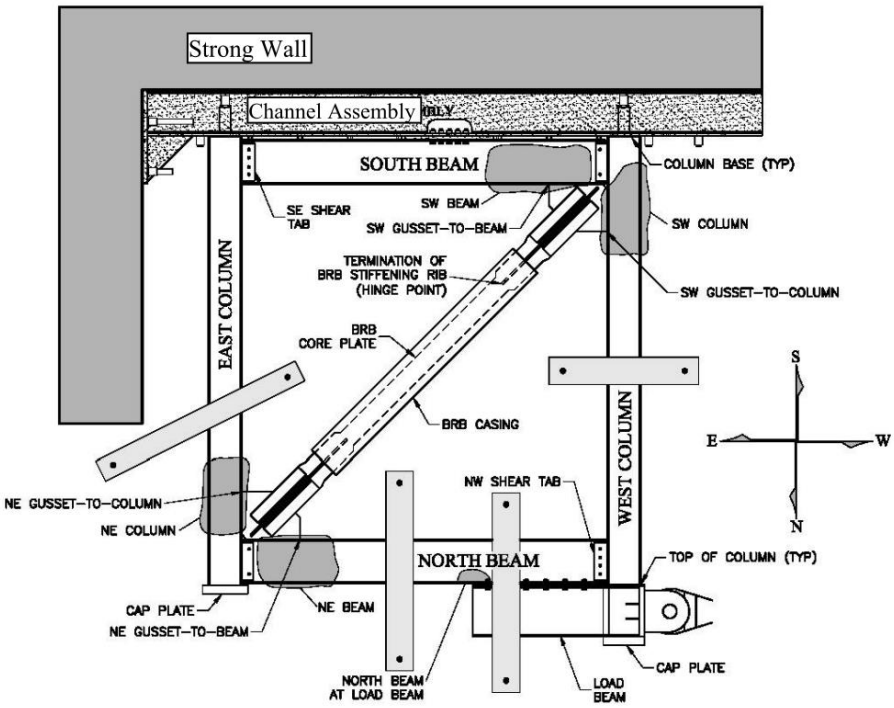

Figure 2.3-11: Experimental test schematic (Christopulos 2005)

Figure 2.3-12: Sway buckling failure of gusset plate (Christopulos 2005)

Figure 2.3-13: Weld fracture of gusset plate connection (Palmer et al. 2014)

Web yielding was also observed in each test despite current AISC web yielding equations suggesting that the expected forces in the web would not lead to yielding. Christopulos (2005) observed that the web shear forces were concentrated in a much shorter length than the gusset plate connection. Beam web buckling also occurred in most tests. Fracture of the beam flange was noted in the first BRB test; this was similar to testing done by Mahin et al. (2004).

The thesis shows that gusset plates that are tapered instead of square performed better with buckling of the beam webs occurring at larger drifts. The cause of this was believed to be due to a reduction in connection length resulting in less restriction to rotational deformation.

One test involved re-orientating the BRB so that the flat core was perpendicular to the gusset plate plane. This was done to see how much increasing the rotational resistance at the end of the BRB would improve overall performance. The thesis observed that the re-orientated BRB did not change the amount of damage in the BRB frame but did alter the location of the damage in some areas. Small amounts of hinging occurred against the weak axis, but the in-plane stiffness of the gusset plate prevented large deformations. Eventually, the BRB frame still failed out-of-plane with hinging occurring in the strong axis of the BRB. The hinge formed at a much slower rate than the BRBs orientated with the core parallel to the gusset plate plane causing the frame to undergo larger maximum drift and total energy dissipation.

This is an interesting finding as it again supports the idea that the end of a BRB has relatively low rotational stiffness, as buckling could occur even when the core plate was perpendicular to the gusset plate.

2.3.5 Koetaka et al. (2008)

Koetaka et al. (2008) tested a full-scale single storey, 1-bay BRB frame in inverted chevron configuration under cyclic loading to investigate varying beam rotational stiffness on buckling capacity. Lateral stiffeners were moved further from the beam centre in each test to reduce beam rotational stiffness. The paper shows that when lateral stiffeners are separated far enough apart, buckling occurred during compression and the out-of-plane displacement increased with each cycle. A test schematic of the BRB frame can be seen in Figure 2.3-14 and buckling of the system can be seen in Figure 2.3-15.

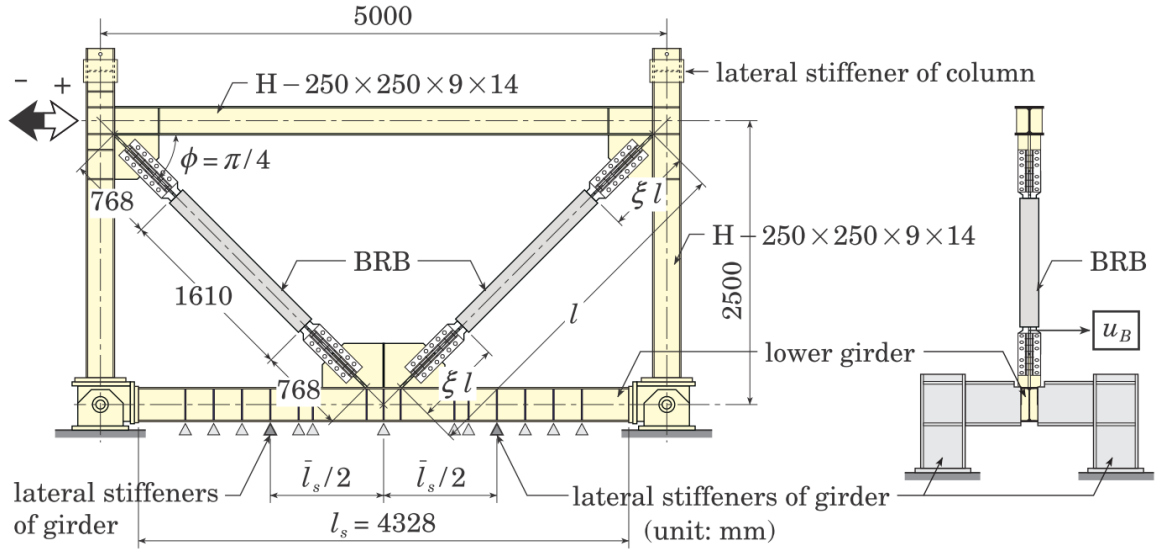

Figure 2.3-14: Experimental test schematic for inverted chevron BRB frame with repositionable lateral stiffeners (Koetaka et al. 2008)

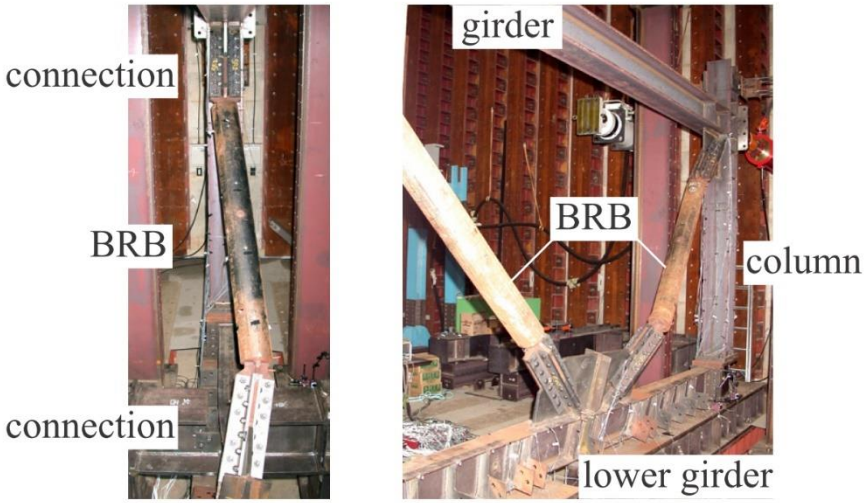

Figure 2.3-15: Sway buckling of inverted chevron BRB frame (Koetaka et al. 2008)

The design of the BRB in this test was a circular tube, as the core, inside a larger circular tube, as the restraining member. This can be seen in Figure 2.3-16. The ends of the core circular tube were attached to a cruciform connection by a 32 mm circular plate. This is an interesting detail as it would be expected that this unique BRB would have relatively high rotational stiffness at the BRB ends, and a hinge would not be expected to form. However, it can be seen by the tests that a hinge did form, indicating a relatively low rotational stiffness.

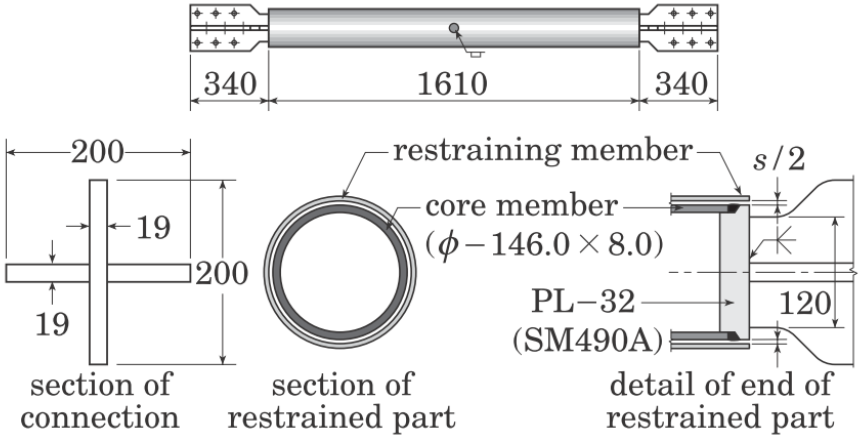

Figure 2.3-16: Circular tube BRB design with plate cap end (Koetaka et al. 2008)

Although the gusset plate does not buckle during these tests, the paper shows that the BRB end can hinge easily and that the beam rotational stiffness must be carefully considered if a chevron configuration frame is used.

2.3.6 Ma et al. (2008)

Ma et al. (2008) investigated all-steel BRBs by uniaxial cyclic loading tests and full-scale sub-assemblage testing. The intended outcome of the paper was to prove the validity of the all-steel BRB design used.

Before the sub-assemblage testing, it was noted that the bottom gusset plate had a visible out-of-plane imperfection due to a manufacturing error. The paper has not specified how large this deformation was. It was decided the test would still occur. Two lateral supports were attached to each side of the column to restrict out-of-plane deformation of the sub-assemblage. Buckling of the gusset plate occurred during the fourth cycle at a storey drift of 1.25 %, as seen in Figure 2.3-17.

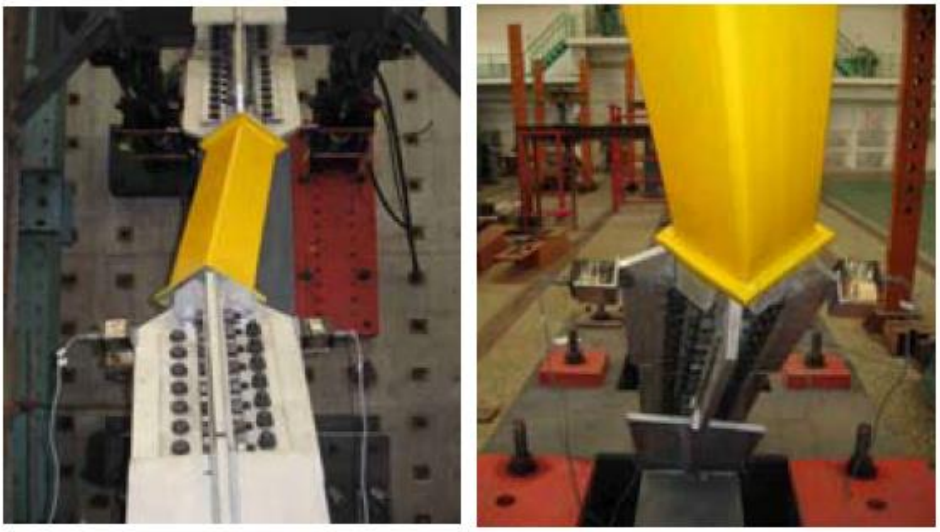

Figure 2.3-17: Sway buckling of gusset plate and BRB end hinging for sub-assemblage test (Ma et al. 2008)

The paper determines that the buckling failure was a result of the initial imperfection of the gusset plate. No consideration has been made of the contribution of the BRB end plastic hinge to the failure, which can be seen in Figure 2.3-18. The rotational stiffness of the cruciform shaped BRB end would be expected to be reasonably high. However, it is clear from the experimental result that it was not sufficient to prevent a mechanism from forming and sway buckling occurring.

Figure 2.3-18: Hinge formation at BRB end post-buckling (casing removed) (Ma et al. 2008)

The results of this paper should not be dismissed due to the manufacturing error of the gusset plate. If the imperfection was relatively small, it may be within the likely range of out-of-plane deformation that would be expected for a BRB frame that is under bi-directional loading. This type of loading can easily occur in an earthquake, and so this experimental test may suggest that sufficient out-of-plane storey drift could decrease the buckling capacity of the BRB system, resulting in failure. Most BRB frames are only tested under in-plane loading, and the effects of bidirectional loading on buckling capacity have not been researched.

2.3.7 Chou et al. (2012)

Chou et al. (2012) experimentally tested a single storey, one bay BRB frame with a diagonal BRB configuration (Figure 2.3-19) to observe the effects of frame action forces on single and double gusset plates. The top gusset plate buckled by sway during the experiment at a significantly lower force than expected, indicating that the buckling design method used is not always conservative.

During the experiment, the gusset plate buckled out-of-plane at an axial force of 693 kN in the BRB, at an inter-storey drift of 0.63 %. This was lower than the maximum compression capacity of the BRB of 913 kN. The failure mechanism, as shown in Figure 2.3-20, indicates that the gusset plate buckled by sway and a hinge formed at the end of the BRB.

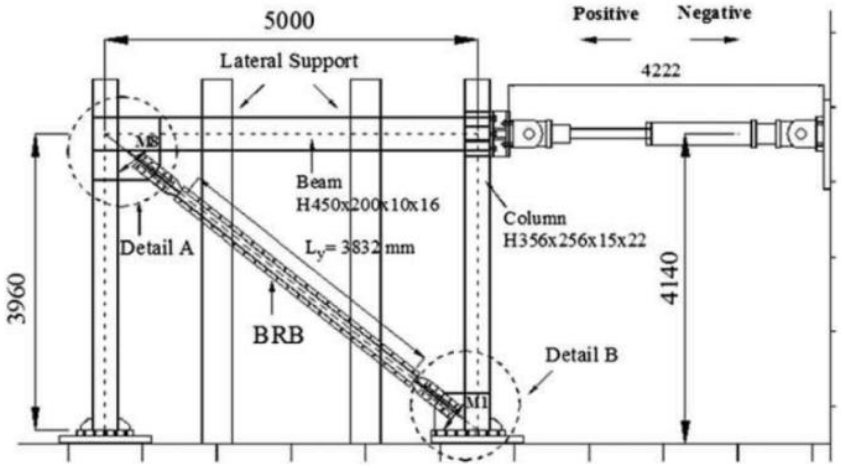

Figure 2.3-19: Experimental test schematic for diagonal configuration BRB frame (Chou et al. 2012)

Figure 2.3-20: Sway buckling of top gusset plate and BRB end hinge formation (Chou et al. 2012)

The BRB used was a unique design. Two C channels were bolted together to form the outer casing and then filled with concrete. The non-yielding cruciform segment extended 100 mm inside the core, approximately equal to the core width. This would indicate relatively low BRB end rotational stiffness (Matsui et al. 2010).

The gusset plate was designed to be susceptible to out-of-plane movement and considered the Thornton method in conjunction with AISC specifications (AISC 2005a) using K = 1.2. This method estimated the gusset plate buckling capacity to be 1157 kN, which was considered acceptable as it was larger than the maximum compression capacity of 914 kN. The gusset plate was also stiffened further with a central stiffener. The beam-column joints of this BRB frame were likely to be considerably rigid with additional beam and column web stiffeners at the ends of the gusset plate. After the gusset plate had buckled early, it was suggested by Chou et al. (2012) that K = 2.0 be used for design. This has been discussed further in Section 2.4.10.

The frame was also tested with free-edge stiffeners added to the gusset plate to increase the stiffness. This modification prevented the buckling failure from occurring again. Chou et al. (2012) noted that the addition of free-edge stiffeners has the additional benefit of reducing normal stresses at the gusset plate tips and gusset strut deformation. This can help prevent weld fractures due to frame action.

2.3.8 Hikino et al. (2012)

Hikino et al. (2012) tested two different BRBs in a chevron configuration frame to compare the effects of changing BRB end rotational stiffness. A standard BRB was used in the first test with the non-yielding segment embedded into the BRB casing 1.5 times the depth of the yielding segment which was equal to the minimum ratio suggested by Takeuchi et al. (2009). The second test was identical except for using a BRB with a reduced non-yielding segment embedment length to yielding width ratio of 0.4. Neither specimen violated the AISC seismic provisions (AISC 2005b).

The first test behaved excellently and did not buckle. The second test, however, buckled by sway with both ends of the BRB hinging and the beam joint twisting out-of-plane, as seen in Figure 2.3-21. An interesting finding was that the BRB behaving in tension in the chevron frame provided little rotational restraint at the beam joint and did not restrain buckling deformation.

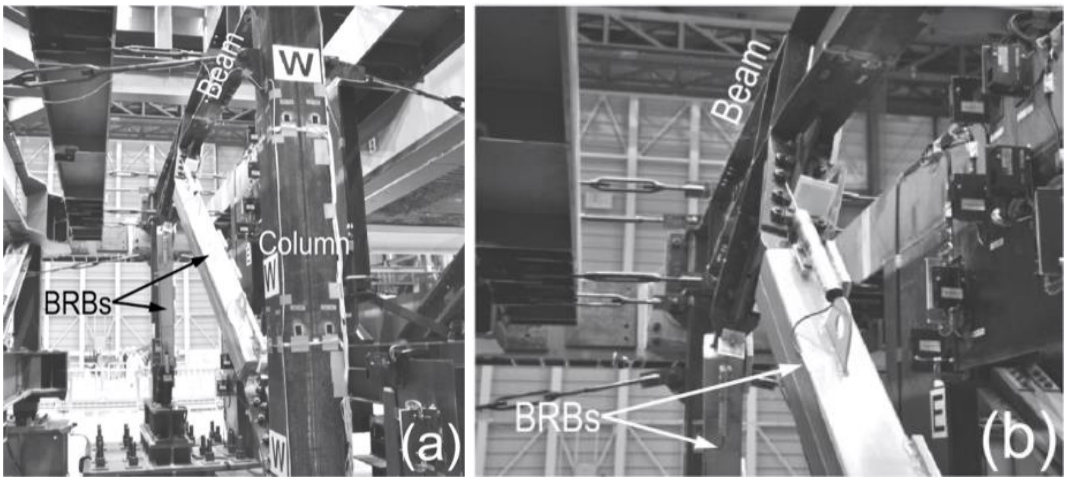

Figure 2.3-21: Sway buckling of BRB in chevron configuration frame (Hikino et al. 2012)

The gusset plate did not buckle in this experiment. Instead, the low beam joint rotational stiffness and the low rotational stiffness at the BRB end lead to the buckling failure. The gusset plate was stiffened at the centre of the splice plate from the BRB end to the beam

joint. The buckling failure shows that the BRB frame should be considered as a system when considering buckling capacity.

2.3.9 Takeuchi et al. (2014)

Takeuchi et al. (2014) tested six BRB specimens axially in a single diagonal sub-assemblage, as shown in Figure 2.3-22. The experiment investigated the effects of adjusting the non-yielding segment embedment depth, gusset plate stiffness, casing shape and the debonding gap between the core plate and the restraining mortar. A 1 % out-of-plane drift was simulated to consider the worst case. Because the test was a sub-assemblage, the beam-column joints were seen as rigid.

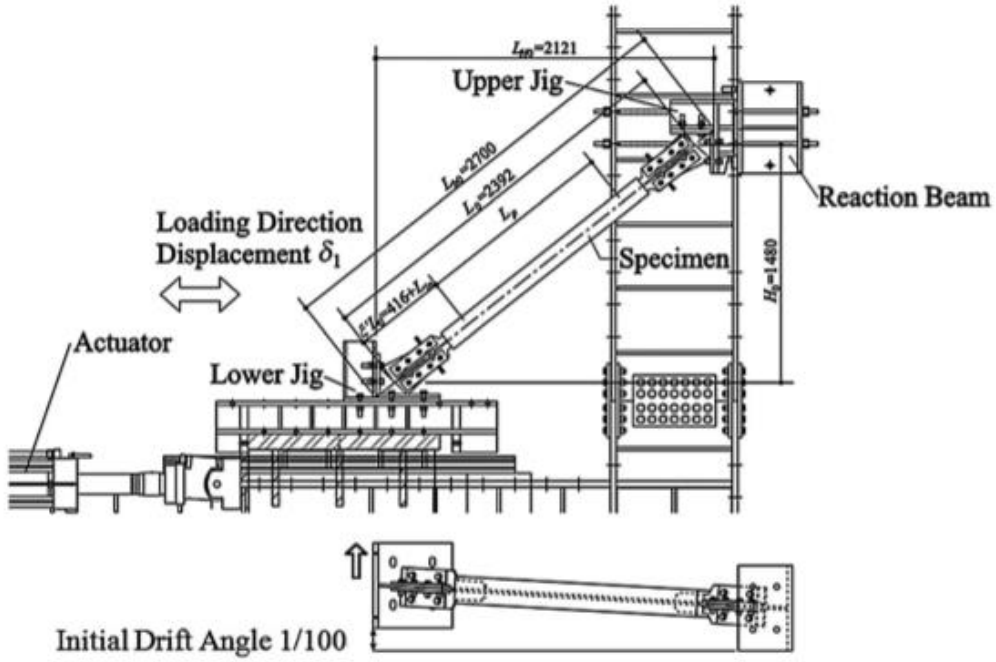

Figure 2.3-22: Experimental test schematic for diagonal BRB in sub-assemblage (Takeuchi et al. 2014)

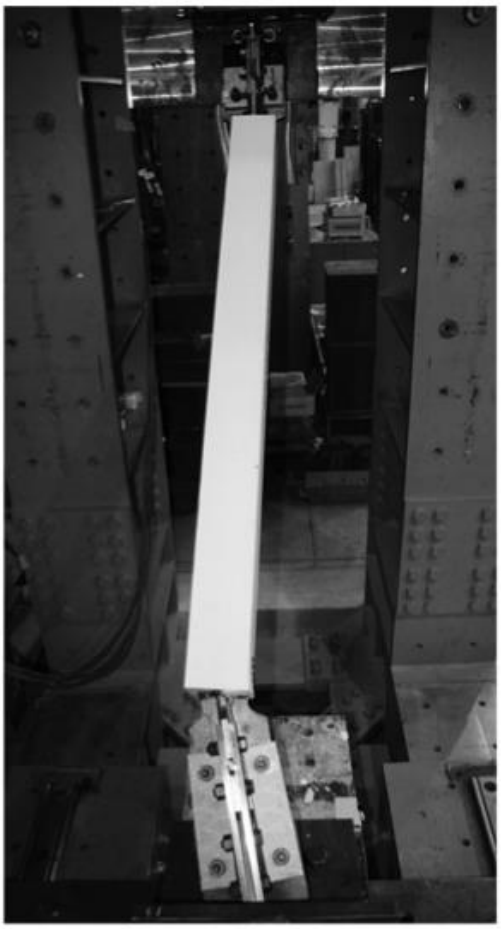

Figure 2.3-23: Sway buckling of BRB in sub-assemblage (Takeuchi et al. 2014)

The tests showed that buckling occurred by hinging of the BRB end and sway buckling failure for most experimental tests. Using gusset plates stiffened with free-edge stiffeners, the BRB system was able to remain stable up to an axial deformation of 3 %. Buckling occurred at lower normalised axial deformations when the non-yielding segment embedment length decreased, the debonding gap increased and when the casing was circular over rectangular. An example failure can be seen in Figure 2.3-23.

It is interesting to note that buckling failure occurred for two specimens with an embedment depth of 2.0 and a large debonding gap. Work by Matsui et al. (2010) and Takeuchi et al. (2009) had previously indicated that failure would not occur at this embedment depth. The buckling capacity was significantly higher than specimens tested with an embedment depth of 1.0. It is clear that the BRB end rotational stiffness significantly affects the buckling capacity of the BRB system.

2.3.10 Takeuchi et al. (2015)

Takeuchi et al. (2015) experimentally tested a chevron configuration BRB sub-assemblage to investigate the modifications to the design method proposed by Takeuchi et al. (2014) to account for chevron configuration BRB frames. The test considered a range of stiffness of beam joints, gusset plates and BRB restrainer ends. It also considered a 1 % out-of-plane storey drift. A schematic of the experimental test has been presented in Figure 2.3-24.

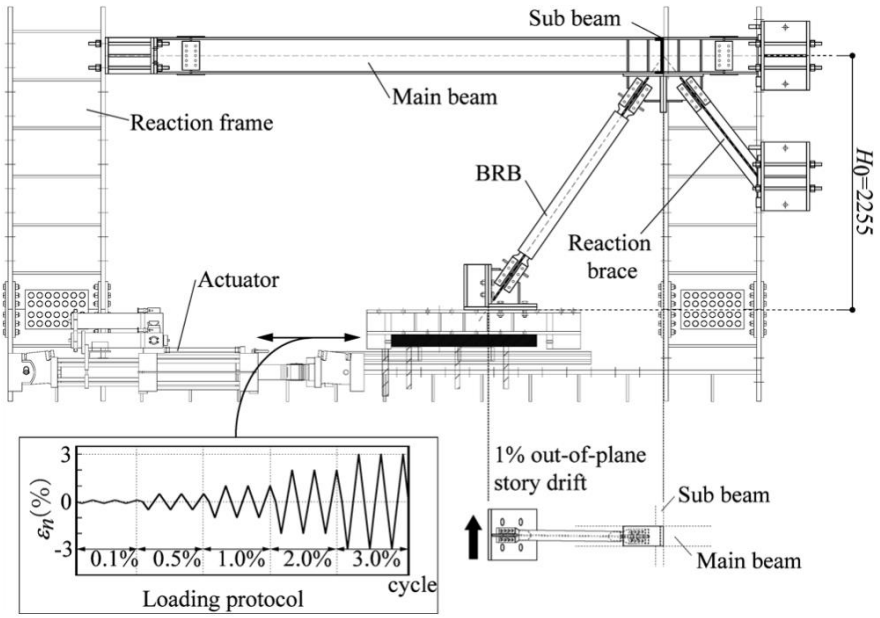

Figure 2.3-24: Experimental test schematic for chevron configuration BRB sub-assemblage (Takeuchi et al. 2015)

Of the six experimental tests performed, two were expected to buckle before the maximum compression capacity of the BRB was reached. Test L-RN'2 was estimated to buckle at 371 kN using the proposed design method and buckled at 527 kN during the experimental test. Test L-RN0 was estimated to buckle at 256 kN and instead buckled at 339 kN. These results show that the design method was conservative for both tests. An example of the buckled gusset plate can be seen in Figure 2.3-25.

Figure 2.3-25: Sway buckling of BRB in chevron configuration sub-assemblage (Takeuchi et al. 2015)

L-RN'2 was identical to L-RN0 except the BRB used had a non-yielding segment insertion length equal to two times the yield core plate width, whereas L-RN0 had zero non-yielding segment insertion length. This shows that buckling capacity of the system can be increased by increasing non-yielding segment insertion length as it increases the BRB restrainer end rotational stiffness. The results also agree with Takeuchi et al. (2014), that a non-yielding segment insertion equal to two is not always sufficient to prevent buckling.

The test H-RN'2 did not buckle by sway failure during the experiment. This was because the test used stiffened gusset plates and a substantially stronger beam joint. The beam joint was strengthened by sub-beams equal to the depth of the main beam being attached perpendicular to the main beam at the centre of the beam joint. This ensured that the beam rotational stiffness was relatively large. In L-RN'2, the beam joint was strengthened only by two tension rods and so it had relatively lower beam rotational stiffness. The test of H-RN'2 shows that well designed BRB frames can perform adequately without sway buckling occurring if all elements are relatively stiff.

2.4 Gusset Plate Buckling Design Methods

This section details the different gusset plate design methods available to estimate the buckling capacity of a gusset plate in compression. Most of these methods have been developed for gusset plates in concentrically braced frames, but many have been applied to gusset plates in BRB frames. A number of design methods have also been developed for the specific case of gusset plates in BRB frames. It should be noted that discussion of the assumptions and limitations of each method can be found in Chapter 3.

2.4.1 Whitmore Method (1952)

The Whitmore method (Whitmore 1952) was developed to estimate the compressive or tensile yield capacity of a gusset plate. It is not used as an estimate of a gusset plate's compressive buckling capacity. However, some experimental tests have done so (Hu and Cheng 1987). The method is important to review as it forms the foundation for the Thornton Method (Section 2.4.2).

The method considers an effective width of the gusset plate to determine the yield capacity. This effective width is based on the bolt or weld spacing of the splice plates that connect the brace to the gusset plate. To determine the Whitmore effective width, b_e, Equation 2.4-1 is used. Thornton and Lini (2011) provided additional guidance on modifying b_e when the width is larger than the gusset plate geometry. Figure 2.4-1 presents a graphical representation of the Whitmore width for both (a) bolted joint, and (b) welded joint gusset plate connections.

$$b_e = b_b + 2l_b \tan\theta \qquad 2.4\text{-}1$$

where:

b_e Whitmore effective width

b_b width between outermost splice plate bolts or width between splice plate welds

l_b length between outermost splice plate bolts or length of splice plate welds

θ dispersion angle, to be taken as 30° as per Figure 2.4-1

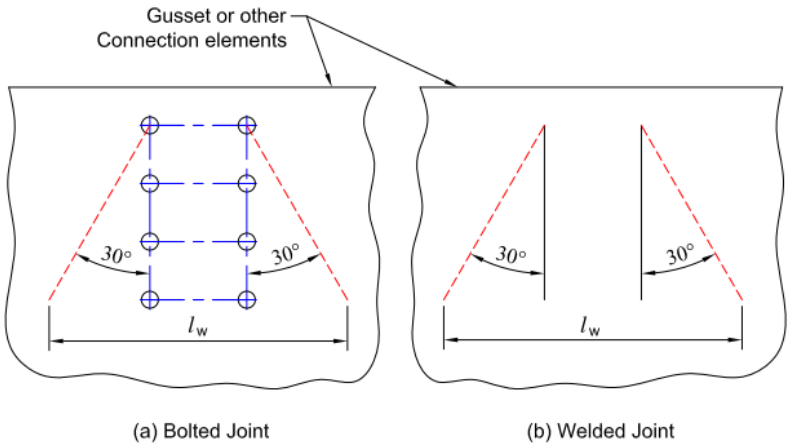

Figure 2.4-1: Whitmore width, indicated as l_w on the figure, for gusset plates with a) bolted or b) welded joints (Thornton and Lini 2011)

The tensile or compression yield capacity, P_y, of the gusset plate is calculated through Equation 2.4-2, which follows the yield capacity concept of area multiplied by yield stress.

$$P_y = b_e t_g F_y \qquad 2.4\text{-}2$$

where:

P_y yield capacity

t_g gusset plate thickness

F_y yield stress

It is interesting to note that the compression and tension yield capacities are largely independent of the gusset plate geometry besides the thickness of the gusset plate and the limiting of the Whitmore width should it exceed the boundaries of the gusset plate.

Experimental testing was performed by Whitmore on ¼ scale aluminium Warren truss joint gusset plates. The paper shows that the Whitmore method was conservative in predicting both compressive and tensile yield capacity. This has been explored further in Section 2.2.1.1.

2.4.2 Thornton Method (1984)

Thornton (1984) developed a method to determine the compressive buckling capacity of a gusset plate by considering the gusset plate as an effective column strip. It is implemented in several standards as a way to determine local buckling capacity of a gusset plate (AISC 2005a; Standards New Zealand 1997).

The method compares the maximum compression stress imposed on the gusset plate as determined by the Whitmore method to the maximum allowable stress from Specification Table 3-36 (AISC 1984). Table 3-36 compares the slenderness ratio of the gusset plate to the

critical buckling stress for steel with F_y = 36 ksi. This table is based on the AISC column buckling curve which accounts for elastic and inelastic buckling as well as other column buckling factors such as member out-of-straightness, residual stresses and accidental eccentricities.

The method can be applied without the use of Table 3-36 by directly solving the AISC column curve equations. Equations 2.4-3 to 2.4-6 calculate the buckling force capacity instead of stress capacity.

$$r = \frac{t_g}{\sqrt{12}} \qquad \text{2.4-3}$$

$$\lambda_c = \frac{KL}{\pi r}\sqrt{\frac{F_y}{E}} \qquad \text{2.4-4}$$

$$P_{cr} = (0.658)^{{\lambda_c}^2} b_e t_g F_y \qquad \lambda_c \leq 1.5 \qquad \text{2.4-5}$$

$$P_{cr} = \left(0.877/{\lambda_c}^2\right) b_e t_g F_y \qquad \lambda_c > 1.5 \qquad \text{2.4-6}$$

where:

r	radius of gyration
λ_c	slenderness coefficient
K	effective length factor
L	Thornton length
π	pi
E	elastic modulus
P_{cr}	gusset plate buckling capacity

The radius of gyration is based on the simplification of the relationship between the second moment of area and area of rectangular sections. The effective length factor of the gusset plate is based on fixed-fixed end conditions which are idealised as K = 0.5. Thornton (1984) recommends using K = 0.65 as it cannot always be guaranteed that the ends are fully rigid.

The equivalent column length used is commonly referred to as the Thornton length. Thornton proposed that the length should be measured from the centre of the Whitmore width to the beam-column interface to the gusset plate in a line parallel to the brace. This was considered to be conservative as it is usually the maximum unsupported length of the gusset plate. Thornton also proposed that a length, L_{ave}, obtained by averaging the lengths L_1, L_2, and

L_3, be used, as shown in Figure 2.4-2. The average length is most commonly considered (Yam and Cheng 1993).

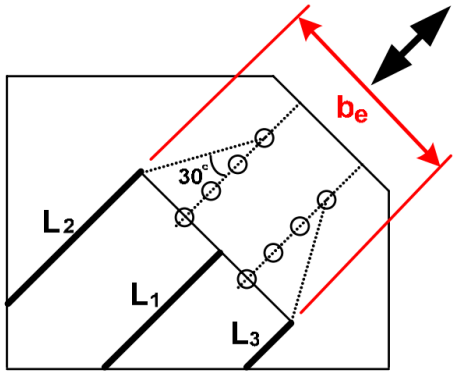

Figure 2.4-2: Gusset plate diagram indicating Thornton lengths (Tsai and Hsiao 2008)

Equation 2.4-5 considers a stocky member. When $\lambda_c \leq 1.5$, the member will undergo inelastic buckling behaviour as a result of the member yielding. Equation 2.4-6 considers when $\lambda_c > 1.5$, indicating a slender member that will buckle elastically. Both curve equations consider other column effects that reduce the buckling capacity of the member including initial imperfections, and accidental eccentric loading. Equation 2.4-5 also considers residual stress effects. These capacity reductions were developed considering column members and their applicability to gusset plates has not been considered.

Thornton (1984) did not provide any experimental evidence to validate the method. The method has been found to be conservative in experimental tests by Gross (1990) and Yam and Cheng (1993).

2.4.3 Modified Thornton Method (1994)

A common criticism of using the Thornton method for gusset plate buckling is that it can be too conservative for some gusset plates (Dowswell 2006; Sheng et al. 2002; Yam and Cheng 1994). It has been found that a number of gusset plates can buckle at up to four times the expected buckling capacity (Yam and Cheng 1993). For this reason, the modified Thornton method was devised by Yam and Cheng (1994) to be a less conservative estimate of a gusset plate's buckling capacity.

The method states that the dispersion angle used to calculate the Whitmore width should be 45^0 instead of 30^0 such that Equation 2.4-1 becomes Equation 2.4-7. It also suggests that the Thornton length used can be determined from the end of the splice plate for relatively rigid splice plates, instead of the last bolt row, to the beam-column interface. Taking the

average or maximum Thornton length can be used for a more conservative estimate. The method does not consider an average length taken from the splice plate end to the beam-column interface. The method was evaluated using the Canadian column curves in CAN/CSA-S16.1-M89 (CSA 1989) instead of the AISC column curve used by Thornton.

$$b_e = b_b + 2l_b \, tan\, 45° \qquad 2.4\text{-}7$$

The method was developed on the basis of load redistribution after gusset plate yielding prior to buckling. It is only applicable when elastic buckling capacity is significantly larger than yield capacity. Yam and Cheng (1994) recommend the method be only applicable when the Thornton elastic buckling capacity (Equation 2.4-6) is more than two times larger than the Whitmore capacity (Equation 2.4-1).

Like the Thornton method, an effective length factor of 0.65 was used. However, the value was chosen to consider the effects of plate action in the critical region bounded by the beam and column instead of accounting for the fixed-fixed boundary condition. Yam and Cheng compared the method to a range of experiments with both fixed-fixed (K = 0.5) and fixed-roller (K = 1.0) boundary conditions and found the modified Thornton method was a better estimate for both cases than the Thornton method.

Because the modified Thornton method is focussed on inelastic buckling, it is unlikely that this method will be suitable for predicting the buckling capacity for a sway buckling of gusset plates in BRB frames as the failure occurs elastically in most cases.

2.4.4 NZS 3404 Method (1997)

The New Zealand Steel Structures Standard NZS 3404 Parts 1 and 2 (Standards New Zealand 1997) defines gusset plates as connection components in Clause 9.1.9.1 and as such, they are subject to Sections 5, 6, 7, 8, and the appropriate provisions of Section 12. The commentary for this clause (Clause C9.1.9) notes that a gusset plate under compression loading is designed as a column member, with specific provisions relating to Section 6.3 and HERA R4-80 (1994).

To prevent a gusset plate from buckling in compression during seismic loading, a designer must follow Clause 12.9.7.2 (b) which states that for:

> *"Buckling in compression; check member capacity to 6.3 using an effective length (Le) of 0.7 times the clear length."*

This factor is more conservative than the Thornton method which considers effective length factor of 0.65. The commentary for this clause (Clause C12.9.7) states that a comprehensive procedure for gusset plate design is presented in Section 10.7.2 of HERA R4-80 (1994) and that it has been experimentally verified by Gross (1990).

Section 6.3 defines the nominal member capacity of a member subject to axial compression. The nominal member capacity is defined as the nominal section capacity multiplied by the member slenderness reduction factor, α_c. This factor is dependent on effective length, *Le*, the radius of gyration, *r*, material yield strength, F_y, form factor, k_f, and the member section constant, α_b. Clause 9.1.9.2 states that $\alpha_b = 0.5$. Clause 6.2.2 shows that $k_f = 1$ as the effective and gross area of the plate are equal. It will be assumed in this thesis that the effective length, 0.7 times the clear length, refers to either the maximum Thornton length or the average Thornton length of the gusset plate and that both lengths are acceptable.

Clause 12.9.7.3 state that the gusset plate must be designed to accommodate member inelastic rotation. These provisions are necessary for concentrically braced frames where the brace may buckle in compression. When the brace buckles, it is desirable for the gusset plates to rotate out-of-plane to minimise damage to the attached beam-column joint. A BRB is designed as a category 1 or 2 member (Wijanto 2012) and so Clause 12.9.7.3.1 applies, which states that:

> *"Gusset plates connecting category 1 or 2 members should be detailed such that there is a clear length of gusset plate, beyond the end of the member being connected, equal in length to between 2 and 3 times the thickness of the gusset plate."*

The outcome of this clause is shown in Figure 2.4-3, where "2tp" is equal to two times the thickness of the gusset plate.

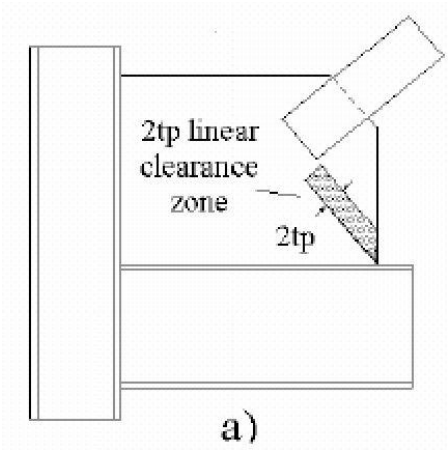

Figure 2.4-3: Clearance required for inelastic rotation in gusset plates (Fussell 2010)

The clause does not match the design philosophy for BRB frames as it is undesirable for a BRB to buckle in compression as a failure mechanism. The application of this clause will result in a gusset plate with a lower flexural stiffness as the Thornton length is unnecessarily increased. This will increase the possibility of sway buckling failure in BRB frames. As such, it is therefore highly recommended that a designer does not apply Clause 19.9.7.3.1 to gusset plates in BRB frames.

2.4.5 HERA R4-80 Method (1994)

The HERA R4-80 method is nearly identical to the NZS 3404 method. However, one major modification has been made. Section 10.7.2 of the New Zealand Structural Steelwork Limit State Design Guides, Volume 1, commonly referred to as HERA R4-80 (HERA 1994), does not match the design provisions of NZS 3404 Clause 12.9.7.2 (b). Instead of $K = 0.7$, it is recommended to use $K = 0.5$. The section also states that the Thornton average length is to be used, instead of the clear length. Apart from these changes, Section 6.3 of NZS 3404 is to be followed to determine gusset plate buckling capacity, the same as the NZS 3404 method.

Although NZS 3404 should take precedent over HERA R4-80, the document is directly referenced in NZS 3404 as a more detailed design procedure for gusset plate buckling indicating that the method is valid under the provisions of NZS 3404 and that a designer could use $K = 0.5$.

2.4.6 Inelastic Plate Buckling Method (2002)

Sheng et al. (2002) found that both the Thornton method and the modified Thornton method are too conservative for large gusset plates with the actual buckling capacity being an average

1.77 times greater than the modified Thornton method estimates. This is due to both methods being unable to account for the effects of plate action properly. Plate action can increase a gusset plate's capacity due to post-buckling strength. Sheng et al. (2002) proposed a method based on the theoretical inelastic plate buckling formula and a constant based on finite element modelling of gusset plates. The gusset plate buckling capacity can be determined by Equation 2.4-8.

$$P_{cr} = \frac{k_g \pi^2 E \sqrt{E_t/E}}{12(1-v^2)\left(b_o/t_g\right)^2} b_1 t_g \qquad 2.4\text{-}8$$

where:

k_g finite element model constant

E_t tangent stiffness modulus

v Poisson's ratio

b_0 short bounded edge length of gusset plate

b_1 bending line length

Sheng et al. (2002) have provided a number of charts to help determine k_g. The constant was found by equating P_{cr} with the buckling capacity of a range of finite element models and was then back-calculated to determine k_g. As such values of k_g are only presented for gusset plate designs that have been modelled. Charts have been provided to allow a designer to interpolate between the modelled gusset plates. The provided charts are non-linear in nature and use only a small amount of data to develop them and so their accuracy may not be sufficient in some cases.

Other researchers have added to the number of possible gusset plates than can be checked with this method through their own finite element models. Chou and Chen (2009) followed Equation 2.4-8 and modelled 33 different gusset plates to determine a variety of k_g values. However, the Whitmore width has been used instead of the full bending line and so the k_g values are not comparable. The study was also limited to central gusset plate connections in chevron configuration BRB frames which can fail by sway failure.

Naghipour et al. (2013) has also provided a range of k_g values based on gusset plate finite element models, including those with free-edge stiffeners, and also uses the Whitmore width instead of b_1. The accuracy of the finite element model was verified with a single gusset plate buckling capacity experiment with fixed end conditions.

As there is not an extensive database of potential gusset plates that have been modelled and evaluated for the inelastic plate buckling method, it is difficult for a designer to apply the

method universally to gusset plate design. Only the finite element models analysed by Chou and Chen consider sway buckling failure but only for a limited number of chevron configuration BRB frames.

Due to the limitation of the method presented by Sheng et al. (2002), particularly the small number of gusset plates that can be considered, the method will not be considered further.

2.4.7 Working Point Method, or Nakamura (2002) Method

Bruneau et al. (2011) recommended the Nakamura method to prevent gusset plate buckling in BRB frames, and this method has been used by some BRB manufacturers in the United States of America as an additional check. This method was incorrectly attributed to Nakamura (2000) and is believed to have been first considered by Tsai et al. (2002) based on design calculations made by Nippon Steel. It will be referred to as the working point method henceforth, due to the effective length of the connection being extended to the working point of the beam-column joint. This is a divergence from other methods where it is assumed the beam-column joint is rigid and does not rotate when the connection has buckled. This method is a check on the sway buckling capacity of the connection transition region at the end of the BRB casing. It is based on the theory that the BRB end must also develop a hinge to form a mechanism for failure.

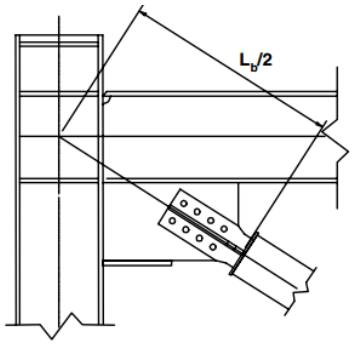

Figure 2.4-4: Connection length used for working point method (Tsai et al. 2002)

The working point method is a simple Euler buckling check where the buckling second moment of area, I_c, is calculated from the non-yielding segment of the BRB outside the casing. The length, L_b, is considered as twice the length from the end of the BRB casing to the work point of the beam-column joint, as shown in Figure 2.4-4 above. The effective length factor of 1.0 is used, but if the length illustrated in Figure 2.4-4 is considered as L_b instead of $L_b/2$, then the effective length factor is essentially 2.0. This would indicate a fixed-free condition exists with the BRB end providing no lateral or rotational restraint. The buckling capacity of the connection can be determined by Equation 2.4-9

$$P_{cr} = \frac{\pi^2 E I_c}{(K L_b)^2} \qquad 2.4\text{-}9$$

where:

I_c second moment of area of non-yielding segment at end of BRB casing

L_b length, from end of BRB casing to centre of beam-column joint (Figure 2.4-4)

The experimental test by Tsai et al. (2002) indicated the method was not conservative, with a buckling capacity demand 1.5 times the yield capacity of the BRB. More information about the test can be found in Section 2.3.1.

2.4.8 Koetaka et al. (2008) Method

Research by Koetaka et al. (2008) primarily focused on the lateral and rotational stiffness of the beam the gusset plate is attached to in chevron configuration frames. The paper does, however, offer a method to determine sway buckling capacity for both diagonal and chevron configuration frames. The method is based on the Euler buckling load of the connection region, encompassing the gusset plate, splice plate connection, and unrestrained non-yielding segment of the BRB. The method is based on a buckling mode shape corresponding to diagram (b) in Figure 2.4-5, which produces a lower buckling capacity than diagram (c). The method can also be modified to consider the condition found in diagram (a), where lateral displacement of the beam joint can occur in chevron configuration frames.

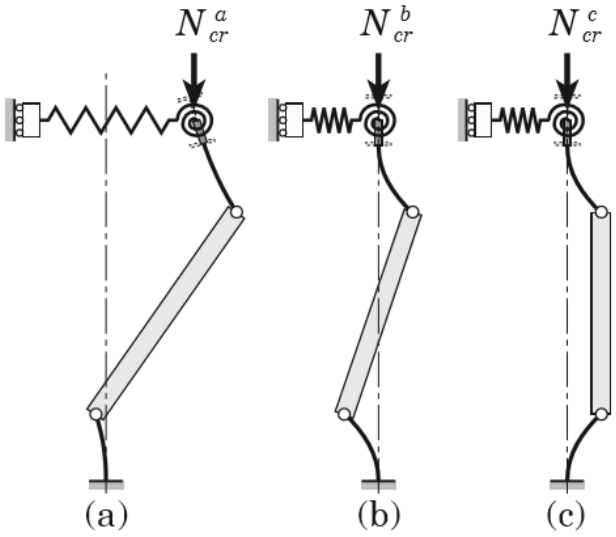

Figure 2.4-5: Out-of-plane buckling mode shapes (Koetaka et al. 2008)

The beam-column joint is assumed to be rigid in this method and so the length, L_c, is considered from the end of the BRB casing to the beam flange. Out-of-plane buckling of the BRB is determined by Equation 2.4-10. It can be seen effective length factor of 2 is used.

$$P_{cr} = (1 - 2\xi)\frac{\pi^2 E I_c}{(2L_c)^2} \qquad 2.4\text{-}10$$

where:

ξ ratio of connection length to BRB casing length

I_c second moment of area of connection

L_c connection length, from end of BRB casing to beam or column flange

The method is similar to Euler buckling but makes consideration to the BRB length. The reduction portion of the equation, $(1 - 2\xi)$, is an approximation derived from the first Taylor series of the sine function, the second Taylor series of the cosine function, and approximating $\frac{\pi^2}{8} = 1$. This method can be applied to both diagonal and chevron configuration frames.

The method was also further modified to consider both the lateral stiffness and rotational stiffness of the beam joint in a chevron configuration BRB frame. Experimental testing was shown to be in relatively good agreement with the method and tests where rotational beam stiffness was lower than what was required by the method resulted in much larger out-of-plane buckling deformations. Further details can be found in Section 2.3.5.

2.4.9 Tsai and Hsiao (2008) Method

Tsai and Hsiao (2008) found that after experimental testing by Tsai et al. (2004), the Thornton method was inadequate for predicting sway buckling failure of gusset plates. They proposed an alteration that considers K = 2.0, instead of K = 0.65, indicating a fixed-free boundary condition. The method follows the Thornton method but considers the Euler column buckling curve instead of the AISC column curve, as seen in Equation 2.4-11. This equation has been rewritten as Equation 2.4-12, considering Equation 2.4-4, to better illustrate the difference. It should be noted that the maximum Thornton length was taken instead of the average Thornton length.

$$P_{cr} = \frac{\pi^2 E}{\left(\frac{KL}{r}\right)^2} b_e t_g \qquad 2.4\text{-}11$$

$$P_{cr} = \left(1.0/{\lambda_c}^2\right) b_e t_g F_y \qquad \lambda_c > 1.5 \qquad \text{2.4-12}$$

The basis for choosing $K = 2.0$, is based on Figure 2.4-6, which suggests that the buckling behaviour of BRBs that fail by sway failure is closer to buckling shape (b) than (c). The diagram indicates the boundary conditions for the gusset plate result in $K < 2.0$ and so $K = 2.0$ should be conservative. It can be seen that an assumption has been made that the gusset plate connection to the beam-column joint is fully fixed, indicating that the beam-column joint is infinitely rigid.

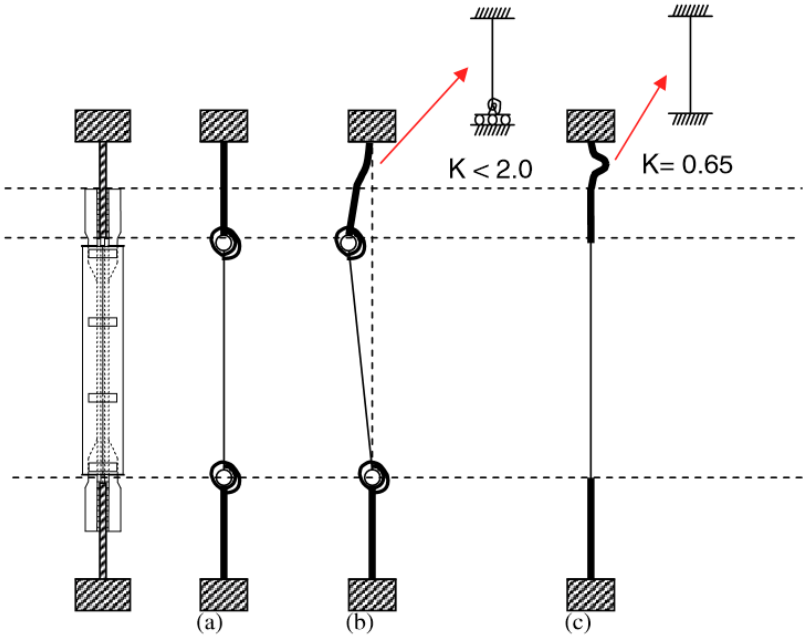

Figure 2.4-6: Buckling shapes and boundary conditions for BRB buckling failure (Tsai and Hsiao 2008)

Using the method, Tsai and Hsiao (2008) found a design capacity of 842 kN. This estimated capacity was considered to be in reasonably good agreement with the experimental buckling capacity of 805 kN. Although this is not conservative, the design capacity is within 5 % of the experiment. More information about the experiment can be found in Section 2.3.2.

2.4.10 Chou et al. (2012) Method

Chou et al. (2012) also found that the Thornton method was inadequate for predicting sway buckling failure of gusset plates. They proposed that the Thornton method is used but with $K = 2.0$, indicating fixed-free boundary conditions. Because this method includes the AISC column curve, it will be more conservative than the Tsai and Hsiao (2008) method which only considers the Euler column curve.

Using the method, Chou et al. (2012) found a design capacity of 759 kN which was within 10 % of the experimental buckling capacity of 693 kN but non-conservative. However, in a later paper (Chou and Liu 2012) the design capacity was calculated to be 614 kN by the same method, which was within 12 % of the experimental capacity and conservative. The difference appears to be explained by different calculation methodologies. The capacity estimate of 759 kN was calculated using a Thornton length considering a central stiffener that was used to strengthen the gusset plate. However, the capacity estimate of 614 kN was calculated using the average Thornton length without regard to the central stiffener.

As the central stiffener provided an increase in gusset plate flexural stiffness that is not considered by the 614 kN estimate, it cannot be determined if the proposed method is conservative.

More information about the experiment can be found in Section 2.3.7

2.4.11 Dowswell (2013) Method

Dowswell (2013) modified the Thornton method to account for variable stress dispersion across the gusset plate, suggesting a wider width than that determined by Whitmore is used. The effective length factor is variable based on the effective width and ranges from 0.35 to 0.5 for corner gusset plates. Through comparison to 91 experimental gusset plate tests, a column curve 0.75 times the AISC column curve is recommended to cover all cases. The method is applicable only to local buckling and does not consider gusset plates that buckle by sway failure.

2.4.12 Takeuchi et al. (2014) Method

Takeuchi et al. (2014) have proposed a design method that builds upon work by (a) Koetaka et al. (2008), which considers the plastic hinge concept, and (b) Matsui et al. (2010) which considers the bending moment transfer concept. The Architectural Institute of Japan Recommendations for Stability Design of Steel Structures states either concept can be implemented to assess and prevent global instability in BRB frames (AIJ 2009). These concepts can be seen in Figure 2.4-7. Takeuchi considers both concepts to develop a method that considers initial imperfections and out-of-plane drifts. The method uses strain energy and moment transfer capacity to determine buckling capacity and has been developed for the collapse mechanisms shown in Figure 2.4-8.

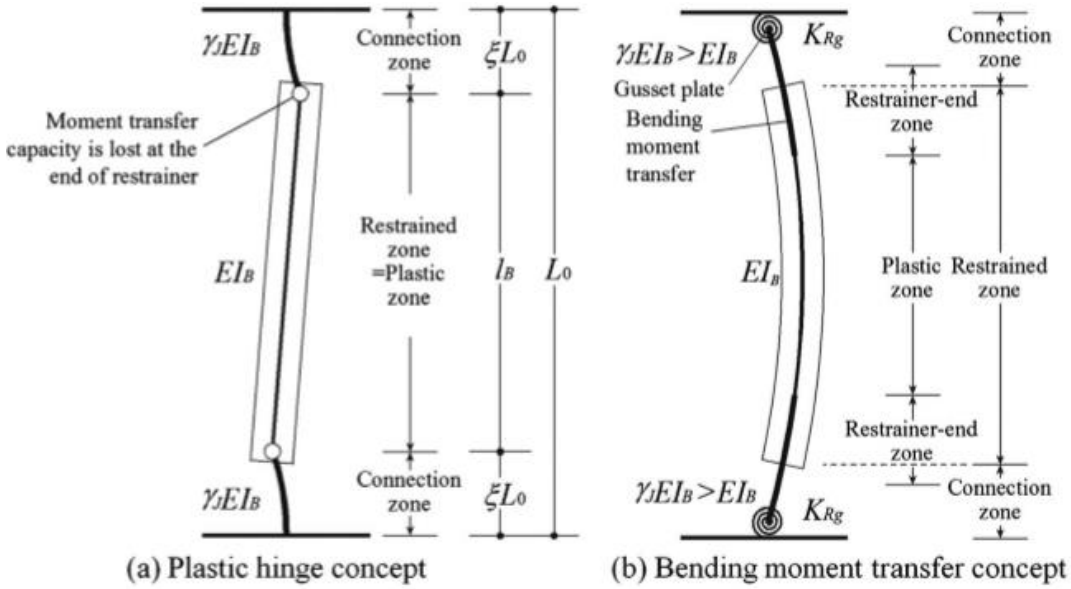

Figure 2.4-7: BRB stability concepts (Takeuchi et al. 2014)

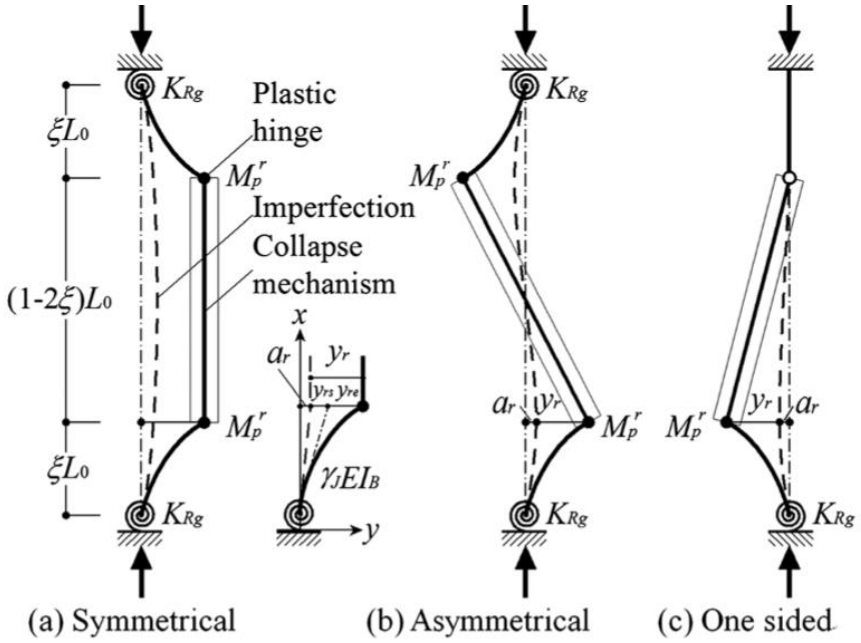

Figure 2.4-8: Potential collapse mechanisms considering imperfection, gusset plate rotational stiffness and plastic hinge formation (Takeuchi et al. 2014)

It has been determined that the asymmetrical collapse mechanism results in the lowest buckling capacity. The buckling capacity for a BRB system assuming elastic springs for gusset plates is calculated through Equation 2.4-13 and Equation 2.4-14. It can be seen in Equation 2.4-13 that the '2' is an effective length factor that modifies the connection length. The terms inside the square root account for the flexibility of the gusset plate affecting the behaviour of the connection region.

$$\lambda_r = \frac{2\xi L_0}{i_c}\sqrt{\frac{{}_{\xi}\kappa_{Rg} + \frac{24}{\pi^2}}{(1-2\xi)\ {}_{\xi}\kappa_{Rg}}} \qquad \text{2.4-13}$$

$$P_{cr1} = \frac{\left(M_p^r - M_0^r\right)/a_r + N_{cr}^r}{\left(M_p^r - M_0^r\right)/a_r N_{cr}^B + 1} \qquad \text{2.4-14}$$

where:

λ_r equivalent slenderness ratio used with the AIJ elasto-plastic column curves to determine N_{cr}^r

ξL_0 connection region length

i_c radius of gyration of connection region

$\xi\kappa_{Rg}$ normalised rotational stiffness of the gusset plate and beam-column joint

ξ ratio of connection length to BRB length

N_{cr}^r elastic buckling strength of the connection region without bending moment transfer capacity

M_p^r moment transfer capacity at the BRB ends

M_0^r initial bending moment at the BRB ends produced by out-of-plane drift

a_r initial imperfection at the BRB end

N_{cr}^B elastic buckling strength of the BRB considering the effects of connection bending stiffness and gusset plate rotational stiffness

P_{cr1} buckling capacity assuming elastic springs for gusset plates

Takeuchi also suggests a second limit on buckling capacity, under the assumption of plastic hinges forming at the gusset plates, as shown in Figure 2.4-9.

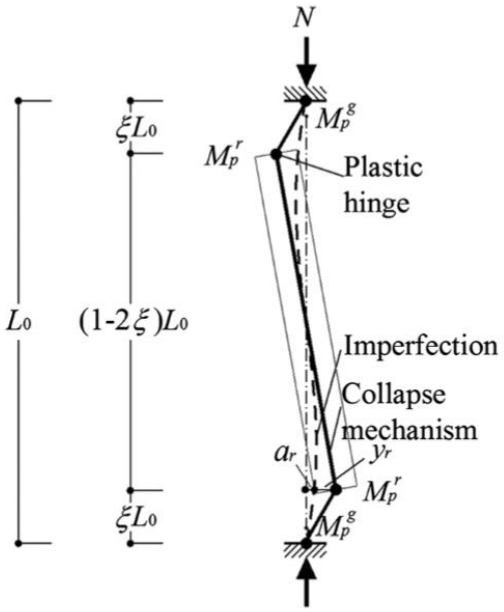

Figure 2.4-9: Collapse mechanism considering plastic hinges at gusset plate ends (Takeuchi et al. 2015)

$$P_{cr2} = \frac{\left[(1-2\xi)M_p^g + M_p^r - 2M_0^r\right]/a_r}{\left[(1-2\xi)M_p^g + M_p^r - 2M_0^r\right]/a_r N_{cr}^B + 1} \qquad 2.4\text{-}15$$

where:

M_p^g plastic bending strength of the gusset plate including axial force effects

P_{cr2} buckling capacity assuming plastic hinges at the gusset plate ends

Equation 2.4-15 calculates the buckling capacity of system assuming plastic hinges form at the gusset plate ends. The minimum of P_{cr1} and P_{cr2} should be taken and checked against the maximum compression capacity of the BRB.

Experimental testing was undertaken to verify the method, and it was shown to predict buckling capacity conservatively in four out of five cases with reasonable accuracy. More details can be found in Section 2.3.9.

2.4.13 Takeuchi et al. (2015) Method

Takeuchi et al. (2015) build upon the work of Takeuchi et al. (2014) by considering chevron configuration BRB frames. It has been noted that the beam joint in chevron frames may not provide sufficient rotational restraint to be regarded as fully rigid so an additional collapse mechanism has been considered. This mechanism has been shown in Figure 2.4-10. Takeuchi has proposed a simplification that combines gusset plate rotational stiffness and beam rotational stiffness. This simplification was found to be conservative.

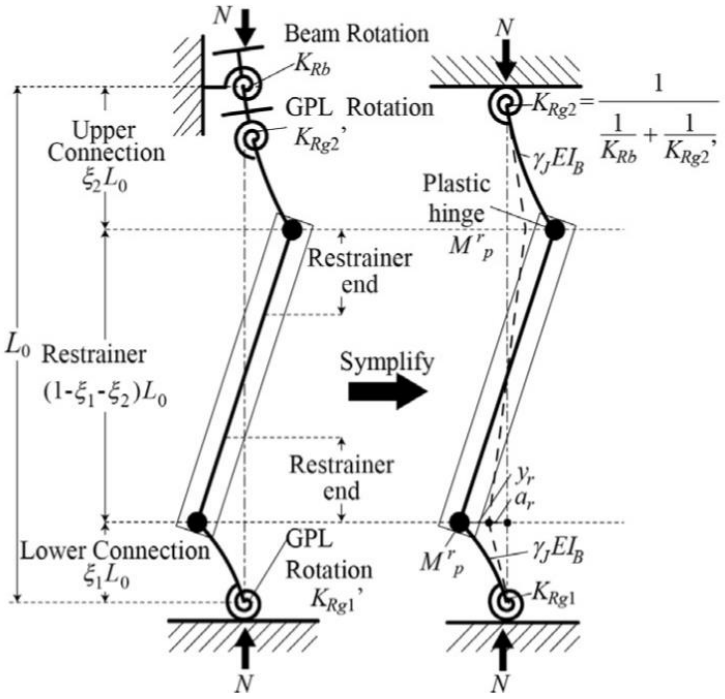

Figure 2.4-10: Collapse mechanism for chevron configuration BRB frames (Takeuchi et al. 2015)

The formulas from Takeuchi et al. (2014) were also modified to consider gusset plates of different designs at each end of the BRB. The updated method was found to be conservative through experimental testing on chevron configuration BRB sub-assemblages by Takeuchi et al. (2015).

2.4.14 Clifton Method (2015)

Clifton proposed a design method in accordance with NZS 3404 Clause 6.7.2 (MacRae and Clifton 2015). NZS 3404 Clause 6.7.2 (Standards New Zealand 1997) states that the connection which is required to brace a compression member shall be designed to resist:

> *"0.025 times the maximum design axial compression force in the member at the position of the support."*

It was proposed that this clause is applicable to gusset plate design where the gusset plate is required to resist 2.5% of the maximum BRB overstrength capacity, $0.025 * N^o_{com,brace}$. This is an empirical formula that has been shown to be satisfactory for estimating design forces on column braces (Mutton and Trahair 1975).

The gusset plate out-of-plane capacity to resist this force is to be determined by yield-line bending. The method thus suggests that if the gusset plate has sufficient capacity from the bending of yield-lines to resist $0.025 * N^o_{com,brace}$, then the gusset plate will not fail out-of-plane. The application of $0.025 * N^o_{com,brace}$ is to be at the end of the BRB at the

junction to the gusset plate. The exact location of the gusset plate yield-lines has not been described.

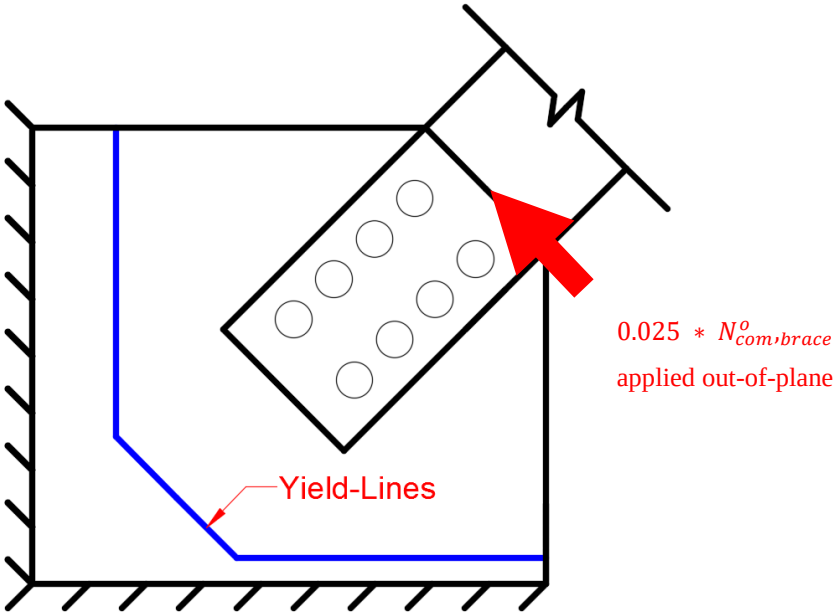

Figure 2.4-11: Diagram of the yield-line method

MacRae and Clifton (2015) also proposed that the gusset plate buckling capacity be considered using the NZS 3404 method described in Section 2.4.4, with an effective length factor of 1.2 using the average Thornton length. This buckling capacity was to be compared to the maximum BRB overstrength capacity multiplied by a safety factor of 3.5. This recommendation considers an equivalent sway buckling column with fixed-roller boundary conditions. This buckling mode does not consider a hinge forming at the BRB end, which has been shown to occur in gusset plate sway buckling in BRB frames (Chou et al. 2012; Hikino et al. 2012; Koetaka et al. 2008; Ma et al. 2008; Takeuchi et al. 2014, 2015; Tsai et al. 2004).

3 GUSSET PLATE DESIGN METHODS

3.1 Introduction

There are a large number of design methods available to determine the buckling capacity of a gusset plate in a BRB frame. It is clear from experimental testing that not all of these methods will result in a conservative prediction of buckling capacity (Chou et al. 2012; Tsai and Hsiao 2008). This chapter seeks to evaluate each method investigated in Section 2.4 against two experimental BRB frame tests that have failed by gusset plate sway buckling. The assumptions and limitations of each method have also been considered to better understand how each method operates and determine why a method may not be able to accurately predict the buckling capacity of a gusset plate.

The experimental BRB tests from Chou et al. (2012) and Tsai et al. (2004) will be evaluated using each design method and compared to the observed experimental buckling capacity. No safety reduction factors will be applied for each design method as the intention is to evaluate each method's accuracy.

The aims of this chapter are to:

6) Discuss the limitations and assumptions made by a number of gusset plate buckling capacity design methods, and
7) Evaluate the buckling capacity design methods against two experimental BRB frame tests that have failed by gusset plate sway buckling to determine their suitability.

3.2 Assumptions and Limitations of Current Design Methods

The following will discuss the limitations and assumptions of the design methods discussed in Section 2.4. The basic assumptions of each design method have been summarised in Table 3.2-1.

Table 3.2-1: Summary of buckling capacity method assumptions

Method	Column Curve	Effective Width*	Length	Effective Length Factor	Other Assumptions
Thornton	AISC	Whitmore $\theta = 30^0$	Average Thornton	0.65	
Modified Thornton	CAN/CSA-S16.1-M89	Whitmore $\theta = 45^0$	Splice plate end to beam/column	0.65	
NZS 3404	NZS 3404 $\alpha_b = 0.5$, $k_f = 1.0$	Whitmore $\theta = 30^0$	Average Thornton	0.7	
HERA R4-80	NZS 3404 $\alpha_b = 0.5$, $k_f = 1.0$	Whitmore $\theta = 30^0$	Average Thornton	0.5	
Working Point	None (Euler elastic buckling)	Connection considered	Beam-Column joint centre to BRB end	2.0	
Koetaka et al. (2008)	None (Euler elastic buckling)	Connection considered	Beam-Column joint edge to BRB end	2.0	Considers BRB length as adjustment factor
Tsai and Hsiao (2008)	None (Euler elastic buckling)	Whitmore $\theta = 30^0$	Maximum Thornton	2.0	
Chou et al. (2012)	AISC	Whitmore $\theta = 30^0$	Average Thornton	2.0	
Takeuchi et al. (2014)	AIJ elasto-plastic	N/A	N/A	2.0	Considers gusset plate as rotational spring
Clifton (2015)	NZS 3404 $\alpha_b = 0.5$, $k_f = 1.0$	Whitmore $\theta = 30^0$	Average Thornton	1.2	Safety factor = 3.5

* dispersion angle, θ, to be used in Equation 2.4-1.

Many of the current design methods available to determine gusset plate buckling capacity are a modification of the Thornton method (Thornton 1984), which assumes that the gusset plate behaves as an equivalent buckling column with an equivalent length equal to the Thornton length and an equivalent width equal to the Whitmore width. Thus, their limitations are often similar when considering buckling length, the second moment of area, and inelastic buckling.

3.2.1 Equivalent Column Length

Many of the buckling methods assume the gusset plate has fixed-fixed boundary conditions. This is considered by using an effective length factor. The theoretical effective length factor for fixed-fixed boundary conditions is 0.5, and this is used by the Hera R4-80 Method (HERA 1994). As these boundary conditions may not be perfectly rigid, it is more common to use an

effective length factor of 0.65. The NZS 3404 method expects the beam-column joint and brace connections to be more flexible. For fixed-fixed conditions, an effective length of 0.7 is used.

The Clifton method considers an effective length factor of 1.2 (MacRae and Clifton 2015). This factor is equivalent to fixed-roller boundary conditions accounting for some flexibility in the beam-column joint. This boundary condition is plausible if both gusset plates buckled at the same time causing the BRB to translate out-of-plane, effectively acting like a roller at the gusset plate interface to the BRB, as seen in Figure 3.2-1. However, this failure has not been observed in experimental testing. It has been shown by Yam and Cheng (1993) and Rabinovitch and Cheng (1993) that the Thornton method is conservative for fixed-roller boundary conditions when using K = 0.65 and so this failure would not be expected to occur.

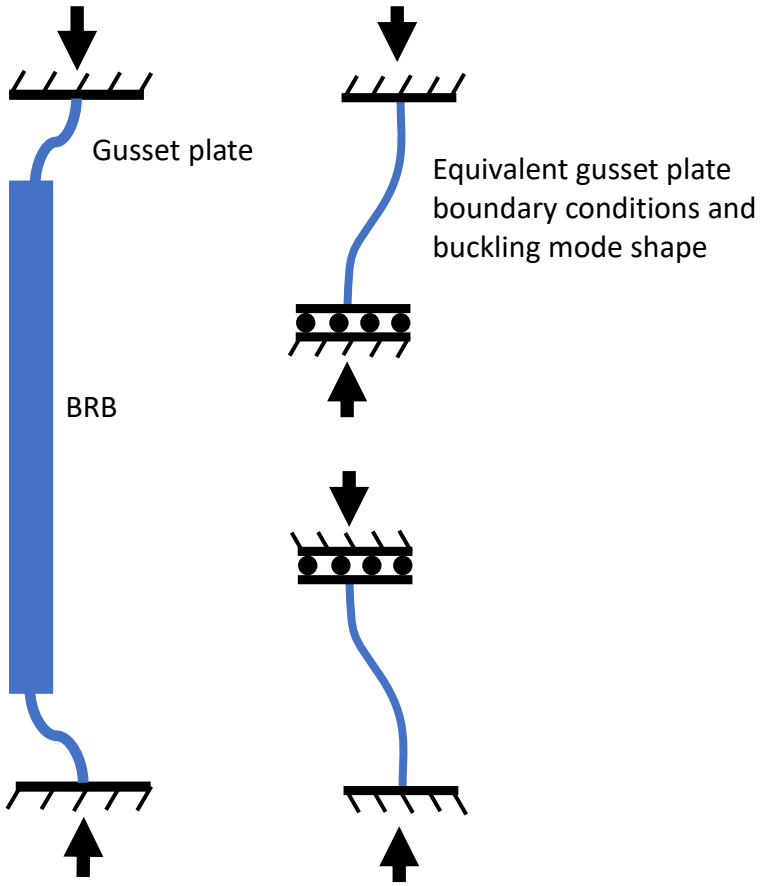

Figure 3.2-1: Failure mechanism, considering both gusset plates buckling, causing BRB out-of-plane translation and fixed-roller boundary conditions

For gusset plate sway buckling in BRB frames, using fixed-free boundary conditions and an effective length factor equal to 2.0 may be appropriate due to the end of the BRB hinging. This failure mechanism can be seen in Figure 3.2-2. Some methods, including the working point method and the methods proposed by Tsai and Hsiao (2008) and Chou et al. (2012) consider K = 2.0. This assumption may not be conservative because it does not consider

any flexibility in the beam-column joint. In the case of chevron configuration BRB frames, beam joints can have significantly lower rotational stiffness than standard beam-column joints. This would indicate the possibility that an effective length factor larger than 2.0 may be appropriate for gusset plates for some BRB frames.

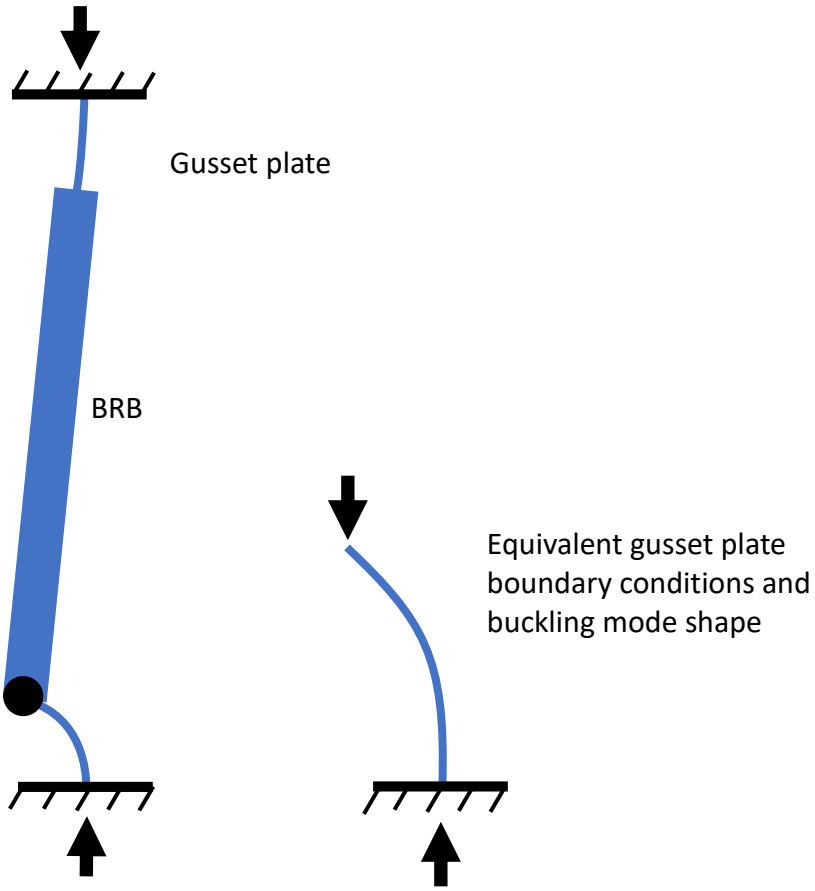

Figure 3.2-2: Failure mechanism, considering BRB end hinging, causing out-of-plane translation and fixed-free boundary conditions

The Tsai and Hsiao (2008) method uses the maximum Thornton length. This length is more conservative than the average Thornton length and may not be a true representation of the equivalent column length.

As to be shown in Section 6.5.8, the Thornton length may not be a reliable indicator of buckling capacity. A parametric study of gusset plates found that buckling capacity can fluctuate as the Thornton length is increased.

The working point method considers an equivalent column length from the end of the BRB restrainer to the centre of the beam-column joint. This is a significantly larger length than the Thornton length. However, the method considers a larger second moment of area.

3.2.2 Second Moment of Area

To account for the second moment of area of the equivalent buckling column, the cross section of the gusset plate is considered by the Whitmore width and the thickness of the gusset plate in most design methods.

The Whitmore width was developed to estimate the yield capacity of the gusset plate. The estimation of yield capacity using the Whitmore method has been found to be over conservative in experimental testing (Gross 1990). This may indicate that the Whitmore width is too large an estimate of the gusset plate width. However, the modified Thornton method considers a modified Whitmore width that is larger, indicating that the standard Whitmore width is not large enough.

It is possible to alter the geometry of a gusset plate without changing the Whitmore width. This is commonly achieved by designers who taper the edges of the gusset plate instead of designing a rectangular section, as seen in Figure 3.2-3. It has been shown in a number of cases, such as in testing by Rabinovitch and Cheng (1993) and Sheng et al. (2002), that decreasing the size of the gusset plate without affecting the Whitmore width (or Thornton length), can result in a lower buckling capacity. This is because the Whitmore width is dependent on splice plate bolt spacing and does not explicitly consider the cross-sectional width of the gusset plate. There may be cases where design methods using the Whitmore width for tapered gusset plates become non-conservative.

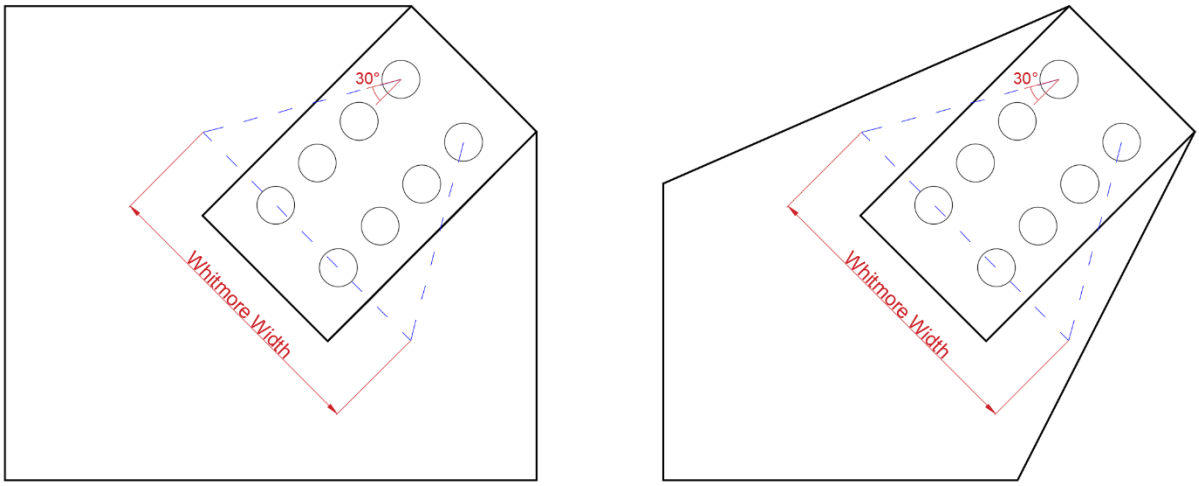

Figure 3.2-3: Gusset plates with different geometric cross sections and equal Whitmore widths

In Section 6.5.7 it is shown that the Whitmore width might not be a reliable indicator of buckling capacity. Using a parametric study, it is found that buckling capacity can fluctuate as the Whitmore width is increased.

The working point method and the method proposed by Koetaka et al. (2008) consider the cross section of the connection region at the face of the BRB restrainer end instead of the gusset plate equivalent cross section. This cross section results in a significantly larger second moment of area as it is generally stiffened. The length considered by these methods includes both the connection region and the gusset plate. Because the cross section changes size over the length considered, it is likely that this assumption is not conservative.

The Koetaka et al. (2008) method also accounts for the length of the BRB in relation to the length of the connection. Most design methods do not consider how other elements in the BRB system affect the gusset plate buckling capacity. However, this assumption is roughly approximated based on the first Taylor series of the sine function which may not be suitably accurate.

3.2.3 Inelastic Buckling

The modulus of elasticity in each of the design methods considered is determined from the elastic response of the steel material used in a gusset plate. When a gusset plate yields, or is close to yielding, the modulus of elasticity will decrease. This means that a gusset plate that buckles inelastically will buckle at a lower capacity than a geometrically identical gusset plate with material properties that allow it to buckle elastically.

A column curve, such as the AISC column curve (AISC 2005a), is applied by some methods to account for this reduction in capacity. The column curve also considers other column buckling reduction factors such as out-of-straightness, residual stresses and accidental eccentricities. It is currently unknown how these reduction factors affect gusset plates, but it is unlikely that the magnitude of the reduction is equal for both columns and gusset plates.

The NZS 3404 method uses the NZS 3404 column curves instead of the AISC column curve. There are five separate column curves in NZS 3404, based on different column residual stress profiles (Standards New Zealand 1997). For gusset plates, $\alpha_b = 0.5$, which indicates a column curve used for I-sections welded from either flame cut plates or as-rolled plates up to 40 mm. The value of 0.5 indicates greater residual stresses leading to a greater stiffness reduction and so this value may be conservative. No experimental studies appear to have been performed to verify the appropriateness of this column curve for gusset plates.

The column curves that are applied are likely to be too conservative for gusset plates. Plate buckling theory indicates that a plate will have additional post-buckling strength when it buckles due to a redistribution of load (Sheng et al. 2002). This is unlike column behaviour and

it has been shown that for local buckling, the Thornton method is often too conservative in predicting gusset plate buckling capacity (Yam and Cheng 1994).

To account for load redistribution after buckling, the modified Thornton method (Yam and Cheng 1994) uses a larger Whitmore width than the Thornton method. Yam and Cheng (1994) recommend that the method is only applied to inelastic gusset plate buckling when the elastic buckling capacity is two times the yield capacity. The modified Thornton method will be less conservative as it predicts a higher buckling capacity.

Some methods, such as that proposed by Tsai and Hsiao (2008) and the working point method do not consider inelastic buckling. These methods will be un-conservative for gusset plates that buckle inelastically. However, they may still be appropriate for gusset plate sway buckling in BRB frames as the buckling capacity is below the yield capacity.

3.2.4 Takeuchi et al. (2014) Method

The Takeuchi et al. (2014) method considers the gusset plate as a rotational spring and not an equivalent buckling column. It also considers the beam-column joints, gusset plates, connections, and the BRB explicitly, as such it will be assessed separately.

The method makes several approximations to reduce the number of terms. This includes assuming that the length of the connection is approximately 1/4 of the BRB length, which may not always be appropriate.

The method considers the Architectural Institute of Japan (AIJ) elasto-plastic column curve for the connection and also explicitly considers the initial imperfection in the BRB system. This is likely to be more realistic than methods that consider only column buckling curve.

It is assumed that the beam-column joint and the gusset plate behave as a single rotational spring. This is a limitation to design as currently, the most effective means of determining the stiffness of this rotational spring is through experimental testing or developing a calibrated finite element model of the beam-column joint and gusset plate. This is time-consuming and can be difficult for a designer to calibrate if experimental testing is not available to confirm the model's validity.

The rotational spring assumption of the gusset plate may be unreasonable as the gusset plate may be large enough in some designs to be more appropriately modelled as a flexural element with length instead of a single point.

Determining the combined rotational stiffness of the gusset plate and beam-column joint is difficult to achieve. Finite element modelling of the gusset plate and beam-column joint is currently the preferred method, though this is time-consuming and requires the use of complex software. A calculation method has been proposed by Kinoshita et al. (2008). However, the method is currently only available in Japanese and is only accurate for rigid beam-column joints. The method becomes non-conservative when beam and column deformation is considered.

The Takeuchi et al. (2014) method assumes a buckling mode shape. This means that the method will be an upper bound solution as the actual buckling mode shape is likely to be unknown to the designer.

Both the experimental tests from Chou et al. (2012) and Tsai et al. (2004) use uniquely designed BRBs. The Takeuchi et al. (2014) method uses equations developed by Matsui et al. (2010) to determine the rotational stiffness at each end of the BRB. Unfortunately, the assumptions of these equations are only applicable to standard rectangular or circular BRBs and are not applicable to the all-steel BRB used by Tsai et al. (2004) or the "sandwiched" BRB used by Chou et al. (2012). As such the Takeuchi et al. (2014) method cannot be evaluated for these experimental BRB frames.

3.2.5 Summary of Design Methods

3.3 Evaluation of Current Design Methods

Each gusset plate buckling capacity design method was compared to two experimentally tested BRB frames which failed by gusset plate sway buckling. The BRB frame tested by Chou et al. (2012) failed at a capacity of 693 kN and the frame tested by Tsai et al. (2004) failed at 805 kN. Table 3.3-1 compares each discussed design method to these two frames. A ratio of each frame's experimental capacity to each design method capacity is presented. The methods which have been found to be non-conservative have been shaded in grey. All calculations made for each design method can be found in Section 10.1 in the appendices for the Chou et al. (2012) experimental BRB frame.

Table 3.3-1: Evaluation of design methods for experimentally tested BRB frames

Design Method	Tsai et al. (2004) Gusset Capacity (kN)	Chou et al. (2012) Gusset Capacity (kN)	Tsai et al. (2004) Capacity / Design Method Capacity	Chou et al. (2012) Capacity / Design Method Capacity
Thornton	2181	1339	0.37	0.52
Modified Thornton	3446	1808	0.23	0.38
NZS 3404	2073	1231	0.39	0.56
HERA R4-80	2180	1331	0.37	0.52
Working Point	1781	3479	0.45	0.2
Koetaka et al. (2008)	1860	3609	0.43	0.19
Tsai and Hsiao (2008)	842	384	0.96	1.8
Chou et al. (2012)	1469	621	0.55	1.12
Clifton (2015)	1780	2178	0.45	0.32

*Non-conservative ratios shaded grey

It can be seen that no method can conservatively predict the buckling capacity of both experimentally tested BRB frames. The Tsai and Hsiao (2008) method is the most accurate for the Tsai et al. (2004) BRB frame and is almost conservative. The method is conservative for the Chou et al. (2012) BRB frame. It is clear that this method requires further investigation to ensure that it can be relied upon for a large range of gusset plates.

The most accurate method for the BRB frame tested by Chou et al. (2012) was the method presented by Chou et al. (2012). However, this method is not conservative for the Tsai et al. (2004) BRB frame. The Chou et al. (2012) method is less conservative than the Tsai and Hsiao (2008) method despite considering the AISC column curve which reduces the estimated buckling capacity. It is clear that the assumption to use average Thornton length over the maximum Thornton length results in a higher estimated buckling capacity which can be non-conservative for gusset plate sway buckling.

The assumption of an effective length factor equal to 2.0 may be reasonable. However, it clearly requires further investigation to ensure it will be accurate for a wide range of gusset plates. Chapter 5 investigates the fixed-free boundary condition assumption further.

Design methods which assumed fixed-fixed boundary conditions are clearly unsuitable for predicting gusset plate sway buckling in BRB frames. The estimated design capacities are significantly higher than the true buckling capacity, making their use highly non-conservative.

The Clifton method did not have the 3.5 safety factor applied in Table 3.3-1 to compare each methods assumptions fairly. It was non-conservative for both frames. It is clear

that assumed boundary conditions of fixed-roller are not sufficient for gusset plate sway buckling. If the 3.5 safety factor were applied, the design method is conservative for both BRB frames. For the Chou et al. (2012) frame, the Clifton method is overly conservative, with the experimental buckling capacity 2.6 times larger than the estimated capacity. This may result in a designer choosing a significantly stiffer gusset plate than required. Gusset plates that are too stiff will increase the demands on the beam-column joint which can lead to damage (Palmer et al. 2016). MacRae and Clifton (2015) recommend the gusset plate be welded to a flexible end plate on one edge to reduce damage.

Both the working point method and the Koetaka et al. (2008) method were not conservative for both BRB frames despite being designed specifically for BRB frames and considering an effective length factor of 2.0. The length considered was also significantly larger than other methods. Considering the second moment of area of the connection region, and not the gusset plate, will not provide an accurate estimate for buckling capacity. The connection region is already significantly stiffer than the gusset plate so an increase in the connection second moment of area is unlikely to result in a significant increase in buckling capacity. This relationship has been explored further in Section 7.6.2.3.

3.4 Conclusion

It is clear that more investigation into the design methods proposed by Chou et al. (2012) and Tsai et al. (2004) is needed to understand better why they are not always conservative, and if adjustments can be made to develop a conservative buckling capacity design method.

The aims at the start of this chapter have been addressed:

1) The limitations and assumptions made by a number of gusset plate buckling capacity design methods have been considered, and a number of the methods are unlikely to be suitable for gusset plate sway buckling in BRB frames.
2) None of the design methods evaluated has been able to estimate the gusset plate buckling capacity of both experimentally tested BRB frames conservatively.

4 FRAME ACTION EFFECTS

4.1 Introduction

Experimental testing has shown that the frame action effect has a negative impact on BRB frame performance (Chou and Liu 2012; Christopulos 2005; Mahin et al. 2004), including indirectly causing gusset plate sway buckling in a number of cases (Christopulos 2005). It has also been shown to cause gusset plate buckling directly when the BRB is in tension (Mahin et al. 2004). It has not been made clear if there is a direct effect on gusset plate buckling, either positive or negative, when the BRB is in compression. Determining the effect of frame action and its magnitude on gusset plate compressive buckling is important as it may help explain why current design methods are unable to predict gusset plate buckling capacity accurately.

To determine the effect of frame action on gusset plate buckling capacity in BRB frames, a finite element model of a BRB frame will be developed and analysed with and without frame action forces. It should be noted that previously published work by Westeneng et al. (2015) used a less refined finite element model and is no longer valid.

The aims of this chapter are to:

1) Develop a reasonable finite element model of an experimentally tested BRB frame that has experienced gusset plate sway buckling failure,
2) Modify the finite element model such that frame action forces can be removed,
3) Compare the buckling capacity of the two finite element models considering frame action forces and no frame action forces to determine the effects of frame action forces on buckling capacity,
4) Evaluate the benefit or detriment of frame action forces to gusset plate design.

4.2 Methodology

To determine the effect of frame action forces on gusset plate buckling capacity, it was proposed that a finite element model of a BRB frame be developed and then displaced until the gusset plate buckled. The BRB frame would be tested with and without frame action forces being applied.

An initial finite element frame model was developed to be verified against experimental testing. The finite element model was then modified to consider two cases: 1) a frame that does not allow frame action forces to affect the attached gusset plate, and 2) a frame that does allow frame action forces.

4.2.1 Experimentally tested BRB Frame Model

The BRB frame from Chou et al. (2012) was chosen to consider the effects of frame action. This choice was made because the frame is a diagonal configuration which has more pronounced frame action effects. The frame is also suitably documented, with enough geometric information available to accurately develop a finite element model. The BRB frame finite element model was able to be validated by comparing its buckling capacity to the experimental test. The model, along with its fixed base boundary conditions, can be seen in Figure 4.2-2.

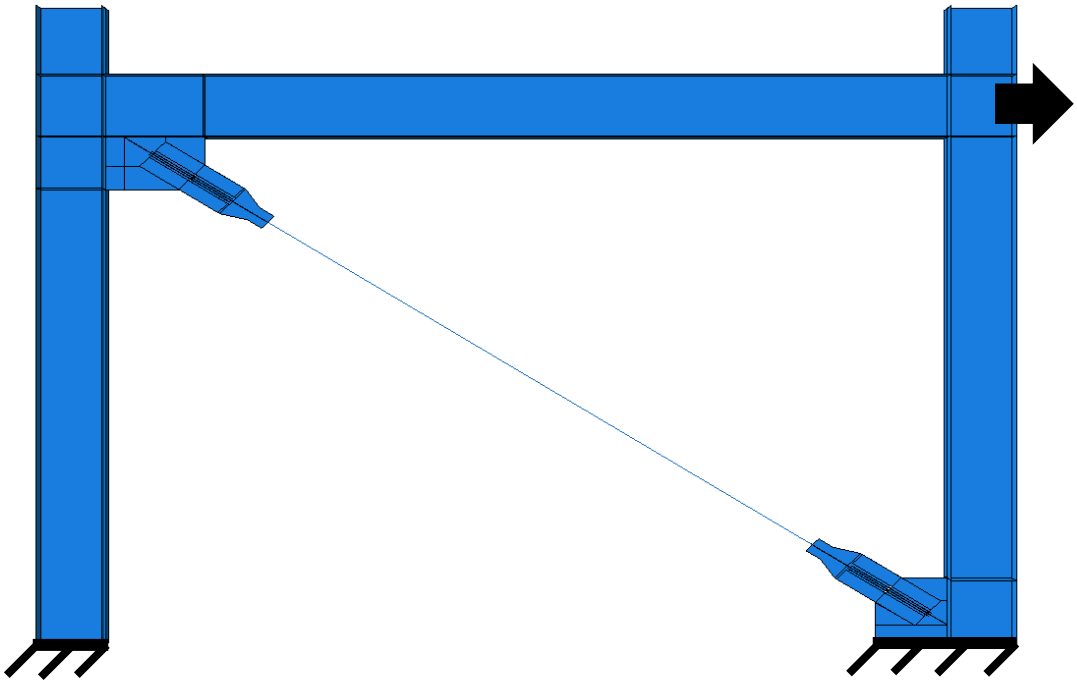

Figure 4.2-1: Boundary conditions for finite element model of Chou et al. (2012) BRB frame

One limitation of choosing this frame to investigate the effects of frame action is that the frame does not have additional gravity load along the beam. Additional gravity loading, such as from a concrete floor diaphragm will preload the gusset plate with some compressive stress from the beam. This may alter the gusset plate buckling capacity.

4.2.2 Frame Action Forces Removed Model

To remove frame action forces from the frame, a reduced model was developed that resulted in the same force being applied to the BRB and prevented the beam-column joint from opening and closing. The boundary conditions of this model can be seen in Figure 4.2-2.

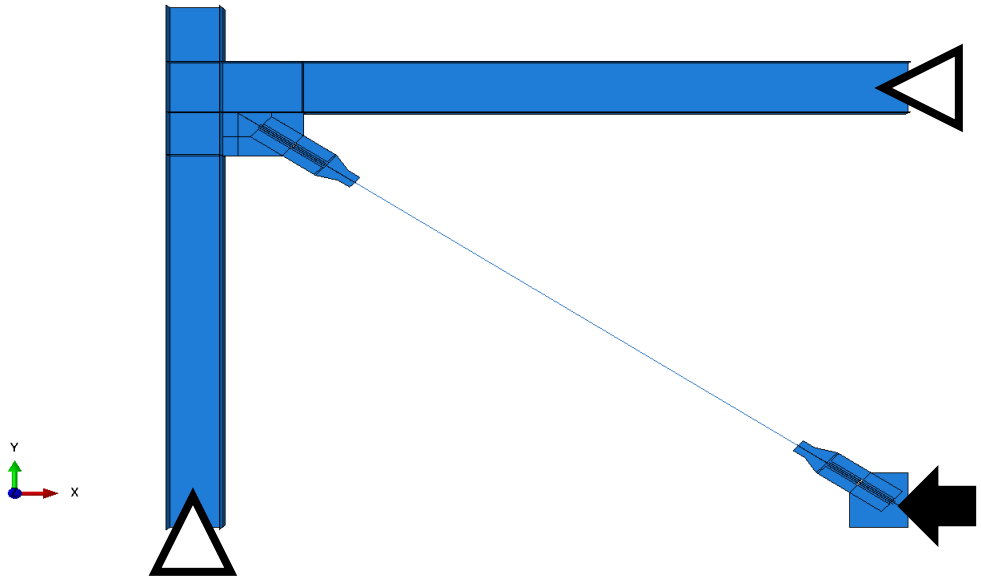

Figure 4.2-2: Boundary conditions for finite element model without frame action forces

Removing frame action forces was achieved by removing the right column from the model and replacing the beam to right column connection with a pin. The left column was also pinned at the base. Instead of the right end of the beam being displaced to cause compression in the BRB, the BRB member itself was displaced to the left at the bottom gusset end. This method is similar to that of Lin et al. (2013) and was verified by observing that no rotation between the beam and column at the joint occurred.

4.2.3 Frame Action Forces model

As the frame action forces removed model has heavily modified the original BRB frame, it was important to develop an additional reduced model that allowed the beam-column joint to open and close. This ensured that the reduced model without frame action forces is a valid model.

The model with frame action forces included is identical to the model without frame action forces but with boundary conditions to allow frame action forces. It can be seen in Figure 4.2-3 that the left column base and the BRB bottom gusset end are fully fixed, and the model is displaced at the right end of the beam. This model was compared to the full finite element model to ensure that the changes did not have a drastic effect on the model's ability to

resemble the experimental data. The model was observed to have rotation between the beam and the column at the joint indicating frame action forces were present.

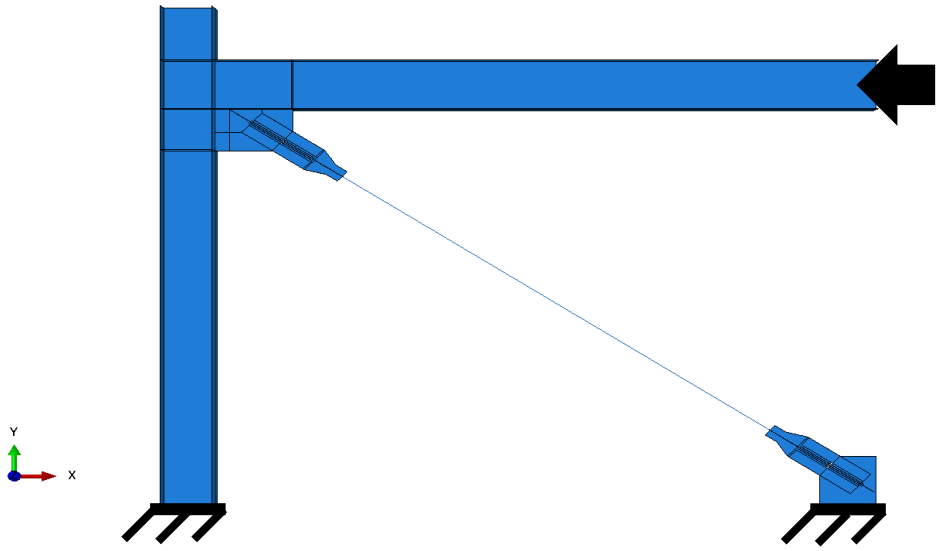

Figure 4.2-3: Boundary conditions for finite element model with frame action forces

4.3 Finite Element Model

All three finite element BRB frame models were developed in Abaqus FEA (Dassault Systemes 2005a) as a representation of the Chou et al. (2012) experimental test frame. All geometric dimensions and materials values were taken from Chou and Liu (2012) and Chou et al. (2012), including Figure 2.3-19 as well as additional gusset plate dimensions from Tsai (2015), which have been presented in Figure 4.3-1.

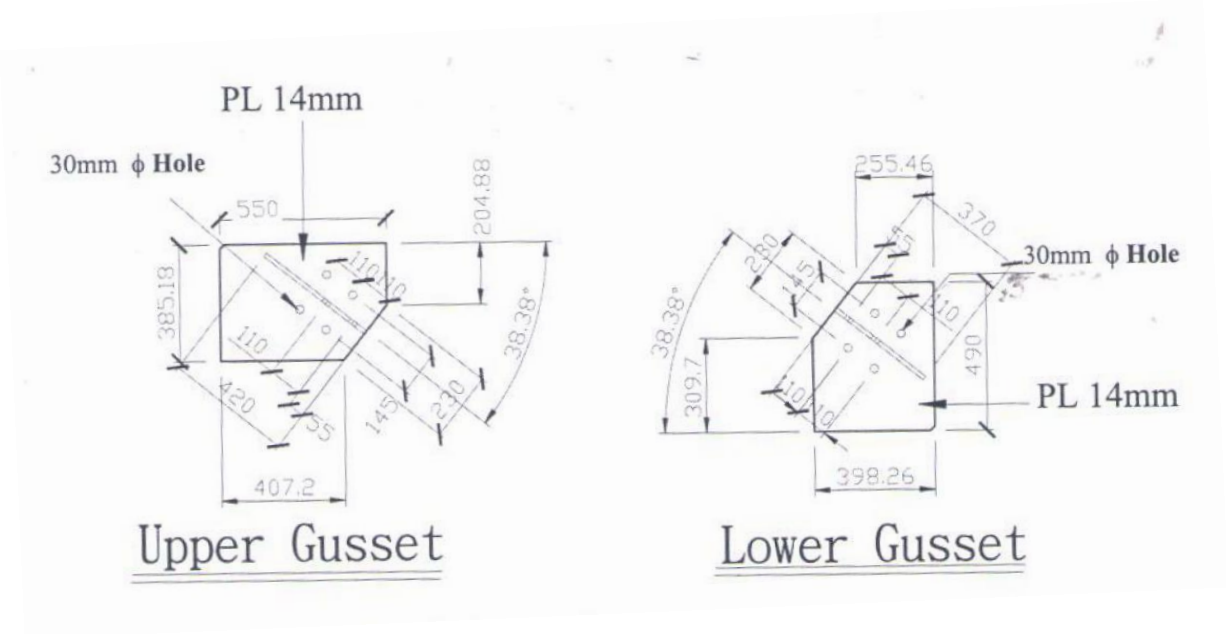

Figure 4.3-1: Gusset plate dimensions and bolt hole locations (Tsai 2015)

4.3.1 Modelling Elements

4.3.1.1 Shell Elements

Shell S4R elements were used to model the beams, columns, gusset plates, and connections. This element type was chosen to form the majority finite element model as it can accurately model thin plates. Additionally, if solid elements were chosen, the computational time of the model would significantly increase.

Shell S4R elements are a four-sided linear general purpose element. They are defined by four nodes. The shell elements also use uniformly reduced integration, which reduces computational time, and avoids shear and membrane locking. Shear locking is an error that can occur in linear four-sided elements where curvature in the element under bending cannot be accurately modelled. It is likely that the shell elements in the BRB frame model will experience significant curvature because of frame action and/or buckling so it is essential that shear locking is avoided.

One issue with using a reduced integration shell element is the potential for hourglass modes that may propagate over the mesh. This occurs when individual elements deform but the overall mesh does not deform. Abaqus applies hourglass control algorithms to prevent this error and visual inspection of the deformed shape can also confirm that undesirable hourglass deformations are not present.

4.3.1.2 Beam Elements

To fully model the BRB, considering the steel core, unbonding medium, concrete filling, and steel outer casing, is very computationally expensive. Modelling the BRB as only the steel yielding core and ignoring the restraining concrete and outer casing is not possible as it will buckle out-of-plane before reaching its compressive yielding capacity.

Most research approaches this issue by modelling the BRB as a truss beam element (Chou and Liu 2012; Lin et al. 2014). This ensures that the yielding behaviour of the BRB is approximated and that the BRB is unable to buckle out-of-plane. However, this approach fails to capture two behaviours: 1) the confining effect from the outer casing and concrete filling that causes the BRB to yield at a force about 1.3 times larger in compression compared to tension, and 2) any out-of-plane deformation that the BRB experiences along its length.

The first behaviour means that for a particular displacement, the compressive force in the BRB is likely to be less than what has occurred in the experimental model. Finite element modelling of BRB frames has determined that the lack of additional compressive force will not

cause a significant difference in frame action forces on the connection region compared to the experimental test (Chou and Liu 2012).

The second behaviour was considered important, as although the BRB has a relatively high stiffness, it is not completely rigid. To account for any small out-of-plane deformation that may occur along the length of the BRB during buckling or otherwise, the BRB element has been modelled as two coupled beam elements instead of a single truss beam. The first beam element considers the BRB yielding core and has elastic and plastic material properties and a geometric profile matching the yielding core dimensions.

The second beam element considers the restraining media of the concrete and the outer steel casing. Because these are unbonded from the yielding core, no axial force will enter the restrainer and it will behave elastically. The geometric profile of the restraining beam must be input in terms of a single material. Equivalent section geometry was determined by modifying the area of the concrete contribution of the BRB by the ratio of elastic moduli of concrete and steel. This allowed a single equivalent section geometry for the restraining beam with a single elastic steel material.

It should be noted that Abaqus can assign a beam section with a generalised profile that allows separate properties for the second moment of area and area. This could be used to define a single BRB beam element with area and material properties associated with the core plate, and inertial properties associated with the restraining media.

However, Abaqus will not allow a generalised profile to be applied if the element has inelastic material properties. As it is essential to model the core plate yielding behaviour, the generalised profile cannot be used. Using two coupled beam elements was found to be the most appropriate and simple solution.

Coupling of yielding core beam and restraining beam

To couple the yielding core beam element and the restraining beam element together, coupling constraints were used. The two beams were coupled in all degrees of freedom except axially. This means that forces that are axially applied to the yielding core will not be transferred to the restraining beam. This is desirable and mimics the behaviour of the unbonding medium in a BRB preventing the transfer of axial force to the restraining elements. Because the other degrees of freedom are constrained, if the core plate was to buckle out-of-plane, it would engage the stiffness of the restraining beam and be unable to do so.

The master nodes were defined on the yielding core beam, with the slave nodes defined on the restraining beam. This was considered sensible as the yielding core beam influences the behaviour of the restraining beam.

To ensure that the restraining beam is still in the same location as the yielding core beam throughout an analysis, a single couple in the centre of the beam elements was constrained in all degrees of freedom. This will not introduce the same axial force that the yielding core beam is experiencing into the restraining beam as there is no other couple or link between the restraining beam and the rest of the finite element model to develop a reaction force.

The two beam elements are coupled by kinematic coupling. Abaqus offers three different coupling types: kinematic, continuum distributing, and structural distributing (Dassault Systemes 2005b). Kinematic coupling constraints are the strictest and impose rigid body motion between the reference master node and slave node for both translation and rotation. Continuum distributing constraints couple translation and rotation of the master node to the average translation of the slave nodes. Finally, structural distributing constraints couple translation and rotation of the master nodes to the average translation and rotation of the slave nodes.

This study determined that kinematic coupling was suitable to constrain the restraining beam to the yield core beam. This is because multiple couplings were used along the length of the beam. If there were not a sufficient number of couplings, the restraining beam was not able to prevent higher mode buckling of the yield core beam, as seen in Figure 4.3-2. It was determined that 1/16 times the length of the yielding core was an appropriate coupling spacing to prevent higher mode buckling. It is likely that this could be further optimised.

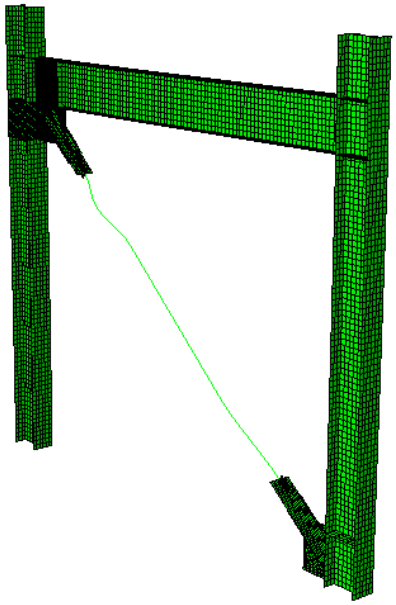

Figure 4.3-2: Buckling failure of BRB due to higher mode buckling

Sizing of BRB beam elements

Inside the restraining casing, the BRB consists of a non-yielding segment and the yielding core segment. By modelling the BRB as a coupled beam, it is difficult to include both segments while still accurately modelling the hinging behaviour that has been observed at the BRB end. Figure 4.3-3 shows how the BRB was detailed for the Chou et al. (2012) frame. The BRB used was a unique design with two C channels bolted together to form the outer steel casing. This design has been verified as performing like a standard BRB configuration with a stable hysteresis loop (Chou and Chen 2010).

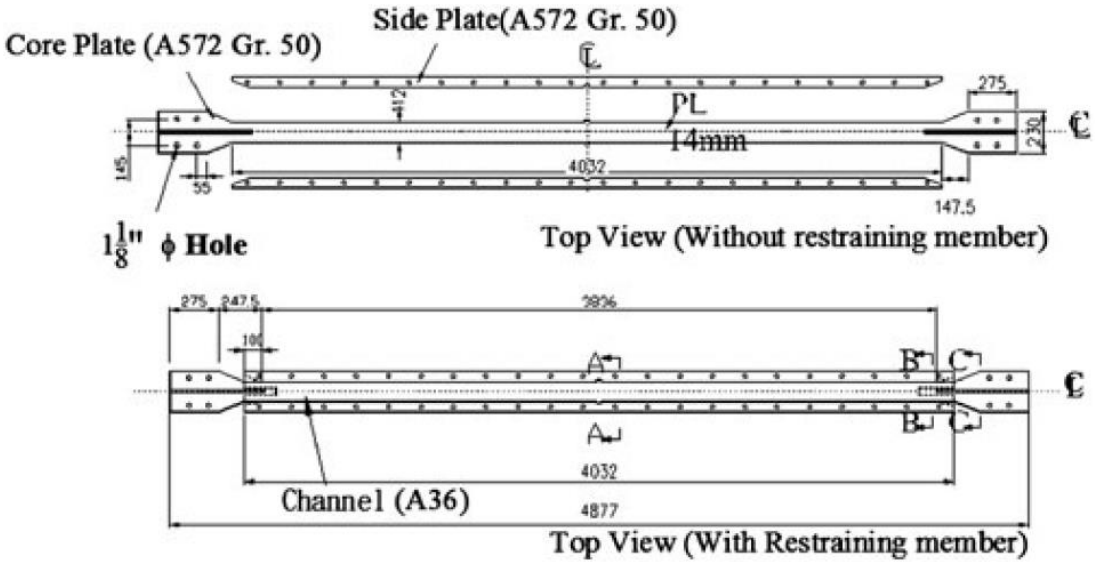

Figure 4.3-3: Schematic of BRB design used in experimental test (Chou et al. 2012)

In this case, the non-yielding segment of the BRB consists of a stiffener that extends inside the BRB casing by 100 mm. Based on the experimental results detailed in Chou and Liu (2012) and Chou et al. (2012), it has been assumed that the hinge has formed at the end of this stiffener at the start of the yielding segment. For this reason, the yielding core beam and the restraining beam in the finite element model considers only the yielding core length between the ends of the stiffener, as shown in Figure 4.3-4.

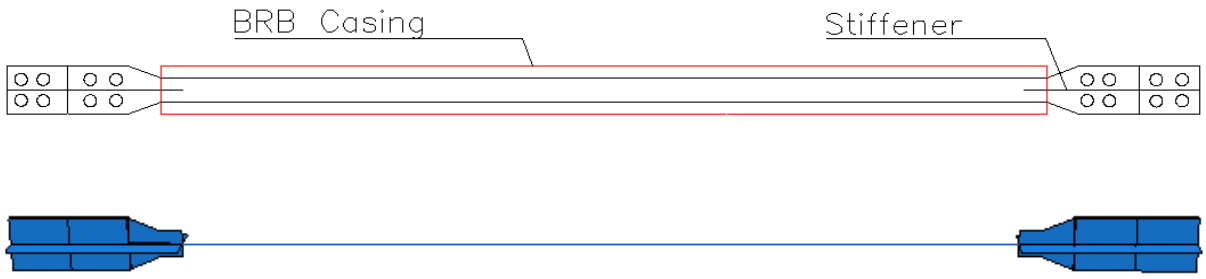

Figure 4.3-4: Comparison of BRB schematic and finite element model of BRB

Because of this decision, the finite element model will be conservative in its behaviour. There will be no additional stiffness provided by the BRB casing to the 100 mm non-yielding segment of the BRB. This assumption is likely to be valid as the BRB core will bend inside the casing once hinging occurs. This assumption has also been made by Chou and Liu (2012) in their finite element model.

4.3.2 Material properties

All material properties have been defined from Chou and Liu (2012) and Chou et al. (2012) and have been displayed in Table 4.3-1.

Table 4.3-1: Material properties used in finite element model

Element	Elastic Modulus (GPa)	Yield Strength (MPa)	Ultimate Strength (MPa)
BRB Yield Core	200	390	527
BRB Steel Casing	200	250	400
BRB Concrete	27.8*	-	35
Gusset Plate	200	385	525
Beam	200	344	448
Column	200	344	448

* Calculated using $E_c = 4700\sqrt{f_c'}$

4.3.3 Boundary Conditions

The boundary conditions of each of the three finite element models have been described in Section 4.2. Boundary conditions are either fully fixed in all degrees of freedom or pinned to allow unrestrained rotation about the out-of-plane axis.

4.3.4 Loading Regime

The finite element models have been loaded through applied displacements. In Abaqus, the maximum displacement was defined as the boundary condition of the displacement node. During analysis, the model will linearly displace until the maximum displacement has been reached at the final time step.

A displacement based loading regime instead of a force based loading was crucial to accurately determine the buckling capacity. If the model was force based, the force will continue to be applied to the model after it has buckled, making the exact buckling load unclear. By using displacement, the force inside the gusset plate will not increase after buckling.

4.3.5 Constraints between Shell Elements

Tie constraints were used to connect the columns, beam, gusset plates, and stiffeners together. These are master-slave constraints that tie translation and rotation between the selected nodes. Tie constraints are used on the assumption that they behave as a perfect weld between elements. It will not be possible to identify locations of any weld tear-out or degradation. For the particular experimental test being investigated by Chou et al. (2012), this was not a concern.

4.3.6 Constraints between Gusset Plate and Splice Plate

The splice plates that connect the BRB to the gusset plate are bolted in the experimental test. Some gusset plate finite element models assume that the splice plate is perfectly tied to the gusset plate through a surface tie constraint such as Chou and Chen (2009). However, to increase the accuracy of the model, the bolt connection has been modelled.

It was decided that mesh independent fasteners would be used to model the bolt connections. This allowed easier manipulation of the gusset plate and splice plate meshes, and reduced the time taken to model the bolts. To apply mesh independent fasteners to the model, reference points were placed at the centre of each bolt location on one splice plate. From there,

the following code was required to be entered into the keyword editor as it cannot be implemented through Abaqus' graphical user interface (GUI):

```
*FASTENER, INTERACTION NAME=Bolt1, PROPERTY=BoltProp,
      REFERENCE NODE SET=BoltNodes1, RADIUS OF
      INFLUENCE=12.5, SEARCH RADIUS=50
PositiveSplicePlateSurface
GussetPlateSurface
NegativeSplicePlateSurface


*FASTENER PROPERTY, NAME=BoltProp
12.5
1,5
```

Each bolt location was defined in the reference node set "BoltNodes1" and specified the fastener property "BoltProp". "BoltProp" defines the bolts to have a radius of 12.5 mm and specifies the degrees of freedom that are constrained. Abaqus requires the first and last degrees of freedom constrained. In this case degrees 1 to 5 were constrained, which indicates that the bolt will constrain the attached plates in all degrees of freedom but will allow rotation about the bolts axis. Because multiple bolts are used to connect the splice plates to the gusset plate, this unconstrained degree of freedom will be constrained in the global sense and will not affect the model.

The list of surfaces, "PositiveSplicePlateSurface", "GussetPlateSurface", and "NegativeSplicePlateSurface" define the plate surfaces which the bolt will connect. The points where the connection occurs are taken from the reference point position in a straight line normal to the plate surfaces. This connects the three surfaces at the location of the bolt translationally in all degrees of freedom and rotationally in two degrees of freedom.

Mesh independent fasteners were also used to connect splice plates to the rib stiffener that is present in this particular BRB frame. This detail can be seen in in the cross-section of the splice plate to gusset plate connection in Figure 4.3-5.

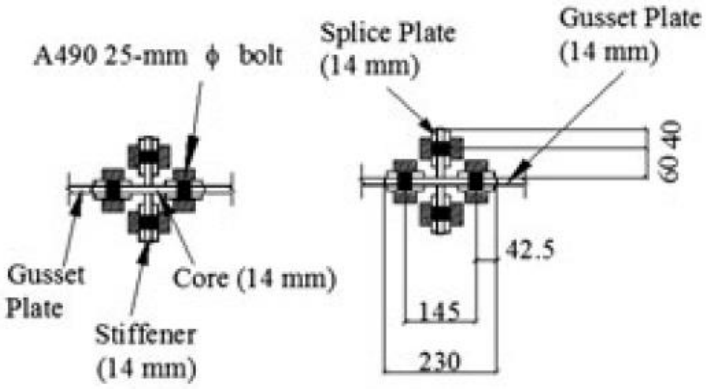

Figure 4.3-5: Cross section of splice plate to gusset plate bolt connection (Chou et al. 2012)

Because of the use of mesh independent fasteners, it has been assumed that the bolts behave rigidly and do not slip during displacement of the BRB frame. This has been considered reasonable based on the Chou et al. (2012) experimental test results.

4.3.7 Initial Imperfection

For the finite element model to buckle correctly in displacement analysis of the BRB frame finite element model, an initial imperfection must be applied. If this imperfection is not applied, the finite element model will remain in-plane and will not buckle even if the capacity in the gusset plate exceeds the buckling capacity. An initial imperfection based on the first buckling mode equal to 1/1000th of the BRB length was chosen. This equates to 3.8 mm at the maximum buckled displacement of the model. To achieve this, the finite element model was run under a buckling analysis which finds the buckling eigenvalue and the deformed shape of the model. This deformed shape was then implemented into the displacement analysis through the following code in the Abaqus model keywords editor:

```
*IMPERFECTION, FILE=ChouFrameBucklingModel, STEP=1
1,3.8
```

The first line tells the model to apply the imperfection from the buckling analysis file. The second line tells the model to apply only the first mode buckling deformation to an amplified displacement of 3.8. It is noted that the imperfection cannot be entered into Abaqus through the program's GUI.

4.3.8 Model Analysis

The model was run as a static – general analysis with non-linear geometry. This involves direct solving of matrices to determine stresses, forces, and deformations of the model. Non-linear geometry is deemed essential due to large displacements occurring in the model which may not otherwise be accurately calculated. The model runs from time zero to one with a maximum time step of 0.01. Abaqus was allowed to automatically reduce the time step required to find convergence. Displacement is applied linearly to the model over the total model run time.

4.3.9 Data Collection

It is difficult to extract the axial force inside the gusset plate in the diagonal reference plane of the BRB directly. However, it can be easily determined by observing at the force inside the yielding core beam element. Due to equilibrium, the axial force inside the BRB must be equal to the total axial force on the gusset plate. A history output was defined in Abaqus that captured the section force inside the BRB yielding core as the model was displaced. After analysis, this section force was able to be graphed against displacement of the frame, as shown in Figure 4.3-6. Buckling capacity will be defined as the maximum section force in the BRB yielding core.

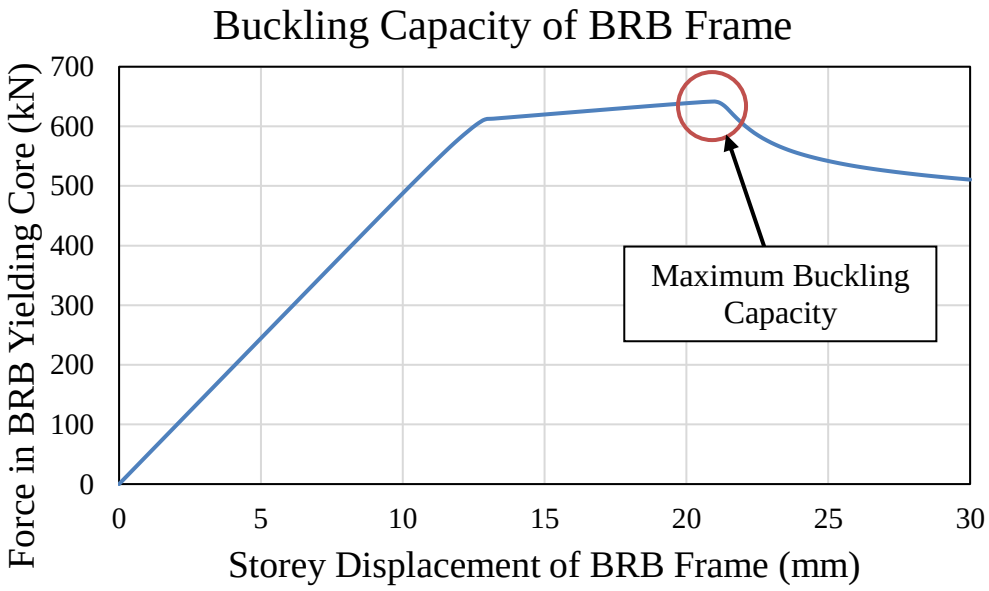

Figure 4.3-6: Force-Displacement relationship of BRB frame indicating buckling capacity

4.3.10 Mesh Size Independence

Mesh size independence was verified for the finite element model by reducing the approximate global mesh size until convergence of buckling capacity was observed. Table 4.3-2 shows the results for different average mesh sizes.

Table 4.3-2: Comparison of mesh sizes and their relationship to buckling capacity

Approximate Mesh Size (mm)	Buckling Capacity (kN)
75	653.3
50	656.8
25	661.7
50 / 25	660.9

It can be seen that there is only a 0.7 % difference between an approximate mesh size of 50 mm and 25 mm. The model is significantly slower computationally with a mesh size of 25 mm and smaller. It was decided to run the model with an approximate mesh size of 50 mm for the beams and columns, and an approximate mesh size of 25 mm for the gusset and splice plates. This allowed the model to take an acceptable amount of time to complete while ensuring accuracy is provided to the most important parts of the model. This was deemed an acceptable solution as there is only 0.1 % difference in buckling capacity between this option and the 25 mm mesh size option.

4.4 Results

4.4.1 Full Finite Element Model

The finite element model buckled at a capacity of 641.7 kN, compared to the experimental buckling capacity of 693 kN. Given the assumptions made in developing the BRB element, it was expected that the finite element model would estimate a lower buckling capacity. As the finite element model is about 8 % of the experimental buckling capacity, it was decided that the finite element model was a reasonably accurate representation of the true behaviour. The buckled shape also accurately matched the experimental model, as shown in Figure 4.4-1.

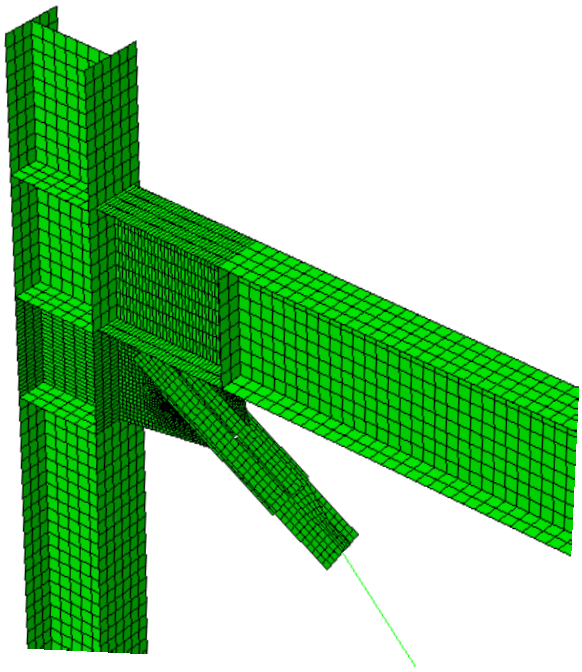

Figure 4.4-1: Buckled gusset plate in finite element model

4.4.2 Reduced Finite Element Model with Frame Action Forces

The reduced finite element model with frame action forces buckled at 627.7 kN. This is less than 3 % lower than the full finite element model. It was decided that the reduced finite element model was an accurate representation of the full finite element model. As such, the reduced finite element model without frame action forces will be sufficient to determine buckling capacity of the Chou et al. (2012) BRB frame when frame action forces are eliminated.

To verify that frame action forces are causing the beam-column joint to open, the deformed angle between the beam gusset plate edge and column gusset plate edge were measured. From the initial 90° angle, the deformed angle was found to be 90.0048° at 5 mm of model displacement and 90.0068° at the displacement equal to when buckling occurred. Although the change in angle deformation appears small, it is clear that the joint is opening and that frame action forces will be applied to the gusset plate.

4.4.3 Reduced Finite Element Model without Frame Action Forces

The reduced finite element model without frame action forces buckled at 593.8 kN. This is about 5 % less than the model with frame action forces. The reduction indicates that frame action has a stabilising effect that improves buckling capacity. During compression of the BRB,

the beam-column joint at the top gusset plate is opening, resulting in a force strut across the gusset plate that is in tension. This strut is perpendicular to axial compression in the gusset plate. It is likely that this tension strut is what stabilises the gusset plate and improved buckling capacity.

The deformed angle between the beam gusset plate edge and the column gusset plate edge was also checked for the reduced finite element model without frame action forces. This study determined that the deformed angle measured 90° at both a displacement of 5 mm and at the displacement equal to when buckling occurred in the model. This indicates that the beam-column joint was not opening during the analysis and is a clear indication that no frame action forces were being applied to the gusset plate.

4.5 Frame Action Forces at Larger Drifts

The reduced model with frame action buckled at a drift of 0.4 %, which is relatively small as BRB frames can be pushed to much larger drifts. Frame action forces increase as drift increases (Chou and Liu 2012). Therefore, it may be possible that BRB frames that experience large drifts are better protected against gusset plate buckling because of frame action forces.

To investigate this behaviour, both the reduced model with frame action and the reduced model without frame action were modified so that the BRB core plate yielded at a lower force. By yielding earlier, the frame will undergo a larger drift before the buckling capacity of the gusset plate has been exceeded.

The material properties of the yielding core beam element were modified for a yield strength of 390 MPa to 250 MPa, reducing the yield capacity from 611 kN to 343 kN. The ultimate strength of the yielding core was also reduced by 140 MPa, such that the slope of the plastic material behaviour did not change. Each of the three finite element models was analysed again and the results can be seen in Table 4.5-1. The reduced model with frame action buckled at approximately 2 % storey drift.

Table 4.5-1: Effect of frame action forces on buckling capacity considering large drifts

	Reduced Model with Frame Action	**Reduced Model without Frame Action**
Buckling Capacity	595.0 kN	553.4 kN

For the BRB frame with 2 % drift at buckling, frame action forces increased the buckling capacity of the gusset plates by 8 % when compared to a model that does not consider

frame action forces. For the BRB frame with only 0.4 % drift at buckling, frame action forces increased the buckling capacity of the gusset plates by 5 %.

This would indicate that the frame action forces do increase buckling capacity of gusset plates at larger drifts. However, this increase is still much smaller than the uncertainty in gusset plate buckling capacity in common gusset plate design methods, as shown in Section 2.4.

4.6 Cyclic Loading

Given that gusset plates have been shown to buckle in tension from frame action forces (Mahin et al. 2004), the effect of cyclic loading on gusset plate buckling in a BRB frame was also considered to ensure that this study is robust.

Repeated cyclic loading is unlikely to have a significant effect on buckling capacity of the gusset plate as the gusset plate should be designed in a way that it behaves elastically for each BRB cycle. The tensile yield capacity of the gusset plate will be designed to be larger than the tensile yield capacity of the BRB.

However, buckling capacity may still be reduced due to cyclic loading. When the BRB is in tension, the beam and column are pinching the gusset plate. There may be a point at which the gusset plate is loaded in compression by the BRB and the gusset plate is still pinched as the BRB transitions from tension loading to compressive loading.

To confirm this hypothesis, the finite element models considering frame action forces and no frame action forces were both linearly displaced to 1 % drift in tension and then in compression. As such, the BRB will initially yield in tension and then yield in compression until a displacement where the forces in the gusset plate cause buckling. A summary of the findings can be found in Table 4.6-1.

Table 4.6-1: Effect of frame action forces on buckling capacity considering cyclic loading

Loading Regime	Reduced Model with Frame Action	Reduced Model without Frame Action
Monotonic	627.7 kN	593.8 kN
Cyclic	576.0 kN	591.4 kN

The consideration of cyclic loading has decreased the buckling capacity of the reduced model with frame action by approximately 8 % when compared to monotonic loading. This would indicate that the gusset plate is still pinched by the beam and column at the time of buckling and so frame action forces have reduced the capacity. This was confirmed by

measuring the deformed angle between the beam and column as 89.957° at the time of buckling.

There are a number of limitations on this finding. It has only been found for one BRB frame analysed by finite element modelling. This BRB frame does not consider the effect that a floor slab on the beam may have on frame action or forces in the gusset plate. Further investigation is recommended, potentially through experimental testing, to quantify the effect.

4.7 Conclusion

It has been shown through finite element modelling of a BRB frame based on experimental testing by Chou et al. (2012), with and without frame action forces, that frame action can have a small effect on increasing gusset plate capacity when the frame is loaded in compression. In contrast to this finding, it was also shown that frame action forces can have a small decrease in gusset plate buckling capacity when the frame is in tension and then compression. It is recommended that further research into frame action forces on buckling capacity is undertaken considering cyclic loading.

The aims at the start of this chapter have been addressed:

1) A reasonable finite element model was developed to be within 10 % of the of an experimentally tested BRB frame's buckling capacity.
2) The finite element model was able to be adjusted such that frame action forces could be removed.
3) Frame action forces can provide 5 % additional buckling capacity at 0.4 % drift and 8 % additional capacity at 2 % drift for the Chou et al. (2012) BRB finite element model. When considering cyclic loading, frame action forces reduced buckling capacity by 8 %.
4) The frame action effect was found to be beneficial to buckling capacity when considering monotonic loading and detrimental to buckling capacity when considering cyclic loading.

5 EVALUATION OF GUSSET PLATE BUCKLING CAPACITY

5.1 Introduction

The gusset plate buckling capacity design methods proposed by Chou et al. (2012) and Tsai and Hsiao (2008) are a simple modification of the Thornton method to predict sway buckling failure in BRB frames. Section 3.3 shows that the method proposed by Tsai and Hsiao (2008) is almost conservative for the experimental frame tested by Tsai et al. (2004) and conservative for the frame tested by Chou et al. (2012). This chapter attempts to determine if the methods are suitable for designing a large number of gusset plates and, if necessary, find what modifications can be made to make the methods suitable.

The proposed methods use an effective length factor equal to 2.0. This indicates that the equivalent buckling column has boundary conditions that are fixed at one end, and free at the other end. Unfortunately, there have been no experimentally tested gusset plates with these boundary conditions. An appropriate way to test these boundary conditions without performing new experimental testing is to use finite element modelling.

Finite element modelling is a useful tool that can approximate experimental results. It can also be used to predict new results due to the versatility of the software used.

A range of gusset plate finite element models was developed based on previous experimental tests. These models were then validated by considering the experimental boundary conditions and comparing the finite element model buckling capacity to the experimental buckling capacity. Finite element models that were considered accurate were modified by changing the boundary conditions to fixed-free. The gusset plate interface to the beam-column joint was fixed in all degrees of freedom and the gusset plate interface to the brace was free in all degrees of freedom.

The buckling capacity of modified gusset plate models was then compared to the design methods proposed by Chou et al. (2012) and Tsai and Hsiao (2008). It could then be determined whether the assumptions made by these methods were valid. Other design methods were also considered.

The aims of this chapter are to:

1) Determine which gusset plate buckling capacity methods are accurate and conservative for experimentally tested gusset plates,
2) Validate finite element models of experimentally tested gusset plates by considering experimental boundary conditions and comparing finite element model buckling capacities to experimental buckling capacities,
3) Modify boundary conditions of validated finite element models to match the assumptions made by Chou et al. (2012) and Tsai and Hsiao (2008),
4) Determine which gusset plate buckling capacity methods are accurate and conservative for finite element models of gusset plates considering fixed-free boundary conditions.

5.2 Experimentally Tested Gusset Plates

By using experimentally tested gusset plates as the basis for the finite element models, the models can be validated based on their buckling capacity. The experimentally tested gusset plates discussed in Section 2.2.1 were evaluated for their suitability. Most papers were found to give sufficient geometric and material information to develop finite element models of the gusset plates.

Some experimentally tested gusset plates were excluded from this study. A number of gusset plates tested by Hu and Cheng (1987) and Yam and Cheng (1993) were eccentrically loaded by only having a single splice plate on one side of the gusset plate. This condition would not be suitable for gusset plates in BRB frames as it would increase the probability of sway buckling failure. Yam and Cheng (1993) also tested gusset plates with additional beam and column moments applied. These tests were not considered due to their similar buckling capacity to the regular gusset plates tested.

The gusset plates considered have been tested with two experimental boundary conditions, fixed-fixed, and fixed-roller. Finite element models with fixed-fixed boundary conditions will have the gusset plate edge that interfaces the beam-column joint fixed in all degrees of freedom and the gusset plate edge that interfaces with the connection region / brace also fixed in all degrees of freedom. Gusset plates were experimentally tested to fixed-roller conditions will be fixed in all degrees of freedom at both edges, except the gusset plate will be free to translate out-of-plane at the beam-column joint interface. This simulates the experimental test conditions where the gusset plate frame was attached to rollers to allow out-of-plane translation.

Gusset plates with fixed-fixed boundary conditions will have a theoretical effective length factor equal to 0.5 and gusset plates with fixed-roller boundary conditions will have an effective length factor equal to 1.0.

A summary of the experimentally tested gusset plates chosen for finite element modelling has been presented in Table 5.2-1 showing both geometric and material information. Figure 5.2-1 shows where geometric measurements have been taken. Gusset plates have been labelled based on each paper's authors, Gross and Cheok (1988), Hu and Cheng (1987), Naghipour et al. (2013), Rabinovitch and Cheng (1993), Sheng et al. (2002) and Yam and Cheng (1993).

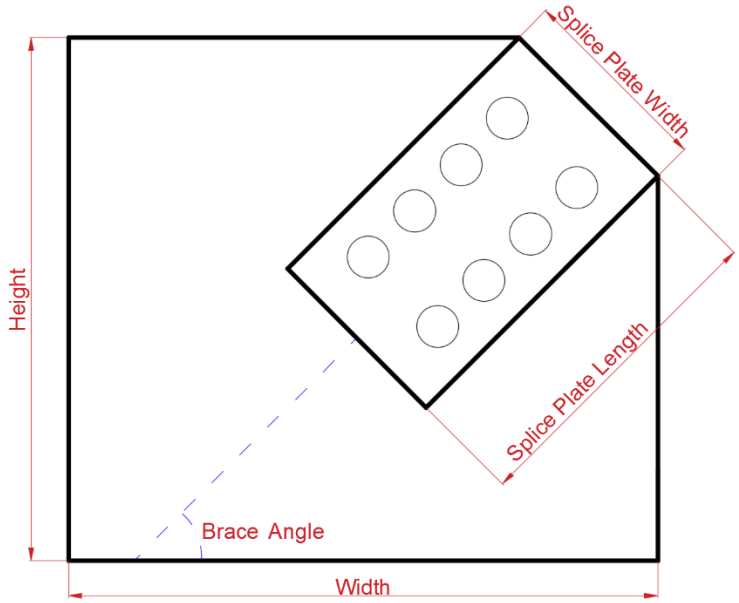

Figure 5.2-1: Gusset plate geometric information

Table 5.2-1: Summary of experimental gusset plates to be developed into finite element models

Gusset name	Height (mm)	Width (mm)	Thickness (mm)	Modulus of Elasticity (GPa)	Yield Strength (MPa)	Gusset Plate Angle (°)	Splice Width (mm)	Splice Depth (mm)	Experiment Effective Length
GC01	279.4	584.2	6.35	200	324	30	146	152	0.5
HC01	550	850	6.7	211	505	45	185	447	0.5
HC02	550	850	3.11	197	240	45	185	447	0.5
HC03	700	850	6.7	211	505	45	185	447	0.5
HC04	700	850	3.11	197	240	45	185	447	0.5
HC05	550	850	6.7	211	505	45	185	447	1
HC06	550	850	3.11	197	240	45	185	447	1
HC07	700	850	6.7	211	505	45	185	447	1
HC08	700	850	3.11	197	240	45	185	447	1
N01	500	500	8	210	300	45	200	230	0.5
RC01	450	550	9.32	206	449	45	148	380	1
RC02	450	550	6.18	206	443	45	148	380	1
RC03	450	550	9.32	206	449	45	148	380	1
S01	400	500	13.3	207.6	295	45	148	240	1
S02	400	500	13.3	207.6	295	45	148	380	1
S03	400	500	9.87	210.2	305	45	148	240	1
S04	400	500	9.87	210.2	305	45	148	380	1
S05	310	440	13.3	207.6	295	45	148	240	1
S06	200	390	13.3	207.6	295	45	148	240	1
S07	200	390	9.87	210.2	305	45	148	240	1

Gusset Name	Height (mm)	Width (mm)	Thickness (mm)	Modulus of Elasticity (MPa)	Yield Strength (MPa)	Gusset Plate Angle (°)	Splice Width (mm)	Splice Depth (mm)	Experiment Effective Length
YC01	400	500	13.3	207.6	295	45	148	310	1
YC02	400	500	9.8	210.2	305	45	148	310	1
YC03	400	500	6.5	210.2	305	45	148	310	1
YC04	400	500	13.3	207.6	295	45	148	310	1
YC05	400	500	9.8	210.2	305	45	148	310	1
YC06	400	500	6.5	210.2	305	45	148	310	1
YC07	700	850	13.3	207.6	295	45	148	450	1
YC08	700	850	9.8	210.2	305	45	148	450	1

5.3 Accuracy of Buckling Capacity Methods

To help investigate the most appropriate method for predicting sway buckling capacity, it was decided that the method must also be acceptable in predicting local buckling capacity.

As only the gusset plate is being looked at for this chapter, only some of the methods outlined in Section 2.4 are applicable. These methods have been summarised in Table 5.3-1.

Table 5.3-1: Summary of local buckling capacity methods investigated

Method	Column Curve	Effective Width	Length	Effective Length Factor
Thornton (max)	AISC	Whitmore $\theta = 30^0$	Maximum Thornton	0.65
Thornton (ave)	AISC	Whitmore $\theta = 30^0$	Average Thornton	0.65
Thornton, K=1 (ave)	AISC	Whitmore $\theta = 30^0$	Average Thornton	1.0
NZS 3404 (max)	NZS 3404 $\alpha_b = 0.5$, $k_f = 1.0$	Whitmore $\theta = 30^0$	Maximum Thornton	0.7
NZS 3404 (ave)	NZS 3404 $\alpha_b = 0.5$, $k_f = 1.0$	Whitmore $\theta = 30^0$	Average Thornton	0.7
HERA R4-80	NZS 3404 $\alpha_b = 0.5$, $k_f = 1.0$	Whitmore $\theta = 30^0$	Average Thornton	0.5
Modified Thornton	CAN/CSA-S16.1-M89	Whitmore $\theta = 45^0$	Splice plate end to beam/column	0.65
Euler	None (Euler elastic buckling)	Whitmore $\theta = 30^0$	Maximum Thornton	0.65

Because both the maximum and average Thornton lengths are acceptable, they will both be investigated for the Thornton method and the NZS3404 method. The Thornton method will also be investigated considering $K = 1.0$ for gusset plates that have been tested under fixed-roller boundary conditions. This is true for the majority of the experimental tests. As the buckling behaviour of the gusset plate appears to be highly dependent on boundary conditions, the validity of the relationship between effective length factor and buckling capacity can be analysed for the Thornton method.

The papers which use fixed-roller boundary conditions do not use $K = 1.0$ for design and instead used $K = 0.65$, with generally conservative results (Hu and Cheng 1987; Rabinovitch and Cheng 1993; Sheng et al. 2002; Yam and Cheng 1993). This would indicate that the Thornton method should be noticeably conservative for gusset plates designed to their actual boundary conditions.

The Euler method, using a maximum Thornton length, has been included at this stage to relate it to the proposed method by Tsai and Hsiao (2008) that will be investigated during the sway buckling stage. This method is unlikely to be accurate for a number of the experimental tests as it does not consider inelastic buckling.

5.3.1 Design Capacity and Experimental Buckling Capacity

In Table 5.3-2, the experimental buckling capacity for each experimentally tested gusset plate has been divided by design capacity calculated by the buckling capacity design methods considered. The result is a calculation of error in estimating capacity that can be used to show which design methods are the most conservative and the most accurate. If a method is found not to be conservative for a particular gusset plate, this has been shaded grey. The raw data for these calculations can be found in Table 10.2-1 in the appendices.

Table 5.3-2: Experimental buckling capacity to design capacity ratio for experimentally tested gusset plates

Gusset Plate	Thornton (max)	Thornton (ave)	Thornton, K = 1.0 (ave)	NZS 3404 (max)	NZS 3404 (ave)	HERA R4-80 (ave)	Modified Thornton	Euler (max)
GC01	4.28	1.86	1.61	5.43	2.35	1.80	2.97	3.76
HC01	3.71	2.12	-	4.22	2.57	1.48	2.38	3.08
HC02	4.16	1.24	-	4.57	1.54	0.91	2.67	3.71
HC03	2.75	1.58	-	3.13	1.91	1.10	1.77	2.29
HC04	4.31	1.28	-	4.73	1.59	0.94	2.77	3.84
HC05	1.79	1.03	2.43	2.04	1.24	0.72	1.15	1.49
HC06	3.63	1.08	2.55	3.98	1.34	0.79	2.33	3.23
HC07	1.54	0.88	2.09	1.75	1.07	0.62	0.99	1.28
HC08	2.65	0.79	1.87	2.91	0.98	0.58	1.70	2.36
N01	1.64	1.19	-	2.20	1.59	1.09	1.11	1.36
RC01	1.34	1.14	1.31	1.62	1.25	1.14	0.84	0.65
RC02	1.93	1.33	1.83	2.60	1.57	1.31	1.21	1.49
RC03	1.26	0.92	1.81	1.71	1.21	0.86	0.79	1.06
S01	2.15	2.03	2.39	2.46	2.25	2.04	1.42	0.73
S02	1.59	1.54	1.56	1.66	1.52	1.50	0.99	0.14
S03	2.30	2.07	2.81	2.86	2.43	2.05	1.52	1.25
S04	1.70	1.61	1.64	1.83	1.62	1.58	1.06	0.26
S05	1.96	1.85	2.18	2.24	2.05	1.86	1.29	0.67
S06	1.63	1.54	1.81	1.87	1.71	1.55	1.08	0.56
S07	1.77	1.59	2.16	2.20	1.87	1.57	1.17	0.96
YC01	1.75	1.68	1.79	1.89	1.77	1.68	1.11	0.31
YC02	1.72	1.60	1.80	1.95	1.73	1.61	1.09	0.54
YC03	1.74	1.47	1.94	2.19	1.71	1.46	1.11	1.00
YC04	1.57	1.47	1.56	1.73	1.54	1.47	1.00	0.35
YC05	1.60	1.41	1.57	1.86	1.52	1.42	1.02	0.61
YC06	1.89	1.41	1.81	2.47	1.62	1.41	1.20	1.25
YC07	1.36	1.18	1.80	1.77	1.45	1.15	0.84	0.90
YC08	1.69	1.29	2.71	2.28	1.73	1.18	1.04	1.40
AVE.	**2.19**	**1.43**	**1.96**	**2.58**	**1.67**	**1.32**	**1.41**	**1.45**
STD. DEV.	**0.92**	**0.35**	**0.39**	**1.03**	**0.38**	**0.40**	**0.61**	**1.11**

*Non-conservative ratios shaded grey

All methods are, on average, conservative. In most cases where a method is not conservative for a particular gusset plate, it occurs in experiments which were tested with fixed-roller boundary conditions, indicating the worst possible case.

The HERA R4-80 method (HERA 1994) is not conservative for a number of cases including gusset plates which were tested with fixed-fixed boundary conditions. This is because it idealised these boundary conditions with K = 0.5. It is therefore recommended that this method not be used in design for gusset plates in general.

The Euler method is also not conservative. This is expected as it does not consider inelastic buckling. Conversely, the modified Thornton method was not conservative in a number of cases because it only considers inelastic buckling.

The Thornton method considering the average Thornton length is the most used method, and this method is the most accurate while being conservative within one standard deviation. This standard deviation is quite large, indicating that the method is not precise. It would be expected that similar results occur when fixed-free boundary conditions are considered.

5.4 Finite Element Model

The finite element model of the gusset plates follows most of the same modelling decisions made in Section 4.3. In this chapter, only the gusset plate and splice plates are modelled. The splice plates are only modelled to the edge of the gusset plate. Boundary conditions are applied to the gusset plate edges corresponding to the interface to the beam-column joint and the splice plate edges corresponding to the interface with the connection region / brace, as seen in Figure 5.4-1.

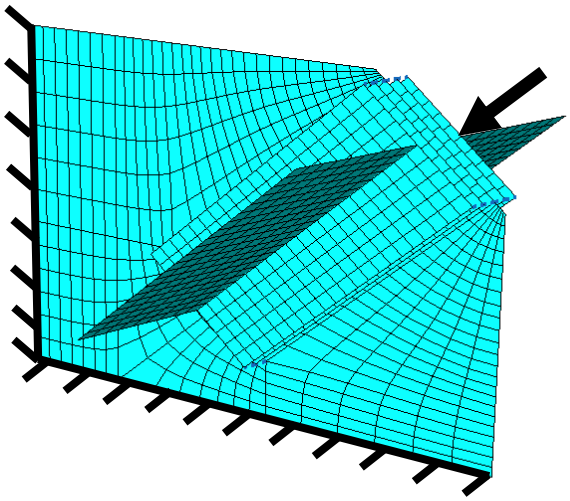

Figure 5.4-1: Gusset plate finite element model with fixed-free boundary conditions

5.4.1 Model Displacement

Displacement is applied to the model through a single reference node with the appropriate boundary conditions of the model and a displacement that compresses the model axially. This

reference node is tied to the splice plate edges at the brace end in all degrees of freedom. This allows the splice plate edges to follow the displacement of the reference node. The force, as a result of this displacement, is then able to transfer through the splice plates to the mesh independent fasteners that simulate the bolts (see Section 4.3.6) and then through the gusset plate itself.

5.4.2 Splice Plate Contact Modelling

The force path does not account for the frictional contact between the splice plates and the gusset plate. This is because Abaqus does not automatically model contact between two parts in an analysis. This would cause some of the force to transfer directly from the splice plates to the gusset plate instead of entirely through the bolts. This could have been modelled directly using frictional contact behaviour in Abaqus, although this is computationally expensive. Alternatively, the splice plate surface could have been tied to the gusset plate surface directly and the bolts ignored. This may be a more accurate assumption of the load path; however, this assumption cannot be directly compared to the design methods.

Each design method uses the Whitmore width which is based on the position of the bolt locations and not the edges of the splice plates to determine the width of the equivalent column. By using bolts to transfer the entirety of the load path, the assumptions of the design methods can be more directly compared to the finite element models.

This assumption does lead to an issue in the finite element model. Because bolts have been modelled to transfer the force through the splice plates to the gusset plate, no interaction between the splice plate and the gusset plate has been modelled. As such, the splice plates will not provide additional stiffness to the gusset plate. This additional stiffness would increase the gusset plate buckling capacity. Figure 5.4-2 demonstrates the behaviour by showing that the splice plates do not follow the deformation of the gusset plate.

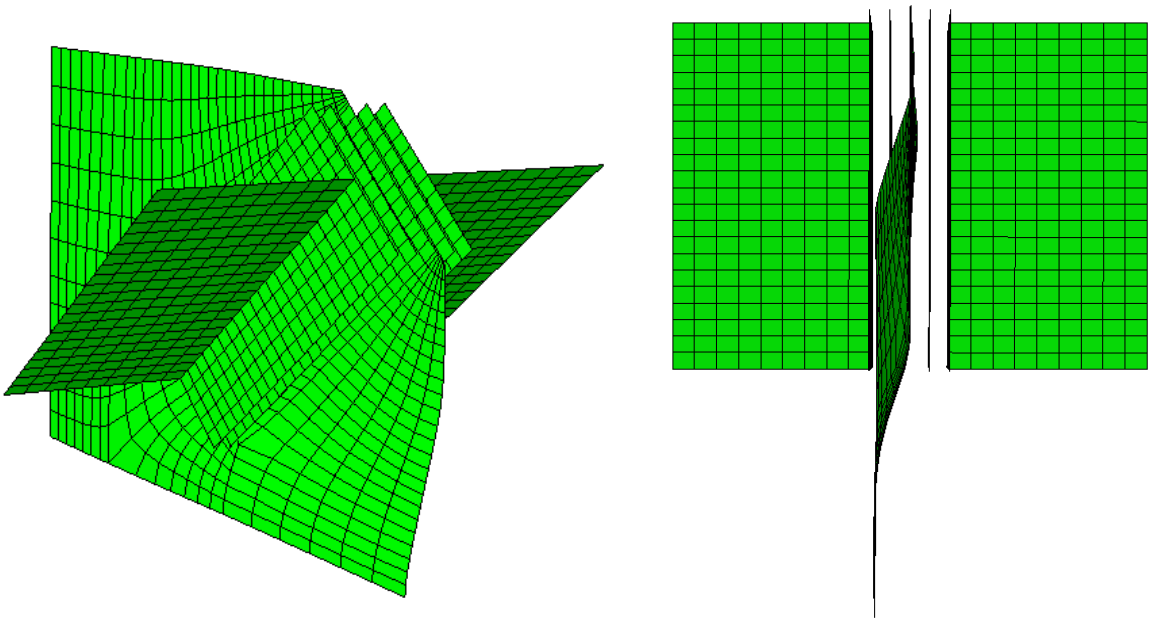

Figure 5.4-2: Buckled gusset plate model under fixed-roller boundary conditions without splice plate contact modelling

A solution was found to account for the interaction between splice plates and gusset plates by connecting the corners of the splice plates to the gusset plate through connectors. The connectors constrained the splice plate and gusset plate rigidly only in the direction perpendicular to the plane of the gusset plate. By only constraining in this one direction, the connectors will not aid in transferring force from the splice plate to the gusset plate. As such, all the forces from the applied displacement enter the gusset plate through the bolt fasteners.

5.4.3 Output

To find the buckling capacity of the gusset plate model, the reaction force along the gusset plate interface to the beam-column joint was considered. By summing the reaction force in the same axis at the displacement imposed on the gusset plate, the total force being applied to the model was found. This was a simple solution that was deemed to be accurate due to equilibrium. Like the output from the finite element model in Section 4.3, the maximum force in the model was determined to be the buckling capacity of the gusset plate as the force noticeably dropped after buckling occurred.

5.5 Accuracy of Finite Element Models

To determine if the finite element models of the experimental test gusset plates are suitable to be evaluated with fixed-free boundary conditions, they must first be validated. The models

were validated by comparing the buckling capacities of experimentally tested gusset plates with the buckling capacities of finite element models using the same experimental boundary conditions.

As finite element models will never exactly match experimental results, a threshold must be used to determine which models are suitable. It was decided that if the finite element model predicts a buckling capacity that is within 10 % of the experimentally tested gusset plate's buckling capacity, then this model is validated.

In Table 5.5-1, the finite element models with buckling capacity that are within 10 % of the experimental gusset plates have been shaded in grey. These models will be used in the fixed-free boundary condition analysis as it has been shown that they closely resemble real experimental behaviour.

Table 5.5-1: Comparison of finite element models to experimentally tested gusset plates

	Experimental Gusset Plate Buckling Capacity	Finite Element Model Buckling Capacity	FEM Capacity/ Experiment Capacity
GC01	516	732	1.42
HC01	914	1230	1.35
HC02	141	226	1.61
HC03	678	1058	1.56
HC04	146	151	1.04
HC05	442	791	1.79
HC06	122	142	1.16
HC07	380	628	1.65
HC08	90	93	1.04
N01	403	804	1.99
RC01	1682	2077	1.23
RC02	1128	1080	0.96
RC03	907	1161	1.28
S01	1626	1818	1.12
S02	2349	2494	1.06
S03	1143	1166	1.02
S04	1867	1818	0.97
S05	1480	1591	1.08
S06	1232	1257	1.02
S07	878	837	0.95
YC01	1956	1995	1.02
YC02	1356	1484	1.09
YC03	742	711	0.96
YC04	1720	1938	1.13
YC05	1210	1191	0.98
YC06	728	712	0.98
YC07	1606	1840	1.15
YC08	1010	1061	1.05
		Average	**1.20**
		Standard Deviation	**0.27**

*Finite element models within 10% of experimental capacity shaded grey

It can be seen that only 15 of the 28 finite element models had buckling capacities within 10 % of the experimental test buckling capacities. The models within the 10 % threshold will be considered validated and have their boundary conditions modified to fixed-free conditions to analyse the assumptions made by Chou et al. (2012) and Tsai and Hsiao (2008). It should be noted that HC04 and HC08 are the same gusset plate tested with fixed-fixed and fixed-roller boundary conditions respectively.

It is likely that the major reason some finite element models did not meet the 10 % threshold is that the boundary conditions imposed on the model are too rigid. When a degree of freedom is fixed in Abaqus, it is considered completely rigid. In reality, there will be some rotation or displacement occurring at this boundary, which will decrease the gusset plate's buckling capacity. It is, therefore, likely that a number of the finite element models fail to capture this behaviour from the experimental tests.

In the experimental tests by Rabinovitch and Cheng (1993), bolt slip was observed in RC01 and RC03, but not RC02. This behaviour was not captured in the finite element models and may contribute to why these finite element models over predicted the buckling capacities. Additionally, these gusset plates were the only ones to be tested under cyclic loading, with tensile yielding observed.

The least accurate finite element model was based on the experimental test from Naghipour et al. (2013). With a finite element buckling capacity of 1.99 times the experimental capacity, there is a significant behaviour that was not captured by the finite element model. This is likely to be the result of the finite element model assuming all degrees of freedom are fixed at the gusset plate – brace interface. However, this was not observed to be true in the experiment, with this end of the gusset plate both rotating and translating out-of-plane as a result of deformations in the I-beam. A more accurate finite element model could be developed by modelling the attached I-beam. However, this is not the same modelling technique that has been used for every other gusset plate, and so the gusset plate model will not be considered.

5.6 Fixed – Free Boundary Conditions

Each finite element model discussed in Section 5.5 that was found to meet the acceptable threshold has been considered an accurate representation of experimental buckling behaviour. The boundary conditions of these models will now be updated such that the gusset plate interface to the beam-column joint is fixed in all degrees of freedom and that the gusset plate interface to the brace is free to laterally translate out-of-plane and rotate out-of-plane. This gusset plate end is fixed such that it will not rotate torsionally or in-plane and will not laterally translate in-plane. This is unlikely to have a large effect on the gusset plate buckling capacity as these fixed degrees of freedom correspond to behaviour in the strong axis of the gusset plate which is not being considered.

To consider the accuracy of the design methods considering fixed-free boundary conditions, the same methods in Section 5.3 have been considered. Table 5.6-1 is updated from

Table 5.3-1, but with the effective length factor updated to the new boundary conditions. Most methods consider K = 2.0, as per the recommendations by Chou et al. (2012) and Tsai and Hsiao (2008). However, the NZS 3404 methods consider K = 2.2 in accordance with NZS 3404 Clause 4.8.3.2 (Standards New Zealand 1997) to account for non-rigidity of boundary conditions.

Table 5.6-1: Summary of sway buckling capacity methods investigated

Method	Column Curve	Effective Width	Length	Effective Length Factor
Thornton (max)	AISC	Whitmore $\theta = 30^0$	Maximum Thornton	2
Chou et al. (2012) (Thornton ave)	AISC	Whitmore $\theta = 30^0$	Average Thornton	2
NZS 3404 (max)	NZS 3404 $\alpha_b = 0.5$, $k_f = 1.0$	Whitmore $\theta = 30^0$	Maximum Thornton	2.2
NZS 3404 (ave)	NZS 3404 $\alpha_b = 0.5$, $k_f = 1.0$	Whitmore $\theta = 30^0$	Average Thornton	2.2
HERA R4-80	NZS 3404 $\alpha_b = 0.5$, $k_f = 1.0$	Whitmore $\theta = 30^0$	Average Thornton	2
Modified Thornton	CAN/CSA-S16.1-M89	Whitmore $\theta = 45^0$	Splice plate end to beam/column	2
Tsai and Hsiao (2008) (Euler)	None (Euler elastic buckling)	Whitmore $\theta = 30^0$	Maximum Thornton	2

5.7 Accuracy of Sway Buckling Capacity Methods

The finite element model's buckling capacity considering fixed-free boundary conditions can now be directly compared to the buckling capacity design methods considering fixed-free boundary conditions. Table 5.7-1 shows the buckling capacity found in the finite element models divided by each buckling capacity design method. If the ratio is less than unity, this indicates that the design method is not conservative for that particular gusset plate. This has been highlighted in the table by cells that are shaded grey.

Table 5.7-1: Finite element model buckling capacity to design capacity ratio for fixed-free boundary conditions

Gusset Plate	Thornton (max)	Chou et al. (2012)	NZS 3404 (max)	NZS 3404 (ave)	HERA R4-80	Modified Thornton	Tsai and Hsiao (2008)
HC04/HC08	2.52	0.75	2.69	0.82	0.68	0.47	2.25
RC02	2.29	0.88	2.58	1.07	0.90	0.86	1.95
S02	1.08	0.80	1.39	0.86	0.84	0.55	0.63
S03	3.39	2.29	3.98	2.79	2.35	0.64	2.83
S04	1.11	0.63	1.55	0.71	0.68	0.47	0.87
S05	2.23	1.51	2.79	2.00	1.72	0.52	1.88
S06	1.61	1.09	2.02	1.45	1.24	0.38	1.36
S07	1.79	1.21	2.11	1.47	1.25	0.34	1.50
YC01	1.47	1.02	2.05	1.36	1.22	0.67	1.21
YC02	1.74	0.97	2.21	1.35	1.17	0.66	1.45
YC03	2.06	1.13	2.40	1.39	1.18	0.78	1.72
YC05	3.61	1.44	4.43	2.01	1.75	1.45	3.01
YC06	4.61	1.77	5.29	2.22	1.88	1.86	3.85
YC08	2.61	1.78	2.89	2.02	1.68	1.30	2.17
AVE.	**2.29**	**1.23**	**2.74**	**1.54**	**1.33**	**0.78**	**1.91**
STD. DEV.	**1.00**	**0.47**	**1.11**	**0.60**	**0.49**	**0.45**	**0.87**

*Non-conservative predictions of finite element sway model shaded grey

It can be seen that the Thornton method considering the maximum Thornton length and the NZS 3404 method considering the maximum Thornton length are the only two methods that are conservative for all cases. The Thornton method considering the maximum Thornton length is more accurate than the NZS 3404 method as it has an average closer to unity and a smaller standard deviation. This average of 2.29 is, however, quite conservative and indicates that a designer using this method would design a gusset plate with about twice the buckling capacity than what is necessary for in-plane loading.

The modified Thornton method is the least conservative at predicting gusset plate buckling capacity for fixed-free boundary conditions. This was to be expected as the philosophy behind the method is to be less conservative at predicting buckling capacity. The method considered inelastic plate buckling effects to increase the predicted buckling capacity. This does not occur in the gusset plates that have buckled elastically and so the method over predicts the buckling capacity of the finite element models.

The method proposed by Chou et al. (2012) is not conservative for a number of cases, and three of these cases fall within the standard deviation. The method is, on average, the closest to predicting the buckling capacity.

The method proposed by Tsai and Hsiao (2008) is not conservative for two gusset plates. These two cases fall outside one standard deviation from the mean value. The method is less accurate than the Chou et al. (2012) method but more accurate than the Thornton method considering the maximum Thornton length.

5.8 Comparison to Sway Buckling Failure in BRB Frames

The two methods in Table 5.7-1 that were found to be conservative for all of the finite element model gusset plates tested under fixed-free boundary conditions can now be compared to sway buckling failures in buckling restrained braced frames that were investigated in Chapter 3. These results have been shown in Table 5.8-1.

Table 5.8-1: Prediction of buckling capacity for sway buckling failure in experimental BRB frames

BRB Frame	Experimental Buckling Capacity (kN)	Thornton – max (kN)	NZS 3404 – max (kN)	Experiment / Thornton	Experiment / NZS 3404
Chou et al. (2012)	693	337	267	2.06	2.60
Tsai et al. (2004)	805	737	556	1.09	1.45

It can be seen that both methods can conservatively predict the buckling capacity of the experimentally tested BRB frames. However, it is clear that the methods are not very accurate for the Chou et al. (2012) frame. The Thornton method with maximum Thornton length and $K = 2.0$ is a reasonably accurate prediction. As the predictions of buckling capacity are significantly different for the two frames, it can be said that the methods are not very precise.

5.9 Conclusion

This study shows that gusset plates modelled through finite element analysis with fixed-free conditions are unable to have their buckling capacity conservatively estimated by the methods proposed by Chou et al. (2012) and Tsai and Hsiao (2008) for all cases. Therefore, it is recommended that these methods not be used to design gusset plates in BRB frames as their assumptions have been found not to be conservative.

The buckling capacity of gusset plates can be conservatively estimated using the Thornton method with $K = 2.0$, the maximum Thornton length and the AISC column curve. This is also true for the NZS 3404 method using the maximum Thornton length and $K = 2.2$. These methods may be acceptable to design gusset plates in BRB frames. This is supported by

the evidence that the methods are both conservative for gusset plates that fail by sway buckling in experimentally tested BRB frames.

However, these methods should not be used without prejudice. Of the 28 experimentally tested gusset plates, only half could be modelled with enough accuracy to represent their experimental test buckling capacity. As such, there may still be some cases for which the suggested methods are not conservative. The finite element models only considered in-plane monotonic loading only. When out-of-plane and cyclic loading is significant, different recommendations may be required.

Although these methods are conservative, they do not appear to have an accurate relationship to buckling capacity. The standard deviations are also quite large for both methods, indicating that the methods are not very precise in their predictions. This is true for the finite element models with fixed-free boundary conditions, and when comparing the methods to sway buckling of gusset plates in experimentally tested BRB frames.

Additionally, the recommendations of this chapter did not consider any effect of the other elements in the BRB system on the buckling capacity of the gusset plate. This effect has been observed in Crake and Westeneng (2014) and will be explored further in Chapter 7.

The aims at the start of this chapter have been addressed:

1) Of the experimentally tested gusset plate buckling methods considered, the Thornton method and the NZS 3404 method were conservative for all gusset plates when considering the maximum Thornton length. All methods considered were not accurate at determining the experimental buckling capacity and most methods were overly conservative for most cases.
2) A finite element model was developed. However, only 15 out of the 28 gusset plates were suitably accurate in matching the experimental buckling capacity.
3) The validated finite element models were modified to consider fixed-free boundary conditions to match the $K = 2.0$ assumption proposed by Chou et al. (2012) and Tsai and Hsiao (2008).
4) The Thornton method and the NZS 3404 method considering the maximum Thornton length were both able to conservatively predict the buckling capacity of the finite element models of gusset plates considering fixed-free boundary conditions. Although these methods could conservatively predict the buckling capacity of gusset plates in two experimentally tested BRB frames, they do not consider the effects of other elements in the BRB system and may not be suitable for all gusset plates in BRB frames.

6 PARAMETRIC ANALYSIS

6.1 Introduction

It is evident from Chapter 5 that the Thornton method and its derivatives are not accurate and are not always conservative for all gusset plates regardless of boundary condition. To better understand gusset plate behaviour, it was decided to determine which assumptions made by the Thornton method most significantly influence the behaviour. A parametric study has been used to determine which gusset plate parameters do not conform to the proportional relationships assumed by the Thornton method.

Each variable in the Thornton method will be investigated by altering finite element models of gusset plates. The relationship between each variable and the gusset plate buckling capacity for the finite element models will be compared to the relationships in the Thornton method. The relationships will be considered for three different boundary conditions. This is important as experimental testing has considered fixed-fixed and fixed-roller boundary conditions but has not determined if the relationships hold for fixed-free boundary conditions.

It is also important to determine whether the relationships hold true for a range of gusset plates and not just one particular gusset plate design. For this reason, a parametric study that considers all possible combinations of parameter values has been developed. This allows for a large data set that can be reviewed to determine if the proportional relationships assumed by the Thornton method are robust for all gusset plates.

The aims of this chapter are to:

1) Consider a range of parameters that affect the buckling capacity of gusset plates and determine how these parameters are handled by the Thornton method.
2) Develop a parametric study considering suitable parameters.
3) Determine if the relationships between the suitable parameters and buckling capacity match the assumptions made by the Thornton method.
4) Determine if these relationships between suitable parameters and buckling capacity hold true for a wide range of parameter value combinations.

6.2 Parameters Considered

Each parameter in the Thornton method has been considered. A number of these parameters are dependent on other parameters such as the Whitmore width being dependent on bolt width and depth, and these have also been considered.

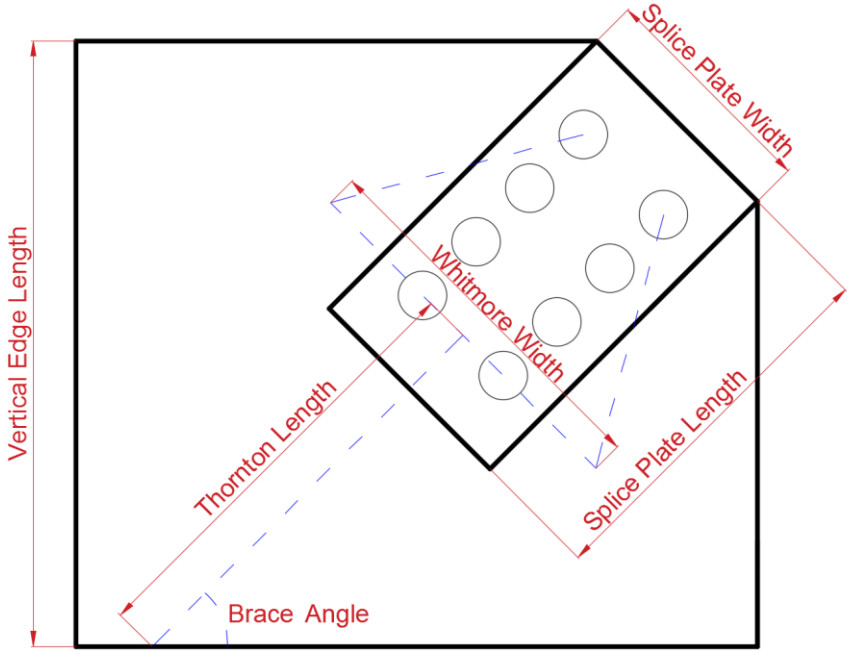

Figure 6.2-1: Diagram of gusset plate dimension parameters investigated

6.2.1 Gusset Plate Thickness

Gusset plate thickness can be considered to be the most critical parameter when designing a gusset plate to prevent buckling. This is because the other parameters available to the designer are largely restrained by brace and frame geometry, available steel material, and brace force. Plate thickness may be restricted based on plate sizes available to the engineer at the time of construction. For BRB frames, it is generally accepted that the plate thickness must be equal to or larger than the BRB core thickness.

Current gusset plate buckling capacity formulas such as the Thornton method assume a cubic relationship between plate thickness and buckling capacity in the elastic buckling range. Experimental testing of gusset plate buckling has mostly found an almost linear relationship for inelastic buckling (Cheng et al. 1994; Yam and Cheng 2002). However, the Thornton method assumes a non-linear relationship.

The gusset plate thicknesses that will be tested in this study can be seen in Table 6.2-1 found in Section 6.2.11.

6.2.2 Modulus of Elasticity

The modulus of elasticity of the gusset plate material is an important variable in determining a gusset plate's buckling capacity. However, it is not likely to have a significant weight on the gusset plate design due to the similarity of values for different steels that are likely to be used in the fabrication of gusset plates.

The Thornton method assumes a linear relationship between modulus of elasticity and buckling capacity for elastic buckling. For inelastic buckling, this relationship is assumed to be $0.658^{\frac{1}{E}}$ based on Equation 2.4-4 and Equation 2.4-5.

The range of modulus of elasticity values can be seen in Table 6.2-1, and these vary from 195 GPa to 210 GPa to consider the likely values that a particular steel may have.

6.2.3 Yield Strength

Yield strength should not have any effect on gusset plates that buckle elastically. This is likely to be the case for gusset plates that buckle by sway. However, for gusset plates that buckle inelastically, yield strength will affect buckling capacity.

The Thornton method assumes a linear relationship between yield strength and buckling capacity for inelastic buckling and no relationship between yield strength and buckling capacity for elastic buckling.

Table 6.2-1 shows the yield strength values used in the parametric study. The values were taken to represent a range of yield strengths that would be reasonably expected for steel in gusset plates.

6.2.4 Whitmore Width

The Whitmore width determines the width of the equivalent buckling column in the Thornton method. It is developed by Equation 2.4-1 and is dependent on the distance between the outermost bolts along the splice plate length and the distance between the outermost bolts along the splice plate width.

For this parametric study, the splice plate length and splice plate width are able to be directly altered. The bolt spacing is then changed as a result of this. As such splice plate length and splice plate width will be directly evaluated against buckling capacity and the Whitmore width will be calculated and then evaluated against buckling capacity. The step size between

parameter values for Whitmore width will not be constant as it is dependent on splice plate length and width.

6.2.5 Splice Plate Length

An increase in splice plate length should increase gusset plate buckling capacity. This is because more of the gusset plate area is strengthened by the splice plates which generally have a significantly higher second moment of area. It is likely this relationship will be non-linear and may not be independent of effective length factor due to the different buckling mode shapes.

The Thornton method does not directly consider splice plate length. Instead, the Thornton length is used to measure the free space between the end of the splice plate and the interface between the gusset plate and the beam-column joint. Adjusting splice plate length will also adjust the bolt spacing between the outermost bolts along the splice plate length. This will result in a change to the Whitmore width.

The relationship indicates that, for both elastic and inelastic buckling, when the splice plate length increases, the Thornton length decreases and thus buckling capacity increases non-linearly.

The values that have been used to alter splice plate length can be seen in Table 6.2-1. The range of values considers long splice plates that are very close to the interface between the gusset plate and the beam-column joint, as well as short splice plates that are shorter than the linear clearance zone described in Figure 2.4-3, which is considered in conventional braced frames.

6.2.6 Splice Plate Width

Splice plate width is not a factor generally considered by design. The Whitmore width is dependent on the bolt spacing width only. However, when bolt spacing is increased, splice plate width usually must also be increased. The finite element model in the parametric analysis proportionally increases bolt spacing when splice plate width is increased.

6.2.7 Brace Angle

Brace angle has not been considered in the Thornton method directly, although it will minimally affect the length of the average Thornton length. Reducing the brace angle from 45°

has been found to cause a minor increase in buckling capacity (Yam and Cheng 1993). It was decided that for every gusset plate, a brace angle of 45° would be used as this will give the minimum capacity.

6.2.8 Thornton Length

The Thornton length determines the length of the equivalent buckling column in the Thornton method. It is dependent on the gusset plate and splice plate geometries.

This parameter is not directly modified in the parametric study as it is dependent on both gusset plate and splice plate geometry. The maximum Thornton length was calculated for each finite element gusset plate model. It should be noted that because the brace angle does not change and remains at 45° for every model in the parametric study, this maximum Thornton length will be the middle Thornton length. This length will be directly proportional to the average Thornton length.

For the Thornton method, the relationship between Thornton length and buckling capacity is $1/L^2$ for elastic buckling and 0.658^{L^2} for inelastic buckling. The inelastic buckling relationship will be different for derivatives of the Thornton method such as the NZS 3404 method due the use of a different column curve.

The Thornton length values considered range from 250 mm to 650 mm. As a result of the length's dependency on gusset and splice plate geometry, the distribution of the values is non-uniform.

6.2.9 Edge Length

Changing the edge lengths of the gusset plates has an effect on gusset plate geometry. By increasing one length, buckling capacity will decrease non-linearly as the Thornton length will be increased. Because the brace angle has been set at 45°, only one edge needs to be changed. It was decided that the horizontal length of the gusset plate along the beam interface would be set at 500 mm. The vertical length of the gusset plate along the column interface was adjusted considering the range of values in Table 6.2-1.

6.2.10 Boundary Conditions

The Thornton method considers the relationship between the effective length factor and buckling capacity to be $1/K^2$ for elastic buckling and 0.658^{K^2} for inelastic buckling.

It is of interest to model the difference between fixed-fixed boundary conditions and fixed-free boundary conditions, and whether this difference has been correctly predicted by the Thornton method. This will provide further evidence to determine if the assumptions made by Chou et al. (2012) and Tsai and Hsiao (2008) are conservative or not.

The different boundary conditions have been considered by their effective length factors and are shown in Table 6.2-1. Each boundary condition has been discussed further.

6.2.10.1 Fixed-Fixed

Fixed-fixed boundary conditions consider a gusset plate that is fully fixed along the interface between the gusset plate and the beam-column joint, and fully fixed at the connection between the gusset plate and the attached BRB. These boundary conditions assume that the weld between the gusset plate and the beam-column joint provides no ductility, that the beam-column joint does not move relative to the BRB, and that the BRB does not form a hinge at the end.

The fixed-fixed boundary condition corresponds to a theoretical effective length factor of 0.5. Because these boundary conditions are perfectly imposed in Abaqus, it does not need to be assumed that the effective length factor is 0.65, as is done in design.

6.2.10.2 Fixed-Roller

The fixed-roller boundary condition considers a gusset plate that is fixed along the interface between the gusset plate and the beam-column joint in all degrees of freedom except for out-of-plane translation. The interface between the gusset plate and the BRB remains fully fixed.

The choice to consider this boundary condition has been made based on a large number of experimentally tested gusset plates that use this condition, as seen in Table 5.2-1. This boundary condition has been tested based on the assumptions shown in Yam and Cheng (1993) which consider that a beam-column joint could translate out-of-plane in relation to the brace.

The boundary conditions result in a buckling behaviour that is considered to be sway buckling. The fixed-roller boundary condition corresponds to a theoretical effective length factor of 1.0. The choice to model this boundary condition also provides a third data point which can show whether the relationship between buckling capacity and boundary conditions is non-linear.

6.2.10.3 Fixed-Free

The fixed-free boundary condition considers a gusset plate where the interface between the gusset plate the beam-column joint is fixed in all degrees of freedom, and the interface between the gusset plate and the BRB free in all degrees of freedom. This indicates that the beam-column joint is fully rigid and that the BRB end forms a perfect hinge.

The boundary conditions result in a sway buckling behaviour with a theoretical effective length factor of 2.0. This is the same effective length factor recommended by Chou et al. (2012) and Tsai and Hsiao (2008) to prevent gusset plate buckling in BRB frames.

6.2.11 Summary of Parameter Values

A summary of the values chosen for each parameter investigated has been presented in Table 6.2-1.

Table 6.2-1: Parameter values chosen for finite element model parametric study

Parameter	Values
Thickness (mm)	5, 10, 15, 20
Modulus of Elasticity (GPa)	195, 200, 205, 210
Yield Strength (MPa)	290, 300, 310
Splice Plate Length (mm)	200, 250, 300
Splice Plate Width (mm)	100, 150, 200
Vertical Gusset Plate Length (mm)	350, 400, 450, 500
Boundary Condition	Fixed-Fixed, Fixed-Roller, Fixed-Free

6.3 Finite Element Model

The gusset plate model used for this parametric study uses the same modelling techniques found in Section 4.3 and Section 5.4 for the development of the gusset plate model. The gusset plate design was modelled based on experimental testing by Yam and Cheng (1993) due to the good relationship between the finite element buckling capacity and experimental buckling capacity found in Section 5.5.

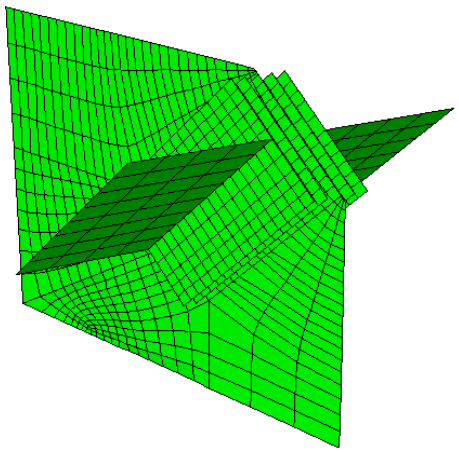

Figure 6.3-1: Finite element model of the representative gusset plate

However, the modelling technique for bolt design required adjustment from the previous models. As splice plate length is a parameter of the investigation, the use of mesh independent fasteners was not appropriate for this design. If the fasteners were used, the splice plate length would increase, but the bolts would not change position. It was not possible to design a script that allowed for the inclusion of additional mesh independent fasteners when the splice plate length increased.

Instead of developing separate models for each splice plate length to run through the parametric analysis, connectors that were dependent on the mesh were used instead. This was achieved by developing a connector section for the bolt that was rigid in each degree of freedom. This connector section was then applied to connectors defined between the splice plates and the gusset plate.

Partitions were used in the splice plates and gusset plates to define the location of the connector bolts, as shown in Figure 6.3-2, where bolt connectors are present at the intersection of partition lines. This does introduce a limitation to the parametric analysis. For every splice plate length, there will always be six bolts connecting the splice plates to the gusset plate. These bolts will be located at each quarter of the length of the splice plate. This is not a true representation of gusset plate design. In longer splice plates, more bolts will be used, and fewer bolts will be used in shorter splice plates. However, it is sufficient to ensure that the force applied to the model transfers from the splice plates through the bolts to the gusset plates when the model is displaced. This is because the bolt fasteners are rigid and so more bolts are not needed to transfer the force.

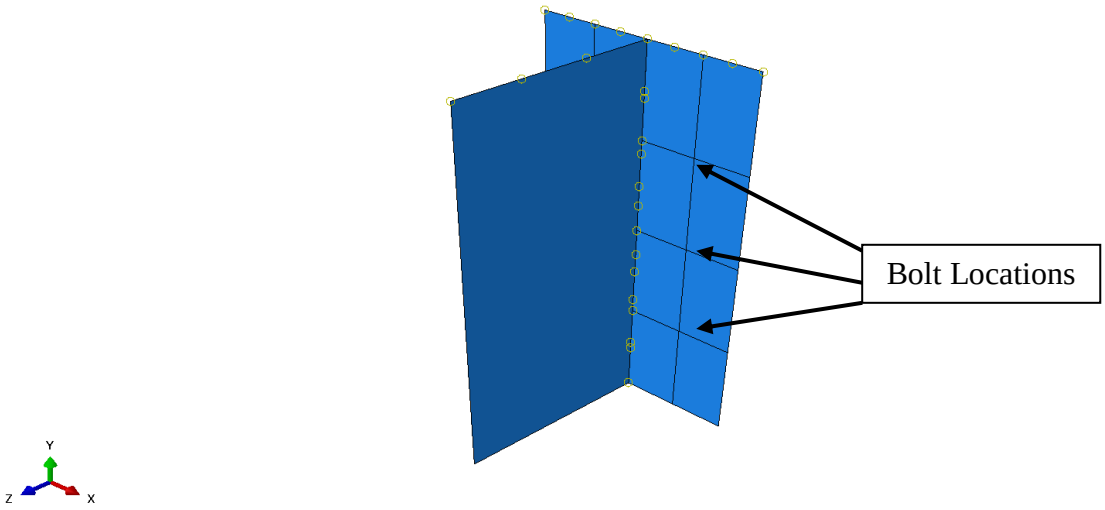

Figure 6.3-2: Splice plate partitions to allow for bolt connections

6.4 Parametric Script Design

Abaqus can use Python scripting to alter finite element models and control the analysis. This can be beneficially used to run a large number of simulations without any user input once the script has been started. A Python input script was developed such that every possible combination of the parameters investigated was covered to create and find the buckling capacity of 5880 finite element models. An output script was also written in Python to process the output files after all the analysis was completed.

6.4.1 Input Script

Nested for loops were used to ensure that each potential gusset plate model was considered. A full copy of the script used can be found in Section 10.3.1 in the appendices. A brief overview of the key behaviour of the script has been presented.

6.4.1.1 Initialisation

The script must be run from the command line using the following code. It can also be run through the Abaqus GUI although the run time of the script is significantly longer. This is critical as although each finite element model only takes several minutes execute, with a large number of models, this run time is significant as each analysis must be run sequentially.

The script first opens the model database that has been previously created. This contains all the geometric and material information used to define the gusset plate model and is necessary. This was achieved through the following code excerpt:

```
mdb=openMdb(pathName="ParametricGussetPlate")
```

To define the different values for each parameter that the script will run through, domains must be developed containing each value. This was achieved for all parameters in the following code excerpt apart from effective length factor.

```
thicknessDomain = [5, 10, 15, 20, 25] # Gusset Thickness
      (mm)
youngsDomain = [195, 200, 205, 210] # Youngs Modulus
      (GPa)
yieldDomain = [290, 300, 310] # Yield Strength (MPa)
a0Domain = [400, 500, 600] # Length of vertical gusset
     plate edge at column interface (mm)
l2Domain = [200, 250, 300] # Length of splice plate (mm)
l3Domain = [100, 150, 200] # Width of splice plate (mm)
```

Effective length factor was required to be manually altered and as such, the script was required to be run three times, for each effective length factor. This was not a limitation of scripting in Abaqus, but instead a choice of efficiency due to the extra code that would be required. This is because the value of the effective length factor does not automatically correspond to the boundary conditions in the model that would need to be altered.

6.4.1.2 Parameter for loops

An example of the for loop has been presented in the code excerpt below. It can be seen that “thicknessParam” takes a particular value in the thickness domain which has been defined above and then sets the value of thickness for the gusset plate section of the gusset plate model. In this case, the gusset plate model is named “YC01-Displacement”.

```
for thicknessParam in thicknessDomain:
           # Adjustment of Thickness Parameter
mdb.models['YC01-Displacement'].sections['Gusset
      Section'].setValues(thickness=thicknessParam)
```

These for loops have been developed for each parameter in the study, using the applicable Abaqus scripting code to adjust the parameter values. This is relatively trivial for gusset plate thickness, modulus of elasticity, and yield strength. However, the length parameters cannot be easily scripted as a change in the geometric shape of the gusset plate or splice plates results in the part and the mesh needing to be regenerated.

When using Abaqus through the GUI, a record of every action is recorded to a text file using the Abaqus scripting language. This has been exploited by adjusting a particular length in the GUI, then copying this behaviour into the script after the part, and mesh has been regenerated. Once this code has been inserted into the parameter script, the value of the length that has been changed can be found and replaced with a parameter variable, allowing the value to be changed in the for loop based on the values in the parameter domain.

This was found to be a good solution and allowed the parametric study to include changes in geometric length. It has however resulted in a large script file that includes some code that is not necessary for the script to run. This is because Abaqus records GUI specific code in the record text file such as updating the view in the GUI.

6.4.1.3 Initial imperfection

After the parameter values have been defined inside each for loop, an eigenvalue and eigenvector analysis to find the buckling mode is created. This is necessary to define the initial imperfection of each model. Parametric models cannot take an initial imperfection of the buckling mode shape if this has been defined for a different geometry. To make the code more efficient, the buckling mode analysis is only updated after a change in geometry, allowing parametric models with changes in material parameters to use the same buckling mode file. The imperfection keywords are then updated in the Abaqus keywords file for the correct buckling mode shape.

6.4.1.4 Displacement Analysis

Finally, the analysis of each parametric model can then begin. The job name and description of each analysis are updated based on the parameter values of that particular model so that each model can be identified by the parametric analysis output script.

```
jobName = 'YC_l3-%s_l2-%s_a0-%s_t%s_E%s_y%s' %(l3Param,
      l2Param, a0Param, thicknessParam, youngsParam,
      yieldParam)
jobDescription = 'YC01 Displacement test where l3-%s l2-
      %s a0-%s t-%s E-%s y-%s' %(l3Param, l2Param,
      a0Param, thicknessParam, youngsParam, yieldParam)
myJob = mdb.Job(name=jobName, model='YC01-Displacement',
      description=jobDescription)
mdb.jobs[jobName].setValues(numCpus=8, numDomains=8)
myJob.submit()
```

6.4.2 Output Script

To process the large number of finite element model output files, a python script was written to collate the output data from each parametric model output database. This can be found in Section 10.3.2 in the appendices.

The output script looked in a designated folder with each parametric output database file. A for loop was used to run through every file in the folder. For each parametric output database, a line was added to an output text file containing the parametric inputs and the maximum buckling capacity.

Buckling capacity was determined by the same method used in Section 5.4.3. The script used a for loop to sum the reaction force of each node at the gusset plate interface with the beam-column joint. This occurred for every time-step in the parametric model output database. The script then identified the time-step with the maximum reaction force sum and output this force as the buckling capacity.

As each output database has not been individually reviewed, a check was required to ensure that the gusset plate did buckle in the analysis. This was achieved by comparing the final reaction force sum in the model with the buckling capacity force. If the final reaction force sum was less than the buckling capacity force, then it was clear that the gusset plate had buckled. If a model were found to have a final force equal to the buckling capacity force, the displacement imposed on the model would be increased until buckling occurred. This was not found to be an issue.

6.5 Results

After the input script had been completed, all 5880 parametric output model databases were analysed. This number is slightly less than the maximum number of theoretical parametric combinations due to some combinations being incompatible with each other. A gusset plate

with a short edge of 350 mm and a long and wide splice plate of 300 mm and 200 mm respectively, was not geometrically valid due to the splice plate extending beyond the bounds of the gusset plate.

The parametric output databases were processed with the parametric output script and then further processed in Matlab (The MathWorks, Inc. 2012). For each parameter, a graph showing the relationship between the parameter and buckling capacity has been produced. All other parameters have been held constant except for each boundary condition. This will determine the relationship if changing the boundary condition is independent of the parameter.

A representative, or baseline, gusset plate has been developed for each parameter value that is held constant, these values are shown in Table 6.5-1.

Table 6.5-1: Parameter values of the representative gusset plate

Parameter	Dimensions
Thickness	10 mm
Modulus of Elasticity	200 GPa
Yield Strength	300 MPa
Splice Plate Length	250 mm
Splice Plate Width	150 mm
Vertical Edge Length	400 mm
Whitmore Width	187.3 mm
Thornton Length	390.0 mm

The relationship between the parameter and buckling capacity has also been compared to the estimated relationship from the Thornton method considering the maximum Thornton length and fixed-free boundary conditions. It is expected that this estimated relationship will always be conservative. The findings from Chapter 5 indicated that the buckling capacity of finite element models with fixed-free boundary conditions will be conservatively estimated using the Thornton method considering the maximum Thornton length.

6.5.1 Gusset Plate Thickness

It can be seen in Figure 6.5-1 that gusset plate thickness has a non-linear relationship with buckling capacity for fixed-free boundary conditions. However, it can be seen that for fixed-fixed and fixed-roller boundary conditions, there is an almost linear relationship. This agrees with observations made by Cheng et al. (1994) and Yam and Cheng (2002). This may indicate that the relationship between thickness and buckling capacity is not independent of boundary condition.

The fixed-free relationship between thickness and buckling capacity is compared to the Thornton method with maximum Thornton length in Figure 6.5-2. The slope of the Thornton method relationship is less than the finite element model relationship. This indicates that the Thornton method conservatively predicts the relationship between buckling capacity and gusset plate thickness for fixed-free boundary conditions.

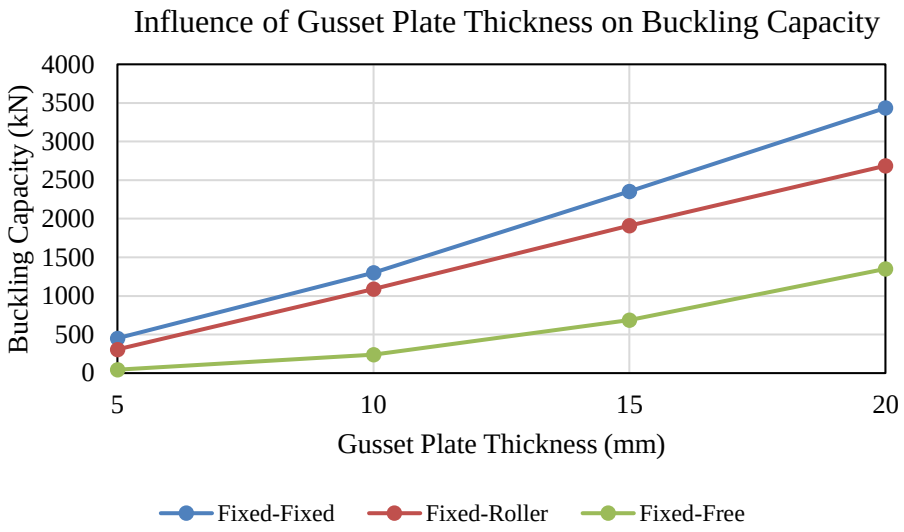

Figure 6.5-1: Influence of thickness on gusset plate buckling capacity

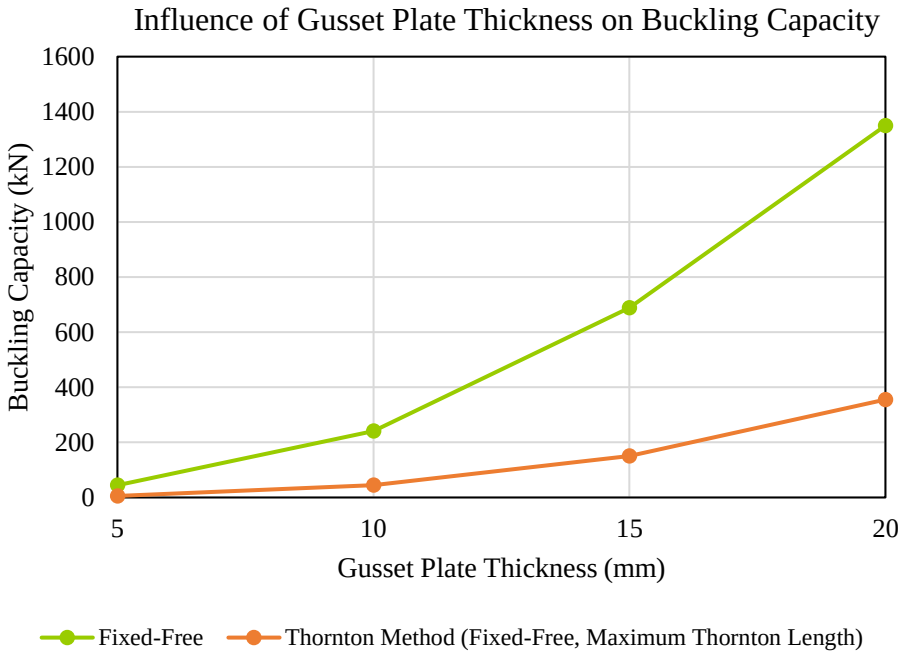

Figure 6.5-2: Comparison of finite element model capacity to estimated capacity considering thickness

6.5.2 Modulus of Elasticity

It can be seen in Figure 6.5-3 that the relationship between modulus of elasticity and buckling capacity is linear for all gusset plate models considering all boundary conditions for the range of interest. As there is not much variation in the values selected for modulus of elasticity, it is unclear if this trend holds true for all values. However, it is likely that all steel used for gusset plates in braced frames will fall within these values, and so it is not necessary to consider outside the range of values.

In Figure 6.5-4, it is clear that the Thornton method considering maximum Thornton length has made an accurate assumption on the modulus of elasticity's relationship to buckling capacity for fixed-free boundary conditions.

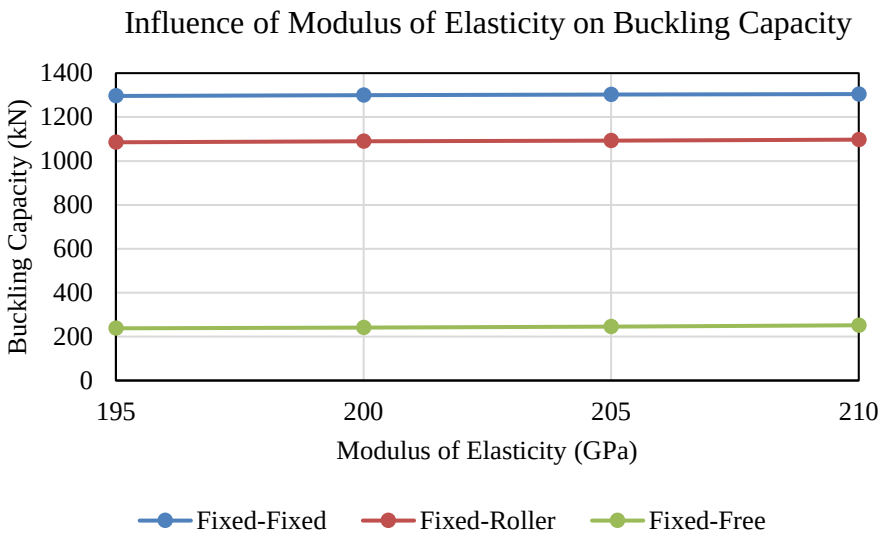

Figure 6.5-3: Influence of modulus of elasticity on gusset plate buckling capacity

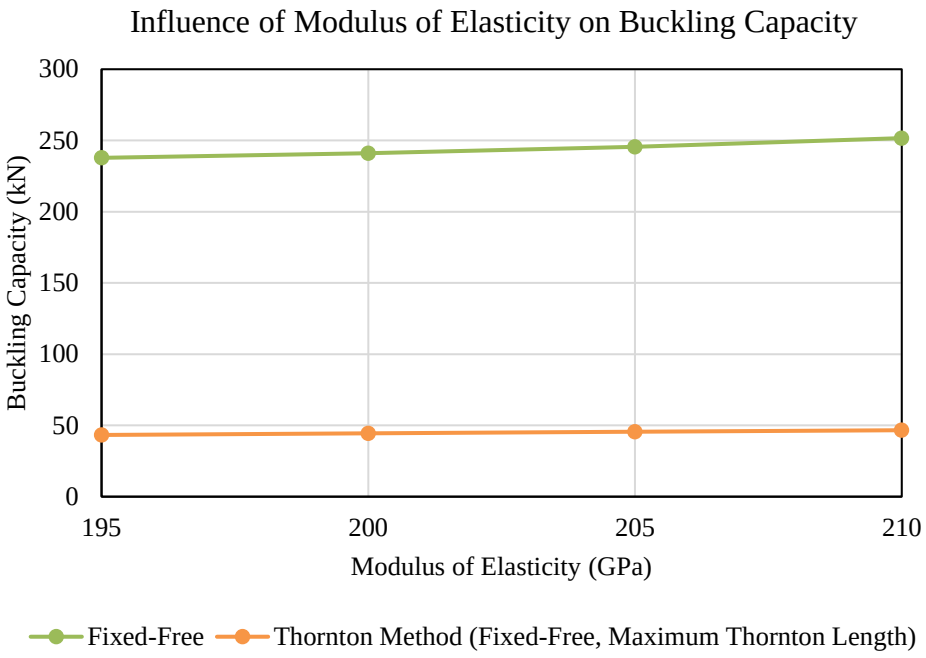

Figure 6.5-4: Comparison of finite element model capacity to estimated capacity considering modulus of elasticity

6.5.3 Yield Strength

Like modulus of elasticity, it clear from Figure 6.5-5 that yield strength has a linear relationship on buckling capacity within the range of likely values for steel gusset plates. This is reasonable for fixed-fixed and fixed-roller boundary conditions which are more likely to buckle inelastically.

Figure 6.5-6 shows that the Thornton method considering maximum Thornton length and fixed-free boundary conditions estimated that the buckling capacity does not change as the yield strength is increased. This is reasonable as the gusset plate is buckling elastically and matches the results of the finite element model.

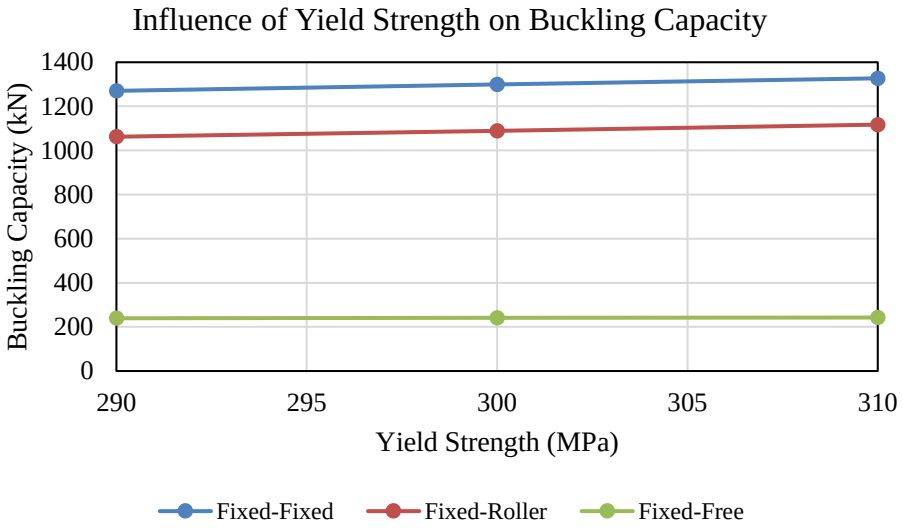

Figure 6.5-5: Influence of yield strength on gusset plate buckling capacity

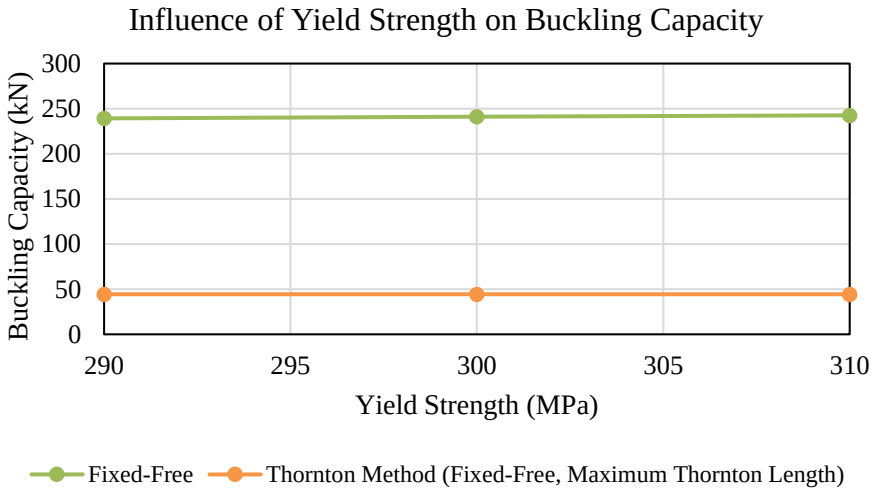

Figure 6.5-6: Comparison of finite element model capacity to estimated capacity considering yield strength

6.5.4 Splice Plate Length

Splice plate length appears to be linearly proportional to buckling capacity for the values considered, as seen in Figure 6.5-7. This is an interesting finding as increasing splice plate length will linearly decrease the maximum Thornton length and linearly increase buckling capacity. However, the maximum Thornton length has an estimated non-linear relationship with buckling capacity by the Thornton method. Depending on the slope of the curves, this may result in a non-conservative estimate of buckling capacity in some cases.

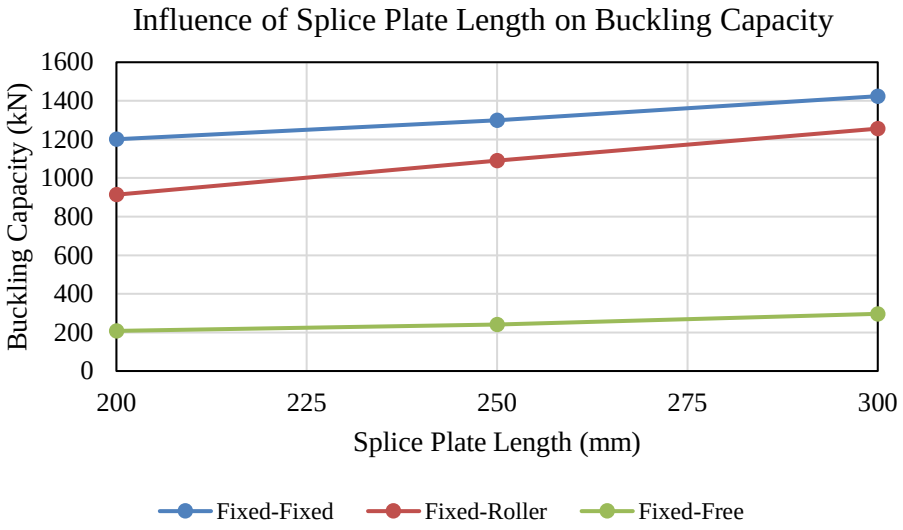

Figure 6.5-7: Influence of splice plate length on gusset plate buckling capacity

6.5.5 Splice Plate Width

It can be seen in Figure 6.5-8, that buckling capacity increases relatively linearly for fixed roller and fixed-free boundary conditions. However, there is a slight nonlinear relationship between splice plate width and buckling capacity for fixed-fixed boundary conditions.

Increasing splice plate width will linearly increase the Whitmore width, which is estimated to be linearly dependent on buckling capacity. It is therefore expected that the Whitmore width will be linearly proportional to buckling capacity for fixed-free boundary conditions based on the splice plate width and splice plate length relationships with buckling capacity.

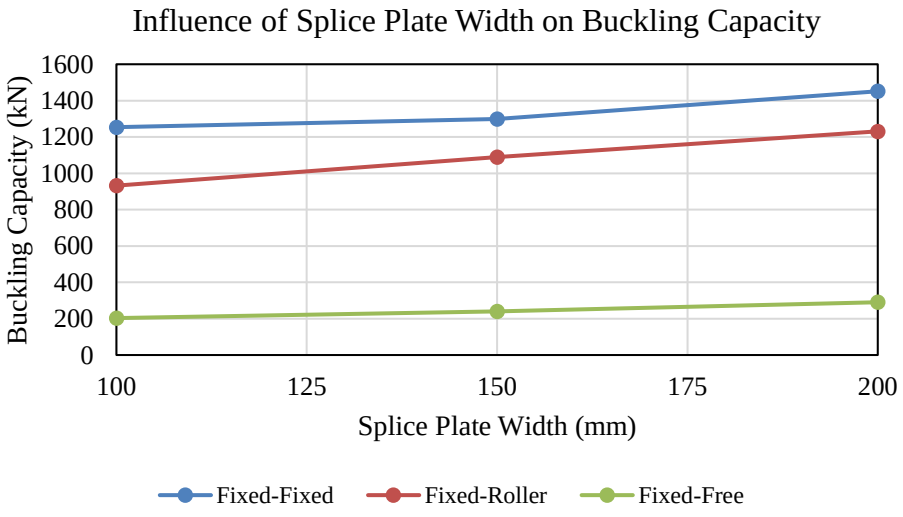

Figure 6.5-8: Influence of splice plate width on gusset plate buckling capacity

6.5.6 Vertical Edge Length

It can be seen in Figure 6.5-9 that when vertical edge length is increased, buckling capacity decreases non-linearly. However, for fixed-fixed boundary conditions, buckling capacity increases when vertical edge length is increased from 400 mm to 450 mm.

Vertical edge length is not a direct parameter used in the Thornton method although it will affect the Thornton length. The inconsistency in the relationship between vertical edge length and buckling capacity may indicate the Thornton length will not have a consistent relationship with buckling capacity in some cases.

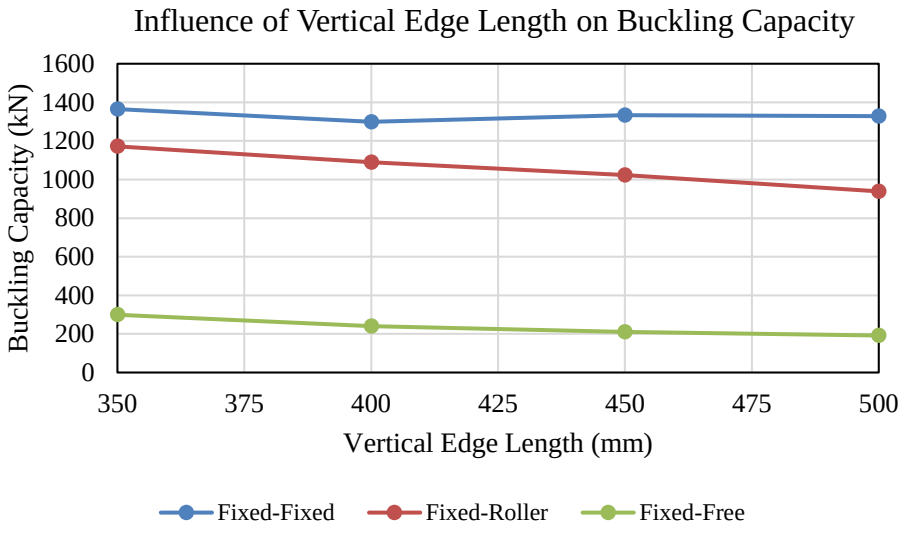

Figure 6.5-9: Influence of vertical edge length on gusset plate buckling capacity

6.5.7 Whitmore Width

The Whitmore width is expected to increase buckling capacity in the Thornton method linearly. It is clear from Figure 6.5-10 that this is not strictly true. There is a general trend that, as the Whitmore width increases, buckling capacity also increases. However, in some cases, there is a decrease in buckling capacity when the Whitmore width increases. This fluctuation in capacity is relatively small but it may contribute to explaining why the Thornton method has a significant variance between the predicted buckling capacity and the true buckling capacity for different gusset plates.

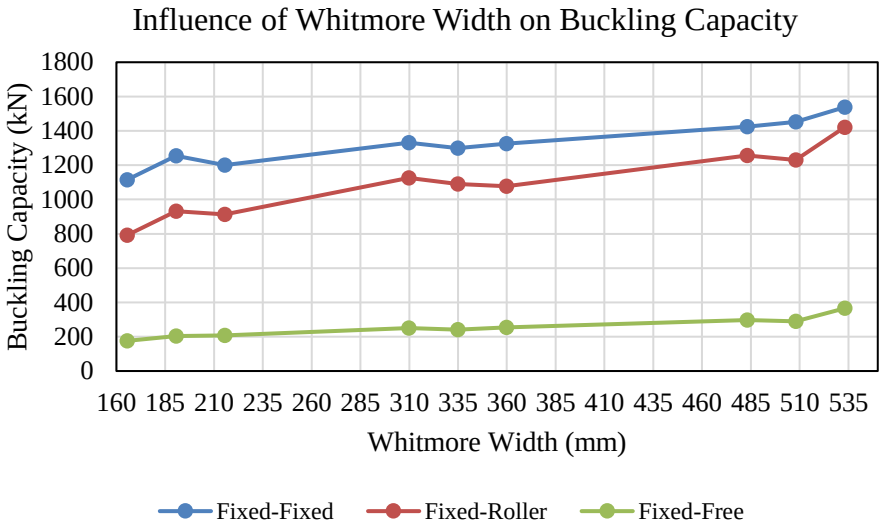

Figure 6.5-10: Influence of Whitmore width on gusset plate buckling capacity

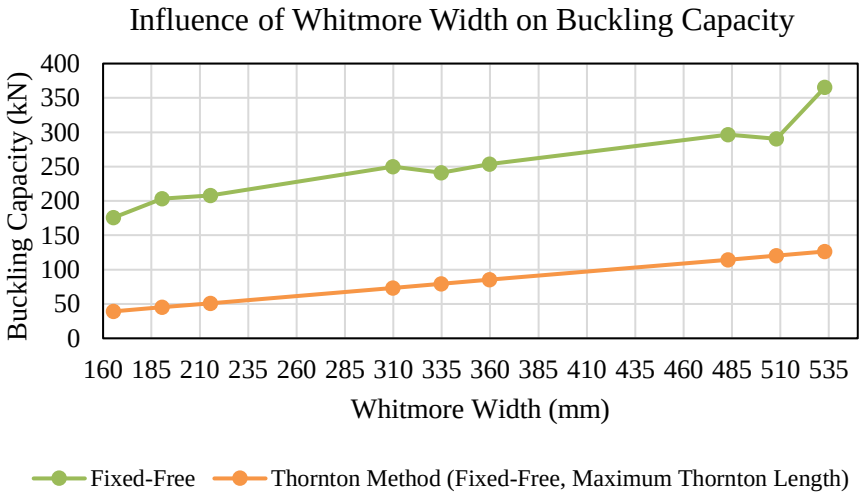

Figure 6.5-11: Comparison of finite element model capacity to estimated capacity considering yield strength

6.5.8 Thornton Length

The Thornton length also shows same fluctuation behaviour as the Whitmore width. It can be seen in Figure 6.5-12 that buckling capacity can either decrease or increase when the Thornton length is increased. This effect is not as strong for gusset plates with fixed-free boundary conditions.

In general, an increase in the Thornton length will cause a decrease in buckling capacity. However, the fluctuation in buckling capacity means that the Thornton method may not always be reliable.

In one case, it can be seen that for K = 1.0 and a Thornton length of 385 mm, the buckling capacity is 840 kN. When the Thornton length is increased to 394 mm, buckling capacity is increased to 1342 kN, a 60 % increase in capacity. Using the relationship in the Thornton method, it would have been expected that buckling capacity would decrease. The Thornton length of 385 mm is the result of a gusset plate with a splice plate length of 200 mm and a vertical edge length of 350 mm.

The fluctuations in capacity are less pronounced for fixed-free boundary conditions, where K = 2.0, with only a 5 % increase in capacity for the same Thornton lengths investigated earlier. As such, these fluctuations may be less of an issue for the methods proposed by Chou et al. (2012) and Tsai and Hsiao (2008).

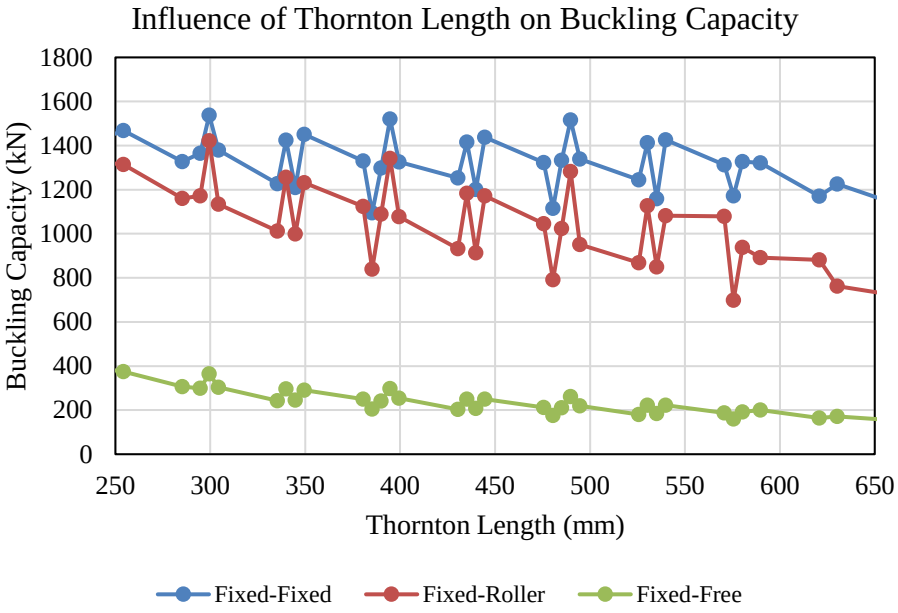

Figure 6.5-12: Influence of Thornton length on gusset plate buckling capacity

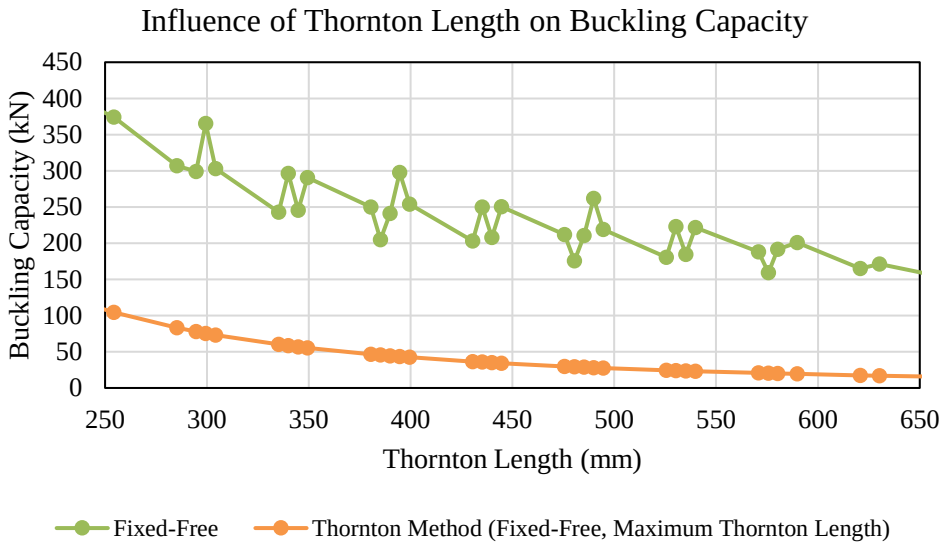

Figure 6.5-13: Comparison of finite element model capacity to estimated capacity considering yield strength

6.6 Parameter Relationship Consistency

The large range of finite element models analysed was used to determine if the parameter relationships remain consistent. By plotting all gusset plate finite element models for each parameter against buckling capacity, it can be visually examined whether the relationship holds true for a wide range of gusset plates. From Figure 6.6-1 through to Figure 6.6-8, the influence of each gusset plate parameter has been plotted against buckling capacity. For each curve on each figure, all other parameters are held constant (except for Whitmore width and Thornton length, which are dependent parameters). If the parameter relationship holds true for all gusset plates tested, only the slope of each curve will vary. This is the result of the other parameters changing between curves.

For example, for Figure 6.6-1, each curve considers four gusset plates that have different thicknesses and all other parameters held constant. The slope of each curve on this figure will be different as they have different parameter values that are being held constant.

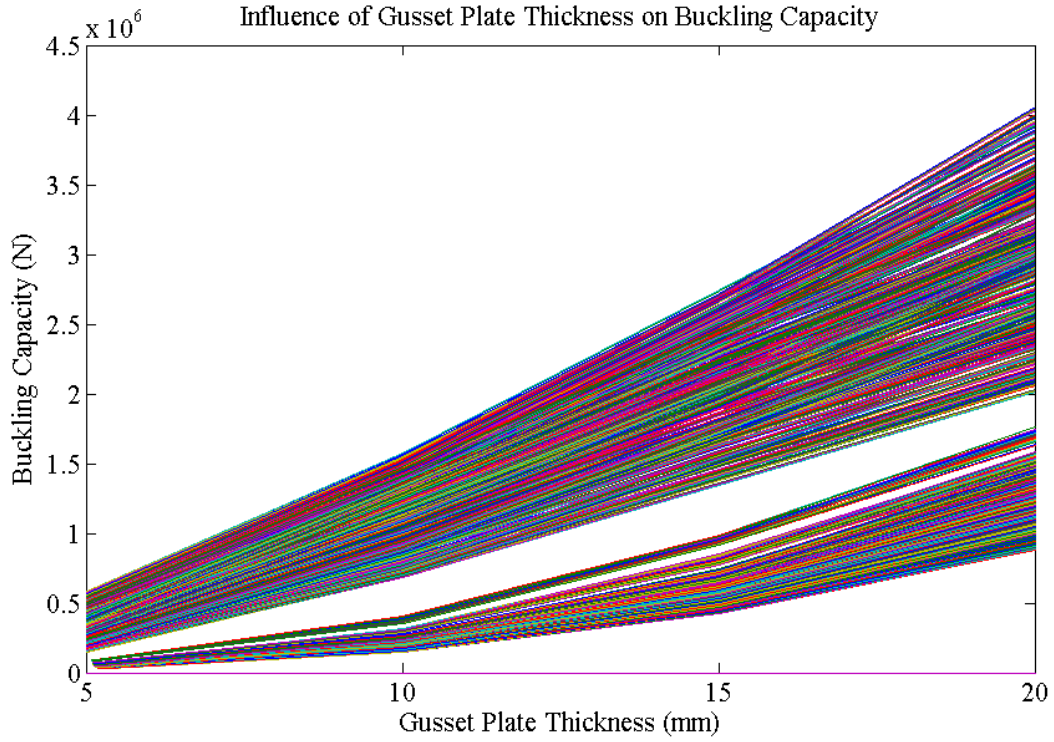

Figure 6.6-1: Influence of thickness on gusset plate buckling capacity

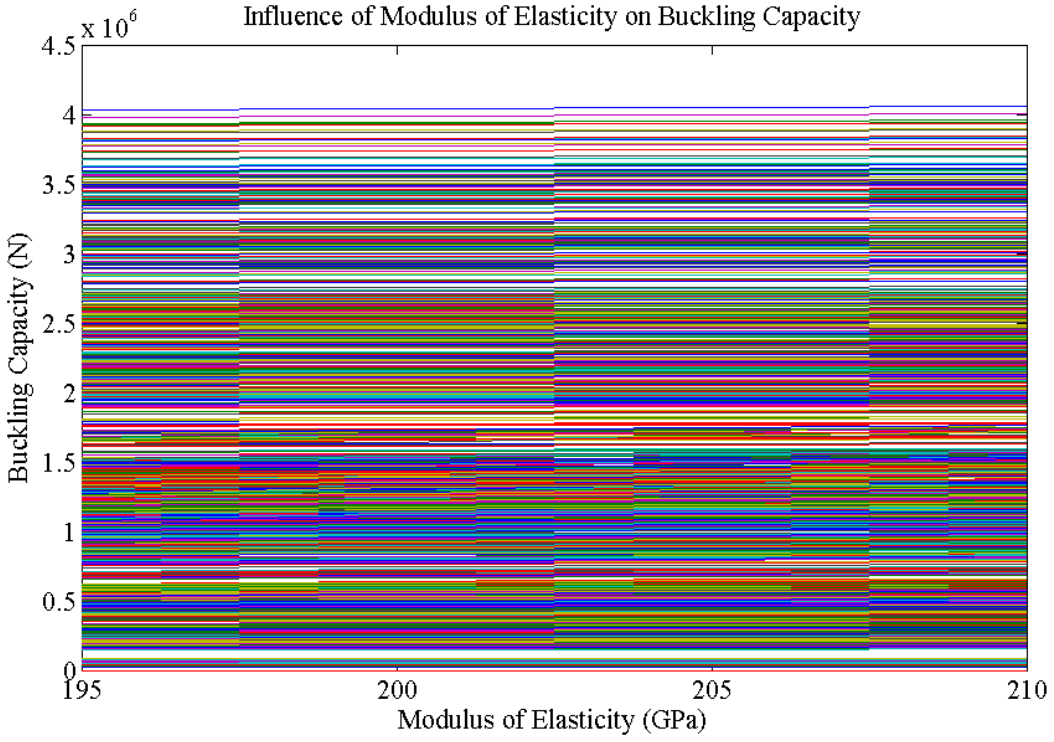

Figure 6.6-2: Influence of modulus of elasticity on gusset plate buckling capacity

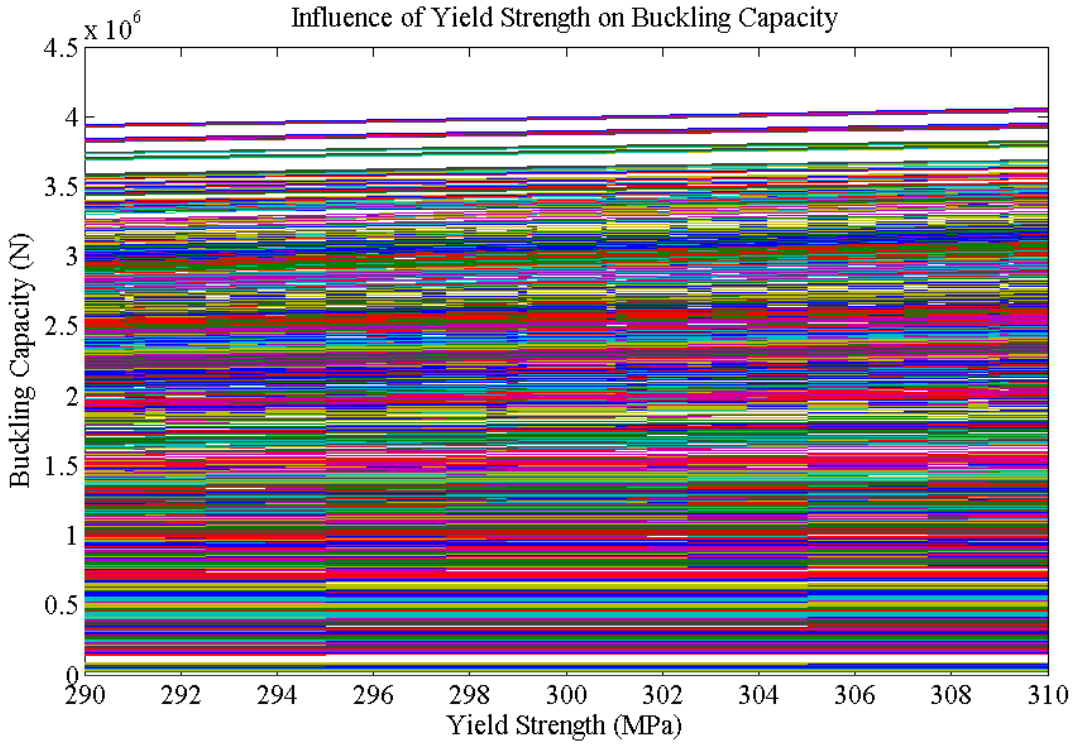

Figure 6.6-3: Influence of yield strength on gusset plate buckling capacity

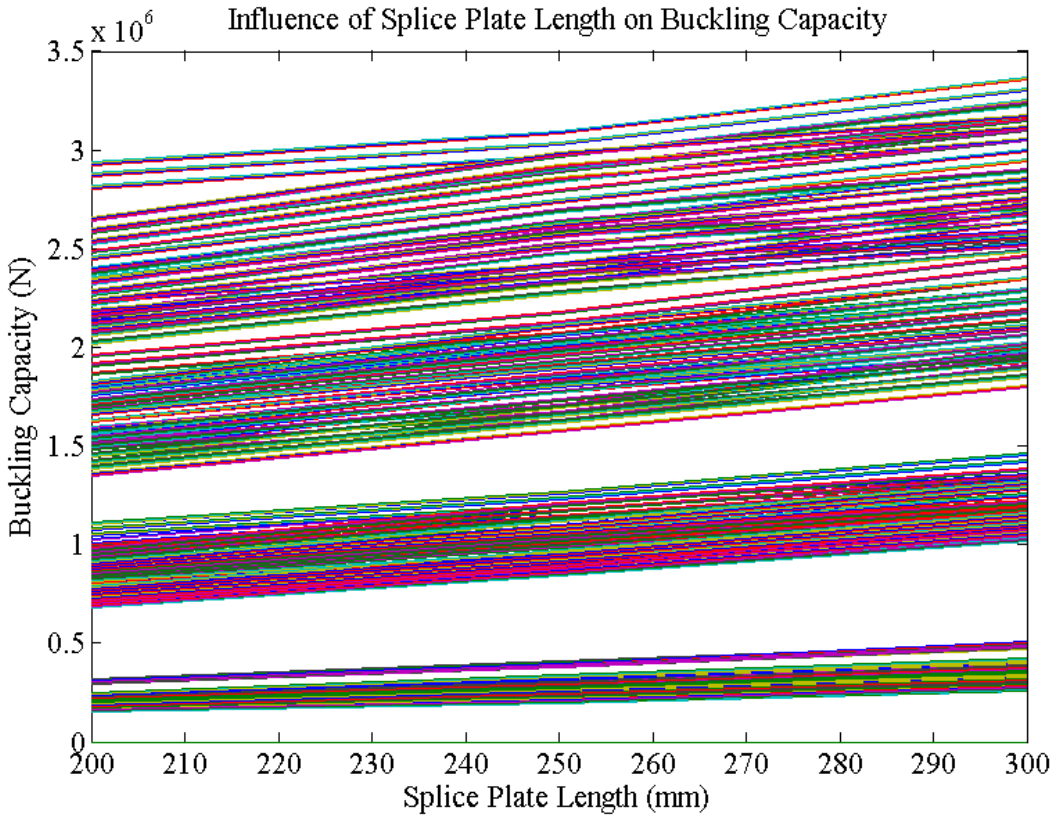

Figure 6.6-4: Influence of splice plate length on gusset plate buckling capacity

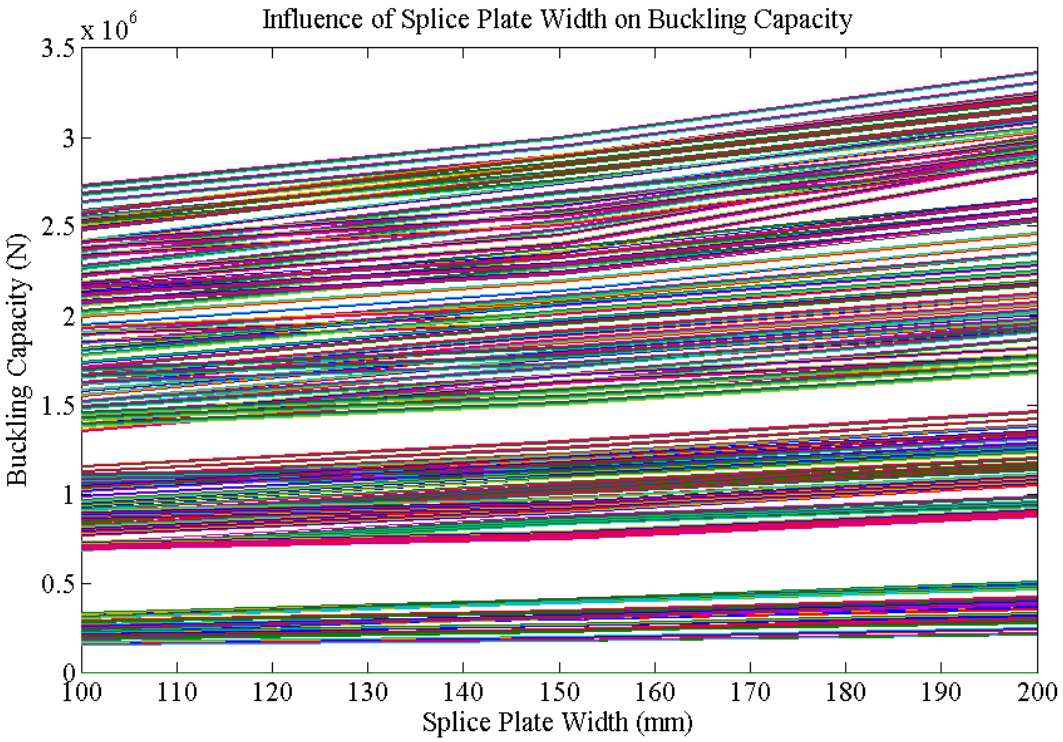

Figure 6.6-5: Influence of splice plate width on gusset plate buckling capacity

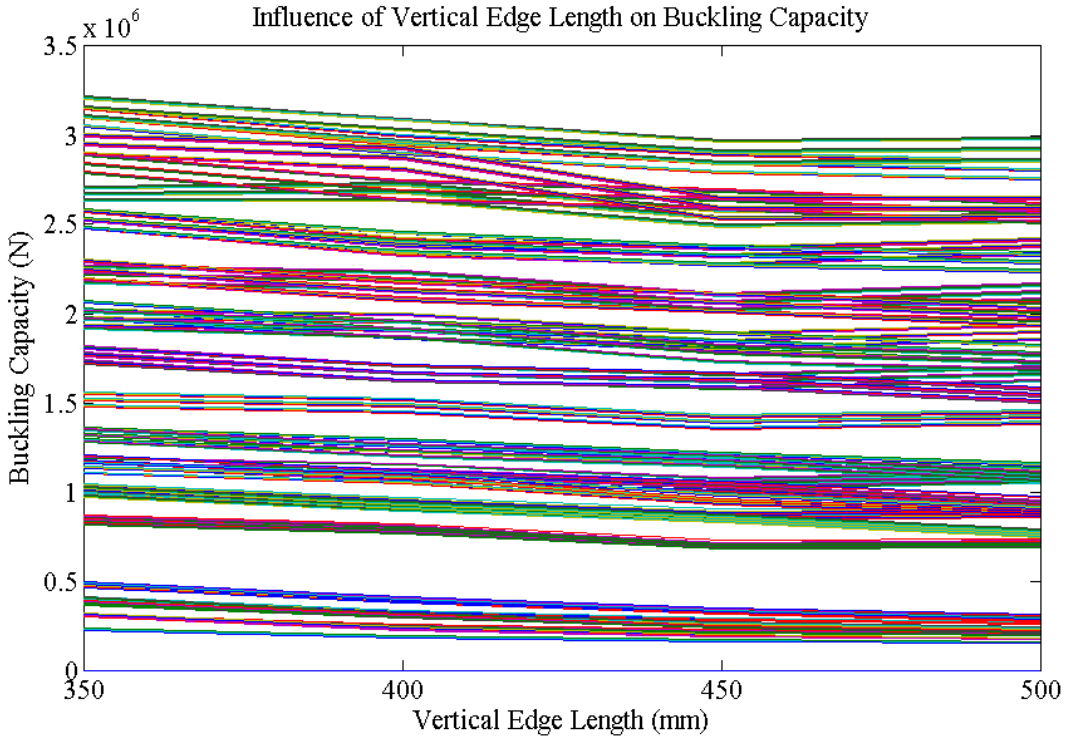

Figure 6.6-6: Influence of vertical edge length on gusset plate buckling capacity

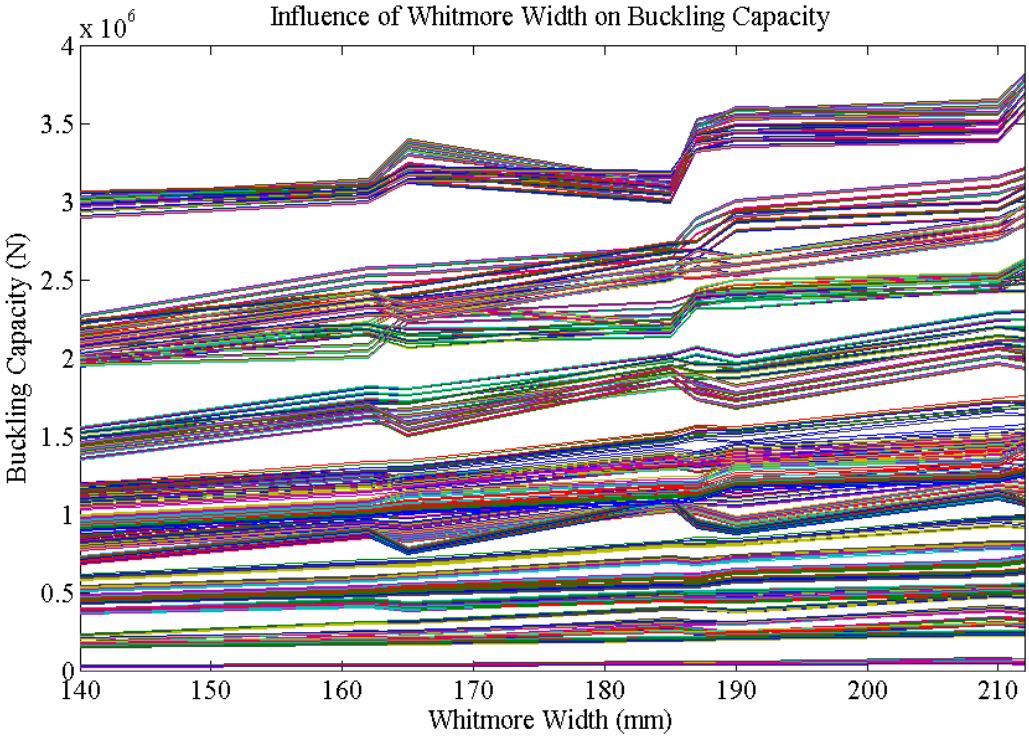

Figure 6.6-7: Influence of Whitmore width on gusset plate buckling capacity

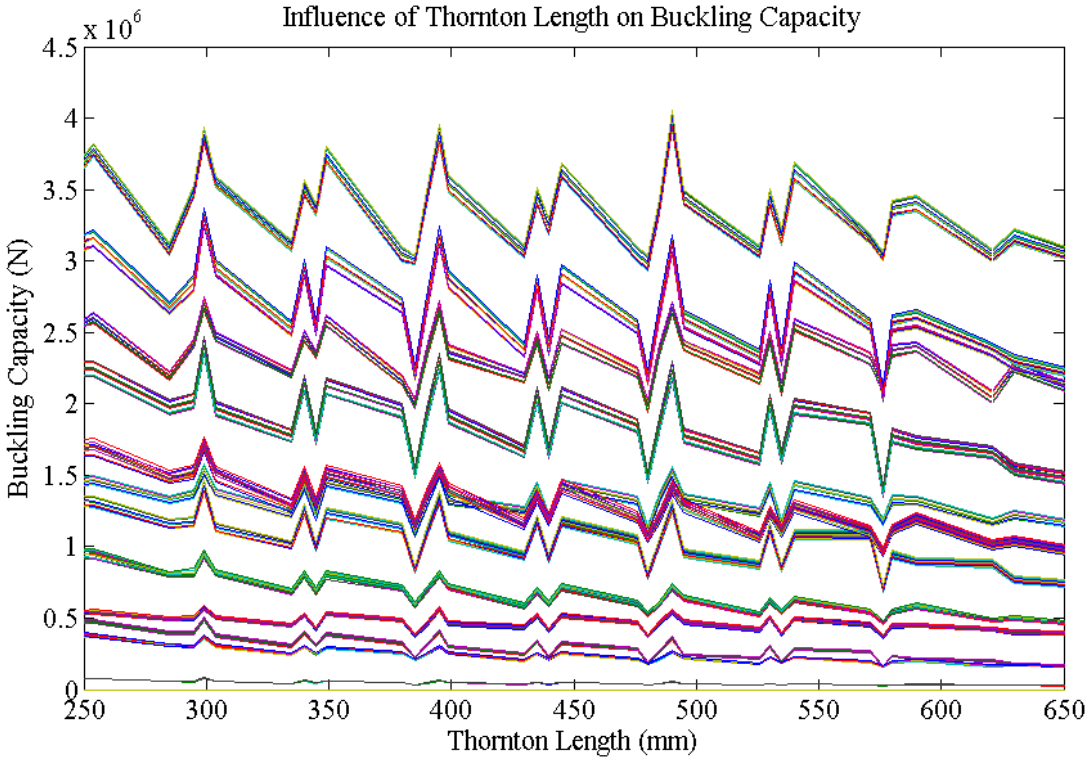

Figure 6.6-8: Influence of Thornton length on gusset plate buckling capacity

Most parameter relationships hold true for all gusset plates as only the slope each curve in the above figures appears to change. However, there are several anomalies.

In Figure 6.6-4, the splice plate length changes from a linearly proportional relationship to a non-linear relationship for the gusset plates with the highest buckling capacities. This appears to the result of these gusset plates having higher buckling capacity at shorter splice plate lengths compared to other gusset plates. As such, this anomaly suggests some gusset plates will have even higher buckling capacities than estimated.

Vertical edge length does not always have a consistent relationship with buckling capacity, as seen in Figure 6.6-6. In general, all gusset plates appear to decrease in buckling capacity as vertical edge length increases, however, there are a number of gusset plates where buckling capacity will increase.

Another key piece of information that can be taken from the figures is the distinct grouping of curves. This is most evident in Figure 6.6-1, where the bottom third of the curves have significantly lower buckling capacity. This is due to these curves having fixed-free boundary conditions. It is clear that gusset plates with fixed-free boundary conditions have significantly lower buckling capacity than those with fixed-free and fixed-roller boundary conditions.

6.7 Conclusion

The parametric study has shown that the standard parameters considered for the Thornton method and its derivatives may not necessarily be relative to buckling capacity in the same way that is expected by the Thornton method. In particular, the Thornton method and the Whitmore width have been shown to not have a reliable proportional relationship with buckling capacity. Although the general trend of these parameters is consistent, small changes in the length or width can lead to an opposite change in buckling capacity than what is expected.

The aims at the start of this chapter have been addressed:

1) A range of parameters that affect the buckling capacity of gusset plates was considered and compared to experimental testing and the Thornton method assumptions.
2) A parametric study was developed using finite element models and python scripting.
3) Since increasing the Thornton length or Whitmore width can sometimes cause an increase or a decrease in capacity, they may not be a reliable parameter for estimating gusset plate buckling capacity

4) Generally, the relationships between suitable parameters and buckling capacity hold true for a broad range of parameter value combinations. However, in some gusset plates, the change in buckling capacity will not follow the trend of the other gusset plates.

7 GP-BRB System Stability Method

7.1 Introduction

It has been shown in the previous chapters that determining buckling capacity of a gusset plate considering the properties of only the gusset plate itself cannot be done accurately, and may not be conservative in a number of cases, especially when considering gusset plates in BRB frames that are particularly susceptible to sway buckling.

It has been shown by a number of research papers that other frame elements can have an effect on the buckling capacity of a gusset plate in a BRB frame (Crake and Westeneng 2014; Takeuchi et al. 2014). Therefore, there is a need for a design method that considers these frame elements.

One promising method is that proposed by Takeuchi et al. (2015) and Takeuchi et al. (2014). This method considers the gusset plate and beam-column joint together with one rotational spring. Their method also considers the BRB and connection flexural stiffness, as well as the BRB end rotational stiffness. The method has been discussed in Sections 2.4.12 and 2.4.13. One of the largest limitations of this method is that the rotational spring that represents the gusset plate is not well defined at present. Experimental testing and finite element methods are the best way to determine this stiffness.

This chapter seeks to develop an alternative buckling capacity design method that considers each of the gusset plates, BRB, BRB restrainer ends, connection regions, and beam-column joints separately. Where appropriate, it will be compared to the method proposed by Takeuchi and his associates.

Because the method explicitly considers the individual elements in the BRB system, the effect of adjusting the stiffness of each element can be investigated to understand buckling behaviour better. The method can also be compared to equivalent buckling column methods such as the Thornton method to see whether the boundary condition assumptions made by Chou et al. (2012) and Tsai and Hsiao (2008) are correct for all BRB frames.

The aims of this chapter are to:

1) Develop a method to consider BRB stability,
2) Determine what potential input variables should be considered,
3) Verify that the method is mathematically correct,
4) Calibrate the method against any experimental information that may exist,
5) Conduct a sensitivity study to consider the effect of changing different parameters such as element rigidity and length,
6) Determine if effective length factor can be assumed to be a constant value such as 2.0,
7) Develop a tentative design procedure.

7.2 Development of Method

Stability and stiffness based approaches were taken to develop the method. There are multiple important flexural elements in the BRB system, and so a design method based on eigenvalue analysis of a stiffness matrix that considers each element of the sub-structural system was deemed to be a reasonable approach to determine the buckling capacity. All the elements in the BRB system were assumed to behave as either as rotational springs or flexural beam elements. The stiffness of these elements was then considered in a single system stiffness matrix, and the critical buckling load was determined by finding the smallest eigenvalue of stiffness matrix.

7.2.1 System Stiffness Matrix

The system stiffness matrix considers the contributions of the various elements in the BRB system. This comprises of the gusset plate flexural stiffness matrix of both gusset plates, the connection region flexural stiffness matrix of both connections between the gusset plates and the BRB, and the BRB flexural stiffness matrix. The matrix has been modified to consider the beam-column joint rotational stiffness, and the BRB end rotational stiffness. BRB end rotational stiffness has been included to account for the fact the ends of the BRB are susceptible to hinging and are often unable to provide full moment transfer (Matsui et al. 2010).

Instead of using the general 4 x 4 beam element stiffness matrix shown in Equation 7.2-1 for each flexural element in the BRB system, a modified beam element stiffness matrix was used to account for P-delta effects.

$$\begin{Bmatrix} V_a \\ M_a \\ V_b \\ M_b \end{Bmatrix} = \frac{EI}{L}\begin{bmatrix} 12/L^2 & 6/L & -12/L^2 & 6/L \\ 6/L & 4 & -6/L & 2 \\ -12/L^2 & -6/L & 12/L^2 & -6/L \\ 6/L & 2 & -6/L & 4 \end{bmatrix}\begin{Bmatrix} \Delta_a \\ \theta_a \\ \Delta_b \\ \theta_b \end{Bmatrix} \qquad 7.2\text{-}1$$

where:

V_X shear force at a particular end of the beam element

M_X moment at a particular end of the beam element

E modulus of elasticity of the beam element

I second moment of area of the beam element

L length of the particular beam element

Δ_X displacement at a particular end of the beam element

θ_X rotation at a particular end of the beam element

The general 4 x 4 beam element stiffness matrix relates displacements and rotations to shear force and moments accounting for the stiffness of the beam element. However, this stiffness does not account for the axial load on the beam element reducing the stiffness. The axial forces in BRB systems are significant, and so it was deemed vital to consider the effects of axial load. This was achieved using stability functions, which modified the matrix seen in Equation 7.2-1 to the stiffness matrix in Equation 7.2-2.

$$\begin{Bmatrix} V_a \\ M_a \\ V_b \\ M_b \end{Bmatrix} = \frac{EI}{L}\begin{bmatrix} f/L^2 & g/L & -f/L^2 & g/L \\ g/L & s & -g/L & r \\ -f/L^2 & -g/L & f/L^2 & -g/L \\ g/L & r & -g/L & s \end{bmatrix}\begin{Bmatrix} \Delta_a \\ \theta_a \\ \Delta_b \\ \theta_b \end{Bmatrix} \quad 7.2\text{-}2$$

$$\phi = \sqrt{\frac{PL^2}{EI}} \quad 7.2\text{-}3$$

$$s = \frac{\phi(\sin\phi - \phi\cos\phi)}{2(1-\cos\phi) - \phi\sin\phi} \quad 7.2\text{-}4$$

$$r = \frac{\phi^2 - \phi\sin\phi}{2(1-\cos\phi) - \phi\sin\phi} \quad 7.2\text{-}5$$

$$f = 2(s+r) - \phi^2 \quad 7.2\text{-}6$$

$$g = s + r \quad 7.2\text{-}7$$

where:

P axial force in beam element

It can be seen the Equation 7.2-2 is dependent on Equations 7.2-3 to 7.2-7. The result is that the stiffness of the beam element is proportional to the applied load on the beam element.

Beam element stiffness matrices considering the P-delta effect have been developed for the gusset plates, connection regions, and the BRB.

The stiffness matrix of each element is then assembled into a system stiffness matrix considering all the elements. Figure 7.2-1 identifies each of the 12 degrees of freedom in the system stiffness matrix and the relationship of each beam element to a complete BRB system.

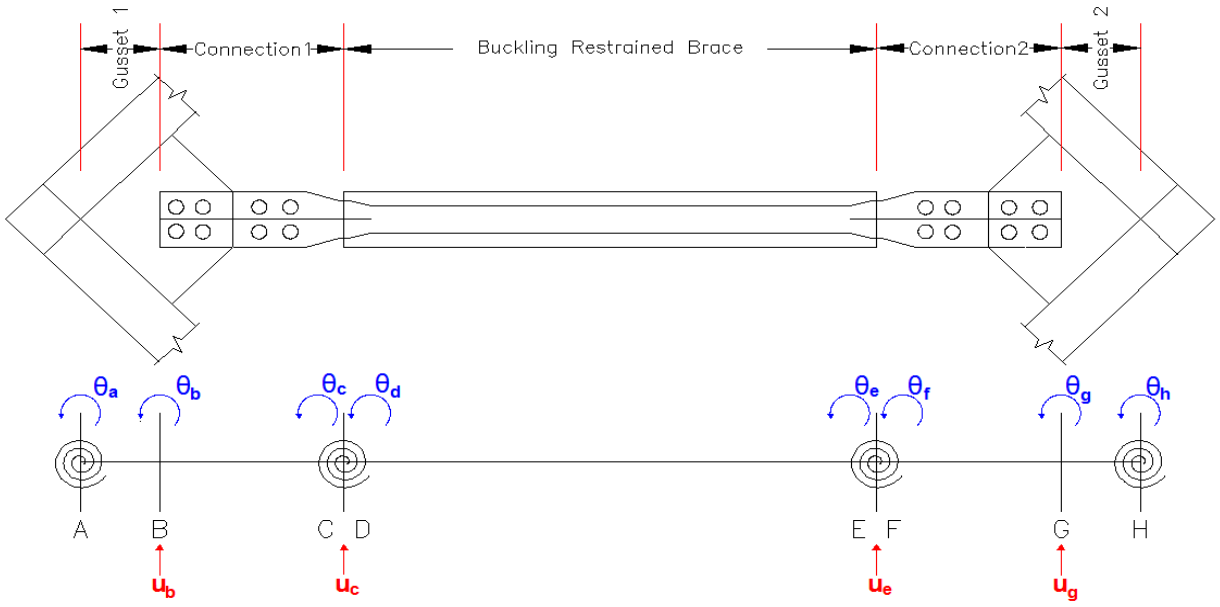

Figure 7.2-1: Components and available degrees of freedom in the system stiffness matrix

7.2.2 Beam-Column Joint

The beam-column joint rotational stiffness is represented by a rotational spring, allowing rotation in the out-of-plane direction, according to Equation 7.2-8. The spring is assumed to be located at the end of the gusset plate and that the lateral displacement there is negligible.

$$\{M_a\} = k_{BC}\{\theta_a\} \qquad 7.2\text{-}8$$

where:

k_{BC} beam-column joint rotational stiffness

If the lateral displacement is not negligible for a particular BRB frame, a more detailed system stiffness matrix could be easily developed considering the beam-column joint as a flexural beam element with a length extending from the end of the gusset plate to the centre of, or far side of, the beam-column joint. The rotational spring could then be implemented at the end of this joint beam element where there is rotation but not displacement. It may be reasonable to assume that this beam-column joint beam element is very stiff.

The use of a beam-column joint as a flexural beam element would be most reasonable when considering BRB systems in chevron configuration BRB frames. These configurations can have beam joints with very low rotational stiffness. This can cause large out-of-plane rotation and displacement as observed in experimental testing by Hikino et al. (2012) and Koetaka and Kinoshita (2009). However, the study by Takeuchi et al. (2015) shows that beam joint rotational stiffness can be accurately modelled at the interface between the gusset and the joint instead of the joint centre. As such, it was decided that using a rotational spring at the end

of the gusset plate instead of modelling the beam-column joint as a flexural element was a reasonable assumption.

7.2.3 Gusset Plate

The gusset plate is modelled as a beam element with flexural stiffness. This follows the assumptions of the Thornton method (and its derivatives) that the gusset plate can be accurately modelled as an equivalent buckling column. This, together with the assumptions commonly used in design, was shown to be generally non-conservative in Chapter 5 and Chapter 6, but it may be conservative if the maximum Thornton length is used, as described in Section 5.7. This is a good choice as the maximum Thornton length is generally the middle length which will be physically valid in the model. This is explored further in Section 7.3.5.

Because the beam-column joint is modelled as a rotational spring at one end of the gusset plate, this end is fixed against any out-of-plane translation. As such the beam element stiffness matrix for the gusset plate can be condensed from Equation 7.2-2 to Equation 7.2-9. This equation also considers the beam-column joint rotational spring by including Equation 7.2-8.

$$\begin{Bmatrix} M_a \\ V_b \\ M_b \end{Bmatrix} = \left(\frac{EI}{L}\right)_G \begin{bmatrix} s + k_{BC} & -g/L & r \\ -g/L & f/L^2 & -g/L \\ r & -g/L & s \end{bmatrix} \begin{Bmatrix} \theta_a \\ U_b \\ \theta_b \end{Bmatrix} \quad 7.2\text{-}9$$

where:

$\left(\frac{EI}{L}\right)_g$ flexural stiffness of the gusset plate

L gusset plate length

7.2.4 Connection Region

The connection region considers the splice plates that attach the gusset plate to the BRB connection outside of the outer casing. It can be considered through Equation 7.2-2 as it is reasonable to consider the connection as a flexural beam element with a particular length and rigidity.

7.2.5 BRB

The BRB has also been considered as a beam element through Equation 7.2-2. However, the restrained portion of the BRB, consisting of the outer casing and concrete filler, is unbonded

from the yielding core plate. This prevents the transfer of axial force into the outer casing and concrete filling. As such, P-delta effects are not present in this portion of the BRB. The general 4 x 4 beam element stiffness matrix from Equation 7.2-1 must be used. The addition of the yielding core plate beam element stiffness and the restrainer beam element stiffness has been shown in Equation 7.2-10.

$$\begin{bmatrix} \frac{12}{L^2}\left(\frac{EI}{L}\right)_R + \frac{f}{L^2}\left(\frac{EI}{L}\right)_C & \frac{6}{L}\left(\frac{EI}{L}\right)_R + \frac{g}{L}\left(\frac{EI}{L}\right)_C & -\frac{12}{L^2}\left(\frac{EI}{L}\right)_R - \frac{f}{L^2}\left(\frac{EI}{L}\right)_C & \frac{6}{L}\left(\frac{EI}{L}\right)_R + \frac{g}{L}\left(\frac{EI}{L}\right)_C \\ \frac{6}{L}\left(\frac{EI}{L}\right)_R + \frac{g}{L}\left(\frac{EI}{L}\right)_C & 4\left(\frac{EI}{L}\right)_R + s\left(\frac{EI}{L}\right)_C & -\frac{6}{L}\left(\frac{EI}{L}\right)_R - \frac{g}{L}\left(\frac{EI}{L}\right)_C & 2\left(\frac{EI}{L}\right)_R + r\left(\frac{EI}{L}\right)_C \\ -\frac{12}{L^2}\left(\frac{EI}{L}\right)_R - \frac{f}{L^2}\left(\frac{EI}{L}\right)_C & -\frac{6}{L}\left(\frac{EI}{L}\right)_R - \frac{g}{L}\left(\frac{EI}{L}\right)_C & \frac{12}{L^2}\left(\frac{EI}{L}\right)_R + \frac{f}{L^2}\left(\frac{EI}{L}\right)_C & -\frac{6}{L}\left(\frac{EI}{L}\right)_R - \frac{g}{L}\left(\frac{EI}{L}\right)_C \\ \frac{6}{L}\left(\frac{EI}{L}\right)_R + \frac{g}{L}\left(\frac{EI}{L}\right)_C & 2\left(\frac{EI}{L}\right)_R + r\left(\frac{EI}{L}\right)_C & -\frac{6}{L}\left(\frac{EI}{L}\right)_R - \frac{g}{L}\left(\frac{EI}{L}\right)_C & 4\left(\frac{EI}{L}\right)_R + s\left(\frac{EI}{L}\right)_C \end{bmatrix}$$

7.2-10

where:

$\left(\frac{EI}{L}\right)_C$ flexural stiffness of the yielding core plate

$\left(\frac{EI}{L}\right)_R$ flexural stiffness of the restrainer including the outer casing and concrete filling

7.2.6 BRB End Rotational Stiffness

The system stiffness matrix explicitly considers the rotational flexibility at the BRB end by assuming the interface between the connection and the BRB end is semi-rigid and governed by a rotational spring. To account for this in the system stiffness matrix, an additional rotational degree of freedom at each BRB end must be added. This ensures that there is a rotational degree of freedom at either side of the rotational spring, which may behave as a hinge. To connect these two rotational degrees of freedom, a rotational spring stiffness matrix has been developed in Equation 7.2-11.

$$\begin{Bmatrix} M_c \\ M_d \end{Bmatrix} = \begin{bmatrix} k_{RE} & -k_{RE} \\ -k_{RE} & k_{RE} \end{bmatrix} \begin{Bmatrix} \theta_c \\ \theta_d \end{Bmatrix} \quad \text{7.2-11}$$

where:

k_{RE} rotational spring stiffness of BRB end

7.2.7 Inelastic buckling behaviour

Without modification, the method will only calculate the elastic buckling capacity of the BRB system. Current buckling capacity methods such as the Thornton method (Thornton 1984) consider inelastic buckling and column reduction factors through columns curves. These curves can be applied to the GP-BRB system stability method.

The NZS 3404 column curve (Standards New Zealand 1997) was chosen given the New Zealand context of this thesis, although other curves such as the AISC column curve (AISC 2005a) can be applied. It should be noted that both curves have been developed considering standard steel columns and their suitability for gusset plates has not been fully investigated.

The column curve can be applied to the method by reducing the rigidity of each beam element before the buckling capacity is calculated. This was achieved using the same method proposed by Lu et al. (2009) for extended direct analysis. An effective rigidity is found by reducing the elastic member rigidity by a stiffness reduction factor that considers inelastic buckling and column reduction factors such as out-of-straightness, residual stresses and accidental eccentricity. The effective rigidity can be found from Equation 7.2-12 to Equation 7.2-14.

$$c = 1.5\,exp(-1.8\alpha_b) - 0.35 \tag{7.2-12}$$

$$SRF_i = 1 - \frac{\left|\frac{N^*}{N_s}\right|}{1 + c\left(1 - \left|\frac{N^*}{N_s}\right|\right)} \tag{7.2-13}$$

$$(\mathrm{EI})_{\mathrm{eff,i}} = SRF_i * (EI)_i \tag{7.2-14}$$

where:

c column curve factor

α_b member section constant, $\alpha_b = 0.5$ for gusset plates

SRF_i stiffness reduction factor

N^* applied axial load on beam element

N_s axial section yield capacity

$(EI)_{eff,i}$ effective rigidity of beam element

The reduction factor has been applied to the gusset plate and the connection region. The BRB restrainer element is not reduced as there is not any axial load applied due to the unbonding layer between the BRB yield core and the restrainer.

7.2.8 Calculation of Buckling Capacity

Once the system stiffness matrix has been assembled from the stiffness matrices of the individual elements in the BRB system, buckling capacity of the system can be found when the applied load, P, is large enough such that the system stiffness matrix is no longer positive definite. This is equivalent to finding the smallest eigenvalue of the matrix.

7.2.9 Matlab Implementation

The system stiffness matrix was scripted into Matlab (The MathWorks, Inc. 2012), and the code can be found in Section 10.4 in the appendices. A for loop was used to increase the applied load in the BRB system. During each iteration of the for loop, the system stiffness matrix was developed.

Cholesky decomposition was used to determine when the matrix is no longer positive definite. This resulted in significant decrease in computation time compared to finding the determinate of the matrix due to the large size of the matrix. Cholesky decomposition was implemented through the following code, where K is the system stiffness matrix, R returns the upper triangular matrix and p returns zero when the matrix is positive definite.

```
[R,p] = chol(K) ;
```

When the matrix is no longer positive definite, p returns a positive integer. The code then determines the first time that a positive integer is returned after the for loop has finished, and the corresponding applied load is the buckling capacity of the BRB system.

7.3 Input Variable Considerations

For the input variables in the GP-BRB system stability method, a number of different values can be chosen, and these have been outlined in this section. It should be noted that flexural stiffness (EI/L) of each element has been considered as two separate variables consisting of flexural rigidity (EI) and length (L) due to the difference in behaviour of the variables in elastic column buckling.

7.3.1 BRB Length

The length of the BRB can be considered as the length of the BRB casing since the casing provides the out-of-plane stiffness of the BRB. However, if a hinge forms inside the casing at the end of the non-yielding region, then it may be reasonable to assume a shorter length equal to the yield length. The critical case will be when the brace has been extended as much as possible by tension and is starting to be compressed, as such it may be reasonable to consider the yield length plus the stroke length. Hinging has also been observed outside the casing (Chen et al. 2004). The casing length is used in the analyses undertaken here.

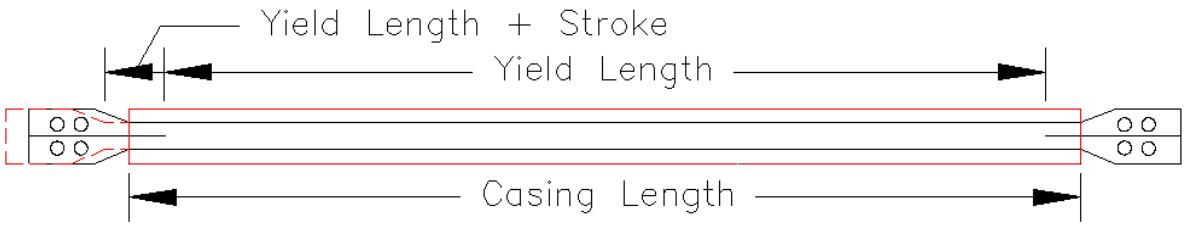

Figure 7.3-1: Potential BRB length selections

7.3.2 BRB Rigidity

The flexural rigidity of the BRB is mostly due to the contribution of the restraining media. This is generally the outside steel casing and the concrete/mortar infill. It is most conservative to assume only the steel casing contributes to the BRB rigidity as some concrete crushing is likely to occur at the BRB ends when a hinge forms. However, concrete contributes about 50 % of the total second moment of area and the modulus of elasticity of concrete is about 15 % of steel. As such it may be overly conservative to ignore the contribution of concrete.

The BRB core plate also provides flexural rigidity to the BRB. This will be a smaller contribution than the concrete or the steel casing, but may provide a noticeable increase in rigidity depending on the core plate shape. It is likely to be reasonable to ignore the contribution of the BRB core plate. After yielding, the core plate has a very low post-elastic stiffness and is assumed as $E_t = 0.05 * E$ where E_t is equal to the tangent modulus of elasticity (Chou and Chen 2010). This significantly reduces the core plate's rigidity and as such the contribution from the core plate to the flexural rigidity of BRB element is minimal.

In some designs, the BRB may be restrained by an all-steel casing with no concrete. Experimental testing has shown these designs have similar behaviour to traditional BRBs (Ma et al. 2008). As such, no special considerations are required to modify the BRB rigidity parameter.

In this study, the steel casing and concrete contribution have been considered, while the yielded steel core has been neglected.

7.3.3 Connection Region Length

Connection region length considers the length between the gusset plate and the BRB casing end.

Several different options for evaluating this length were considered. They were (a) the length from the BRB casing end to the last splice plate bolt, (b) the length from the yielding segment end to the last splice plate bolt, (c) the length from the BRB casing end to the edge of the splice plate, and (d) the length from the yielding segment end to the edge of the splice plate. The four potential lengths have been detailed in Figure 7.3-2.

The choice of BRB casing end or yielding segment end is dependent on the choice of BRB length to remain consistent.

The choice of the length extending to the last splice plate bolt, or the edge of the splice plate is dependent on the choice of gusset plate length. Traditionally, the Thornton length is considered to start from the last bolt in the connection splice (Thornton 1984). However, Yam and Cheng (1994) state that it is reasonable to assume the bolts clamp the connection sufficiently such that only considering a length to the end of the splice plate is more reasonable. For this study, it was decided that method (b) would be used.

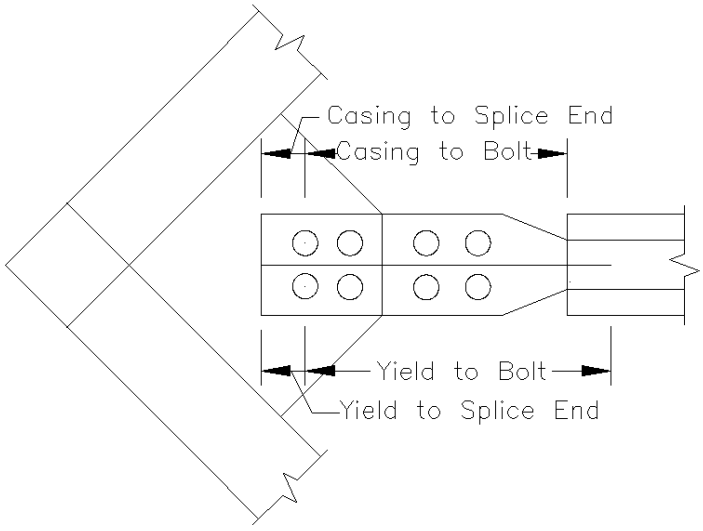

Figure 7.3-2: Potential connection length considerations

7.3.4 Connection Region rigidity

Connection region flexural rigidity can be considered by either the cross section of the connection outside the BRB end or the non-yielding segment cross section inside the BRB end. The latter being the most conservative. It may also be reasonable to consider both cross sections proportionally, as the transition between the two may be large enough such that cross section of the connection outside the BRB is not conservative. It is generally assumed that the gusset plate provides no additional rigidity contribution for the portion of the connection that is spliced to the gusset plate. In this study, the non-yielding segment cross section will be considered.

7.3.5 Gusset Plate Length

Gusset plate length can be taken as either (a) the average Thornton length, (b) the maximum Thornton length, or (c) the length between the end of the splice plate and the beam-column interface.

The length is usually taken as the average Thornton length (Thornton 1984). However, this is not physically valid in the full stability model and would result in an underestimation of the distance between the beam-column joints. The average Thornton length has also been found not to be conservative in a number of cases in Section 5.7.

Taking the maximum Thornton length is likely to result in a conservative estimation of gusset plate flexural stiffness, as evident from the design method study in Section 5.3 and Section 5.7. The distance between the beam-column joints will be overly conservative in cases where the maximum Thornton length is not the middle length.

The length between the end of the splice plate and the beam-column interface has not been investigated thoroughly, and so in this study, the maximum Thornton length has been considered.

7.3.6 Gusset Plate Rigidity

Using the Thornton method, it is possible to find an estimate for gusset plate rigidity. This may not be a reasonable assumption as Section 5 has shown that the Thornton method does not always accurately estimate gusset plate buckling capacity. It may be more accurate to find the gusset plate rigidity from a finite element model. However, this can be time-consuming for a designer.

As this study is considering the middle Thornton length, it is likely that the flexural stiffness of the gusset plate will be conservative by considering gusset plate rigidity from the Thornton method.

7.3.7 Beam-Column Joint Rotational Spring

The beam-column joint cannot always be considered a rigid element with infinite rotational stiffness. For BRBs in chevron configuration, the attached beam can have significantly lower rotational stiffness than a beam-column joint. This joint rotational spring can be conservatively idealised as a pin with zero rotational stiffness. Determining the rotational stiffness of the joint is difficult and may require finite element modelling. Takeuchi provides formulas for beam rotational stiffness for BRB systems in chevron configuration (Takeuchi et al. 2015).

The most conservative option is to assume that the beam-joint in a chevron configuration BRB frame acts as a perfect hinge and so the beam joint rotational spring stiffness is zero.

By assuming the joint as a rotational spring at the end of the gusset plate, the total length of the system is reduced. It may be more reasonable to consider the joint as a rigid link connecting to a pin or rotational spring in the centre of the joint. This has not been investigated further due to the discussion in Section 7.2.2.

7.3.8 BRB End Rotational Spring

The BRB end rotational spring stiffness depends on (a) the embedment length of the non-yielding segment into the BRB casing, (b) whether or not there are collars on the BRB casing end, (c) the properties and confinement of any concrete at the ends of the casing, (d) the extent that there has been tension yield of the BRB, and (e) the detailing of the brace at the end of the casing. It is difficult to quantify these things in general.

Matsui et al. (2010) have developed simple rotational stiffness equations for the elastic and plastic behaviour of simple rectangular or circular cased BRBs. These equations have been found to be in good agreement with experimental data.

The equations show that the rotational stiffness of the BRB end is dependent on the insertion length of the non-yielding segment at the BRB end. The designer has to determine whether the elastic or plastic rotational stiffness is used depending on whether the allowable rotation angle exceeds the pseudo yield point rotation angle. For a number of failures, the BRBs

used have been uniquely designed (such as considering all-steel BRBs), and the assumptions made by Matsui are not valid.

The most conservative option is to assume that a perfect hinge will always form at one BRB end and that the BRB end rotational stiffness is zero.

7.4 Verification of the GP-BRB System Stability Method

It was important to ensure that the method was mathematically correct and that its implementation into Matlab was correct. Mastan2 (Ziemian and Mcguire 2008) is a structural analysis software that performs linear and non-linear analysis. The foundations of the software are based on theoretical and numerical formulations on matrix structural analysis by Mcguire et al. (2000).

By comparing the same BRB system in Mastan2 and the GP-BRB system stability method, it can be verified that the GP-BRB system stability method is a correct implementation.

For this particular comparison, the restrainer component of the BRB will be affected by P-delta forces. This is because it is not possible to separate out the P-delta effect in Mastan2. As such, the GP-BRB system stability method will not implement the 4 x 4 general stiffness matrix for the restrainer component of the BRB and will instead use the modified stiffness matrix with stability functions.

7.4.1 Comparison of GP-BRB System Stability Method and Mastan2

To compare and verify the GP-BRB system stability method against Mastan2, four cases were used considering the experimental test by Chou et al. (2012). This test was chosen as the basis for this comparison, although the Matlab code should match the results of Mastan2 for any value used in any geometric or material property.

It should be noted that the results of this comparison cannot be compared to the experimental buckling capacity because the BRB end rotational stiffness is unknown for the test by Chou et al. (2012), and the assumption made on the BRB restrainer described above. Additionally, only elastic buckling behaviour was considered.

The four cases considered were:

1) Considering infinite rotational stiffness at the beam-column joint and BRB end rotational springs,

2) Considering infinite rotational stiffness at the beam-column joint and one BRB end rotational springs, and one perfectly pinned BRB end rotational spring,
3) Considering infinite rotational stiffness at one beam-column joint and both BRB end rotational springs, and one perfectly pinned beam-column joint rotational spring,
4) Considering beam-column joint and BRB end rotational springs to have some particular rotational stiffness, this is the general case.

Case 2 considers an ideal BRB system that has formed a perfect hinge at one end of the BRB, which is representative of a BRB with very low rotational stiffness at the BRB ends. Case 3 considered an ideal BRB system that has formed a perfect pin at the beam-column joint. This is representative of a chevron configuration BRB frame with a beam joint that has very low rotational stiffness. For Case 4, the rotational stiffness of all rotational springs in the model has been set to $1 * 10^9$ Nmm/rad.

It can be seen in Table 7.4-1 that the Matlab script implementation of the GP-BRB system stability method has an identical buckling capacity to the implementation of the method using Mastan2 software. This indicates that the method has been correctly formulated and is consistent with software that follows matrix structural analysis.

Table 7.4-1: Comparison of calculated buckling capacity from Mastan2 and Matlab script for GP-BRB system stability method

Case Number	Mastan2 Buckling Capacity (kN)	Matlab Script Buckling Capacity (kN)
1	1310.0	1310.0
2	45.1	45.1
3	381.0	381.0
4	754.6	754.5

It should be noted that the accuracy of the Mastan2 buckling capacity has been rounded to the nearest 0.1 kN, and the Matlab script is designed to round down to the nearest 0.1 kN. The accuracy of the Matlab script can be increased by adjusting the step size that the applied load iterates through in the for loop.

7.5 Validation of the GP-BRB System Stability Method

7.5.1 BRB Frame experimental studies

7.5.1.1 Tsai et al. (2004)

Sufficient geometric information is available on the BRB frame that buckled at the ground storey in experimental testing by Tsai et al. (2004). Unfortunately, because an all-steel BRB was used in the experimental test, the equations developed by Matsui et al. (2010) are not valid to determine the BRB end rotational spring stiffness. It is clear that the BRB end had a significant role in the buckling of this gusset plate due to the hinge forming. As such, the GP-BRB system stability method cannot be reliably verified by this experimental test frame.

If it is assumed that both the beam-column joint and BRB end rotational stiffness are infinite, then the GP-BRB system stability method estimates the buckling capacity of the first floor BRB frame tested by Tsai et al. (2004) to be 833 kN. This is slightly larger than the 805 kN buckling capacity found in the experiment.

If the true rotational stiffness of the beam-column joints and the BRB end rotational spring were known, it is likely that the GP-BRB system stability method would conservatively predict buckling capacity. It was observed that the BRB end hinged during the experiment, indicating that the true BRB end rotational stiffness will be less than rigid. The beam-column joints are also unlikely to be fully rigid. As the frame was in chevron configuration, the joint at the centre of the beam will have relatively less rotational stiffness.

Insufficient information is available on the design of the buckled gusset plate on the third storey. Additionally, the hinge formed outside the BRB end in this case and the equations developed by Matsui et al. (2010) cannot be applied.

7.5.1.2 Christopulos (2005)

As described in Section 2.3.4, the Christopulos frame experienced sway buckling failure after the welds connecting the gusset plate to beam column joint degraded during cyclic loading. Frame action effects caused additional stresses on the gusset plate welds which eventually failed in some tests.

Although Christopulos (2005) provides sufficient geometric information to model the frame in the GP-BRB system stability method, the rotational stiffness of the beam-column joint cannot be accurately modelled as the stiffness was constantly decreasing due to the weld degradation.

7.5.1.3 Chou et al. (2012)

The BRB frame experimentally tested by Chou et al. (2012) had the same issues as the frame by Tsai et al. (2004). The design is well documented, but the BRB design is incompatible with the design equations developed by Matsui et al. (2010) due to the unique bolted C channel design of the BRB, and so the BRB end rotational stiffness cannot be determined.

If it is assumed that both the beam-column joint and BRB end rotational stiffness values are infinite, then the GP-BRB system stability method estimates a buckling capacity of 759 kN. This is slightly larger than the experimental buckling capacity of 693 kN and indicates that the BRB end rotational stiffness had an effect on buckling capacity. This matches experimental observations, as the BRB end developed a hinge during the experiment.

Assuming the GP-BRB system stability method is accurate, the BRB end rotational stiffness can be back-calculated. To achieve an estimated buckling capacity of 693 kN using the GP-BRB system stability method, the BRB end rotational stiffness is $1.4 * 10^9$ Nmm/rad, using the inputs from the Chou et al. (2012) experimental test frame and assuming the beam-column joints are rotationally rigid. This is larger than what would be expected for a rotational stiffness that would result in a hinge forming at the BRB end based on findings by Matsui et al. (2010). This indicates that the GP-BRB system stability method would likely be conservative for the Chou et al. (2012) frame if the true BRB end rotational stiffness was known.

7.5.1.4 Hikano et al. (2012)

Not enough gusset plate geometric information has been presented by Hikino et al. (2012) to be suitably used in the GP-BRB system stability method.

7.5.1.5 Takeuchi (2014)

Not enough gusset plate geometric information has been presented by Takeuchi et al. (2014) to be suitably used in the GP-BRB system stability method.

7.5.2 Upcoming Experimental Testing

Due to the lack of information available to accurately model previous experimental buckling sway failures in BRB frames using the GP-BRB system stability method, upcoming experimental testing is planned to be undertaken at the University of Canterbury.

One intended outcome of this experimental testing on a BRB frame is to calibrate the GP-BRB system stability method based on the potential input variables considered in Section 7.3 and then determine if the method is suitable in conservatively predicting buckling failure due to sway buckling in BRB frames.

7.6 Sensitivity Study

Although the method is unable to be fully calibrated and proven as an acceptable design solution, a sensitivity study can be performed to investigate if the model behaviour is reasonable. It can also be used to gather further insight into how each element affects the buckling behaviour of the BRB system. This information can be used to optimise BRB frame design by determining which frame elements have the most influence on buckling capacity. The sensitivity study has only been performed considering elastic buckling behaviour and does not reduce the rigidity of the flexural beam elements to account column curve factors such as residual stresses, accidental eccentricities, or out-of-straightness.

It should be noted that the results are dependent on the particular BRB design and that using a different BRB frame will produce different relationships between buckling capacity and the variable under investigations. This is because, for the assessment of individual element stiffness in Section 7.6.2, all lengths have been held constant and changing the length of an element would affect the relationship. The reverse is true for individual element lengths: the modulus of elasticity and second moment of area have been held fixed for Section 7.6.3.

It should also be noted that when a flexural beam element length is increased in this study, the overall length of the system is increased as no other beam element has been shortened to compensate. This was done to isolate the effect of changing an individual element's length.

The results have been presented in a normalised format as the particular buckling values are not important in the sensitivity study.

7.6.1 Input Parameters

The Chou et al. (2012) experimental BRB frame has been used for this analysis. The BRB end rotational stiffness has been assumed to be $1.4 * 10^9$ Nmm/rad, based on the analysis in Section 7.5.1.1.

The beam-column joint rotational stiffness was assumed to be fully rigid and a large rotational stiffness of $1 * 10^{20}$ Nmm/rad was used. This is an idealisation of a diagonal configuration braced frame although it would not be conservative for design. For chevron

configuration braced frames, it was assumed that one beam joint would act as a perfect pin, giving a rotational stiffness value of 0 Nmm/rad. This would be conservative for design. By plotting both of these boundary conditions, an upper and lower bound can be seen in each figure, indicating the spread of buckling capacity that would result from changing the beam-column joint stiffness.

A summary of all input parameters is presented in Table 7.6-1, and these values have been used to normalise the variable of interest in each graph in this sensitivity study.

Table 7.6-1: Base input parameters used for sensitivity study

Input Parameter	Consideration	Value
Gusset Plate Length	Maximum Thornton length	283 mm
Gusset Plate Second Moment of Area	Thornton method	62197 mm^4
Connection Region Length	BRB casing end to last splice bolt	642.5 mm
Connection Region Second Moment of Area	Non-yielding segment cross-section	11456144 mm^4
BRB Length	BRB casing length	4032 mm
BRB Second Moment of Area	Steel outer casing + Concrete restraining medium	11535865 mm^4 + 16150211 mm^4
Steel Modulus of Elasticity	Steel Material Properties	200 GPa
Concrete Modulus of Elasticity	$E_c = 4700\sqrt{f_c'}$	27.8 GPa
Beam-Column Joint Rotational Stiffness	Value large enough to behave rigidly for diagonal brace configuration, or pinned for chevron brace configuration	$1*10^{20}$ Nmm/rad, or 0 Nmm/rad
BRB End Rotational Stiffness	Back calculated	$1.4*10^9$ Nmm/rad

7.6.2 Influence of Individual Element Rigidity

7.6.2.1 Influence of Gusset Plate Rigidity

Increasing gusset plate rigidity for this particular BRB frame appears to have only a small effect, as seen in Figure 7.6-1. By doubling either the modulus of elasticity or the second moment of area of both gusset plates, the buckling capacity only increases by about 20 %. However, it can be seen that gusset plates with weak flexural rigidity have a significant effect on buckling capacity of the BRB system. This effect is less pronounced for chevron brace configuration frames than diagonal configuration frames.

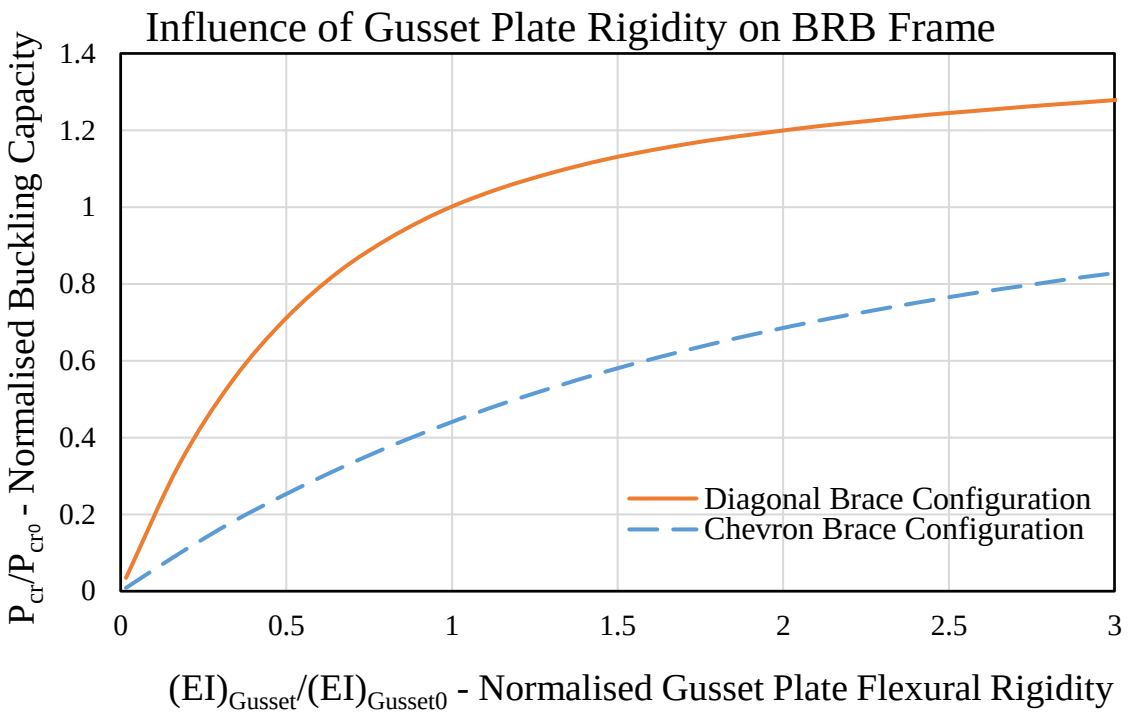

Figure 7.6-1: Influence of gusset plate rigidity on buckling capacity

This non-linear relationship is significantly different from what has been assumed by the Thornton method for elastic buckling of gusset plates which suggests that increasing either the modulus of elasticity or second moment of area should result in an equal increase in buckling capacity when considering elastic buckling. It would appear that by considering the gusset plate as one element in a system of elements, its influence on the system is not as significant when the gusset plate rigidity is large enough. This indicates that increasing gusset plate rigidity has diminishing returns on buckling capacity in a BRB system.

7.6.2.2 Influence of BRB Restrainer rigidity

BRB restrainer rigidity also has a small effect on buckling capacity for this particular BRB frame. This can be seen in Figure 7.6-2, where doubling the rigidity of the BRB restrainer results in about only a 10 % increase in buckling capacity.

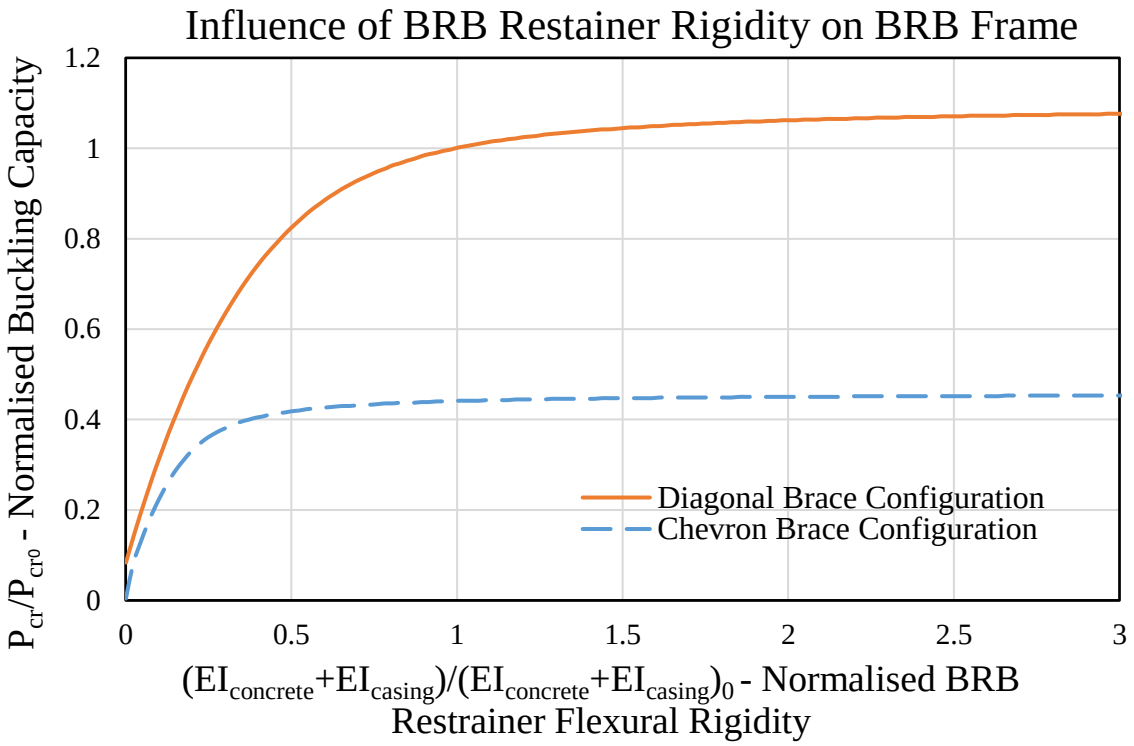

Figure 7.6-2: Influence of BRB restrainer rigidity on buckling capacity

Again, the idea of diminishing returns on increasing flexural rigidity can be seen for BRB restrainer rigidity. It is clear that the relative stiffness of the BRB restrainer compared to other elements in the BRB system is significantly higher for the BRB frame considered. As such, the stiffness must be significantly decreased for buckling capacity to decrease.

7.6.2.3 Influence of Connection Region rigidity

For this particular BRB frame, it can be seen that the connection region's rigidity is large enough that there is almost no effect on buckling capacity when both connection region's rigidity is increased, as seen in Figure 7.6-3. This is reasonable, as the connection stiffness is generally very high in BRB frames due to the relatively short length of connection region and the relatively high second moment of area, when compared to the gusset plate.

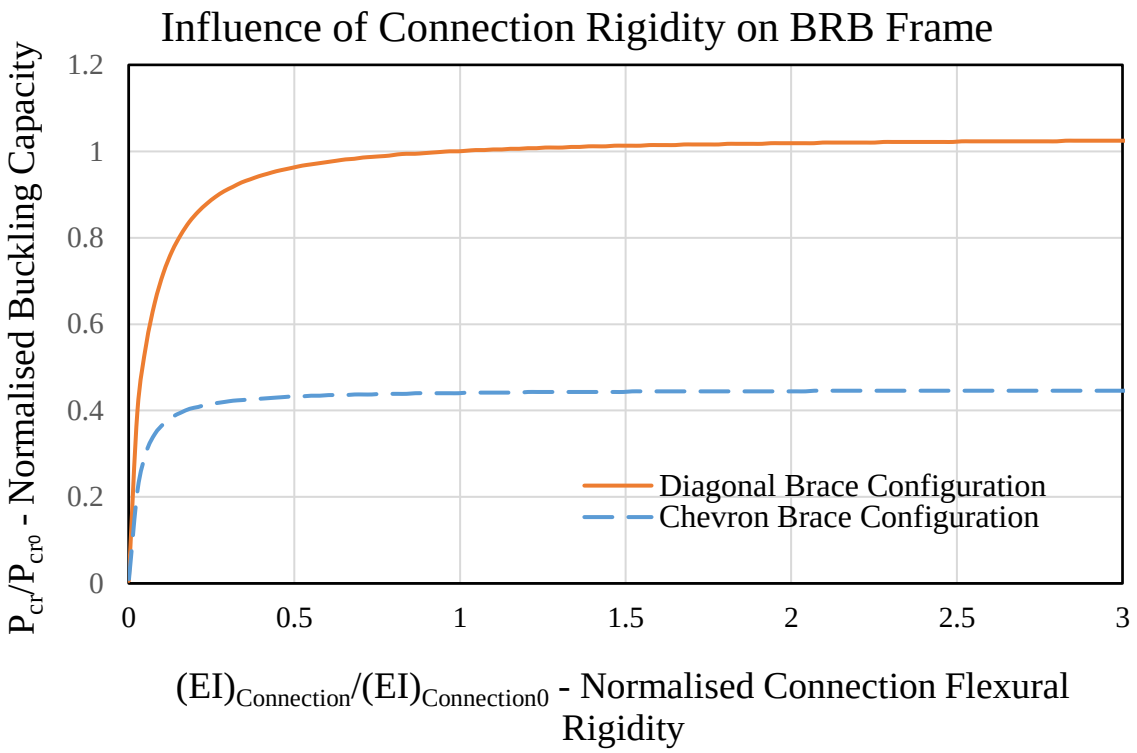

Figure 7.6-3: Influence of connection region rigidity on buckling capacity

Like the other individual elements, when connection rigidity is low enough, buckling capacity rapidly decreases.

7.6.2.4 Influence of BRB End Rotational Stiffness

Increasing BRB end rotational stiffness at both ends of the BRB results in a small increase in buckling capacity. This is seen in Figure 7.6-4, where doubling the BRB end rotational stiffness results in only a 5 % increase in buckling capacity for the diagonal frame configuration.

For the BRB frame investigated, the initial BRB end rotational stiffness was back-calculated based on a buckling capacity that was equal to the experimental test (see Section 7.5.1.3). It is likely that the true BRB end rotational stiffness was less than this. It is, therefore, likely that the effect of increasing BRB end rotational stiffness on the BRB frame tested by Chou et al. (2012) would have a reasonable effect on increasing the BRB system's buckling capacity.

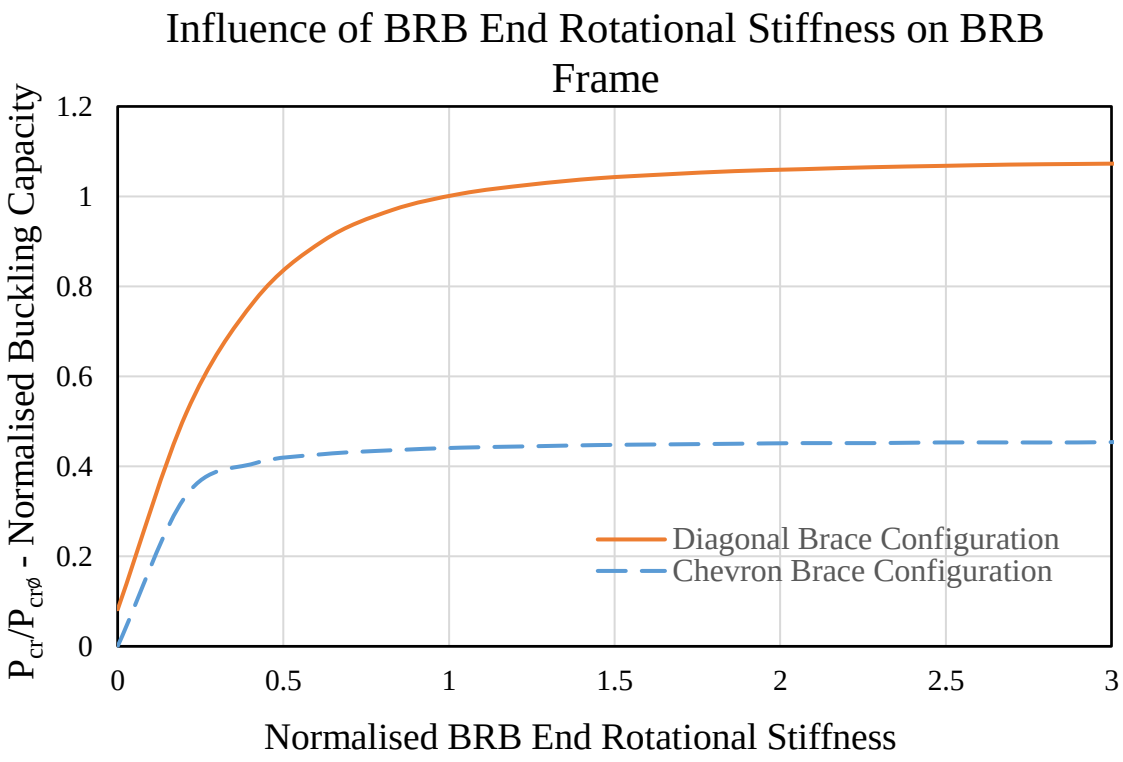

Figure 7.6-4: Influence of BRB end rotational stiffness on buckling capacity

It can be seen from the model that for chevron configuration braced frames, when the BRB end rotational stiffness tends to zero, buckling capacity also tends to zero. This is because a mechanism has been able to form immediately and there is no stiffness in the system. This highlights the danger of designing chevron configuration frames without consideration to beam joint rotational stiffness or BRB end rotational stiffness.

7.6.3 Influence of Individual Element Length

7.6.3.1 Influence of Gusset Plate Length

For this particular BRB frame, it can be seen in Figure 7.6-6 that gusset plate length has a significant effect on buckling capacity. By doubling gusset plate length, the buckling capacity of the system decreases to approximately 40 % of the original capacity.

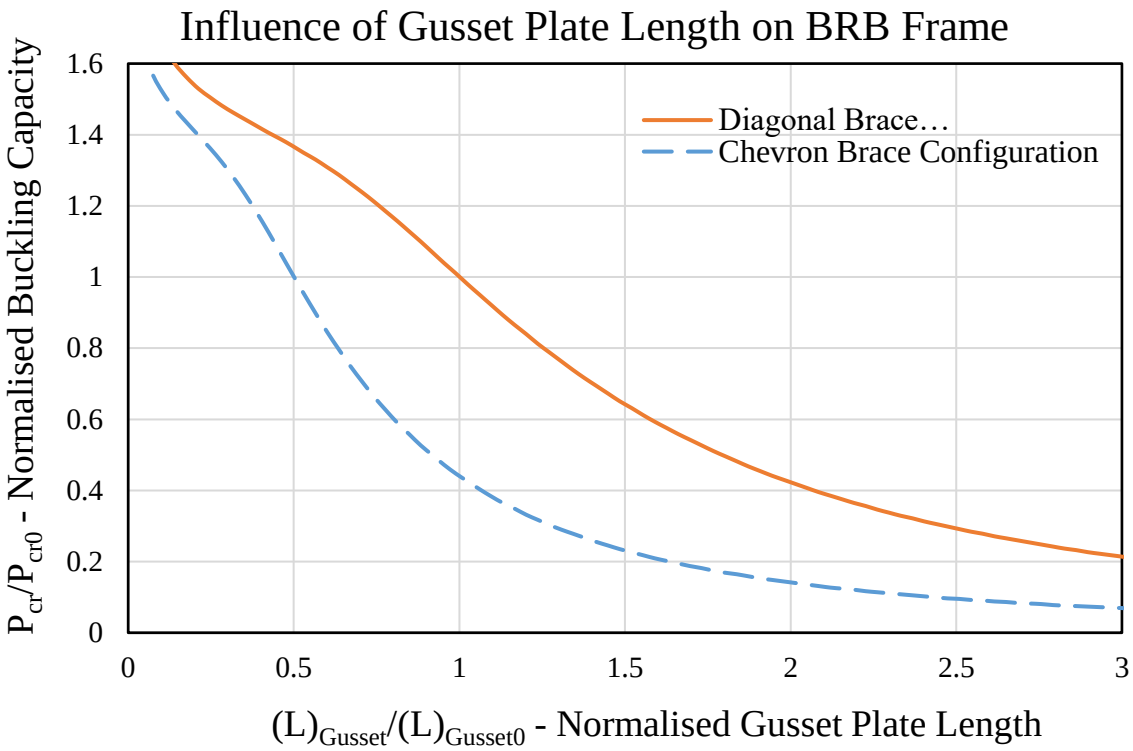

Figure 7.6-5: Influence of gusset plate length on buckling capacity

This is a significant difference compared to the Thornton method and its derivatives which assume that for elastic buckling, doubling gusset plate length should result in buckling capacity decreasing by four times the original capacity.

7.6.3.2 Influence of BRB Length

BRB length has a minor influence on reducing buckling capacity. It can be seen in Figure 7.6-6 that doubling BRB length results in reducing buckling capacity to about 80 % of its original capacity. This is likely because the stiffness of the BRB restrainer in the BRB frame considered is significantly stiffer than other beam elements in the system.

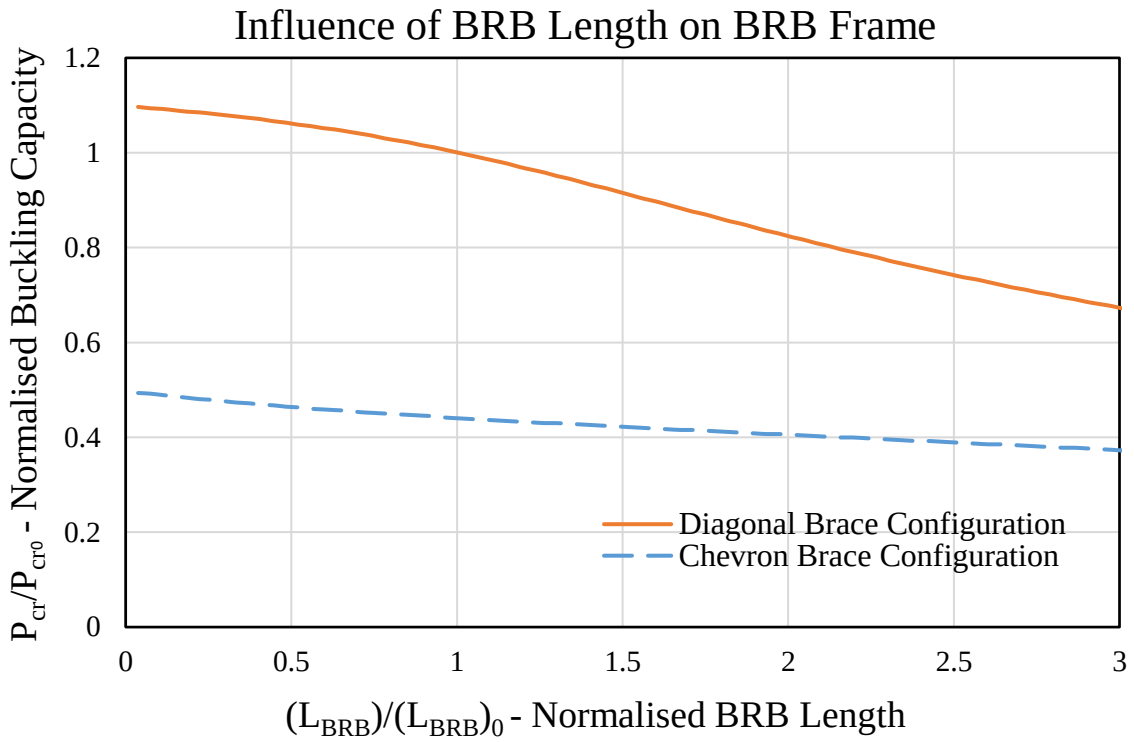

Figure 7.6-6: Influence of BRB length on buckling capacity

In practice, the designer will be limited by frame size and it will not be possible to increase or decrease the length of the BRB by a significant amount. The figure does show that a designer should take extra care when designing with long BRBs, as the buckling capacity of the system may be considerably lower than expected if the influence of the BRB restrainer on buckling capacity is not considered.

7.6.3.3 Influence of Connection Region Length

The behaviour of connection region length appears to fall in between the behaviour of gusset plate length and BRB length. It can be seen in Figure 7.6-7 that doubling the connection length will reduce buckling capacity to about 65 % of the original capacity for a diagonal brace configuration frame. The behaviour of a chevron brace configuration frame is less susceptible to changes in connection length.

Connection length is unlikely to be a variable that can be easily adjusted by the designer on a BRB frame, although it will increase if the gusset plate length is decreased. As the gusset plate has a lower rigidity than the connection region, this will result in a net increase in buckling capacity.

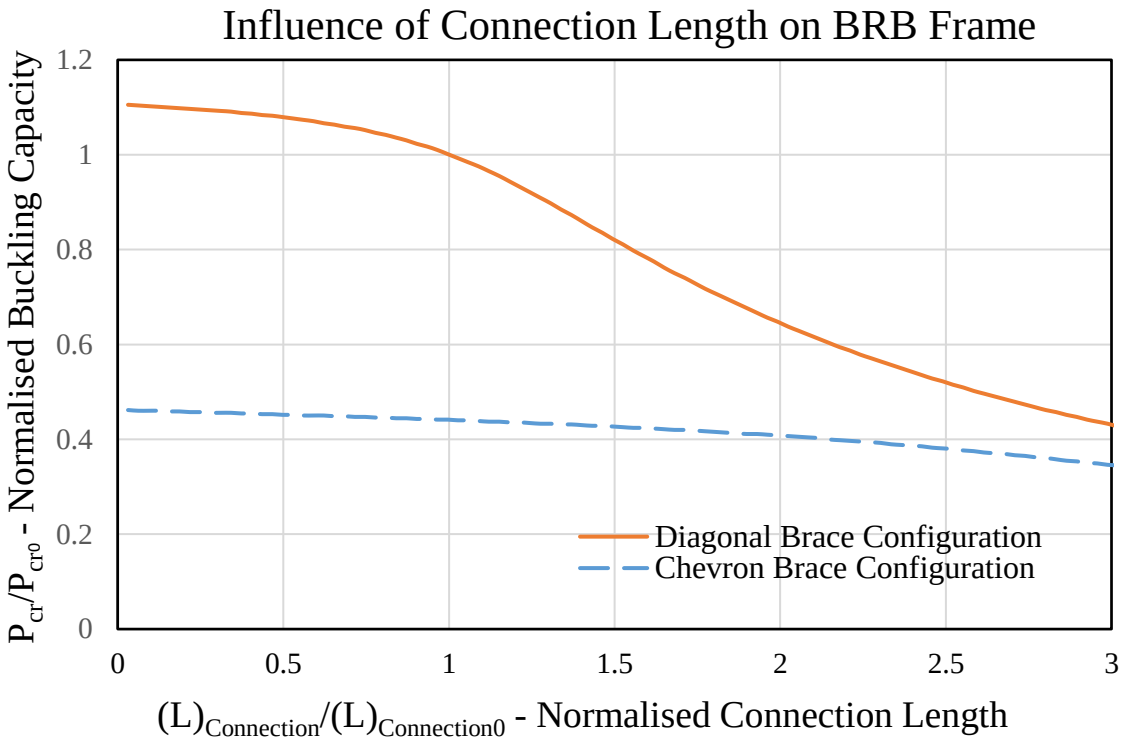

Figure 7.6-7: Influence of connection length on buckling capacity

7.7 Effective Length Factor Comparison

7.7.1 Equivalent Effective Length Factor

Using the Thornton method, the effective length factor of a gusset plate is 0.65, considering fixed-fixed boundary conditions and accounting for the end conditions not being fully rigid. The buckling capacity methods proposed by Chou et al. (2012) and Tsai and Hsiao (2008) assume that when gusset plates buckle in a BRB frame, the effective length factor will be less than 2.0, and that using 2.0 for design will be an upper bound. This is equivalent to fixed-free boundary conditions.

In the GP-BRB system stability method, the behaviour of the gusset plate buckling capacity is affected by the behaviour of other elements in the BRB system. The sensitivity study in Section 7.6 has shown that the other elements in the system can have a significant effect on buckling capacity. The behaviour of other elements in the BRB system can be said to alter the boundary conditions of the gusset plate.

It is possible to develop an equivalent effective length factor for the gusset plate using the GP-BRB system stability method. By using Equation 7.7-1, the equivalent effective length factor that would result in the same elastic buckling capacity as the gusset plate design method

proposed by Tsai and Hsiao (2008) can be found. The Tsai and Hsiao (2008) method has been chosen as it considers elastic buckling and as such the effective length factor can be easily back-calculated.

$$K_{equiv} = \frac{\pi}{\sqrt{\frac{P_{cr}L^2}{EI}}} \qquad 7.7\text{-}1$$

where:

K_{equiv} equivalent effective length factor

P_{cr} gusset plate buckling capacity from GP-BRB system stability method

L middle Thornton length

EI gusset plate flexural rigidity

By finding the equivalent effective length factor, it can be determined whether K = 2.0 is the upper bound effective length factor for gusset plate buckling in BRB frames.

The Tsai and Hsiao (2008) method assumes fixed-free boundary conditions, and the GP-BRB system stability method assumes the gusset plate's boundary conditions are dependent on the other elements in the BRB system. For an accurate comparison, the beam-column joint has been assumed to be fully rigid in the GP-BRB system stability method.

To test whether the effective length factor of a gusset plate in BRB frames is bounded by 2.0, gusset plate rigidity has been increased in the GP-BRB system stability method. It can be seen in Figure 7.7-1, that for diagonal brace configuration BRB frames, a lower bound equivalent effective length factor of 1.0 exists and that this effective length factor can be much larger than 2.0.

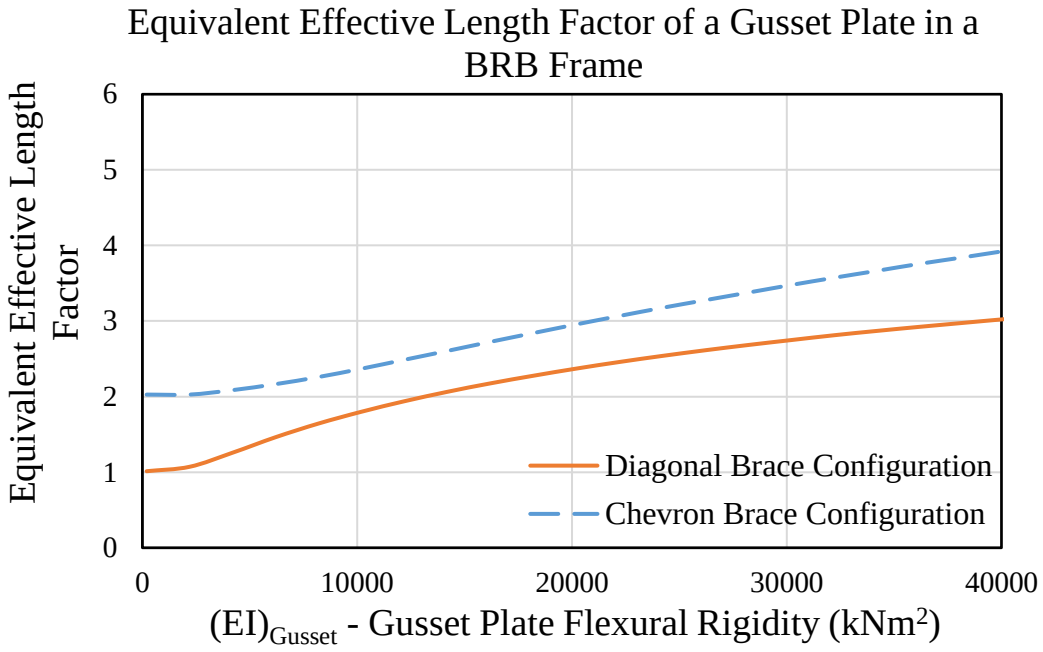

Figure 7.7-1: Equivalent effective length factor of a gusset plate in a BRB frame

The figure indicates that for BRB frames, the minimum effective length factor that is used is 1.0, and not 0.65 as suggested by the Thornton method. This is reasonable as it is possible for the BRB to buckle by a symmetric sway failure in which fixed-roller boundary conditions of both gusset plates could be approximated. This is seen in Figure 2.4-7 for the bending moment transfer concept diagram. This buckling failure has not been observed in BRB experimental testing.

In Equation 7.7-1, the effect of this is that an increase in flexural rigidity results in a smaller increase in buckling capacity, which results in an increase in K_{equiv}.

For both diagonal and chevron configuration brace frames, the equivalent effective length factor can be larger than 2.0. This indicates that the upper bound assumption made by Chou et al. (2012) and Tsai and Hsiao (2008) does not always hold true.

7.7.2 Comparison to Previous Work

Work by Crake and Westeneng (2014) was the precursor to the GP-BRB system stability method. This paper considered only one gusset plate and one BRB element, as shown in Figure 7.7-2. It can be seen that this model is significantly more simplified than the model used in the GP-BRB system stability method.

Figure 7.7-2: Design model for stability method considered (Crake and Westeneng 2014)

The model used by Crake and Westeneng (2014) did not account for the possibility of a hinge forming at the BRB end, and so it assumes full moment transfer is always available. It has been assumed that the beam-column joint provides full restraint to the gusset plate translationally and rotationally. The pinned end of the BRB is a crude approximation of the other gusset plate rotating out-of-plane after buckling has occurred due to its low rotational stiffness. The role of the connection has also been ignored in the model.

None-the-less, the findings related to equivalent effective length factor by Crake and Westeneng (2014) are similar to that found in this chapter, as seen in Figure 7.7-3. The figure compares the research from Crake and Westeneng (2014) with the GP-BRB system stability method considering rigid beam-column joints, rigid BRB end rotational springs, and no stiffness reduction factors so that the method calculates the elastic buckling capacity. This study and the research by Crake and Westeneng (2014) both show that the equivalent effective length factor of the BRB system has a theoretical minimum value of unity and is capable of being larger than 2.0.

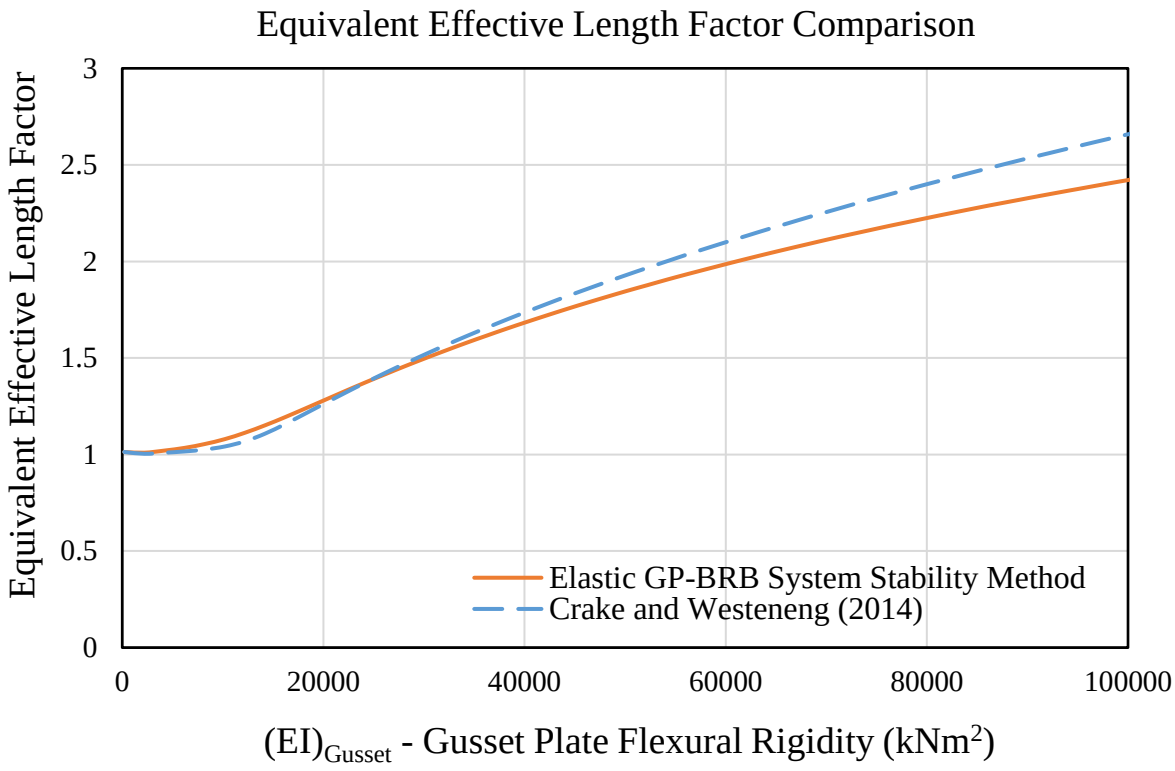

Figure 7.7-3: Equivalent effective length factor comparison between the elastic GP-BRB system stability method and previous research by Crake and Westeneng (2014)

7.8 Comparison to Takeuchi Method

Both the GP-BRB system stability method and the method proposed by Takeuchi et al. (2014) consider buckling capacity as a function of all elements in the BRB system. There are a number of differences and similarities between the GP-BRB system stability method and the Takeuchi method. The GP-BRB system stability method uses a stiffness based approach to calculate buckling capacity instead of the strain energy approach used by the Takeuchi method. The Takeuchi method also assumes a buckling mode shape, whereas the proposed method requires no buckling mode shape assumption. This is significant as because the mode shape is assumed, the Takeuchi method will be an upper bound solution.

The GP-BRB system stability method considers the gusset plate as a beam element instead of a combined rotational spring, as shown in Figure 7.8-1. The rotational stiffness of the combined gusset plate and joint rotational spring is difficult for a designer to determine without finite element software. The flexural stiffness of the gusset plate is usually significantly less than the connection stiffness, so it may be inappropriate to assume the connection length includes the gusset plate length. The Takeuchi method can consider initial known imperfections in the BRB and gusset plate, whereas this is not accounted for explicitly in the version of the

GP-BRB system stability method described here, although it can be done. Both methods can consider accidental eccentricity, yielding and residual stress effects by means of the column curves.

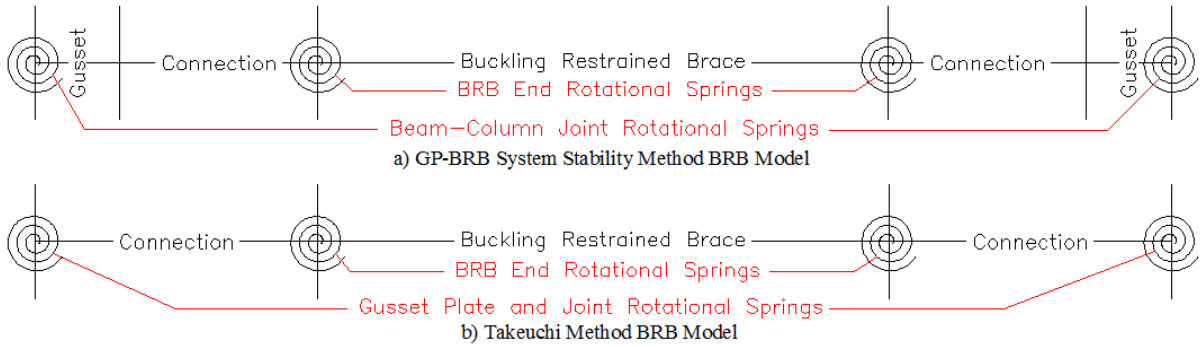

Figure 7.8-1: Comparison between GP-BRB system stability method and Takeuchi method BRB system models

7.9 Future Implementation as a Design Tool

This chapter has developed the GP-BRB system stability method as a tool to consider how other elements in the BRB system affect the buckling capacity of the gusset plate and whether the assumptions made by Chou et al. (2012) and Tsai and Hsiao (2008) are correct. It is possible that the GP-BRB system stability method can be further developed so that it can be used in design to conservatively predict the buckling capacity of gusset plates in a BRB frame for a wide range of cases. The method also requires calibration with experimental testing. This was deemed to be outside the scope of the thesis. However, an outline of some requirements to develop the method into a design tool has been outlined in this section.

7.9.1 Improvements to the GP-BRB system stability method

7.9.1.1 Out-of-Plane Drift

Out-of-plane storey drift of the BRB frame may affect the buckling capacity of the BRB system. This effect has been considered by Takeuchi et al. (2014) as an additional moment that acts on the BRB restrainer end. This ultimately decreases the rotational stiffness of the BRB restrainer end, decreasing buckling capacity. It is likely that the formulas derived by Takeuchi et al. (2014) to account for out-of-plane storey drift can be easily implemented when determining the rotational spring stiffness of the BRB restrainer end.

7.9.1.2 Chevron configuration braced frames

Currently, the GP-BRB system stability method considers only rotational stiffness of the beam joint in a chevron configuration braced frame. Takeuchi et al. (2015) also consider the horizontal stiffness of the beam joint, allowing for a translational spring to represent out-of-plane displacement of the beam joint. This can be easily implemented into the GP-BRB system stability method by modifying the system stiffness matrix so that one beam column joint can also consider translation instead of assuming that the beam-column is fixed for lateral movement. This modification is unlikely to be necessary for most building designs as the beam joint is likely to be attached to a floor slab which will resist out-of-plane displacement of the beam joint. This method could also be used to consider out-of-plane drift of one end.

7.9.1.3 Consideration of frame action forces

It was shown in Chapter 4 that frame action forces can result in a small decrease in buckling capacity when considering cyclic loading. This effect has only been considered for a single case and has not yet been quantified. Further research is recommended and once complete the findings should be incorporated in the GP-BRB system stability method through a reduction factor.

7.9.1.4 Consideration of gusset plate

In the GP-BRB system stability method, the gusset plate is still being considered as an equivalent column. This is likely to be the weakest assumption made by the method considering the poor accuracy of the methods which make this assumption in Chapter 5. The choice of using the middle Thornton length is likely to result in a conservative estimation of the gusset plates flexural stiffness, but this may not always be true. It may be best to determine an equivalent flexural stiffness for the gusset plate by analysing the gusset plate through finite element modelling. This would be more accurate and would allow more complex gusset plate designs, such as those that use free-edge stiffeners to provide additional stiffness. However, this is likely to be time-consuming for the designer unless some form of automation is implemented.

7.9.2 Implementation of the Method as Software

Given the large matrix that is developed in the GP-BRB system stability method, it is likely that the best way for designers to use the method is through computer software. This would

likely be an open source solution and could potentially be cloud based to allow updates when the method is developed to be more accurate.

The use of software could allow more detailed analysis techniques such as allowing the designer to enter the dimensions of the desired gusset plate into the software which could then automatically develop and run a finite element model to determine the equivalent flexural stiffness of the gusset plate. This would result in a more accurate buckling capacity being obtained by the method.

7.9.3 Design Steps

The GP-BRB system stability method has not been proven to be accurate and conservative by this thesis due to an imperfect data set for experimentally tested BRB frames being available. However, if the method can be successfully calibrated, a designer could follow certain design steps to ensure that the gusset plate in a particular BRB frame is strong enough to prevent sway buckling. An example design process has been presented:

1) Consider appropriate input variables based on the BRB frame design for connection region, BRB, BRB restrainer end and beam-column joint,
2) Perform preliminary design of gusset plate based on frame geometry, assume minimum thickness of gusset plate is equal to BRB core thickness,
3) Apply appropriate column curve to reduce buckling capacity to account for member effects such as out-of-straightness and accidental eccentric loading,
4) Apply inputs to the system stiffness matrix,
5) Calculate buckling capacity by finding the smallest eigenvalue of the system stiffness matrix,
6) Check buckling capacity is greater than the maximum compressive strength of the BRB,
7) If buckling capacity is not sufficient, increase system capacity by:
    a) Increasing gusset plate flexural stiffness by increasing thickness or adding free-edge stiffeners,
    b) Increasing BRB end rotational stiffness by increasing non-yielding segment insertion length,
    c) Stiffening the beam joint, particularly if the frame is chevron configuration.

7.10 Conclusion

From the results of this sensitivity study for this particular BRB frame, it can be seen that for all individual elements, when one element has substantially lower flexural rigidity or rotational stiffness, the buckling capacity of the BRB system is significantly reduced. It is, therefore, essential that a designer ensures that all elements are sufficiently stiff.

It has also been seen that for a particular element's rigidity and length, the idea of diminishing returns on buckling capacity is apparent if that particular element is sufficiently stiff enough. This idea means that the overall buckling capacity of the system will not substantially increase when a particular element's stiffness is increased.

An equivalent effective length factor for the gusset plate using the GP-BRB system stability method was found and compared to methods that consider the gusset plate as an equivalent buckling column. It has been shown that the equivalent effective length factor can be larger than 2.0 for a gusset plate and so the assumption made by Chou et al. (2012) and Tsai and Hsiao (2008) that this value will not be greater than 2.0 has been shown to be invalid.

The aims at the start of this chapter have been addressed:

1) A method to consider BRB stability was developed.
2) A range of potential input variables was considered.
3) The method has been found to be mathematically correct by comparing it to matrix structural analysis software.
4) The method has been unable to be calibrated against experimentally tested BRB frames due to a lack of data. However, some assumptions have been made that show the method may be reasonable.
5) The sensitivity study found that individual beam element rigidity and length, and rotational stiffness have different non-linear effects on overall buckling capacity. It was also found that if an element in the BRB system has relatively lower stiffness than other elements in the system, buckling capacity will significantly decrease.
6) An equivalent effective length factor for gusset plates in BRB frames has shown that a constant value, such as $K = 2.0$, is not always sufficient in design.
7) A tentative design procedure has been developed.

8 CONCLUSION

This thesis sets out to investigate gusset plate buckling behaviour in BRB frames. The results of a number of experimental tests on BRB frames have shown that gusset plates can fail by sway buckling at a significantly lower buckling capacity than what has been calculated using previous design methods. Due to the increasingly common use of BRBs as the main lateral load resisting system in structures to resist seismic loading, gusset plate buckling in BRB frames may present a risk to the safety of structures that use BRBs. Through the chapters in this thesis, the behaviour of gusset plate sway buckling was investigated to help reduce the risk of early gusset plate failure. As well as the behaviour of gusset plates buckling by sway, this thesis considered current design methods to find whether a conservative and reasonable estimate of gusset plate buckling capacity could be found so that a designer can manage the risk of gusset plate failure.

In summary, this thesis has shown that:

1) The US-based design methods for BRBs consider the gusset plate as an equivalent column with a Whitmore width and Thornton length, and an effective length factor which is less than unity even though the mode of failure of such gusset plates is generally sway. The effective length factor is generally taken as 0.65 or 0.70 in the AISC and NZ standards, but recommendation from Taiwan suggests using a value of 2.0. Values greater than this are also possible.
2) Finite element modelling replicated behaviour and strengths of gusset plates in BRB system tests. It was found that, of the current design methods investigated, no method was able to conservatively estimate sway buckling capacity for a range of gusset plates. Modifying the current design methods to consider a Whitmore width, maximum Thornton length, and an effective length factor of 2 or greater resulted in a conservative estimation.
3) From 5880 finite element studies of a range of realistic gusset plate connections, a parametric study found variations of Whitmore width and Thornton length did not always produce the expected changes in performance indicating that they may not be reliable for determining gusset plate buckling capacity.

4) Frame action forces decreased the gusset plate buckling capacity under cyclic loading by up to 8% in the analyses undertaken. The decrease due to frame action is relatively small and may be ignored in the design of the gusset plate itself. However, if full strength welds are not provided at the plate edge, then frame action may affect the weld demands, this is not considered in this study.
5) A simple stiffness based system stability method was developed to determine how different BRB system elements affected buckling capacity. Flexibilities of the frame beam-column joint, gusset plate, connection, and BRB are considered together with residual stress and yielding effects. The buckling capacity of the system was determined based on the minimum eigenvalue of the system stiffness matrix. A sensitivity study found that buckling capacity significantly decreases if one element of the system has relatively lower stiffness and this finding was consistent with that from experimental results.
6) In this study, it is shown that gusset plate stability increases by increasing its stiffness. This can be done by adding stiffeners to the gusset plate, by making it thicker, or by reducing its length. Also, high stiffness at the BRB ends is beneficial and this may be increased by increasing non-yielding segment length in the BRB core plate or providing additional rotational restraint. The beam-column joint should also have high stiffness which may be increased through stiffener or web-doubler plates in both the beam and column. The GP-BRB system stability method developed can be used to assist a designer in evaluating stiffness. However, it should be noted that many BRBs may also be subject to out-of-plane deformation. If the system is stiff out-of-plane it may yield under the likely deformations, compromising the in-plane performance. Separate checks may be required to assess this effect which is beyond the scope of this thesis.

9 REFERENCES

AIJ. (2009). *Recommendations for stability design of steel structures*. Architectural Institute of Japan.

AISC. (1984). *Engineering for Steel Construction*. American Institute of Steel Construction (AISC), Chicago, Illinois.

AISC. (1986). *Manual of Steel Construction - Load & Resistance Factor Design*. American Institute of Steel Construction (AISC).

AISC. (2005a). *Specification for Structural Steel Buildings*. American Institute of Steel Construction (AISC), Chicago.

AISC. (2005b). *Seismic provisions for structural steel buildings. ANSI/AISC Standard 341-05*, American Institute of Steel Construction (AISC), Chicago, Illinois.

Bruneau, M., Uang, C. M., and Sabelli, S. R. (2011). *Ductile design of steel structures.* McGraw-Hill Professional.

Chen, C.-H., Hsiao, P.-C., Lai, J.-W., Lin, M.-L., Weng, Y.-T., and Tsai, K.-C. (2004). "Pseudo-dynamic test of a full-scale CFT/BRB frame: Part 2—Construction and testing." *Proceedings of 13th World Conference on Earthquake Engineering*.

Cheng, J. R., Yam, M. C., and Hu, S. (1994). "Elastic buckling strength of gusset plate connections." *Journal of Structural Engineering*, American Society of Civil Engineers, 120(2), 538–559.

Chou, C.-C., and Chen, P.-J. (2009). "Compressive behavior of central gusset plate connections for a buckling-restrained braced frame." *Journal of Constructional Steel Research*, 65(5), 1138–1148.

Chou, C.-C., and Chen, S.-Y. (2010). "Subassemblage tests and finite element analyses of sandwiched buckling-restrained braces." *Engineering Structures*, 32(8), 2108–2121.

Chou, C.-C., and Liu, J.-H. (2012). "Frame and brace action forces on steel corner gusset plate connections in buckling-restrained braced frames." *Earthquake Spectra*, Earthquake Engineering Research Institute, 28(2), 531–551.

Chou, C.-C., Liu, J.-H., and Pham, D.-H. (2012). "Steel buckling-restrained braced frames with single and dual corner gusset connections: seismic tests and analyses." *Earthquake Engineering & Structural Dynamics*, 41(7), 1137–1156.

Christopulos, A. S. (2005). "Improved seismic performance of buckling restrained braced frames." University of Washington.

Crake, M., and Westeneng, B. (2014). "Effects of Stiffened Gusset Plate Connections on Buckling Restrained Brace Frames." *Civil and Natural Resources Engineering Research Conference*, 3, 49–56.

CSA. (1989). *CAN/CSA-S16.1-M89 - Limit States Design of Steel Structures*. Canadian Standards Association (CSA), Rexdale, Ontario.

Dassault Systemes. (2005a). "Abaqus FEA (Version 6.11-2)."

Dassault Systemes. (2005b). *Abaqus Analysis User's Manual*. Simulia.

Dowswell, B. (2006). "Effective Length Factors for Gusset Plate Buckling." *Engineering Journal*, American Society of Civil Engineers, 43(2), 91.

Dowswell, B. (2013). "Gusset Plate Stability Using Variable Stress Trajectories." *10th Pacific Structural Steel Conference*.

Fahnestock, L. A., Ricles, J. M., and Sause, R. (2007). "Experimental evaluation of a large-scale buckling-restrained braced frame." *Journal of structural engineering*, American Society of Civil Engineers, 133(9), 1205–1214.

Fussell, A. (2010). "Heavy Brace Gusset Plate Connections for Braced Steel Frames." *Steel Construction New Zealand*.

Gross, J. L. (1990). "Experimental study of gusseted connections." *Engineering Journal*, 27(3), 89–97.

Gross, J. L., and Cheok, G. (1988). *Experimental Study of Gusseted Connections for Laterally Braced Steel Buildings*. U.S. Department of Commerce, National Institute of Standards and Technology.

HERA. (1994). *New Zealand Structural Steelwork Limit State Design Guides, Volume 1. Hera Report R4-80*. HERA, Manukau City, New Zealand.

Hikino, T., Okazaki, T., Kajiwara, K., and Nakashima, M. (2012). "Out-of-plane stability of buckling-restrained braces placed in chevron arrangement." *Journal of Structural Engineering*, American Society of Civil Engineers, 139(11), 1812–1822.

Hu, S., and Cheng, J. R. (1987). *Compressive behavior of gusset plate connections*. Department of Civil Engineering, University of Alberta.

Kinoshita, T., Koetaka, Y., Inoue, K., and Iitani, K. (2008). "Out-of-plane stiffness and yield strength of cruciform connection for buckling-restrained brace." *Journal of Structure and Construction Engineering, AIJ*, 632, 1865–73.

Koetaka, Y., and Kinoshita, T. (2009). "Design criteria of buckling-restrained brace to prevent out-of-plane buckling." *Journal of Structural and Construction Engineering*, 74(641), 1371–1378.

Koetaka, Y., Kinoshita, T., Inoue, K., and Iitani, K. (2008). "Criteria of buckling-restrained braces to prevent out-of-plane buckling." *Proceedings of 14th World Conference on Earthquake Engineering*.

Lin, M.-L., Weng, Y.-T., Tsai, K.-C., Hsiao, P.-C., Chen, C.-H., and Lai, J.-W. (2004). "Pseudo-Dynamic test of a full-scale CFT/BRB frame: Part 3—analysis and performance evaluation." *Proceedings of 13th World Conference on Earthquake Engineering*.

Lin, P.-C., Tsai, K.-C., Wu, A.-C., and Chuang, M.-C. (2014). "Seismic design and test of gusset connections for buckling-restrained braced frames." *Earthquake Engineering & Structural Dynamics*, 43(4), 565–587.

Lin, S., MacRae, G., Wu, A., Lin, P., and Tsai, K. (2012). "Development and implementation of buckling restrained braces in Taiwan." *The New Zealand Society for Earthquake Engineering Conference*.

Lu, A., Macrae, G., Ziemian, R., Hann, C., Peng, B., and Clifton, C. (2009). "Extended direct analysis of steel frames." *Sesoc Journal*, 22(2), 89–102.

Ma, N., Wu, B., Zhao, J., Li, H., Ou, J., and Yang, W. (2008). "Full scale test of all-steel buckling restrained braces." *14th World Conference on Earthquake Engineering*, International Society for Optics and Photonics.

MacRae, G., and Clifton, C. (2015). "Research on Seismic Performance of Steel Structures." *Steel Innovation Conference 2015*.

Mahin, S., Uriz, P., Aiken, I., Field, C., and Ko, E. (2004). "Seismic performance of buckling restrained braced frame systems." *13th World Conference on Earthquake Engineering*.

Matsui, R., Takeuchi, T., Nishimoto, K., Takahashi, S., and Ohyama, T. (2010). "Effective buckling length of buckling restrained braces considering rotational stiffness at restrainer ends." *7th International Conference on Urban Earthquake Engineering &*

5th International Conference on Earthquake Engineering Joint Conference Proceedings, Center for Urban Earthquake Engineering, 1245–1254.

Mcguire, W., Gallagher, R. H., and Ziemian, R. D. (2000). *Matrix Structural Analysis*. Faculty Books.

Mutton, B. R., and Trahair, N. S. (1975). "Design Requirements for Column Braces." *Civil Engineering Transactions, The institution of Engineers, Australia*, CE17(1), 30–36.

Naghipour, M., Abdollahzadeh, G., and Shokri, M. (2013). "Analysis and design procedure of corner gusset plate connection in BRBFs." *Iranica Journal of Energy & Environment*, 4(3), 271–282.

Nakamura, H., Takeuchi, T., Maeda, Y., Nakata, Y., Sasaki, T., Iwata, M., and Wada, A. (2000). *Fatigue Properties of Practical-Scale Unbonded Braces.* Nippon Steel.

Palmer, K. D. (2012). "Seismic behavior, performance and design of steel concentrically braced frame systems." University of Washington, Seattle, WA.

Palmer, K. D., Christopulos, A. S., Lehman, D. E., and Roeder, C. W. (2014). "Experimental evaluation of cyclically loaded, large-scale, planar and 3-d buckling-restrained braced frames." *Journal of Constructional Steel Research*, 101, 415–425.

Palmer, K. D., Roeder, C. W., and Lehman, D. E. (2016). "Connection Design Recommendations for Improved BRBF Performance." *Engineering Journal*, American Society of Civil Engineers, 53(1), 29–45.

Rabinovitch, J. S., and Cheng, J. R. (1993). *Cyclic Behavior of Steel Gusset Plate Connections*. University of Alberta.

Ralph, R. (1986). "Analysis of Large Bracing Connection Designs for Heavy Construction." *Proceedings of the 1986 National Engineering Conference*.

Sheng, N., Yam, C., and Iu, V. (2002). "Analytical investigation and the design of the compressive strength of steel gusset plate connections." *Journal of Constructional Steel Research*, 58(11), 1473–1493.

Standards New Zealand. (1997). *NZS3404 Part 1 and 2 Steel Structures Standard*. Standards New Zealand.

Takeuchi, T., Matsui, R., and Mihara, S. (2015). "Out-of-Plane Stability Assessment of Buckling-Restrained Braces with Chevron Configurations." *Proceedings of The 8th International Conference on Behaviour of Steel Structures in Seismic Areas*.

Takeuchi, T., Matsui, R., Nishimoto, K., Takahashia, S., and Ohyama, T. (2009). "Effective Buckling Length For Buckling Restrained Braces Considering Rotational Stiffness at Restrainer Ends." *Journal of Structural and Construction Engineering*, Architectural Institute of Japan, 74(639), 925–934.

Takeuchi, T., Ozaki, H., Matsui, R., and Sutcu, F. (2014). "Out-of-plane stability of buckling-restrained braces including moment transfer capacity." *Earthquake Engineering & Structural Dynamics*, 43(6), 851–869.

The MathWorks, Inc. (2012). "MATLAB and Statistics Toolbox Release 2012b."

Thornton, W. (1984). "Bracing Connections for Heavy Construction." *Engineering Journal*, American Society of Civil Engineers, 21 (3), 139–148.

Thornton, W., and Lini, C. (2011). "The Whitmore Section." *Modern Steel Construction*.

Tsai, K.-C. (2015). "Gusset Plate Dimensions (Private Correspondence)."

Tsai, K.-C., and Hsiao, P.-C. (2008). "Pseudo-dynamic test of a full-scale CFT/BRB frame—Part II: Seismic performance of buckling-restrained braces and connections." *Earthquake Engineering & Structural Dynamics*, 37(7), 1099–1115.

Tsai, K.-C., Hsiao, P.-C., Wang, K.-J., Weng, Y.-T., Lin, M.-L., Lin, K.-C., Chen, C.-H., Lai, J.-W., and Lin, S.-L. (2008). "Pseudo-dynamic tests of a full-scale CFT/BRB frame-

Part I: Specimen design, experiment and analysis." *Earthquake Engineering and Structural Dynamics*, 37(7), 1081–1098.

Tsai, K.-C., Hwang, Y.-C., Weng, C.-S., Shirai, T., and Nakamura, H. (2002). "Experimental tests of large scale buckling restrained braces and frames." *Proceedings, Passive Control Symposium*.

Tsai, K.-C., Weng, Y.-T., Lin, S.-L., and Goel, S. (2004). "Pseudo-dynamic Test of A Full-scale CFT/BRB Frame: Part 1-Performance Based Specimen Design." *Proceedings of 13th World Conference on Earthquake Engineering*.

Uang, C. M., Masayoshi, N., and Tsai, K. C. (2004). "Research and application of buckling-restrained braced frames." *International Journal of Steel Structures*, 4(4), 301–313.

Wakabayashi, M., Nakamura, T., Katagihara, A., Yokoyama, H., and Morisono, T. (1973). *Experimental study on the elastoplastic behavior of braces enclosed by pre-cast concrete panels under horizontal cyclic loading – Parts 1 & 2*. Architectural Institute of Japan.

Walbridge, S., Grondin, G., and Cheng, J. J. (2005). "Gusset plate connections under monotonic and cyclic loading." *Canadian Journal of Civil Engineering*, NRC Research Press, 32(5), 981–995.

Watanabe, A., Hitomi, Y., Saeki, E., Wada, A., and Fujimoto, M. (1988). "Properties of brace encased in buckling-restraining concrete and steel tube." *Proceedings of Ninth World Conference on Earthquake Engineering*, 719–724.

Westeneng, B., Lee, C.-L., and MacRae, G. (2015). "Early Failure of Gusset Plates in Buckling Restrained Brace Frames." *Steel Innovation Conference 2015*.

Whitmore, R. (1952). *Experimental investigation of stresses in gusset plates*. Engineering Experiment Station, University of Tennessee.

Wigle, V. R., and Fahnestock, L. A. (2010). "Buckling-restrained braced frame connection performance." *Journal of Constructional Steel Research*, 66(1), 65–74.

Wijanto, S. (2012). "Behaviour and Design of Generic Buckling Restrained Brace Systems." The University of Auckland.

Yam, M. C., and Cheng, J. R. (1993). *Experimental investigation of the compressive behavior of gusset plate connections*. Department of Civil Engineering, University of Alberta.

Yam, M. C., and Cheng, J. R. (1994). *Analytical investigation of the compressive behavior and strength of steel gusset plate connections*. Department of Civil Engineering, University of Alberta.

Yam, M., and Cheng, J. (2002). "Behavior and design of gusset plate connections in compression." *Journal of Constructional Steel Research*, 58(5), 1143–1159.

Yamamoto, K., Akiyama, N., and Okumura, T. (1985). "Elastic analysis of gusseted truss joints." *Journal of Structural Engineering*, American Society of Civil Engineers, 111(12), 2545–2564.

Ziemian, R. D., and Mcguire, W. (2008). "Mastan2 (Version 3.2.0)."

10 APPENDICES

10.1 Gusset Plate Design Method Calculations

10.1.1 Thornton Method (1984) Calculations

$L_c := 207.2\ mm$ $k := 0.65$

$t_g := 14\ mm$ $b_e := 272\ mm$

$F_y := 385\ MPa$ $E := 200000\ MPa$

$$r := \frac{t_g}{\sqrt{12}} \qquad r = 4.041\ mm$$

$$\lambda_c := \frac{k \cdot L_c}{\pi \cdot r} \cdot \sqrt{\frac{F_y}{E}} \qquad \lambda_c = 0.465$$

Lamda less than 1.5 therefore use Pcr1

$$P_{cr1} := 0.658^{\lambda_c^2} \cdot F_y \cdot b_e \cdot t_g$$

$$P_{cr2} := \frac{0.877}{\lambda_c^{\ 2}} \cdot F_y \cdot b_e \cdot t_g$$

$P_{cr1} = 1339\ kN$

10.1.2 Modified Thornton Method (1994) Calculations

$b_b := 145\ mm$ $\quad l_b := 110\ mm$

$b_e := b_b + 2\ l_b \cdot \tan(45\ °)$ $\quad b_e = 365\ mm$

$L := 200\ mm$ $\quad k := 0.65$

$t_g := 14\ mm$

$F_y := 385\ MPa$ $\quad E := 200000\ MPa$

$r := \frac{t_g}{\sqrt{12}}$ $\quad r = 4.041\ mm$

$\lambda_c := \frac{k \cdot L}{\pi \cdot r} \cdot \sqrt{\frac{F_y}{E}}$ $\quad \lambda_c = 0.449$ $\quad$ Lamda less than 1.5 therefore use Pcr1

$P_{cr1} := 0.658^{\lambda_c^2} \cdot F_y \cdot b_e \cdot t_g$

$P_{cr2} := \frac{0.877}{\lambda_c^{\ 2}} \cdot F_y \cdot b_e \cdot t_g$

$P_{cr1} = 1808\ kN$

10.1.3 NZS 3404 Method (1997) Calculations

$L := 207.2\ mm$ $k := 0.7$

$k_f := 1.0$ $f_y := 385\ MPa$

$\alpha_b := 0.5$ $t_g := 14\ mm$

$b_e := 272\ mm$

$r := \frac{t_g}{\sqrt{12}}$ $r = 0.004\ m$

$\lambda_n := \frac{(k \cdot L)}{r} \cdot \sqrt{k_f} \cdot \sqrt{\frac{f_y}{250\ MPa}}$ $\lambda_n = 44.536$

$\alpha_a := \frac{(2100 \cdot (\lambda_n - 13.5))}{\lambda_n^{\,2} - 15.3 \cdot \lambda_n + 2050}$ $\alpha_a = 19.443$

$\lambda := \lambda_n + \alpha_a \cdot \alpha_b$ $\lambda = 54.258$

$\eta := 0.00326 \cdot (\lambda - 13.5)$ $\eta = 0.133$

$\xi := \frac{\left(\frac{\lambda}{90}\right)^2 + 1 + \eta}{2 \cdot \left(\frac{\lambda}{90}\right)^2}$ $\xi = 2.059$

$\alpha_c := \xi \cdot \left(1 - \sqrt{\left(1 - \left(\frac{90}{\xi \cdot \lambda}\right)^2\right)}\right)$ $\alpha_c = 0.839$

$N_s := b_e \cdot t_g \cdot f_y$ $N_s = 1466.1\ kN$

$P_{cr} := \alpha_c \cdot N_s$ $P_{cr} = 1230.7\ kN$

10.1.4 Hera R4-80 Method (1994) Calculations

$L := 207.2\ mm$ $k := 0.5$

$k_f := 1.0$ $f_y := 385\ MPa$

$\alpha_b := 0.5$ $t_g := 14\ mm$

$b_e := 272\ mm$

$r := \frac{t_g}{\sqrt{12}}$ $r = 0.004\ m$

$\lambda_n := \frac{(k \cdot L)}{r} \cdot \sqrt{k_f} \cdot \sqrt{\frac{f_y}{250\ MPa}}$ $\lambda_n = 31.811$

$\alpha_a := \frac{(2100 \cdot (\lambda_n - 13.5))}{\lambda_n^{\ 2} - 15.3 \cdot \lambda_n + 2050}$ $\alpha_a = 14.932$

$\lambda := \lambda_n + \alpha_a \cdot \alpha_b$ $\lambda = 39.277$

$\eta := 0.00326 \cdot (\lambda - 13.5)$ $\eta = 0.084$

$\xi := \frac{\left(\frac{\lambda}{90}\right)^2 + 1 + \eta}{2 \cdot \left(\frac{\lambda}{90}\right)^2}$ $\xi = 3.346$

$\alpha_c := \xi \cdot \left(1 - \sqrt{\left(1 - \left(\frac{90}{\xi \cdot \lambda}\right)^2\right)}\right)$ $\alpha_c = 0.908$

$N_s := b_e \cdot t_g \cdot f_y$ $N_s = 1466.1\ kN$

$P_{cr} := \alpha_c \cdot N_s$ $P_{cr} = 1330.9\ kN$

10.1.5 Working Point Method (2002) Calculations

$L_b := 1274.8\ mm$ $k := 2$

$I_c := 11456144\ mm^4$ $E := 200000\ MPa$

$$P_{cr} := \frac{\pi^2 \cdot E \cdot I_c}{(k \cdot L_b)^2} \qquad P_{cr} = 3478.8\ kN$$

10.1.6 Koetaka et al. Method (2008) Calculations

$L_{BRB} := 4032\ mm$ $E := 200000\ MPa$

$L_c := 922\ mm$ $I_c := 11456144\ mm^4$

$$\xi := \frac{L_c}{L_{BRB}} \qquad \xi = 0.229$$

$$P_{cr} := \frac{\pi^2 \cdot E \cdot I_c}{(2 \cdot L_c)^2}(1 - 2 \cdot \xi) \qquad P_{cr} = 3608.9\ kN$$

10.1.7 Tsai and Hsiao Method (2008) Calculations

$L := 283\ mm$ $k := 2$

$t_g := 14\ mm$ $b_e := 272\ mm$

$E := 200000\ MPa$

$$r := \frac{t_g}{\sqrt{12}} \qquad r = 4.041\ mm$$

$$P_{cr} := \frac{\pi^2 \cdot E}{\left(\frac{k \cdot L}{r}\right)^2} b_e \cdot t_g$$

$P_{cr} = 383.2\ kN$

10.1.8 Chou et al. Method (2012) Calculations

$L := 207.2\ mm$ $k := 2$

$t_g := 14\ mm$ $b_e := 272\ mm$

$F_y := 385\ MPa$ $E := 200000\ MPa$

$r := \frac{t_g}{\sqrt{12}}$ $r = 4.041\ mm$

$\lambda_c := \frac{k \cdot L}{\pi \cdot r} \cdot \sqrt{\frac{F_y}{E}}$ $\lambda_c = 1.432$ Lamda less than 1.5 therefore use Pcr1

$P_{cr1} := 0.658^{\lambda_c^2} \cdot F_y \cdot b_e \cdot t_g$

$P_{cr2} := \frac{0.877}{\lambda_c^{\ 2}} \cdot F_y \cdot b_e \cdot t_g$

$P_{cr1} = 621.4\ kN$

10.2 Gusset Plate Capacity Calculations

10.2.1 Experimentally Tested Gusset Plate Capacity Calculations

Table 10.2-1: Experimentally tested gusset plate capacities using various calculation methods (Raw Data)

	Thornton (max)	**Thornton (ave)**	**Thornton, K = 1.0 (ave)**	**NZS 3404 (max)**	**NZS 3404 (ave)**	**HERA R4-80**	**Modified Thornton method**	**Euler**	**Buckling Capacity**
GC01	120.5	276.7	321.1	95.1	219.6	287.5	174.0	137.4	516.0
HC01	246.6	430.5	727.5	216.7	355.8	616.8	384.2	296.6	914.0
HC02	33.8	113.4	188.2	30.7	91.3	155.2	52.6	37.9	140.6
HC03	246.6	430.5	727.5	216.7	355.8	616.8	384.2	296.6	678.2
HC04	33.8	113.4	188.2	30.7	91.3	155.2	52.6	37.9	145.5
HC05	246.6	430.5	181.9	216.7	355.8	616.8	384.2	296.6	441.7
HC06	33.8	113.4	47.9	30.7	91.3	155.2	52.6	37.9	122.4
HC07	246.6	430.5	181.9	216.7	355.8	616.8	384.2	296.6	380.1
HC08	33.8	113.4	47.9	30.7	91.3	155.2	52.6	37.9	89.6
N01	246.1	339.4	162.5	183.5	253.1	369.0	361.8	295.6	403.3
RC01	1253.1	1481.3	1282.6	1038.6	1349.0	1472.9	2007.2	2602.6	1682.0
RC02	584.0	850.1	615.3	433.4	718.3	861.2	935.5	758.8	1128.0
RC03	718.5	990.2	502.3	531.7	748.7	1060.0	1150.9	856.1	907.0
S01	755.2	799.8	679.5	659.7	722.2	796.0	1144.3	2216.0	1626.0
S02	1476.8	1524.1	1508.9	1414.4	1541.8	1570.3	2370.0	17147.3	2349.0
S03	496.2	552.7	407.0	399.5	470.2	558.6	751.9	917.0	1143.0
S04	1095.0	1161.9	1140.2	1018.6	1155.1	1184.5	1757.4	7095.7	1867.0
S05	755.2	799.8	679.5	659.7	722.2	796.0	1144.3	2216.0	1480.0
S06	755.2	799.8	679.5	659.7	722.2	796.0	1144.3	2216.0	1232.0
S07	496.2	552.7	407.0	399.5	470.2	558.6	751.9	917.0	878.0
YC01	1119.3	1162.8	1091.2	1032.9	1105.2	1161.5	1759.2	6251.7	1956.0
YC02	789.9	849.4	752.5	696.1	781.7	844.2	1241.5	2532.4	1356.0
YC03	426.7	503.2	382.1	338.2	433.6	506.6	670.6	738.9	742.0
YC04	1093.7	1168.8	1104.4	994.5	1116.5	1169.3	1719.0	4909.9	1720.0
YC05	755.8	857.7	770.0	649.7	794.5	852.6	1188.0	1988.9	1210.0
YC06	386.0	514.5	402.7	295.2	448.8	516.0	606.7	580.3	728.0
YC07	1179.9	1360.3	892.0	906.5	1107.1	1397.6	1919.2	1784.2	1606.0
YC08	597.8	783.9	372.2	443.7	583.5	854.6	972.4	722.7	1010.0

10.2.2 Fixed-Free Boundary Condition Finite Element Model Calculations

Table 10.2-2: Fixed-Free boundary conditions finite element model capacities using various calculation methods (Raw Data)

	Finite Element Capacity	**Thornton (max)**	**Thornton (ave)**	**NZS 3404 (max)**	**NZS 3404 (ave)**	**HERA R4-80**	**Modified Thornton**	**Euler**
HC04	9	3.6	12.0	3.4	11.0	13.2	19.1	4.0
RC02	156	68.2	176.6	60.5	145.9	172.9	182.3	80.1
S02	1144	1062.3	1432.2	822.7	1328.7	1358.5	2098.2	1811.2
S03	274	80.8	119.7	68.9	98.4	116.4	429.4	96.9
S04	652	590.0	1033.9	422.0	919.2	954.4	1398.2	749.5
S05	441	197.8	293.0	158.0	220.4	257.0	849.0	234.1
S06	319	197.8	293.0	158.0	220.4	257.0	849.0	234.1
S07	145	80.8	119.7	68.9	98.4	116.4	429.4	96.9
YC01	802	546.6	784.2	390.9	589.5	656.8	1190.6	660.3
YC02	389	223.2	401.1	176.1	287.6	331.8	590.3	267.5
YC03	134	65.1	118.5	55.9	96.2	113.6	172.7	78.0
YC05	632	175.3	439.8	142.6	314.1	360.5	434.7	210.1
YC06	236	51.1	133.1	44.7	106.5	125.6	126.8	61.3
YC08	166	63.7	93.1	57.4	82.3	98.5	127.8	76.3

10.3 Parametric Analysis Scripts

10.3.1 Parametric Design Input Script

```
Note: Code is run through an Abaqus command line prompt with
the following line:

abaqus cae nogui=gussetInputScript)

# Required imports to run code
from abaqus import *
from abaqusConstants import *
import sys
import os

# Opens model database containing gusset plate models
mdb=openMdb(pathName="GussetPlateParametricModelK05")

# Domains containing all parameter values
thicknessDomain = [5, 10, 15, 20] # mm
youngsDomain = [195, 200, 205, 210] # GPa
yieldDomain = [290,300,310] # MPa
a0Domain = [350, 400, 450, 500] # mm
l2Domain = [200, 250, 300] # mm
l3Domain = [100, 150, 200] # mm
kDomain = [0.5, 1, 2] # Manually modified

# Default Parameters (Required for initial buckling job)
thicknessParam = 5
youngsParam = 195000
yieldParam = 290
a0Param = 400
l2Param = 200
l3Param = 100.0

# Adjust timestep if necessary
mdb.models['GussetPlate-
DisplacementModel'].steps['Displacement'].setValues(
initialInc=0.01, maxInc=0.01)

# Adjust Displacement if necessary
mdb.models['GussetPlate-
DisplacementModel'].boundaryConditions['DisplacementNode'].set
Values(u2=-20.0)

for l3Param in l3Domain:

# Length adjustment required for gusset plate adjustment due
to Abaqus geometry handling
```

```
halfL3Param = (l3Param + 15.0)/2.0

# Adjustment of l3 for Buckling Model
session.viewports['Viewport:
1'].setValues(displayedObject=None)
p = mdb.models['GussetPlate-BuckleModel'].parts['Plate
240x148x13']
session.viewports['Viewport: 1'].setValues(displayedObject=p)
p = mdb.models['GussetPlate-BuckleModel'].parts['Plate
240x148x13']
s = p.features['Shell planar-1'].sketch
mdb.models['GussetPlate-
BuckleModel'].ConstrainedSketch(name='__edit__',
objectToCopy=s)
s1 = mdb.models['GussetPlate-
BuckleModel'].sketches['__edit__']
g, v, d, c = s1.geometry, s1.vertices, s1.dimensions,
s1.constraints
s1.setPrimaryObject(option=SUPERIMPOSE)
p.projectReferencesOntoSketch(sketch=s1,
upToFeature=p.features['Shell planar-1'],
filter=COPLANAR_EDGES)
d[1].setValues(value=l3Param, )
s1.unsetPrimaryObject()
p = mdb.models['GussetPlate-BuckleModel'].parts['Plate
240x148x13']
p.features['Shell planar-1'].setValues(sketch=s1)
del mdb.models['GussetPlate-BuckleModel'].sketches['__edit__']
p = mdb.models['GussetPlate-BuckleModel'].parts['Plate
240x148x13']
p.regenerate()
p1 = mdb.models['GussetPlate-BuckleModel'].parts['Splice
Flange']
session.viewports['Viewport: 1'].setValues(displayedObject=p1)
p = mdb.models['GussetPlate-BuckleModel'].parts['Splice
Flange']
s = p.features['Shell planar-1'].sketch
mdb.models['GussetPlate-
BuckleModel'].ConstrainedSketch(name='__edit__',
objectToCopy=s)
s2 = mdb.models['GussetPlate-
BuckleModel'].sketches['__edit__']
g, v, d, c = s2.geometry, s2.vertices, s2.dimensions,
s2.constraints
s2.setPrimaryObject(option=SUPERIMPOSE)
p.projectReferencesOntoSketch(sketch=s2,
upToFeature=p.features['Shell planar-1'],
filter=COPLANAR_EDGES)
d[1].setValues(value=l3Param, )
s2.unsetPrimaryObject()
```

```
p = mdb.models['GussetPlate-BuckleModel'].parts['Splice
Flange']
p.features['Shell planar-1'].setValues(sketch=s2)
del mdb.models['GussetPlate-BuckleModel'].sketches['__edit__']
p = mdb.models['GussetPlate-BuckleModel'].parts['Splice
Flange']
p.regenerate()
p1 = mdb.models['GussetPlate-BuckleModel'].parts['Gusset-
Plate']
session.viewports['Viewport: 1'].setValues(displayedObject=p1)
p = mdb.models['GussetPlate-BuckleModel'].parts['Gusset-
Plate']
s = p.features['Partition face-1'].sketch
mdb.models['GussetPlate-
BuckleModel'].ConstrainedSketch(name='__edit__',
objectToCopy=s)
s1 = mdb.models['GussetPlate-
BuckleModel'].sketches['__edit__']
g, v, d, c = s1.geometry, s1.vertices, s1.dimensions,
s1.constraints
s1.setPrimaryObject(option=SUPERIMPOSE)
p.projectReferencesOntoSketch(sketch=s1,
upToFeature=p.features['Partition face-1'],
filter=COPLANAR_EDGES)
d[1].setValues(value=l3Param, )
s1.unsetPrimaryObject()
p = mdb.models['GussetPlate-BuckleModel'].parts['Gusset-
Plate']
p.features['Partition face-1'].setValues(sketch=s1)
del mdb.models['GussetPlate-BuckleModel'].sketches['__edit__']
p = mdb.models['GussetPlate-BuckleModel'].parts['Gusset-
Plate']
p.regenerate()
p = mdb.models['GussetPlate-BuckleModel'].parts['Gusset-
Plate']
s = p.features['Shell planar-1'].sketch
mdb.models['GussetPlate-
BuckleModel'].ConstrainedSketch(name='__edit__',
objectToCopy=s)
s2 = mdb.models['GussetPlate-
BuckleModel'].sketches['__edit__']
g, v, d, c = s2.geometry, s2.vertices, s2.dimensions,
s2.constraints
s2.setPrimaryObject(option=SUPERIMPOSE)
p.projectReferencesOntoSketch(sketch=s2,
upToFeature=p.features['Shell planar-1'],
filter=COPLANAR_EDGES)
d[4].setValues(value=halfL3Param, )
s2.unsetPrimaryObject()
```

```
p = mdb.models['GussetPlate-BuckleModel'].parts['Gusset-
Plate']
p.features['Shell planar-1'].setValues(sketch=s2)
del mdb.models['GussetPlate-BuckleModel'].sketches['__edit__']
p = mdb.models['GussetPlate-BuckleModel'].parts['Gusset-
Plate']
p.regenerate()
session.viewports['Viewport:
1'].partDisplay.setValues(mesh=ON)
session.viewports['Viewport:
1'].partDisplay.meshOptions.setValues(
meshTechnique=ON)
session.viewports['Viewport:
1'].partDisplay.geometryOptions.setValues(
referenceRepresentation=OFF)
a = mdb.models['GussetPlate-BuckleModel'].rootAssembly
session.viewports['Viewport: 1'].setValues(displayedObject=a)
a = mdb.models['GussetPlate-BuckleModel'].rootAssembly
a.regenerate()
session.viewports['Viewport:
1'].assemblyDisplay.setValues(mesh=ON,
optimizationTasks=OFF, geometricRestrictions=OFF,
stopConditions=OFF)
session.viewports['Viewport:
1'].assemblyDisplay.meshOptions.setValues(
meshTechnique=ON)
a = mdb.models['GussetPlate-BuckleModel'].rootAssembly
partInstances =(a.instances['S01-Gusset-1'],
a.instances['Plate 240x148x13-1'],
a.instances['Plate 240x148x13-2'], a.instances['Flange2'],
a.instances['Flange1'], a.instances['Splice Web-1'],
a.instances['Splice Web-2'], )
a.generateMesh(regions=partInstances)

# Adjustment of l3 for Displacment Model
p1 = mdb.models['GussetPlate-DisplacementModel'].parts['Plate
240x148x13']
session.viewports['Viewport: 1'].setValues(displayedObject=p1)
p = mdb.models['GussetPlate-DisplacementModel'].parts['Plate
240x148x13']
s = p.features['Shell planar-1'].sketch
mdb.models['GussetPlate-
DisplacementModel'].ConstrainedSketch(name='__edit__',
objectToCopy=s)
s1 = mdb.models['GussetPlate-
DisplacementModel'].sketches['__edit__']
g, v, d, c = s1.geometry, s1.vertices, s1.dimensions,
s1.constraints
s1.setPrimaryObject(option=SUPERIMPOSE)
p.projectReferencesOntoSketch(sketch=s1,
```

```
upToFeature=p.features['Shell planar-1'],
filter=COPLANAR_EDGES)
d[1].setValues(value=l3Param, )
s1.unsetPrimaryObject()
p = mdb.models['GussetPlate-DisplacementModel'].parts['Plate
240x148x13']
p.features['Shell planar-1'].setValues(sketch=s1)
del mdb.models['GussetPlate-
DisplacementModel'].sketches['__edit__']
p = mdb.models['GussetPlate-DisplacementModel'].parts['Plate
240x148x13']
p.regenerate()
p1 = mdb.models['GussetPlate-DisplacementModel'].parts['Splice
Flange']
session.viewports['Viewport: 1'].setValues(displayedObject=p1)
p = mdb.models['GussetPlate-DisplacementModel'].parts['Splice
Flange']
s = p.features['Shell planar-1'].sketch
mdb.models['GussetPlate-
DisplacementModel'].ConstrainedSketch(name='__edit__',
objectToCopy=s)
s2 = mdb.models['GussetPlate-
DisplacementModel'].sketches['__edit__']
g, v, d, c = s2.geometry, s2.vertices, s2.dimensions,
s2.constraints
s2.setPrimaryObject(option=SUPERIMPOSE)
p.projectReferencesOntoSketch(sketch=s2,
upToFeature=p.features['Shell planar-1'],
filter=COPLANAR_EDGES)
d[1].setValues(value=l3Param, )
s2.unsetPrimaryObject()
p = mdb.models['GussetPlate-DisplacementModel'].parts['Splice
Flange']
p.features['Shell planar-1'].setValues(sketch=s2)
del mdb.models['GussetPlate-
DisplacementModel'].sketches['__edit__']
p = mdb.models['GussetPlate-DisplacementModel'].parts['Splice
Flange']
p.regenerate()
p1 = mdb.models['GussetPlate-
DisplacementModel'].parts['Gusset-Plate']
session.viewports['Viewport: 1'].setValues(displayedObject=p1)
p = mdb.models['GussetPlate-DisplacementModel'].parts['Gusset-
Plate']
s = p.features['Partition face-1'].sketch
mdb.models['GussetPlate-
DisplacementModel'].ConstrainedSketch(name='__edit__',
objectToCopy=s)
s1 = mdb.models['GussetPlate-
DisplacementModel'].sketches['__edit__']
```

```
g, v, d, c = s1.geometry, s1.vertices, s1.dimensions,
s1.constraints
s1.setPrimaryObject(option=SUPERIMPOSE)
p.projectReferencesOntoSketch(sketch=s1,
upToFeature=p.features['Partition face-1'],
filter=COPLANAR_EDGES)
d[1].setValues(value=l3Param, )
s1.unsetPrimaryObject()
p = mdb.models['GussetPlate-DisplacementModel'].parts['Gusset-
Plate']
p.features['Partition face-1'].setValues(sketch=s1)
del mdb.models['GussetPlate-
DisplacementModel'].sketches['__edit__']
p = mdb.models['GussetPlate-DisplacementModel'].parts['Gusset-
Plate']
p.regenerate()
p = mdb.models['GussetPlate-DisplacementModel'].parts['Gusset-
Plate']
s = p.features['Shell planar-1'].sketch
mdb.models['GussetPlate-
DisplacementModel'].ConstrainedSketch(name='__edit__',
objectToCopy=s)
s2 = mdb.models['GussetPlate-
DisplacementModel'].sketches['__edit__']
g, v, d, c = s2.geometry, s2.vertices, s2.dimensions,
s2.constraints
s2.setPrimaryObject(option=SUPERIMPOSE)
p.projectReferencesOntoSketch(sketch=s2,
upToFeature=p.features['Shell planar-1'],
filter=COPLANAR_EDGES)
d[4].setValues(value=halfL3Param, )
s2.unsetPrimaryObject()
p = mdb.models['GussetPlate-DisplacementModel'].parts['Gusset-
Plate']
p.features['Shell planar-1'].setValues(sketch=s2)
del mdb.models['GussetPlate-
DisplacementModel'].sketches['__edit__']
p = mdb.models['GussetPlate-DisplacementModel'].parts['Gusset-
Plate']
p.regenerate()
session.viewports['Viewport:
1'].view.setValues(nearPlane=1276.32,
farPlane=1552.11, width=785.398, height=506.114,
viewOffsetX=23.5703,
viewOffsetY=3.25644)
session.viewports['Viewport:
1'].partDisplay.setValues(mesh=ON)
session.viewports['Viewport:
1'].partDisplay.meshOptions.setValues(
meshTechnique=ON)
```

```
session.viewports['Viewport:
1'].partDisplay.geometryOptions.setValues(
referenceRepresentation=OFF)
a = mdb.models['GussetPlate-DisplacementModel'].rootAssembly
session.viewports['Viewport: 1'].setValues(displayedObject=a)
a = mdb.models['GussetPlate-DisplacementModel'].rootAssembly
a.regenerate()

session.viewports['Viewport:
1'].assemblyDisplay.setValues(mesh=ON,
optimizationTasks=OFF, geometricRestrictions=OFF,
stopConditions=OFF)
session.viewports['Viewport:
1'].assemblyDisplay.meshOptions.setValues(
meshTechnique=ON)
a = mdb.models['GussetPlate-DisplacementModel'].rootAssembly
partInstances =(a.instances['S01-Gusset-1'],
a.instances['Plate 240x148x13-1'],
a.instances['Plate 240x148x13-2'], a.instances['Flange2'],
a.instances['Flange1'], a.instances['Splice Web-1'],
a.instances['Splice Web-2'], )
a.generateMesh(regions=partInstances)

for l2Param in l2Domain:

# Adjustment of Buckling Model
p = mdb.models['GussetPlate-BuckleModel'].parts['Plate
240x148x13']
s = p.features['Shell planar-1'].sketch
mdb.models['GussetPlate-
BuckleModel'].ConstrainedSketch(name='__edit__',
objectToCopy=s)
s1 = mdb.models['GussetPlate-
BuckleModel'].sketches['__edit__']
g, v, d, c = s1.geometry, s1.vertices, s1.dimensions,
s1.constraints
s1.setPrimaryObject(option=SUPERIMPOSE)
p.projectReferencesOntoSketch(sketch=s1,
upToFeature=p.features['Shell planar-1'],
filter=COPLANAR_EDGES)
d[0].setValues(value=l2Param, )
s1.unsetPrimaryObject()
p = mdb.models['GussetPlate-BuckleModel'].parts['Plate
240x148x13']
p.features['Shell planar-1'].setValues(sketch=s1)
del mdb.models['GussetPlate-BuckleModel'].sketches['__edit__']
p = mdb.models['GussetPlate-BuckleModel'].parts['Plate
240x148x13']
p.regenerate()
```

```
p1 = mdb.models['GussetPlate-BuckleModel'].parts['Splice
Flange']
session.viewports['Viewport: 1'].setValues(displayedObject=p1)
p = mdb.models['GussetPlate-BuckleModel'].parts['Splice
Flange']
s = p.features['Shell planar-1'].sketch
mdb.models['GussetPlate-
BuckleModel'].ConstrainedSketch(name='__edit__',
objectToCopy=s)
s2 = mdb.models['GussetPlate-
BuckleModel'].sketches['__edit__']
g, v, d, c = s2.geometry, s2.vertices, s2.dimensions,
s2.constraints
s2.setPrimaryObject(option=SUPERIMPOSE)
p.projectReferencesOntoSketch(sketch=s2,
upToFeature=p.features['Shell planar-1'],
filter=COPLANAR_EDGES)
d[0].setValues(value=l2Param, )
s2.unsetPrimaryObject()
p = mdb.models['GussetPlate-BuckleModel'].parts['Splice
Flange']
p.features['Shell planar-1'].setValues(sketch=s2)
del mdb.models['GussetPlate-BuckleModel'].sketches['__edit__']
p = mdb.models['GussetPlate-BuckleModel'].parts['Splice
Flange']
p.regenerate()
p1 = mdb.models['GussetPlate-BuckleModel'].parts['Splice Web']
session.viewports['Viewport: 1'].setValues(displayedObject=p1)
p = mdb.models['GussetPlate-BuckleModel'].parts['Splice Web']
s = p.features['Shell planar-1'].sketch
mdb.models['GussetPlate-
BuckleModel'].ConstrainedSketch(name='__edit__',
objectToCopy=s)
s1 = mdb.models['GussetPlate-
BuckleModel'].sketches['__edit__']
g, v, d, c = s1.geometry, s1.vertices, s1.dimensions,
s1.constraints
s1.setPrimaryObject(option=SUPERIMPOSE)
p.projectReferencesOntoSketch(sketch=s1,
upToFeature=p.features['Shell planar-1'],
filter=COPLANAR_EDGES)
d[0].setValues(value=l2Param, )
s1.unsetPrimaryObject()
p = mdb.models['GussetPlate-BuckleModel'].parts['Splice Web']
p.features['Shell planar-1'].setValues(sketch=s1)
del mdb.models['GussetPlate-BuckleModel'].sketches['__edit__']
p = mdb.models['GussetPlate-BuckleModel'].parts['Splice Web']
p.regenerate()
p1 = mdb.models['GussetPlate-BuckleModel'].parts['Gusset-
Plate']
```

```
session.viewports['Viewport: 1'].setValues(displayedObject=p1)
p = mdb.models['GussetPlate-BuckleModel'].parts['Gusset-
Plate']
s = p.features['Shell planar-1'].sketch
mdb.models['GussetPlate-
BuckleModel'].ConstrainedSketch(name='__edit__',
objectToCopy=s)
s2 = mdb.models['GussetPlate-
BuckleModel'].sketches['__edit__']
g, v, d, c = s2.geometry, s2.vertices, s2.dimensions,
s2.constraints
s2.setPrimaryObject(option=SUPERIMPOSE)
p.projectReferencesOntoSketch(sketch=s2,
upToFeature=p.features['Shell planar-1'],
filter=COPLANAR_EDGES)
s2.unsetPrimaryObject()
del mdb.models['GussetPlate-BuckleModel'].sketches['__edit__']
p = mdb.models['GussetPlate-BuckleModel'].parts['Gusset-
Plate']
s = p.features['Partition face-1'].sketch
mdb.models['GussetPlate-
BuckleModel'].ConstrainedSketch(name='__edit__',
objectToCopy=s)
s1 = mdb.models['GussetPlate-
BuckleModel'].sketches['__edit__']
g, v, d, c = s1.geometry, s1.vertices, s1.dimensions,
s1.constraints
s1.setPrimaryObject(option=SUPERIMPOSE)
p.projectReferencesOntoSketch(sketch=s1,
upToFeature=p.features['Partition face-1'],
filter=COPLANAR_EDGES)
d[0].setValues(value=l2Param, )
s1.unsetPrimaryObject()
p = mdb.models['GussetPlate-BuckleModel'].parts['Gusset-
Plate']
p.features['Partition face-1'].setValues(sketch=s1)
del mdb.models['GussetPlate-BuckleModel'].sketches['__edit__']
p = mdb.models['GussetPlate-BuckleModel'].parts['Gusset-
Plate']
p.regenerate()
a = mdb.models['GussetPlate-BuckleModel'].rootAssembly
a.regenerate()
a = mdb.models['GussetPlate-BuckleModel'].rootAssembly
session.viewports['Viewport: 1'].setValues(displayedObject=a)
session.viewports['Viewport: 1'].assemblyDisplay.setValues(
optimizationTasks=OFF, geometricRestrictions=OFF,
stopConditions=OFF)
session.viewports['Viewport:
1'].assemblyDisplay.setValues(mesh=ON)
```

```
session.viewports['Viewport:
1'].assemblyDisplay.meshOptions.setValues(
meshTechnique=ON)
a = mdb.models['GussetPlate-BuckleModel'].rootAssembly
partInstances =(a.instances['S01-Gusset-1'],
a.instances['Plate 240x148x13-1'],
a.instances['Plate 240x148x13-2'], a.instances['Flange2'],
a.instances['Flange1'], a.instances['Splice Web-1'],
a.instances['Splice Web-2'], )
a.generateMesh(regions=partInstances)

# Adjustment of Displacement Model
p = mdb.models['GussetPlate-DisplacementModel'].parts['Gusset-
Plate']
s = p.features['Partition face-1'].sketch
mdb.models['GussetPlate-
DisplacementModel'].ConstrainedSketch(name='__edit__',
objectToCopy=s)
s1 = mdb.models['GussetPlate-
DisplacementModel'].sketches['__edit__']
g, v, d, c = s1.geometry, s1.vertices, s1.dimensions,
s1.constraints
s1.setPrimaryObject(option=SUPERIMPOSE)
p.projectReferencesOntoSketch(sketch=s1,
upToFeature=p.features['Partition face-1'],
filter=COPLANAR_EDGES)
d[0].setValues(value=l2Param, )
s1.unsetPrimaryObject()
p = mdb.models['GussetPlate-DisplacementModel'].parts['Gusset-
Plate']
p.features['Partition face-1'].setValues(sketch=s1)
del mdb.models['GussetPlate-
DisplacementModel'].sketches['__edit__']
p = mdb.models['GussetPlate-DisplacementModel'].parts['Gusset-
Plate']
p.regenerate()
p1 = mdb.models['GussetPlate-DisplacementModel'].parts['Splice
Web']
session.viewports['Viewport: 1'].setValues(displayedObject=p1)
p = mdb.models['GussetPlate-DisplacementModel'].parts['Splice
Web']
s = p.features['Shell planar-1'].sketch
mdb.models['GussetPlate-
DisplacementModel'].ConstrainedSketch(name='__edit__',
objectToCopy=s)
s2 = mdb.models['GussetPlate-
DisplacementModel'].sketches['__edit__']
g, v, d, c = s2.geometry, s2.vertices, s2.dimensions,
s2.constraints
s2.setPrimaryObject(option=SUPERIMPOSE)
```

```
p.projectReferencesOntoSketch(sketch=s2,
upToFeature=p.features['Shell planar-1'],
filter=COPLANAR_EDGES)
d[0].setValues(value=l2Param, )
s2.unsetPrimaryObject()
p = mdb.models['GussetPlate-DisplacementModel'].parts['Splice
Web']
p.features['Shell planar-1'].setValues(sketch=s2)
del mdb.models['GussetPlate-
DisplacementModel'].sketches['__edit__']
p = mdb.models['GussetPlate-DisplacementModel'].parts['Splice
Web']
p.regenerate()
p1 = mdb.models['GussetPlate-DisplacementModel'].parts['Splice
Flange']
session.viewports['Viewport: 1'].setValues(displayedObject=p1)
p = mdb.models['GussetPlate-DisplacementModel'].parts['Splice
Flange']
s = p.features['Shell planar-1'].sketch
mdb.models['GussetPlate-
DisplacementModel'].ConstrainedSketch(name='__edit__',
objectToCopy=s)
s1 = mdb.models['GussetPlate-
DisplacementModel'].sketches['__edit__']
g, v, d, c = s1.geometry, s1.vertices, s1.dimensions,
s1.constraints
s1.setPrimaryObject(option=SUPERIMPOSE)
p.projectReferencesOntoSketch(sketch=s1,
upToFeature=p.features['Shell planar-1'],
filter=COPLANAR_EDGES)
d[0].setValues(value=l2Param, )
s1.unsetPrimaryObject()
p = mdb.models['GussetPlate-DisplacementModel'].parts['Splice
Flange']
p.features['Shell planar-1'].setValues(sketch=s1)
del mdb.models['GussetPlate-
DisplacementModel'].sketches['__edit__']
p = mdb.models['GussetPlate-DisplacementModel'].parts['Splice
Flange']
p.regenerate()
p1 = mdb.models['GussetPlate-DisplacementModel'].parts['Plate
240x148x13']
session.viewports['Viewport: 1'].setValues(displayedObject=p1)
p = mdb.models['GussetPlate-DisplacementModel'].parts['Plate
240x148x13']
s = p.features['Shell planar-1'].sketch
mdb.models['GussetPlate-
DisplacementModel'].ConstrainedSketch(name='__edit__',
objectToCopy=s)
```

```
s2 = mdb.models['GussetPlate-
DisplacementModel'].sketches['__edit__']
g, v, d, c = s2.geometry, s2.vertices, s2.dimensions,
s2.constraints
s2.setPrimaryObject(option=SUPERIMPOSE)
p.projectReferencesOntoSketch(sketch=s2,
upToFeature=p.features['Shell planar-1'],
filter=COPLANAR_EDGES)
d[0].setValues(value=l2Param, )
s2.unsetPrimaryObject()
p = mdb.models['GussetPlate-DisplacementModel'].parts['Plate
240x148x13']
p.features['Shell planar-1'].setValues(sketch=s2)
del mdb.models['GussetPlate-
DisplacementModel'].sketches['__edit__']
p = mdb.models['GussetPlate-DisplacementModel'].parts['Plate
240x148x13']
p.regenerate()
session.viewports['Viewport:
1'].partDisplay.setValues(mesh=ON)
session.viewports['Viewport:
1'].partDisplay.meshOptions.setValues(
meshTechnique=ON)
session.viewports['Viewport:
1'].partDisplay.geometryOptions.setValues(
referenceRepresentation=OFF)
a = mdb.models['GussetPlate-DisplacementModel'].rootAssembly
session.viewports['Viewport: 1'].setValues(displayedObject=a)
a = mdb.models['GussetPlate-DisplacementModel'].rootAssembly
a.regenerate()
session.viewports['Viewport:
1'].assemblyDisplay.setValues(mesh=ON,
optimizationTasks=OFF, geometricRestrictions=OFF,
stopConditions=OFF)
session.viewports['Viewport:
1'].assemblyDisplay.meshOptions.setValues(
meshTechnique=ON)
a = mdb.models['GussetPlate-DisplacementModel'].rootAssembly
partInstances =(a.instances['S01-Gusset-1'],
a.instances['Plate 240x148x13-1'],
a.instances['Plate 240x148x13-2'], a.instances['Flange2'],
a.instances['Flange1'], a.instances['Splice Web-1'],
a.instances['Splice Web-2'], )
a.generateMesh(regions=partInstances)
session.viewports['Viewport:
1'].assemblyDisplay.setValues(mesh=OFF)
session.viewports['Viewport:
1'].assemblyDisplay.meshOptions.setValues(
meshTechnique=OFF)
```

```
for a0Param in a0Domain:

# Adjustment of length a0 for Buckling Model
p1 = mdb.models['GussetPlate-BuckleModel'].parts['Gusset-
Plate']
session.viewports['Viewport: 1'].setValues(displayedObject=p1)
session.viewports['Viewport:
1'].partDisplay.setValues(mesh=ON)
session.viewports['Viewport:
1'].partDisplay.meshOptions.setValues(
meshTechnique=ON)
session.viewports['Viewport:
1'].partDisplay.geometryOptions.setValues(
referenceRepresentation=OFF)
p = mdb.models['GussetPlate-BuckleModel'].parts['Gusset-
Plate']
s = p.features['Shell planar-1'].sketch
mdb.models['GussetPlate-
BuckleModel'].ConstrainedSketch(name='__edit__',
objectToCopy=s)
s2 = mdb.models['GussetPlate-
BuckleModel'].sketches['__edit__']
g, v, d, c = s2.geometry, s2.vertices, s2.dimensions,
s2.constraints
s2.setPrimaryObject(option=SUPERIMPOSE)
p.projectReferencesOntoSketch(sketch=s2,
upToFeature=p.features['Shell planar-1'],
filter=COPLANAR_EDGES)
s=mdb.models['GussetPlate-BuckleModel'].sketches['__edit__']
s.parameters['a0'].setValues(expression=str(a0Param))
s2.unsetPrimaryObject()
p = mdb.models['GussetPlate-BuckleModel'].parts['Gusset-
Plate']
p.features['Shell planar-1'].setValues(sketch=s2)
del mdb.models['GussetPlate-BuckleModel'].sketches['__edit__']
p = mdb.models['GussetPlate-BuckleModel'].parts['Gusset-
Plate']
p.regenerate()
a1 = mdb.models['GussetPlate-BuckleModel'].rootAssembly
a1.regenerate()
#: Warning: Mesh deleted in 3 regions of instance 'S01-Gusset-
1' due to geometry association failure.
a = mdb.models['GussetPlate-BuckleModel'].rootAssembly
session.viewports['Viewport: 1'].setValues(displayedObject=a)
session.viewports['Viewport:
1'].assemblyDisplay.setValues(mesh=OFF)
session.viewports['Viewport:
1'].assemblyDisplay.meshOptions.setValues(
meshTechnique=OFF)
```

```
session.viewports['Viewport:
1'].assemblyDisplay.setValues(mesh=ON)
session.viewports['Viewport:
1'].assemblyDisplay.meshOptions.setValues(
meshTechnique=ON)
a = mdb.models['GussetPlate-BuckleModel'].rootAssembly
partInstances =(a.instances['S01-Gusset-1'],
a.instances['Plate 240x148x13-1'],
a.instances['Plate 240x148x13-2'], a.instances['Flange2'],
a.instances['Flange1'], a.instances['Splice Web-1'],
a.instances['Splice Web-2'], )
a.generateMesh(regions=partInstances)

# Adjustment of length a0 for Displacement Model
p = mdb.models['GussetPlate-DisplacementModel'].parts['Gusset-
Plate']
s = p.features['Shell planar-1'].sketch
mdb.models['GussetPlate-
DisplacementModel'].ConstrainedSketch(name='__edit__',
objectToCopy=s)
s1 = mdb.models['GussetPlate-
DisplacementModel'].sketches['__edit__']
g, v, d, c = s1.geometry, s1.vertices, s1.dimensions,
s1.constraints
s1.setPrimaryObject(option=SUPERIMPOSE)
p.projectReferencesOntoSketch(sketch=s1,
upToFeature=p.features['Shell planar-1'],
filter=COPLANAR_EDGES)
s=mdb.models['GussetPlate-
DisplacementModel'].sketches['__edit__']
s.parameters['a0'].setValues(expression=str(a0Param))
s1.unsetPrimaryObject()
p = mdb.models['GussetPlate-DisplacementModel'].parts['Gusset-
Plate']
p.features['Shell planar-1'].setValues(sketch=s1)
del mdb.models['GussetPlate-
DisplacementModel'].sketches['__edit__']
p = mdb.models['GussetPlate-DisplacementModel'].parts['Gusset-
Plate']
p.regenerate()
a = mdb.models['GussetPlate-DisplacementModel'].rootAssembly
a.regenerate()
a = mdb.models['GussetPlate-DisplacementModel'].rootAssembly
session.viewports['Viewport: 1'].setValues(displayedObject=a)
session.viewports['Viewport: 1'].assemblyDisplay.setValues(
optimizationTasks=OFF, geometricRestrictions=OFF,
stopConditions=OFF)
session.viewports['Viewport:
1'].assemblyDisplay.setValues(mesh=ON)
```

```
session.viewports['Viewport:
1'].assemblyDisplay.meshOptions.setValues(
meshTechnique=ON)
a = mdb.models['GussetPlate-DisplacementModel'].rootAssembly
partInstances =(a.instances['S01-Gusset-1'],
a.instances['Plate 240x148x13-1'],
a.instances['Plate 240x148x13-2'], a.instances['Flange2'],
a.instances['Flange1'], a.instances['Splice Web-1'],
a.instances['Splice Web-2'], )
a.generateMesh(regions=partInstances)

# Development of Buckling Job
buckleJobName = 'Buckle_k%s_l3-%s_l2-%s_a0-%s' %(kParam,
l3Param ,l2Param ,a0Param)
jobDescription = 'Buckling test to define imperfection for
Buckle_k%s_l3-%s_l2-%s_a0-%s' %(kParam, l3Param ,l2Param
,a0Param)
buckleJob = mdb.Job(name=buckleJobName, model='GussetPlate-
BuckleModel', description=jobDescription)

#Submission of Buckling Job
buckleJob.submit()
mdb.jobs[buckleJobName].waitForCompletion()

# Update imperfection in displacement model to first buckling
mode shape
imperfection = '*IMPERFECTION, STEP=1, FILE=%s\n1,2'
%(buckleJobName)
mdb.models['GussetPlate-
DisplacementModel'].keywordBlock.synchVersions(
storeNodesAndElements=False)
mdb.models['GussetPlate-
DisplacementModel'].keywordBlock.replace(373, imperfection)

for yieldParam in yieldDomain:

# Adjustment of Youngs Modulus Parameter
mdb.models['GussetPlate-DisplacementModel'].materials['Gusset
Material'].plastic.setValues(table=((yieldParam, 0.0), (556.1,
0.1)))

for youngsParam in youngsDomain:

#Adjustment of Yield Stress Parameter
youngs = youngsParam * 1000 # Change to MPa
mdb.models['GussetPlate-DisplacementModel'].materials['Gusset
Material'].elastic.setValues(table=((youngs, 0.3), ))

for thicknessParam in thicknessDomain:
```

```
# Adjustment of Thickness Parameter
mdb.models['GussetPlate-DisplacementModel'].sections['Gusset
Section'].setValues(thickness=thicknessParam)

# Development of Job
jobName = 'k%s_l3-%s_l2-%s_a0-%s_t%s_E%s_y%s' %(kParam,
l3Param, l2Param, a0Param, thicknessParam, youngsParam,
yieldParam)
jobDescription = 'Gusset Plate Displacement Model where l3-%s
l2-%s a0-%s t-%s E-%s y-%s' %(l3Param, l2Param, a0Param,
thicknessParam, youngsParam, yieldParam)
myJob = mdb.Job(name=jobName, model='GussetPlate-
DisplacementModel', description=jobDescription)
mdb.jobs[jobName].setValues(numCpus=4, numDomains=4)

#Submission of Job
myJob.submit()
mdb.jobs[jobName].waitForCompletion()
```

10.3.2 Parametric Design Output Script

```
## Gusset Plate Output Script ##

#  The script takes ODB output from gussetInputScript and
finds the maximum reaction force for each ODB and then writes
it to file

# Required imports to run code
from odbAccess import *
from abaqusConstants import *
from odbMaterial import *
from odbSection import *
from array import *
import sys, os, re

# Changes the directory to where ODB is located
os.chdir(r'F:\working\ODB')

# Opens the data recording file
dispFile = open('/working/Output/OutputData.dat','a')

# Loop runs for every ODB in the directory
for filename in os.listdir('.'):

print filename

# Opens the ODB abaqus file
odb = openOdb(path=filename)

# Resets the reaction force sum and array for each file
RForce = 0
array = []

# Loop runs for every frame in the ODB file
for frame in odb.steps['Displacement'].frames:

# Finds the reaction force for each node in the Boundary set
frameRF = frame.fieldOutputs['RF']
nodes = odb.rootAssembly.nodeSets['BOUNDARY']
nodeRF = frameRF.getSubset(region=nodes)

# Loop runs for every node in a single frame and adds up the
reaction force of each node
for v in nodeRF.values:
RForce = RForce + v.data[1]

# Sum of node reaction forces added to array of reaction force
sum for all frames
array.append(RForce)
```

```
# Resets the reaction force sum for each frame
RForce = 0

# Writes to file parameters, maximum reaction force of all
frames, last frame reaction force

# Pulls numbers out of file name, as unable to extract lengths
from ODB
parameters = str(filename)
values = re.findall(r'\d+', parameters)

parameterK = int(values[0])
parameterL3 = int(values[2])
parameterL2 = int(values[4])
parameterA0 = int(values[6])
parameterB0 = 500


# Calculates middle Thornton Length as L1
if (parameterA0/parameterB0) < 1
      parameterL1 = parameterA0 / cos(45) - parameterL2 -
(parameterL3 / 2) * tan(45)
      else
      parameterL1 = parameterB0 / cos(45) - parameterL2 -
(parameterL3 / 2) * tan(45)

# Pulls certain values from ODB directly
parameterThick = odb.sections['Section-ASSEMBLY_S01-GUSSET-
1__PICKEDSET2'].thickness
parameterYoungs = odb.materials['Gusset
Material'].elastic.table[0][0]
parameterYield = odb.materials['Gusset
Material'].plastic.table[0][0]

# Writes parameters and buckling capacity in a single line in
output text file.

dispFile.write('%s   %10.4E   %10.4E   %10.4E   %10.4E
%10.4E   %10.4E   %10.4E   %10.4E   %10.4E   %10.4E\n' %
(filename, parameterK, parameterL1, parameterL2, parameterL3,
parameterA0, parameterYoungs, parameterYield, parameterThick,
max(array), array[-1]))

dispFile.close()
print 'Script Complete'
```

10.4 GP-BRB System Stability Method Matlab Code

```
% GP-BRB System Stability Method Script
% Benjamin Westeneng

% This script has been written for Matlab R2012b to implement
% the GP-BRB system stability method. It considers the
% individual elements of the BRB system and combines them
% into a system stiffness matrix that considers P-delta
% effects. When the system stiffness matrix is found to
% no longer be positive definite, this corresponds to the
% buckling capacity of the GP-BRB system

% Applied force on system stiffness matrix, accuracy to 1 kN
appliedForceVector = 1000:1000:1000000000 ;

Dvector = [];
Pvector = [];

% Function Handles for stability functions
Phi = @(P,L,E,I) sqrt((P*L^2)/(E*I));
s = @(Phi) (Phi*(sin(Phi)-Phi*cos(Phi)))/(2*(1-cos(Phi))-
Phi*sin(Phi)) ;
r = @(Phi) ((Phi^2) - (Phi*sin(Phi)))/((2*(1-cos(Phi)))-
(Phi*sin(Phi))) ;
f = @(s,r,Phi) 2*(s + r)-Phi^2 ;
g = @(s,r) s + r ;

for i = appliedForceVector

% Rotational Spring Inputs
kBeamColumn1 = 1e20 ; % N mm / rad
kBeamColumn2 =  1e20 ; % N mm / rad
kRestrainerEnd1 = 1e20  ; % N mm / rad
kRestrainerEnd2 = 1e20  ; % N mm / rad

% Gusset 1 Inputs
pG1  = i ; % N applied force
lG1  = 283; % mm maximum Thornton length
eG1  = 200000 ; % MPa modulus of elasticity
iG1  = 62197 ; % mm^4 second moment of area (Thornton Method)
aG1  = 3808 ; % mm^2 area (Whitmore Method)
fyG1 = 385 ; % MPa yield stress
NsG1 = aG1*fyG1; % N yield force

% Connection 1 Inputs
pC1  = i ; % N applied force
lC1  = 642.5 ; % mm connection length
eC1  = 200000 ; % MPa modulus of elasticity
iC1  = 11456144 ; % mm^4 second moment of area
```

```
aC1  = 6020 ; % mm^2 connection area
fyC1 = 385 ; % MPa yield stress
NsC1 = aC1*fyC1; % N yield force

% BRB Restrainer Inputs
lB = 4032 ; % mm BRB casing length
eB = 200000 ; % MPa modulus of elasticity
iB = 11535865+(16150211*(27800/200000)) ; % mm^4 second moment
of area

% Connection 2 Inputs
pC2  = i ; % N applied force
lC2  = 642.5 ; % mm connection length
eC2  = 200000 ; % MPa modulus of elasticity
iC2  = 11456144 ; % mm^4 second moment of area
aC2  = 6020 ; % mm^2 connection area
fyC2 = 385 ; % MPa yield stress
NsC2 = aC2*fyC2; % N yield force

% Gusset 2 Inputs
pG2  = i ; % N applied force
lG2  = 283 ; % mm maximum Thornton length
eG2  = 200000 ; % MPa modulus of elasticity
iG2  = 62197 ; % mm^4 second moment of area (Thornton Method)
aG2  = 3808 ; % mm^2 area (Whitmore Method)
fyG2 = 385 ; % MPa yield stress
NsG2 = aG2*fyG2; % N yield force

%EI Strength Reduction Factors
c = 1.5*exp(-1.8*0.5)-0.35;

srfC1 = 1-((i/NsC1)/(1+c*(1-i/NsC1)));
srfC2 = 1-((i/NsC2)/(1+c*(1-i/NsC2)));
srfG1 = 1-((i/NsG1)/(1+c*(1-i/NsG1)));
srfG2 = 1-((i/NsG2)/(1+c*(1-i/NsG2)));

% EI/L of each input
eilB  = (eB*iB/lB) ; % no reduction as no load on restrainer
eilC1 = (eC1*iC1/lC1) * srfC1 ;
eilC2 = (eC2*iC2/lC2) * srfC2 ;
eilG1 = (eG1*iG1/lG1) * srfG1 ;
eilG2 = (eG2*iG2/lG2) * srfG2 ;

% Gusset 1 Stability Functions
PhiG1 = Phi(pG1,lG1,eG1,iG1*srfG1) ;
sG1 = s(PhiG1) ;
rG1 = r(PhiG1) ;
fG1 = f(sG1,rG1,PhiG1) ;
gG1 = g(sG1,rG1) ;
```

```
% Connection 1 Stability Functions
PhiC1 = Phi(pC1,lC1,eC1,iC1*srfC1) ;
sC1 = s(PhiC1) ;
rC1 = r(PhiC1) ;
fC1 = f(sC1,rC1,PhiC1) ;
gC1 = g(sC1,rC1) ;

% Connection 2 Stability Functions
PhiC2 = Phi(pC2,lC2,eC2,iC2*srfC2) ;
sC2 = s(PhiC2) ;
rC2 = r(PhiC2) ;
fC2 = f(sC2,rC2,PhiC2) ;
gC2 = g(sC2,rC2) ;

% Gusset 2 Stability Functions
PhiG2 = Phi(pG2,lG2,eG2,iG2*srfG2) ;
sG2 = s(PhiG2) ;
rG2 = r(PhiG2) ;
fG2 = f(sG2,rG2,PhiG2) ;
gG2 = g(sG2,rG2) ;

% Stiffness matrix Development
K00 = sG1*eilG1 + kBeamColumn1 ;
K01 = -gG1/lG1*eilG1 ;
K02 = rG1*eilG1 ;

K10 = K01 ;
K11 = fG1/lG1^2*eilG1 + fC1/lC1^2*eilC1 ;
K12 = -gG1/lG1*eilG1 + gC1/lC1*eilC1 ;
K13 = -fC1/lC1^2*eilC1 ;
K14 = gC1/lC1*eilC1 ;

K20 = K02 ;
K21 = K12 ;
K22 = sG1*eilG1 + sC1*eilC1 ;
K23 = -gC1/lC1*eilC1 ;
K24 = rC1*eilC1 ;

K31 = K13 ;
K32 = K23 ;
K33 = fC1/lC1^2*eilC1 + 12/lB^2*eilB ;
K34 = -gC1/lC1*eilC1  ;
K35 = 6/lB*eilB  ;
K36 = -12/lB^2*eilB ;
K37 = 6/lB*eilB ;

K41 = K14 ;
K42 = K24 ;
K43 = K34 ;
K44 = sC1*eilC1 + kRestrainerEnd1 ;
```

```
K45 = -kRestrainerEnd1;

K53 = K35 ;
K54 = K45;
K55 = 4*eilB + kRestrainerEnd1 ;
K56 = -6/lB*eilB ;
K57 = 2*eilB ;

K63 = K36 ;
K65 = K56 ;
K66 = fC2/lC2^2*eilC2 + 12/lB^2*eilB ;
K67 = -6/lB*eilB ;
K68 = gC2/lC2*eilC2;
K69 = -fC2/lC2^2*eilC2;
K610 = gC2/lC2*eilC2;

K73 = K37 ;
K75 = K57 ;
K76 = K67 ;
K77 = 4*eilB + kRestrainerEnd2 ;
K78 = -kRestrainerEnd2;

K86 = K68 ;
K87 = K78;
K88 = sC2*eilC2 + kRestrainerEnd2;
K89 = -gC2/lC2*eilC2;
K810 = rC2*eilC2 ;

K96 = K69;
K98 = K89;
K99 = fC2/lC2^2*eilC2 + fG2/lG2^2*eilG2;
K910 = - gC2/lC2*eilC2 + gG2/lG2*eilG2 ;
K911 = gG2/lG2*eilG2 ;

K106 = K610;
K108 = K810;
K109 = K910;
K1010 = sC2*eilC2 + sG2*eilG2 ;
K1011 = rG2*eilG2 ;

K119 = K911;
K1110 = K1011;
K1111 = sG2*eilG2 + kBeamColumn2 ;

% full system stiffness matrix development
K = [ K00, K01, K02, 0, 0, 0, 0, 0, 0, 0, 0, 0;
      K10, K11, K12, K13, K14, 0, 0, 0, 0, 0, 0, 0;
      K20, K21, K22, K23, K24, 0, 0, 0, 0, 0, 0, 0;
      0  , K31, K32, K33, K34, K35, K36, K37, 0, 0, 0, 0;
      0  , K41, K42, K43, K44, K45, 0, 0, 0, 0, 0, 0;
```

```
      0  , 0  , 0  , K53, K54, K55, K56, K57, 0, 0, 0, 0;
      0  , 0  , 0  , K63, 0, K65, K66, K67, K68, K69, K610, 0;
      0  , 0  , 0  , K73, 0  , K75, K76, K77, K78, 0, 0, 0;
      0  , 0  , 0  , 0  , 0  , 0, K86, K87, K88, K89, K810, 0;
      0  , 0  , 0  , 0  , 0, 0, K96, 0, K98, K99, K910, K911 ;
      0  , 0  , 0, 0, 0, K106, 0, K108, K109, K1010, K1011;
      0  , 0  , 0  , 0  , 0  , 0, 0, 0, 0,K119, K1110, K1111];

% Cholesky decomposition of system stiffness matrix
% d becomes greater than 0 when matrix no longer
% positive definite indicating buckling failure
[R,d] = chol(K) ;

% Vectors for positive definite indicator,
% equivalent effective length factor, applied force
Dvector = [Dvector d] ;
Pvector = [Pvector i] ;

% Break to stop applied force loop when matrix
% no longer positive definite
if d > 0
     break
end
end

% Location variable to determine applied force when
% matrix no longer positive definite, result is
% conservative rounding down.
LOC=[size(Dvector,1) find(Dvector(end,:)>0,1)] ;
Pcr = Pvector(LOC(2)-1);
```